TUMOUR IMMUNOLOGY GROUP
WEATHERALL INSTITUTE OF MOLECULAR MEDICINE
NUFFIELD DEPARTMENT OF MEDICINE
MEDICAL SCIENCES DIVISION
UNIVERSITY OF OXFORD

"The role of Tryptophan and the mTOR pathway in T cell fate determination"

Thesis submitted
for the degree of
Doctor of Philosophy

Ioannis Karydis

October 2013
Trinity Term 2013

Abstract

The adaptive immune response forms an essential part of the cancer immuno-editing process, whereby nascent malignant cells are detected and destroyed prior to forming tumours. The process is tightly controlled to minimise collateral damage to healthy tissue. One of the mechanisms evolved for this purpose and frequently co-opted by malignant cells is the creation of a microenvironment scarce in essential amino-acids through the use of catabolic enzymes such as Indoleamine 2,3-dioxygenase (IDO) , responsible for the rate-limiting step in tryptophan catabolism. The evolutionary conserved GCN2 and mTORC1 pathways respond to amino-acid starvation by triggering emergency homeostatic response programmes that aim to conserve nutrients by shutting down biosynthetic pathways, slowing cell cycle progression and facilitating autophagy. This research project focuses on elucidating the interaction between IDO activity and these pathways and its implications for the immune-editing process.

The role of the mTOR kinase as a regulator of T cell fate following exposure to cognate antigen has recently become apparent. Experiments described herein confirm that in murine and human models of T cell activation exposure to tryptophan starvation results in significant mTORC1 inhibition and a modified phenotype with reduced Tbet expression, altered cytokine secretion profile, greatly impaired proliferative capability and expanded $CD4^{+}$ $FoxP3^{+}$ $CD25^{high}$ subpopulations. Additional results confirmed that the action of IDO is sufficient to deplete tryptophan from the microenvironment to levels sufficient to depress the mTORC1 axis and trigger GCN2 activity even in tumour cell lines. Lower extracellular tryptophan levels were necessary to perturb these pathways In IDO expressing cell lines, suggesting that compensatory mechanisms allow continued proliferation of malignant cells in the face of conditions that severely impede an anti-cancer immune response. In conclusion, manipulation of the mTORC1 axis via IDO-induced tryptophan depletion is an important tumour immune-escape mechanism that can be a target for cancer immunotherapies.

Dedicated to my wife and our successful joint experiment –
a case where IDO directly led to “I do”!

Acknowledgements

First of all I would like to thank my supervisor, Professor Vincenzo Cerundolo for offering me the opportunity to join his lab and enter the exciting world of tumour immunology just as it finally entered the mainstream and subsequently mentoring and guiding me throughout this project – without his support this task would have never come to fruition.

I would also like to express my gratitude to my clinical supervisor, Professor Mark Middleton, who originally put me in touch with Prof. Cerundolo and subsequently provided invaluable clinical input; furthermore without his assistance in securing protected time for me to finish writing up, this thesis would have never been completed on time!

In addition I am eternally grateful to Dr Jonathan Silk who introduced me to the vagaries of laboratory science and IDO in particular and provided constructive and insightful guidance and supervision throughout my time in the lab. Dr Val Macaulay opened my eyes to the wonders of the mTOR pathways and initiated me to the field of phosphoprotein analysis. Drs Uzi Gileadi and Carmela De Santo also offered invaluable practical advice at several stages of this project – flow cytometry would likely still be a mystery for me without them! I benefitted from the input of virtually everybody in the tumour immunology group, and in particular the “level 7” team – the communal coffee brainstorming sessions formed an integral part of my time in the lab.

I have to thank my family back in Greece without whose guidance and support I wouldn’t be here –and in particular my mother whose personal fight against cancer inspired me to become an oncologist in the first place, my father who spurred me on to strive towards academic excellence and guided my educational path with clear vision and my grandfather who sadly passed away before this project was complete.

Finally, the biggest thanks has to go to Laura, my long suffering wife - words are not enough to express my gratitude to her: Not only did she provide direct help throughout our joint time in the lab starting almost from day 1 when she taught me how to effectively use HPLC; most importantly she steadfastly supported me through the dark days of me trying to write-up and working full time as a medic while she was almost single-handedly managing the fallout of our most successful joint experiment – our adorable son whose laughter kept my spirits up while I was taming the sea of data that came out of 3.5 years of experiments!

Table of Contents

Chapter 1: Introduction

1.1. The Immune system and cancer

1.1.1. Cancer immunoediting

The suggestion that the immune system is involved in protecting the host from cancer development dates from the early 20th century[1], however it was not formally introduced as the "cancer immunosurveillance" hypothesis until more than 50 years later by Burnet and Thomas[2]. As a result of the emerging understanding of the underlying immunobiology they predicted that the immune system was responsible for eliminating continuously arising transformed cells.

Initially this prediction was not confirmed when it was put to the test utilising the best available model of immunodeficiency at the time, nude mice[3]. A series of experiments by Stutman et al[4,5] using CBA/H strain nude mice failed to show any differences in rates of spontaneous or carcinogen induced neoplasia between these mice and wild-type controls.

These results initially discredited the hypothesis for several decades until advances in our understanding of the underlying immunological mechanisms revealed a number of caveats (summarised by Dunn et al[6]) that invalidated the conclusions drawn from these experiments. One of the biggest issues that had not been appreciated initially was the presence of detectable numbers of functional T cell populations[7] as well as fully functional natural killer cells and underlying nearly normal innate immunity.

At around this time an increasing volume of direct experimental results from animal experiments[6] as well as corroborative human data accumulated pointing towards the existence of a functional immunosurveillance process:

Initially it was shown that in mice Interferon gamma ("IFN-γ") inhibits the growth of transplanted tumours[8] and protects against the formation of both induced and spontaneous tumours[9] . In addition mice lacking perforin – which is essential for the cytolytic function of cytotoxic T and natural killer ("NK") lymphocytes[10]– were also shown to be more susceptible to both induced[11] and spontaneous[12] tumour formation.

The most conclusive evidence supporting the role of the adaptive immune system in controlling and shaping tumour growth came from experiments employing gene-modified mice that were unable to produce any T, B or natural killer T ("NKT") lymphocytes by virtue of not having a functional recombinase activating gene 2 ("RAG2")[13]. $RAG2^{-/-}$ mice were particularly suitable as a model because RAG2 deficiency only affects cells that need to undergo recombination of their antigen receptor - lymphocytes - and thus DNA repair was not affected in somatic cells otherwise.

An important study by Shankaran et al[14] demonstrated that $RAG2^{-/-}$ mice developed both induced and spontaneous tumours much more frequently than wild-type controls; moreover tumours from immunodeficient $RAG2^{-/-}$ mice were much more likely to be rejected when transplanted into syngeneic immunocompetent mice than tumours grown from immunocompetent mice. The implication was that the presence of an intact immune system not only protects against tumour formation but also drives the selection of tumours that are less immunogenic.

Over the last decade or so, the maturation of transgenic mouse techniques and the increasing availability of highly specific blocking monoclonal antibodies have allowed us to conduct increasingly intricate experiments slowly dissecting the underlying immunological mechanisms.

The interplay of the immune system with cancer is now understood to be driven by a process described as "immunoediting"[15]. This is thought to be dynamic and comprising three distinct phases: elimination, equilibrium and escape.

1.1.2. Tumour elimination

The first stage of the immunoediting process is thought to take place continuously in immunocompetent multicellular organisms. During this phase the immune system continuously monitors the organism for the development of new transformed cells with malignant potential and destroys them before they develop into outright malignant tumours.

While there is no direct evidence of this occurring in vivo, strong indirect evidence has come from animal experiments where individual parts of the immune system are specifically disabled, either via employing transgenic models with well-defined immune deficiencies, or by using wild-type animals with targeted use of neutralising monoclonal antibodies.

It is important to note that these experiments are based on de-novo carcinogenesis (e.g. via carcinogens / tumour suppressor mutations) rather than transplanted tumours as these by default have already escaped immune monitoring in the original host.

The earliest definitive evidence came from experiments using $RAG2^{-/-}$ mice where carcinogen induced tumours were more frequent than in wild-type controls as mentioned earlier[14]. Subsequent studies confirmed that carcinogen induced tumours were more frequent in mice who lacked αβ or γδ T cells[16], lacked CD1d-restricted NKT cells[17], lacked[11] or were insensitive[9] to IFN-γ or type I interferons[18] , lacked perforin[11] , IL12 or IL23[19], lacked eosinophils[20] or had their NK cell population depleted by specific antibody treatment[21] .

Studies observing the development of spontaneous tumours in mice have been more difficult as they have relatively short life-span and long telomeres; the incidence of spontaneous tumours in immunocompetent inbred strains varies but is in the region of 0-20% over their lifespan[22]. Nevertheless several studies have now been able to confirm an increased incidence of specific types of spontaneous cancer in mice with well-defined immunodeficiencies; for example $RAG2^{-/-}$ mice are susceptible to intestinal and lung neoplasms[14], $Pfp^{-/-}$ mice lacking perforin develop B cell lymphomas[23] and IFN-$\gamma^{-/-}$ mice that cannot express IFN-γ develop lung adenocarcinomas on a BALB/c background[12]. Combining immunodeficiencies sometimes results in non-overlapping pro-neoplastic effects, e.g. $RAG2^{-/-}$ $Stat1^{-/-}$ mice develop also mammary malignancies as well as lung and colonic adenocarcinomas[14].

More recently, the development of mouse strains predisposed to earlier development of cancer has allowed to extend these observations, for example mice with a heterozygous mutation in the p53 gene- that are genetically predisposed to develop

a multitude of cancers[24]-develop more aggressive tumours with an earlier onset in the presence of additional immunodeficiencies such as loss of perforin[23], or NKT cells[17] .

In addition to animal data there has been a significant accumulation of observational data in humans supporting a role of the immune system in suppressing the development of cancer. AIDS patients have long been known to be at increased risk of several malignancies (reviewed by Boshoff and Weiss in [25]) . Often these are virus associated such as lymphomas secondary to EBV and Kaposi's sarcomas secondary to HHV8, however the incidence of some non-virally induced tumours, most notably lung adenocarcinomas[26,27] is 3.5 times more common than in the wider population even when corrected for confounding factors such as smoking habit.

As the number of organ transplant recipients is increasing, this has provided researchers with access to a population that requires maintenance immunosuppression for prolonged periods of time. As these patients are followed up very closely there is a wealth of data that can be compared with standardised incidences in the general population. An increase in cancer incidence could be seen for a range of malignancies, although the exact changes depended on the immunosuppressive regime used[28]; kidney transplant recipients exhibit an up to 3-fold increase in the incidence of a range of malignancies including cancers that are not known to be related to infections such as lung, colon and pancreas[29]. The incidence of skin cancers in particular is particularly increased – 2 to tenfold for malignant melanoma[30] and up to 200-fold for non-melanoma skin cancers[31] .

The most convincing data in humans supporting the role of the immune system in eliminating spontaneously occurring tumours comes from observations of spontaneous immune responses to cancer. Antibody responses against tumour antigens in patient sera have been described for a long time (reviewed by Reuschenbach M, et al[32]). Cross reactivity between tumour antigens and naturally occurring self-antigens occasionally results in tolerance breakdown and the development of "paraneoplastic" autoimmune disorders. These can sometimes precede the clinical detection of cancer for number of years[33] and sometimes cytotoxic as well as humoral responses are also seen[34]. Spontaneously regressing

melanocytic lesions associated with clinically significant cytotoxic T cell responses against tumour antigens[35,36] are perhaps the best examples of a successful elimination phase of immunoediting in humans and stimulated research in immunotherapies against melanoma that eventually led to the development of multiple successful immunotherapeutic approaches.

1.1.3. Immune equilibrium

The second stage of the immunoediting process refers to the situation where latent tumours are prevented from spreading and or growing directly as a result of the actions of the host immune system. This is a dynamic state of affairs where a strong immune response successfully contains but fails to completely eradicate a tumour cell population that has been selected to manifest immunoevasive abilities. It is inherently unstable as a shift in the balance of power can occur at any point – either due to external factors altering the immune system functioning or due the gradual accumulation of mutations by the cancer that eventually accrue such an advantage that they can no longer be contained.

Direct evidence for an existence of such a state in vivo is now available; in a seminal paper Koebel et al[37] demonstrated that utilising a model based on applying low dose carcinogen on naïve wild-type mice. In the absence of additional treatment only a minority of treated animals developed tumours. When the tumour free animals were subsequently rendered immune deficient by treatments that targeted their adaptive immune system such selective $CD4^+$ or $CD8^+$ cell depletion up to 50% of them developed sarcomas at the site of the previous carcinogen injection. Interestingly, when these tumours were transplanted to immunocompetent mice they were highly immunogenic with up to 40% of them being outright rejected. In contrast the much rarer spontaneous tumours arising in the absence of immunosuppression were much less immunogenic; these findings fitted well with the concept of immunoediting.

In humans indirect evidence for the existence of a state of immune equilibrium comes from studies of tumour-infiltrating lymphocytes (“TILs”). While these are present to some extent in all tumours, their relative abundance has now been shown to be closely associated with prognosis. This phenomenon was initially described in

melanomas[38] but was subsequently confirmed to hold true for multiple other tumour types including oesophageal[39] and ovarian[40] cancers. In colorectal cancer in particular[41] a close association was demonstrated between patient survival and the nature of the immune response - in terms of the type of cells involved, their location and density .

1.1.4. Immune escape

The last stage of the immunoediting process refers to events taking place once immune controls fail and the cancer cells are able to grow and spread free of the influence of the immune system. While this can occasionally occur without any change in the underlying physiology of the cancer cells – for example if the host becomes immunosuppressed due to an unrelated cause – in the majority of cases the tumour accumulates genetic changes under strong immunological selection pressure and eventually reaching the critical mass needed to escape immunosurveillance.

A large number of potential tumour escape strategies have been seen reported in the literature for both animal models and from human studies; they can broadly be subdivided in changes affecting the phenotype of the tumour cell itself and the gain of the ability to modify their local microenvironment in a way that disrupts the immunosurveillance network.

The simplest way for a cancer cell to avoid detection from the adaptive immune system is to alter its antigen processing and presentation pathways – loss of TAP1, MHC class I ,β2m, LMP2 and development of Interferon insensitivity through mutation or epigenetic silencing have all been reported[42,9].

In addition the expression of immunogenic neoantigens whose presence is not critical for the malignant clone's survival and growth will be heavily negatively selected. This has been observed in human patients, particularly where the use of immunotherapy was successful in triggering a robust immune response against the primary tumour but there was subsequent disease progression with new lesions no longer expressing antigens detected in the primary against whose specific responses were detectable[43,44] .

Even if the cytotoxic lymphocytes do manage to detect and target tumour cells, the latter can still escape destruction by developing resistance to cell lysis e.g. through expressing mutated inactive forms of death receptors such as Fas[45] and TRAIL-R1&2[46] or by upregulating anti-apoptotic molecules such as BCL-X_L[47]. In addition the upregulation of regulatory molecules such as PD-L1[48] and HLA-E[48] can dampen the activity of or even outright kill responding T cells.

An alternative route to disturbing the immunosurveillance network - that potentially has more far reaching consequences- is manipulating the tumour microenvironment in a way that inhibits the function of the adaptive and innate immune systems. This allows for multiple adaptations to evolve independently in a heterogeneous genetically unstable population. These changes individually may have been too weak to have an effect when expressed by small clonal groups of malignant cells, however when they come together in the population they can have an additive or even super-additive effect and be successful in inactivating particular aspects of the immune monitoring process.

What's more in doing so they provide the opportunity for cells to develop additional mutations that otherwise would have been selected against due to their immunogenicity - even if those clones themselves do not possess the necessary cellular machinery to deflect the immune system. In this way a genetically heterogeneous tumour may be able to collectively develop highly aggressive characteristics even when the likelihood of an individual cell clone developing all the necessary genetic and epigenetic changes would be very low.

Manipulation of the local microenvironment can occur in a number of ways. Firstly tumour cells can secrete soluble factors that directly inhibit important aspects of both the innate and adaptive immune responses. The presentation of tumour antigens in an immunogenic fashion by dendritic cells in local lymph nodes can be stopped by preventing their migration[49], activation[50] or simply by preventing them from processing antigen in the first place[51]. Immunosuppressive cytokines secreted by tumour cells themselves such as TGF-β[50] can have wide ranging effects and inactivate multiple facets of the immune response.

In addition, through a number of mechanisms, some of which are not completely understood, tumours can either recruit a variety of immunoregulatory cells whose presence and activity precludes an effective local immune response, such as regulatory T cells (reviewed by Terabe et al in [52]), myeloid derived suppressor cells (reviewed by Gabrilovic et al in [53]) and plasmacytoid dendritic cells[54].

Depletion of essential nutrients from the local microenvironment is another mechanism physiologically used for dampening down excessive or unwanted immune responses by various immunoregulatory cells (e.g., arginine and cysteine by myeloid derived suppressor cells[55], tryptophan by numerous dendritic cell subsets (summarised by Harden et al in[56]). Tumour cells can co-opt this mechanism either indirectly by promoting the presence of the appropriate cell types in the local microenvironment, or - in the case of tryptophan – express the relevant enzyme, indoleamine 2,3-dioxygenase (IDO) that catalyses the rate limiting step in tryptophan metabolism.

It is the role of tryptophan depletion in facilitating immune escape and the specific underlying mechanisms and processes involved particularly with regards to its effects on T cell function that form the focus of this research project.

1.2. Tryptophan catabolism and cancer

1.2.1. Tryptophan catabolism in mammals

L-Tryptophan is the least abundant of all dietary amino-acids. It cannot be synthesised de novo in humans and thus in its absence protein synthesis eventually will stop, which is particularly important for rapidly dividing cells such as T lymphocytes responding to antigenic stimulation.

It furthermore plays a vital role in a number of physiological processes by providing the raw materials in the form of its direct catabolites for the biosynthesis of a number of important bioactive compounds, including the neurotransmitter serotonin, the neurohormone melatonin and a number of kynurenine metabolites, the latter feeding into nicotinamide dinucleotide (NAD^+) synthesis.

The main metabolic pathway responsible for the breakdown of dietary tryptophan is the kynurenine pathway[57]. The initial- and rate limiting- reaction in this pathway is the cleavage of the 2,3-double bond of the indole ring of tryptophan through the incorporation of molecular oxygen to form N-formylkunurenine that is then rapidly converted to L-kynurenine.

In humans and most mammals two enzymes are known to be responsible for this reaction in vivo: Indoleamine 2,3-dioxygenase ("IDO") (EC 1.13.11.52) and tryptophan 2,3-dioxygenase ("TDO") (EC 1.13.11.11). Both are heme containing but differ significantly in their structure, substrate specificities and tissue expressing patterns:

TDO is a tetrameric enzyme that is enantiomer specific – it can only metabolise the naturally occurring L-Tryptophan stereoisomer. It is naturally expressed in high levels in liver [58] and is thought to be the main enzyme responsible for controlling systemic tryptophan levels, though recently it has also been found to be expressed in brain where it may regulate the production of neuroactive tryptophan catabolites[59].

In contrast IDO is a monomeric enzyme that has a broader range than TDO- it was originally isolated from rabbit intestine as a D-tryptophan degrading enzyme[60]. It is expressed ubiquitously, particularly in lung, gut, epididymis, thymus and the placenta[61,62] though baseline expression levels are low. Its expression and activity can

be dramatically upregulated in response to stimuli such as IFN-γ in a number of cell types including fibroblasts[63], monocytes[64] and in particular dendritic cells (reviewed by Harden in[56]).

An additional third enzyme called indoleamine 2,3-dioxygenase-2("IDO2") was discovered in 2007; this has 43% homology at the amino acid level with IDO and is situated next to it on chromosome 8 in mice and humans. It is expressed in a number of murine tissues including liver, kidney and brain[65]. The distribution of IDO2 expression in humans is an open question; transcription of the human IDO2 gene is complex with several different alternative transcripts one of which appears to lack any enzymatic activity in in vitro assays[66]. While there is some evidence that the mouse isoform has some enzymatic activity[67]– albeit lower than IDO - nevertheless it has not been possible so far to conclusively prove that human IDO2 can function as a tryptophan catabolising enzyme (reviewed by Fatokun in[68]).

On the other hand IDO2 protein expression has been detected in pancreatic cell lines[69] and IDO2 mRNA has been isolated from gastric, colonic and renal tumours[70] , but in the absence of evidence of enzymatic activity its physiological role remains unclear.

1.2.2. Indoleamine 2,3-dioxygenase and the immune system

It is now thought likely that IDO originally evolved as a defence molecule deployed when triggered by inflammatory stimuli with the aim to inhibit pathogen growth by depleting tryptophan from the local microenvironment– an action that it is still capable of performing, as IDO function plays an important role in inhibiting the intracellular replication of pathogens such as Chlamydia psittaci[71] and Toxoplasma gondii[72].

Over time it became integrated in processes that balance the immune response to contain the pathogens minimising collateral tissue damage e.g. in the context of fungal infections[73] .

The first clear evidence that IDO has bona-fide immunoregulatory capabilities came from a series of seminal experiments by Mellor and Munn[74] that showed that in mice IDO inhibition resulted in rapid T cell induced rejection of allogeneic concepti. Subsequent studies of autoimmunity in animal models expanded this concept. Utilising the prototypical model of T-cell mediated autoimmune disease, experimental autoimmune encephalomyelitis ("EAE"), a large body of evidence accumulated (summarised and expanded in Yan et al[75]) that supports a significant role for IDO in controlling immune cell-mediated inflammation of the CNS. Collagen-induced arthritis ("CIA") in mice is much more severe in IDO-deficient mice[76], while intra-articular delivery of IDO gene ameliorates its effects[77] .

There are several ways in which IDO is thought to be able to mediate its immunoregulatory effects. The most straightforward one to conceptually visualise is that of tryptophan starvation from the local microenvironment; activation of the GCN2 pathway as a result of insufficient tryptophan to load on transfer RNAs ("tRNAs") has been shown to lead to inhibition of T cell proliferation[78] . On the other hand kynurenine downstream metabolites also have a direct effect on T cell function (reviewed in by Opitz et al in[79]*;* the aryl hydrocarbon receptor (AHR) has recently been implicated as a potential direct target of kynurenine[80].

There is still a great deal of uncertainty regarding whether tryptophan depletion or kynurenine production plays a more important role ; some studies have actually implicated that both are needed to achieve the effect in specific settings[81] ; it is likely the underlying immunological circumstances dictate their relative roles in a given setting.

1.2.3. Tryptophan catabolism and cancer

The potential role of tryptophan catabolising enzymes and in particular IDO has as tumour immune escape mechanisms has been extensively investigated. The ratio of kynurenine to tryptophan in human cancer patients has been found to correlate with disease activity and prognosis[82],[83].

Expression of IDO in the tumour cells themselves or in cells of the local microenvironment has been shown to confer a significantly worse prognosis in a range of tumour types including ovarian[84], colorectal[85], endometrial[86], uterine[87], pancreatic[88] and non-small-cell lung[89].

A hint as to why this might be the case comes from studies of immune cell populations found at the tumour site or at draining lymph nodes; $CD3^+$ and $CD8^+$ T cell infiltration was reduced in tumour specimens of IDO expressing colorectal[85], ovarian[90] and endometrial[91] cancers. Interestingly no studies have reported a significant decrease in $CD4^+$ T cell infiltration though the presence of a relatively increased $CD4^+CD25^+FoxP3^+$ regulatory T cell ("Treg") population may be partly responsible for this[61].

In animal models, transfection of IDO into tumour cells prevents their rejection by pre-immunized hosts[92,93] , but the antitumor effect of IDO is dependent on a fully competent immune system.

A recent study by Holmgaard et al[94] has demonstrated that CTLA-4 and PD-1 targeting neutralising antibodies are much more effective in inhibiting tumour growth in IDO knockout versus wild-type mice; conversely IDO inhibition was strongly synergistic with CTLA-4 blockade in mediating rejection of both IDO expressing and non-expressing tumours. This finding illustrates that multiple redundant immunoregulatory mechanisms are in play and may explain to some extent why IDO knockout mice do not have an obvious phenotype.

It should finally be noted that constitutive TDO expression has recently also been detected in several human tumour types particularly malignant glioma, hepatocellular carcinoma, melanoma, and bladder cancer and functional studies confirmed that its activity is sufficient to trigger immunologically meaningful effects[80,95].

1.3. Cellular mechanisms involved in detection of amino-acid sufficiency

All mammalian cells require a constant supply of essential amino acids ("a.a.") to meet their homeostatic and growth demands. Under restrictive nutrient conditions they need to be able to modify their metabolic pathways to conserve limited resources by restricting translation to essential proteins only, stimulating autophagy and if possible increasing the uptake of extracellular a.a. To achieve this several interacting molecular pathways have evolved that are conserved from yeasts to mammals, the best studied of which are the mTORC1 and GCN2 pathways.

1.3.1. The mTORC1 pathway

The mTORC1 pathway acts as a gatekeeper for cellular growth and proliferation by integrating signals regarding energy via AMPK[96,97] amino acid availability via the Rag GTPases and the "Ragulator" complex[98–100], mitogen/growth factor stimulation via the Akt[101], ERK1/2[102] and p90RSK1[103] kinases and cellular stress via p53[104].

mTORC1 itself is a multiprotein complex[105] consisting of the mechanistic target of rapamycin ("mTOR") Serine/Threonine Kinase in association with the raptor protein that acts as a scaffolding/adaptor protein to facilitate substrate binding and provide specificity. Other proteins such as GβL/mLST8, deptor and PRAS40 provide additional substrate specificity, localisation and regulatory functions[106].

Through raptor it binds to proteins containing a "TOS" motif[107] such as S6 Kinase and 4E-BP1 and phosphorylates them; alternatively it can use them as scaffold bringing it close to its substrate e.g. an association with the "TOS" motif in the promoter binding transcription factor TFIIIC allows targeting of the transcriptional repressor protein Maf1 and thus stimulation of tRNA transcription[108].

S6 protein is a component of the 40S ribosomal protein whose phosphorylation at several serine residues is essential to allow the translation of RNAs that contain a 5'

terminal oligopyrimidine sequence. As an activated S6 Kinase is the main kinase driving its activity and that is directly driven by an active mTORC1 pathway, phosphorylated S6 is often used as a surrogate marker for mTORC1 activity, particularly as there are highly specific antibodies against its phosphorylated form that offer much better signal/noise ratios than other available options. Kinases from alternative pathways (such as the MEK/ERK axis) can under certain circumstances also drive low level phosphorylation, particularly at serine residue 236 ("Ser236") hence why phosphorylation at serine residues 240 and 244 ("Ser240"/ "Ser244") is generally a better readout for determining mTORC1 status by S6.

mTORC1 activation results in increased protein & lipid synthesis , promotes cell cycle progression and mitochondrial biogenesis and inhibits autophagy[106].

The mTOR kinase is also an essential component of the mTORC2 protein complex whose regulation and function are much less understood. It is known to phosphorylate Ser473 of Akt activating it [109] and thus can be thought of as being upstream of mTORC1; however prolonged exposure to rapamycin – a mTORC1 specific inhibitor – results in mTORC2 disassembly and thus inhibition[110] in ~20% cell lines tested, suggesting the existence of cellular phenotype specific feedback mechanisms.

1.3.2. The GCN2 pathway and interaction with mTOR

The general control nonderepressible 2("GCN2") pathway acts as an emergency brake in the presence of amino acid depletion. The GCN2 kinase is activated by the presence of uncharged tRNAs and phosphorylates eIF2α[111]; this results in reduced translation of most mRNAs apart from a select few such as ATF4, ATF5 and GADD34, thus triggering the "amino acid response"(AAR). This is a stress response[112,113] that involves upregulation of several a.a. biosynthesis and salvage enzymes and transporter proteins while inhibiting cell growth.

Both pathways are finely tuned, as their prolonged activation in the presence of continuing amino acid deficiency would eventually be counterproductive; they are inhibited after a period of time by feedback mechanisms [114,115]. Furthermore, there is accumulating evidence that they are interlinked: mTORC1 activity appears essential

for the expression of CHOP, a transcription factor expressed downstream of eIF2α that is essential for the AAR[116]. On the other hand, mTORC1 activity itself is modulated both positively[117] and negatively[118] in the presence of phosphorylated eIF2α and appears to be part of a feedback loop controlling tRNA expression levels[119] .

1.4. The mTORC1 pathway, tryptophan depletion and T cell fate

Activation of naïve T cells places significant nutritional requirements on them in order to proliferate and differentiate into their effector roles; a wide variety of nutrient transporters including amino acid transporters such as CD98[120] are upregulated in response to Akt signalling in an mTORC1 dependent manner[121]. Amino acid deprivation during this critical period can result in radical changes in their developmental programme or even its complete abortion; limiting the availability of cysteine[55]and arginine[122] have been shown to be mechanisms employed by myeloid derived suppressor cells to achieve dampening of the immune response.

The mTOR kinase appears to be intricately involved with the process of cell fate determination. mTORC1 inhibition modulates the immune response of activated naïve $CD4^+$ T cells, inhibiting their differentiation to Th1, Th2 and Th17 subtypes[123,124], while promoting FoxP3 expression and Treg cell fate[125]. In $CD8^+$ T cells on the other hand, proliferation is relatively spared; instead mTORC1 inhibition following activation promotes a shift towards a memory instead of effector cell phenotype by reversing the balance between Tbet and Eomesodermin transcription factor expression[126,127] . The mTORC2 pathway was also recently shown to be essential for $CD4^+$ naïve T cell differentiation into Th1 and Th2 cell fates, through distinct signalling pathways - Akt and PKCθ respectively[124].

T cells being activated in a low tryptophan environment as the result of IDO activity are likely to have their mTORC1 pathway influenced both directly through the Rag-GTPase /Ragulator pathway and indirectly by feedback from the GCN2 pathway. This would provide a way for IDO expressing cells to directly influence the differentiation fate of naïve T cells and would be particularly important for tumour cells that might not be able to express the same array of cytokines or co-stimulatory molecules that professional antigen presenting cells would.

1.5. Aims

This project attempts to clarify the position of the mTORC1 pathway in the interplay between tumour cells and the immune system during the process of immunoediting. In particular it focuses on tryptophan deprivation via IDO expression as an immune escape mechanism and attempts to derive information, in particular temporal and quantitative dose-response curves that may prove useful in designing cancer immunotherapeutic strategies.

The underlying hypothesis that is being addressed in this project is that active IDO expression exerts a direct effect on the mTORC1 and GCN2 pathways through tryptophan depletion in both tumour cells and T lymphocytes thus directing cell growth patterns and phenotype determination.

The first results chapter (chapter 2) describes experiments designed to investigate the effects of tryptophan depletion on the mTORC1 pathway of the tumour cell itself; the second and third chapter (chapters 3 and 4) address the question of mTORC1 inhibition and resulting changes in T cell fate by tryptophan depletion due to IDO activity in murine and human T cell models respectively.

The specific aims addressed in chapter 2 relate to investigating the interplay of IDO expression and tumour cell themselves:

- Validation of murine and human tumour cell line models that can be used for elucidating the effect of IDO expression on the mTORC1 pathway
- Investigating the effect of active IDO expression on the mTORC1 and GCN2 pathways in tumour cell lines and the role that tryptophan depletion plays in this process
- Comparing the effects of IDO expression in cis or trans by tumour cells versus environmental tryptophan depletion.
- Establishing an experimental method to quantify mTORC1 pathway activity in individual cells in culture.

- Determining dose response curves for extracellular tryptophan concentration versus mTOC1 pathway activity for active IDO expressing and non-expressing cell lines.

The specific aims addressed in chapters 3 and 4 relate to the effects of IDO activity via tryptophan depletion in the local microenvironment in murine and human T cells respectively:

- Establishing and validating protocols for the detection and quantification of mTORC1 pathway activity and for testing the effect of low extracellular tryptophan levels in activated murine and human T cells.
- Determining the timecourse of mTORC1 pathway activation in human and murine $CD4^+$ and $CD8^+$ T cells in the presence and absence of tryptophan in the extracellular environment.
- Ascertaining the phenotypic effects of activating human and murine $CD4^+$ and $CD8^+$ T cells under tryptophan limiting conditions
- Investigating the interplay between the strength of TCR signalling and downstream mTORC1 activity when tryptophan availability is limiting
- Ascertaining whether media preconditioned by IDO expressing cells have comparable effects on activated T cells to tryptophan depleted media.

Chapters 2-4: Results

Chapter 2. IDO and inhibition of the mTOR pathway in tumour cell lines.

2.0. Introduction

The main hypothesis running through this research project is that one of the main mechanisms through which IDO exerts its immunomodulatory effects is inhibition of the mTORC1 pathway by triggering a starvation signal through consumption of tryptophan in the extracellular media.

However the mechanisms through which nutrient starvation inhibits mTORC1 activity are universal and conserved across eukaryotic cells. Therefore one would expect that IDO expression either by the tumour cells themselves or induced in cells populating the tumour microenvironment should also affect the malignant cell themselves.

The experiments described in this first chapter aim to elucidate how a microenvironment that is tryptophan depleted and kynurenine rich as a result of IDO activity would affect the tumour cells themselves, particularly focusing on mTORC1 pathway activity and attempt to glean at how the cancer cells would address this issue.

2.1. The mTORC1 pathway is active and suppressible by rapamycin and tryptophan deprivation in the EG7 cell line

Initial experiments were carried out using the EG7 thymoma cell line to determine its baseline mTORC1 activity levels and sensitivity to inhibition by rapamycin. Viability and growth rates were not affected over 6 hours at concentrations up to 250nM. A rapamycin concentration of 10nM appeared to be sufficient to exert an inhibitory effect on S6 phosphorylation at Ser240 (Figure 2.1a.) therefore 20nM was chosen as the standard concentration to use as a positive control for mTORC1 pathway inhibition in subsequent experiments.

To investigate the effect of tryptophan deprivation in the presence and absence of constitutive IDO activity the murine thymoma EG7 cell line- wild-type or stably transfected with GFP and IDO ("EG7-C7") - was used. EG7 transfected with GFP alone ("EG7-GFP") was used in some experiments as an additional control.

Standard R10 culture media based on RPMI1640 contain at least 25µM tryptophan; to allow control of the amount of tryptophan available to growing cells custom made tryptophan-free RPMI1640 was used to prepare "T10" tryptophan depleted media. This type of culture media is not completely tryptophan-free as it still contains 10% Fetal Calf Serum ("FCS") that is needed for the EG7 cell lines to grow properly.

FCS does contain tryptophan – as part of the proteins contained within it but also more importantly as free amino-acid in amounts that are highly variable between batches, so that even otherwise tryptophan-free media containing 10% FCS can end up with tryptophan concentrations in excess of 2µM.

Despite this, prolonged (>24hours) culture in tryptophan depleted 10% FCS containing media caused mTORC1 axis inhibition as seen by reduced S6 Ser240 phosphorylation in all three EG7 cell lines studied that was equivalent to the effect of 20nM Rapamycin by 36h (Figure 2.1b.,bottom panel). Moreover, in IDO expressing cell line this was happening earlier (Figure 2.1b., top panel), consistent with the effect of IDO expression resulting in earlier exhaustion of tryptophan in the media.

It is worth mentioning that culture of EG7 cells in tryptophan depleted media for 36 hours did result in reduced growth rates that were similar to those seen in the presence of mTORC1 inhibition by 20nM rapamycin using normal R10 media (Figure 2.1c.). The effect was most marked in the IDO expressing EG7-C7 cells, likely because any residual present in the tryptophan depleted media would be rapidly catabolised by IDO leading to complete tryptophan starvation.

Figure 2.1. The mTOR pathway is active and suppressible by rapamycin and tryptophan deprivation in the EG7 wild-type cell line

EG7 wild-type cells were plated in 6 well plates in R10 media at a concentration of $2*10^5$ cells/ml; rapamycin was immediately added to reach pre-specified concentrations in different wells. After 6 hours the cells were harvested, lysed and assayed by western blotting for total and phospho(Ser240)S6.

2.1a. The mTORC1 pathway is active and suppressible by rapamycin in the EG7 wild-type cell line

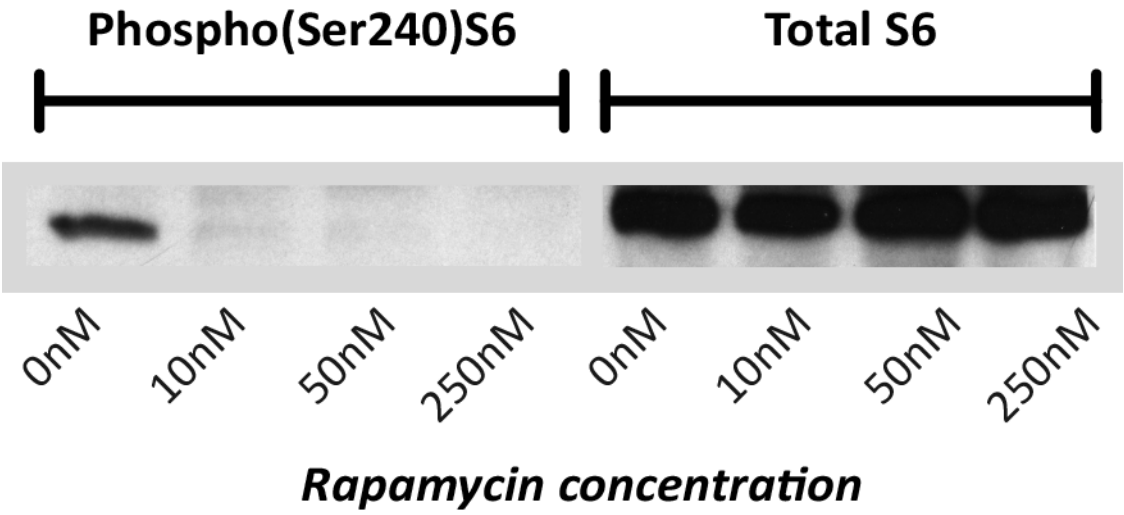

2.1a. Rapamycin inhibits S6 phosphorylation in the EG7 wild-type cell line.

10nM rapamycin in culture media is sufficient to almost completely abolish phosphorylation of S6 at Ser240 as seen by the absence of phospho(Ser240)S6 bands in the relevant lanes; total S6 expression was not significantly changed.

EG7-GFP and EG7-C7 cells were plated in 6 well plates in R10 or tryptophan depleted T10 media at a concentration of $2*10^5$ cells/ml; rapamycin was immediately added to control groups at a final concentration of 20nM. At appropriate timepoints cells were harvested, lysed and assayed by western blotting for total and phospho(Ser240)S6.

2.1b. Tryptophan deprivation results in inhibition of mTORC1 activity in EG7 cells regardless of IDO activity

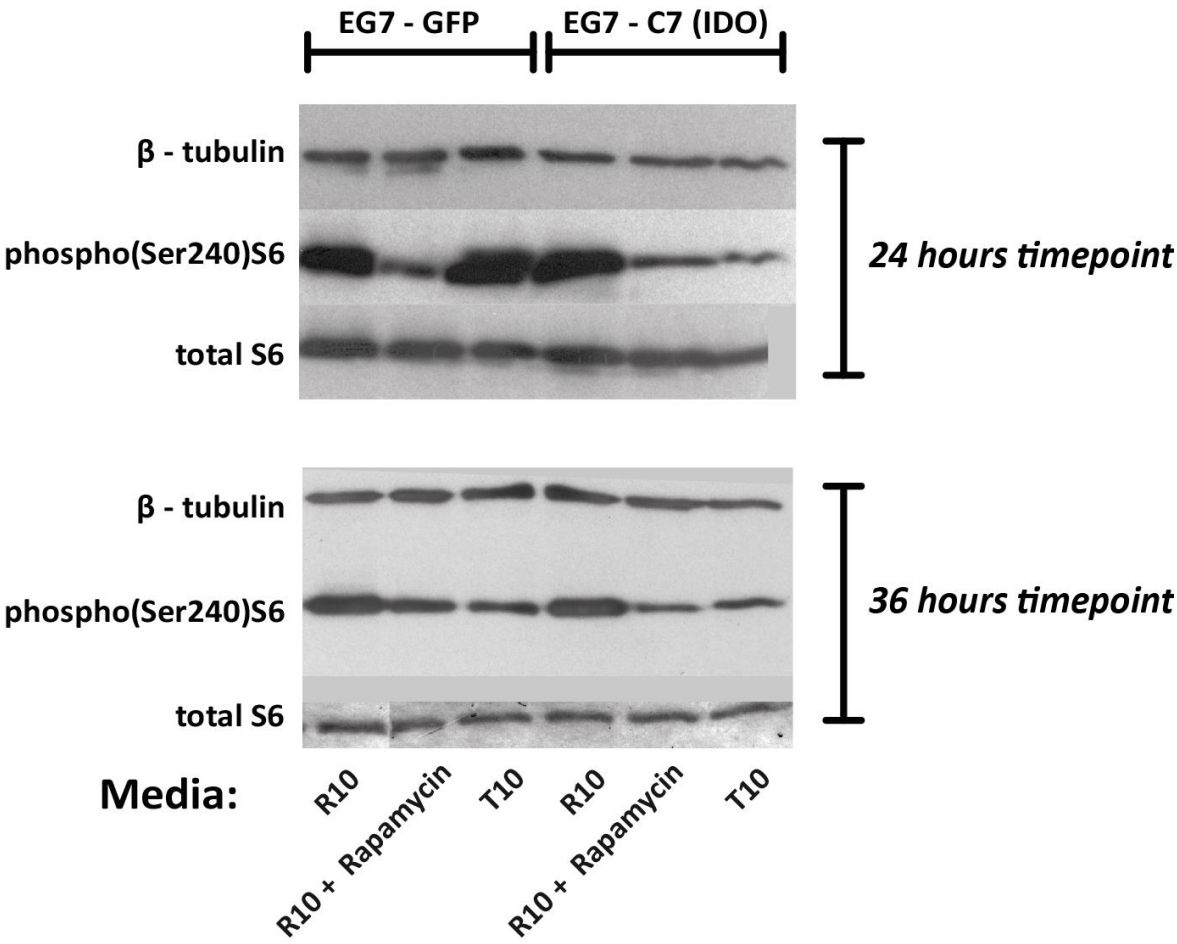

2.1b. Culture in tryptophan depleted media for more than 24hours results in inhibition of S6 phosphorylation at Ser240 in EG7 cells regardless of IDO activity.

Western blots of EG7-GFP (non-IDO expressing, left lanes) and EG7-C7 (IDO expressing, right lanes) cells revealing that at 36 hours ***(bottom panel)*** the mTORC1 inhibitory effect of culture in tryptophan depleted T10 media is similar to that of 20nM rapamycin as measured by phosphorylation of S6 at Ser240. This effect is visible at earlier timepoints ***(top panel)*** in the IDO expressing cell line.

2.1c. Tryptophan deprivation and mTORC1 inhibition both suppress cell growth to a similar extent in EG7 cells

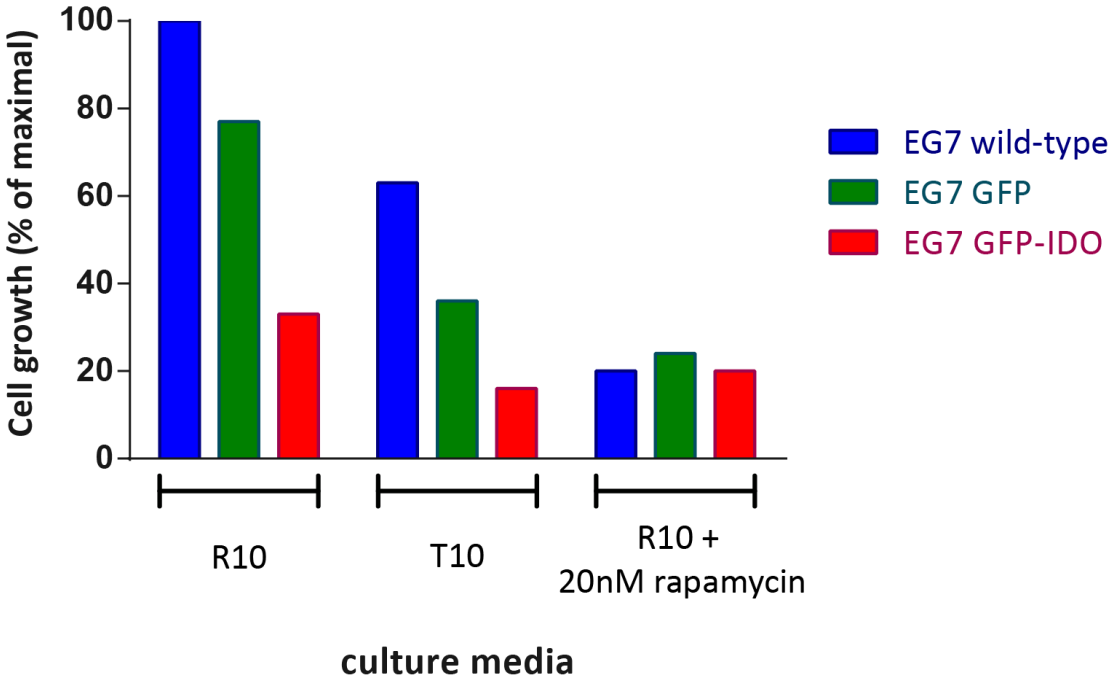

2.1c. Proliferation of EG7 wild-type, GFP and IDO-GFP transfected cells is inhibited by culture in tryptophan depleted media.

Graph demonstrating that culture in tryptophan depleted T10 media results in reduced proliferation in wild-type, GFP transfected and most noticeably GFP-IDO transfected cells. In the latter case the extent of inhibition is similar to that seen in all cell groups when 20nM rapamycin is added to the media at t=0.

2.2. IDO is expressed functionally in the HeLa-IDO transfected cell line

The EG7 cell line - as well as related transfected cell lines such as the GFP-IDO transfected EG7-C7 – are rapidly proliferating cell lines and very sensitive to nutrient depletion. Specifically they cannot reliably be used in experiments with FCS-free media for prolonged periods of time as a significant proportion of cells will undergo necrosis. What's more their rapid growth uses up additional nutrients in culture confounding the effect of tryptophan depletion.

For these reasons HeLa wild-type and transfected cell lines were used for subsequent experiments due to their slower growth rates and greater resistance to FCS/nutrient depletion compared to EG7 cell lines; it should be noted that for these lines human IDO was used. To help design further experiments, the rate of tryptophan catabolism was quantitated (Figure 2.2., right panel). HeLa-IDO transfected cell lines consumed tryptophan more than 3 times faster than wild-type cells.

When HeLa-IDO are plated at a density of $2*10^5$ cells/ml in R10, tryptophan is completely depleted from the supernatants within 45 hours at an approximate rate of 0.58µM/hour (Figure 2.2., left panel). The fact that this effect is due to IDO activity is evidenced by the concomitant production of kynurenine that can be detected in media from HeLa-IDO cultures but not from HeLa-wt.

Figure 2.2. IDO is expressed functionally in the HeLa-IDO transfected cell line

HeLa wild-type and IDO transfected lines were plated at $2*10^5$ cells/ml in R10 media. Supernatants were harvested at pre-specified timepoints and analysed by HPLC.

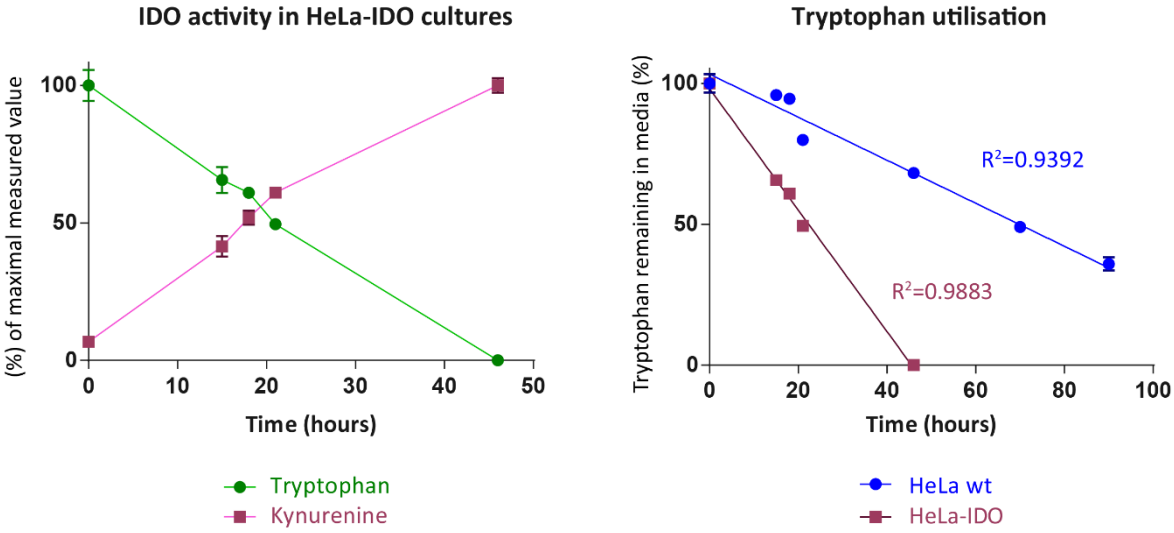

2.2. Functional IDO expression by transfected HeLa-IDO cells results in rapid tryptophan consumption and production of kynurenine in media.

(Right panel): Plot comparing and contrasting the rate of tryptophan consumption in HeLa wild-type and HeLa IDO cells; for both cell lines and within the timescales measured tryptophan consumption could be modelled by linear regression with a reasonably good fit. The rate was at least 3 times faster for the IDO transfected line compared with wild-type cells.

(Left panel): Graph demonstrating the timecourse of tryptophan and kynurenine concentrations in supernatants from HeLa-IDO cultures. Kynurenine was not detected in HeLa wild-type supernatants above baseline values at any timepoints.

2.3. Tryptophan acts together with FCS to modulate the mTORC1 pathway in HeLa cells.

HeLa wild-type cells respond to tryptophan withdrawal by inhibiting S6 phosphorylation within 3 hours (Figure 2.3a.). The effect is not as dramatic as that seen in the EG7 cell line as the detectable baseline levels of phospho-S6 appear to be lower but is comparable to starvation with EBSS (Earle's balanced salt solution, osmotically balanced culture media containing no organic nutrients) and to exposure to 20nM rapamycin.

Activation of the mTORC1 pathway in HeLa cells is also heavily modulated by the presence of FCS in cultured media. Culturing in FCS and tryptophan-free media for 6 hours results in a significant reduction in S6 phosphorylation; this is only partially rescued by the addition of tryptophan or FCS at time 0 in concentrations of less than 4% (Figure 2.3b.).

Tryptophan and FCS appear to work together to stimulate the mTORC1 axis: When the levels of FCS used in tryptophan-free RPMI1640 is less than 4%, the addition of tryptophan further stimulates S6 phosphorylation (Figure2.3c.). Tryptophan effects reach a plateau at concentrations above 5µM (data not shown).

At FCS concentrations above 5% it becomes increasingly difficult to reliably detect the effect of additional small amounts (<5µM) of tryptophan in S6 phosphorylation by western blotting in short term (<6 hour) cultures. This is partially because of the higher baseline levels of S6 phosphorylation, but also because media with >5% FCS can contain >2µM tryptophan obfuscating the effect of exogenously added tryptophan.

Figure 2.3. Tryptophan acts together with FCS to modulate the mTORC1 pathway in HeLa cells.

HeLa and EG7 wild-type cells were cultured for 24hours in R10 media at plating densities of $2*10^5$ cells/ml. After 24 hours media was exchanged to fresh R10, EBSS or tryptophan depleted T10 - with additives (20nM rapamycin, 50µM tryptophan and or 2mM L-Glutamine where appropriate. Cells were harvested and lysed for western blotting 3 hours later.

2.3a. Tryptophan deprivation inhibits the mTORC1 pathway in HeLa and EG7 wild-type cells rapidly

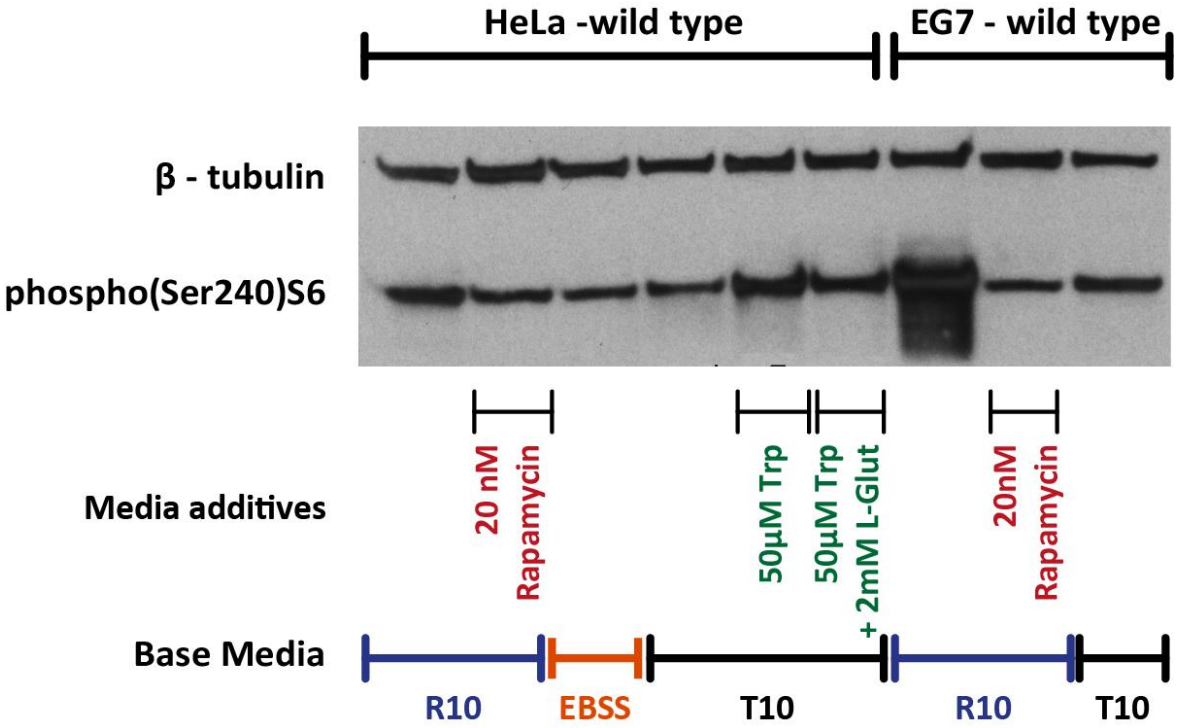

2.3a. S6 phosphorylation at Ser240 is inhibited in wild-type EG7 and HeLa cells under conditions of tryptophan deprivation.

Western blot of lysates after 3 hours of culture in new media demonstrating that in the absence of additional tryptophan cells cultured in tryptophan depleted T10 media exhibit markedly reduced levels of phosphorylation of S6 at Ser240 as compared with controls cultured in R10 tryptophan replete media or T10 media where additional tryptophan has been added.

HeLa wild-type cells were washed in EBSS and plated at $2*10^5$ cells/ml in R10, EBSS or tryptophan and FCS-free T0 media in the presence of different amounts of tryptophan and FCS; 6 hours later they were harvested, lysed and probed by western blotting for phosphorylation of S6 at Ser240.

2.3b. The mTORC1 pathway of HeLa cells is highly sensitive to media tryptophan and FCS concentrations

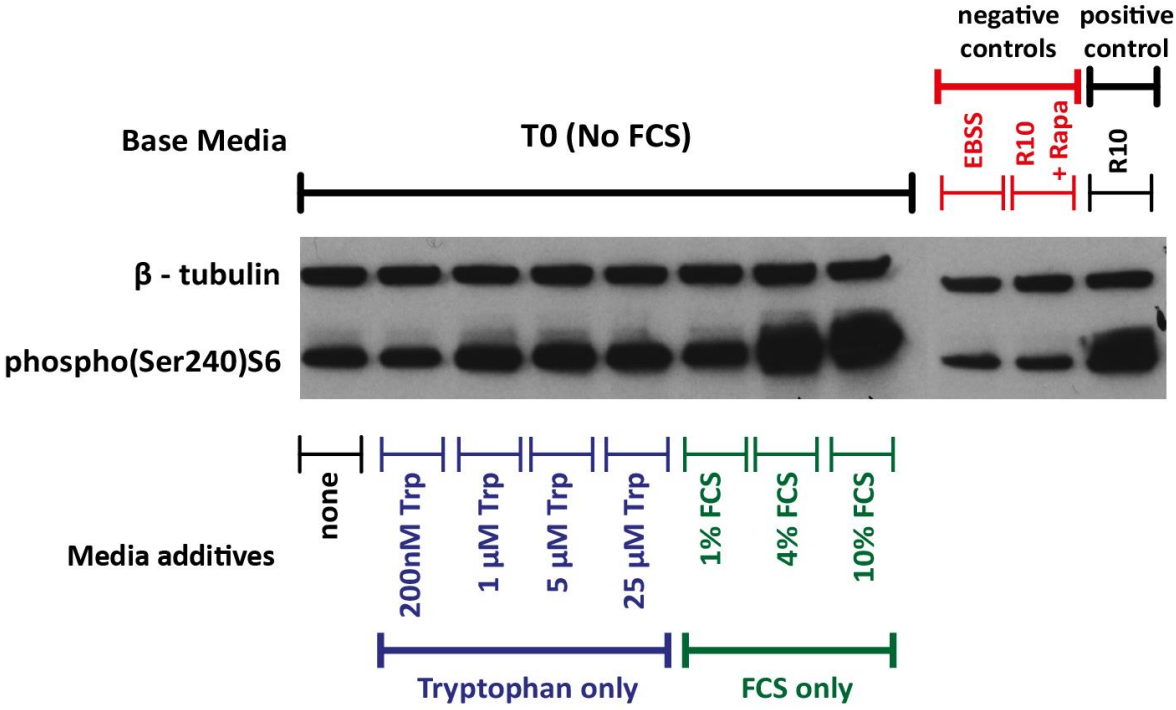

2.3b. Phosphorylation of S6 at Ser240 is highly sensitive to media FCS and tryptophan concentrations in HeLa cells.

Western blot of lysates after 6 hours of culture demonstrating dramatic inhibition of S6 phosphorylation at Ser240 when cells are cultured in T0 media that contain no FCS or tryptophan. The addition of >1µM tryptophan rescues mTORC1 activity to some extent, however only the addition of >4% FCS to media results in S6 phosphorylation levels approaching those seen in the positive controls.

HeLa wild-type cells were washed in EBSS, plated at $2*10^5$ cells/ml in tryptophan and FCS-free T0 media with the addition of varying amounts of FCS and tryptophan. They were harvested after 6h, lysed and probed by western blotting for phosphorylation of S6 at Ser240.

2.3c. Tryptophan acts together with FCS to stimulate the mTORC1 axis

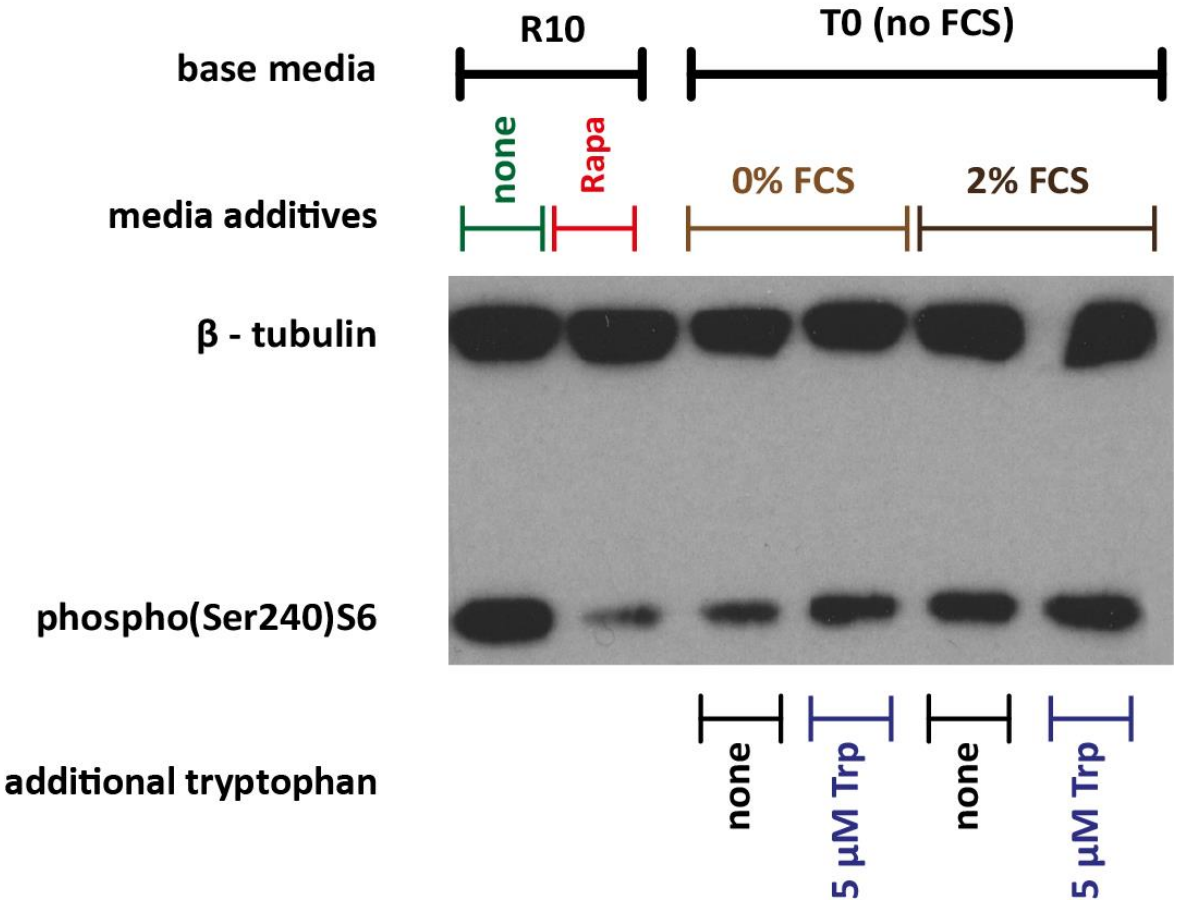

2.3c. Tryptophan acts together with FCS to stimulate S6 phosphorylation at Ser240.

Western blot of lysates after 6 hours of culture demonstrating that the addition of tryptophan increases levels of S6 phosphorylation at Ser240 both in the presence and absence of FCS and acts in concert with it to activate the mTORC1 pathway.

2.4. The GCN2 pathway in HeLa cells is activated by tryptophan depletion independently of the mTORC1 pathway; IDO expression lowers the threshold at which activation takes place.

As mentioned earlier, the mTORC1 and GCN2 pathways are the 2 best known pathways that respond to amino-acid depletion from the local microenvironment. To establish whether they are co-ordinately controlled in the same way in wild-type and IDO expressing cells, they were assayed using HeLa wild-type and IDO-transfected cell lines.

The cells were left to rest overnight in tryptophan replete R10 media and then briefly (for 3 hours) cultured in tryptophan and FCS-free T0 media to which pre-specified amounts of tryptophan was added in individual treatment groups. In the absence of additional tryptophan GCN2 activation and mTORC1 inhibition was seen in both cell lines (Figure2.4a.).

The threshold for GCN2 activation appeared to be higher in wild-type HeLa cells, as GCN2 activation was seen in treatment groups where extracellular tryptophan levels were low but not completely exhausted (50-100nM as measured by HPLC (Figure2.4b.).

In IDO expressing cells only groups with prolonged exposure to complete tryptophan deprivation activated their GCN2 pathway; interestingly phospho(Ser240)S6 levels appeared to be subjectively less reduced for the same amount of measured extracellular tryptophan in IDO expressing cells compared to wild-types and this effect was further investigated in subsequent experiments.

It is worth noting that inhibition of mTORC1 directly by rapamycin was insufficient to trigger GCN2 activation confirming that mTORC1 inhibition is not sufficient to activate the GCN2 pathway.

Figure 2.4. Raised threshold for activation of the GCN2 pathway in IDO expressing cells

HeLa wild-type and IDO cells were plated in R10 overnight. In the morning the plates were washed in PBS and media changed to tryptophan-free T0 media; in different wells varying amounts of tryptophan were added (0-50µM final concentrations). 3 hours later supernatants were collected and analysed by HPLC while the cells were lysed in situ and probed by western blot for phospho-S6, GCN2 and phospho-GCN2

2.4. GCN2 and mTORC1 pathways are coordinately activated by tryptophan depletion.

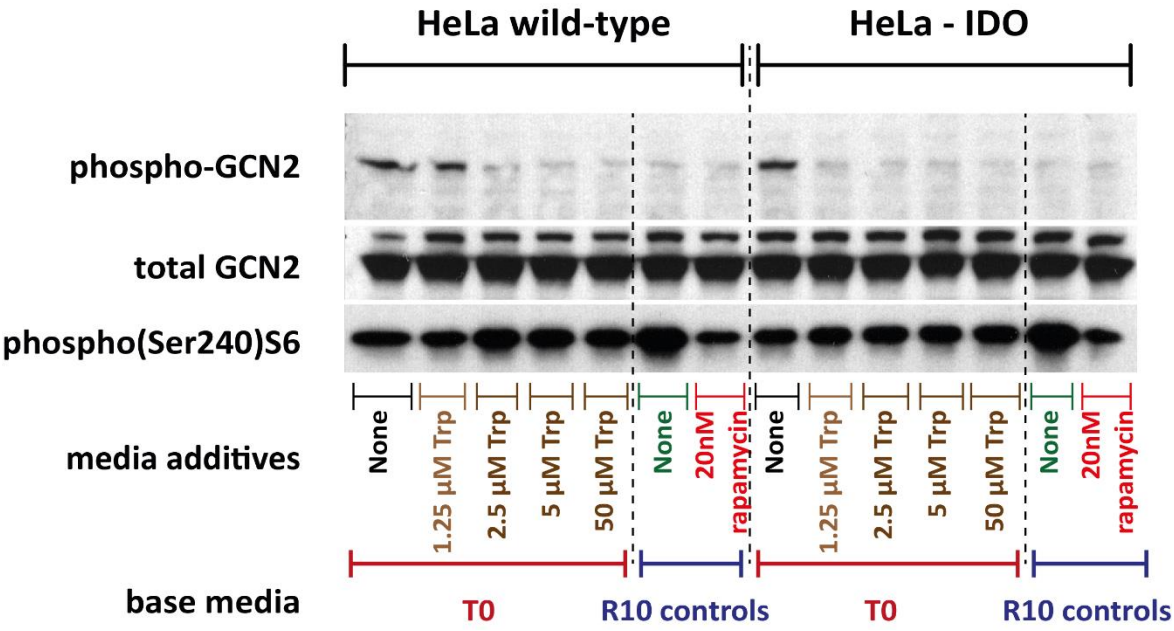

2.4a. Tryptophan depletion results in activation of the GCN2 pathway in HeLa wild-type and IDO-transfected cell lines. ***(top panel)*** Western blot of lysates after 3 hours of culture demonstrating that tryptophan depletion triggers phosphorylation of GCN2 and inhibits phosphorylation of S6 at different thresholds of extracellular tryptophan concentration as measured by HPLC ***(bottom panel)*** in wild-type and IDO expressing HeLa cells.

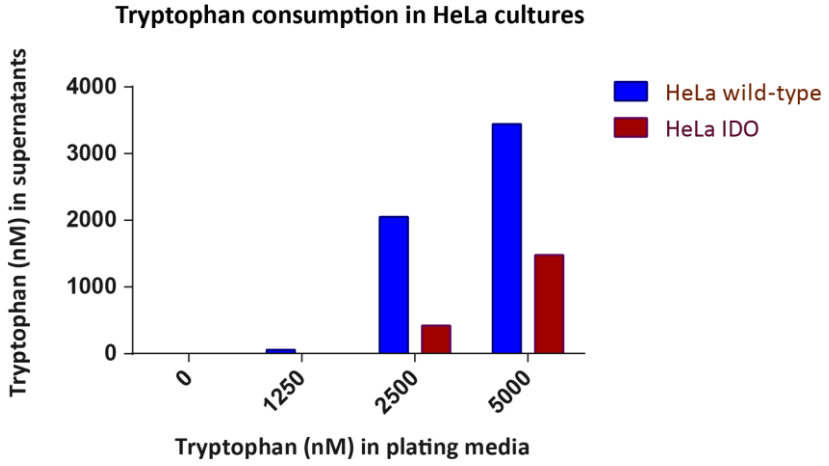

2.5. The presence of active IDO on its own is not sufficient to inhibit the mTOR pathway in HeLa cells in the presence of tryptophan.

While IDO can exert an effect on mTORC1 directly through tryptophan depletion, there is a possibility that the production of kynurenine – or further downstream metabolites- might also influence mTORC1 activity.

To further investigate this a series of experiments was conducted utilizing HeLa derived cell lines to see if the presence of active IDO on its own was sufficient to modulate the mTORC1 pathway in the presence of abundant tryptophan.

To this effect HeLa IDO transfected cells were used again. As an additional positive control interferon γ ("IFN-γ") treated HeLa wild-type cells were used; IFN-γ is known to induce IDO expression in several cell types in vitro and in-vivo[62] and IDO expression by these cells would occur in more physiological context.

The functional activity of IDO expressed as a result of IFN-γ applied to HeLa wild-type cells was confirmed by HPLC (Figure 2.5a.) as measured by the ability of IFN-γ treated HeLa wild-type cells to rapidly consume tryptophan and produce kynurenine in their culture media.

In the actual experiment, even when cultured in media long enough to produce physiologically significant[81] amounts of Kynurenine (>8μM in the HeLa- IDO groups and >15μM in the IFN-γ treated HeLa wild-type groups) phosphorylation of S6 at Ser240 did not appear significantly impaired in IDO expressing lines compared to untreated wild-type cells (Figure 2.5b.) in the presence of sufficient tryptophan in the media – in all treatment groups tryptophan levels in supernatants taken immediately prior to harvesting were >3μM.

Figure 2.5. The presence of active IDO on its own is not sufficient to inhibit the mTORC1 pathway in HeLa cells in the presence of tryptophan.

HeLa - IDO, HeLa -GFP and HeLa wild-type cells were plated at $2*10^5$ cells/ml in R10 in 6-well plates in the presence or absence of 20nM rapamycin or IFN-γ(50ng/ml). 20 hours later the media was changed in some wells to EBSS to stimulate complete nutrient starvation, while in other wells 50µM tryptophan was added. Supernatants were harvested 4 hours later and kynurenine and tryptophan concentrations were determined by HPLC, while cells were lysed in situ and probed for phosphorylated(Ser240) S6 by western blotting.

2.5a. IFN-γ induces active IDO expression in HeLa cells

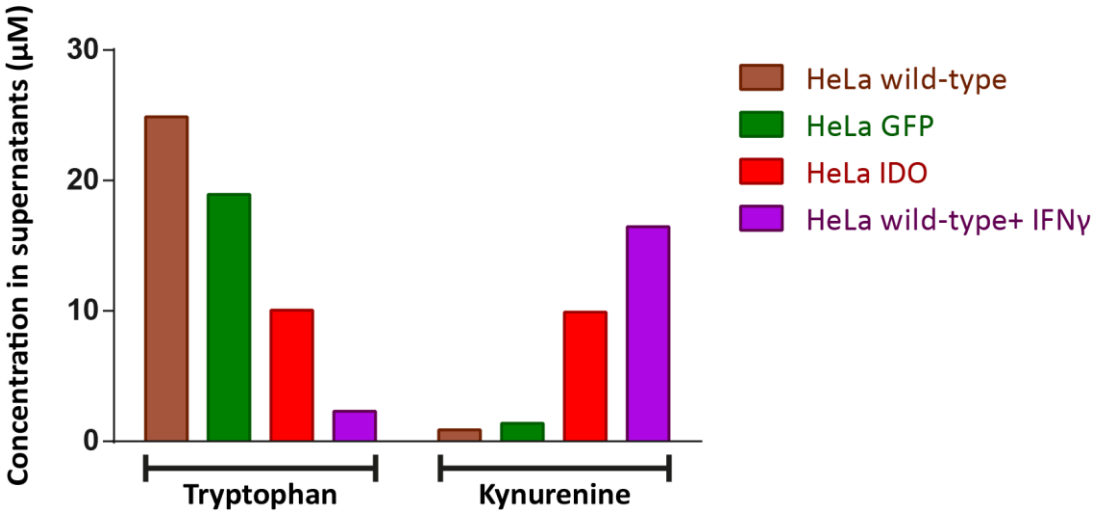

2.5a. IFN-γ induces active IDO expression in HeLa cells.

HPLC analysis results confirming induction of functional IDO as evidenced by tryptophan consumption and kynurenine production in IFN-γ treated wild-type HeLa cells.

2.5b. Kynurenine production per se does not inhibit the mTORC1 pathway

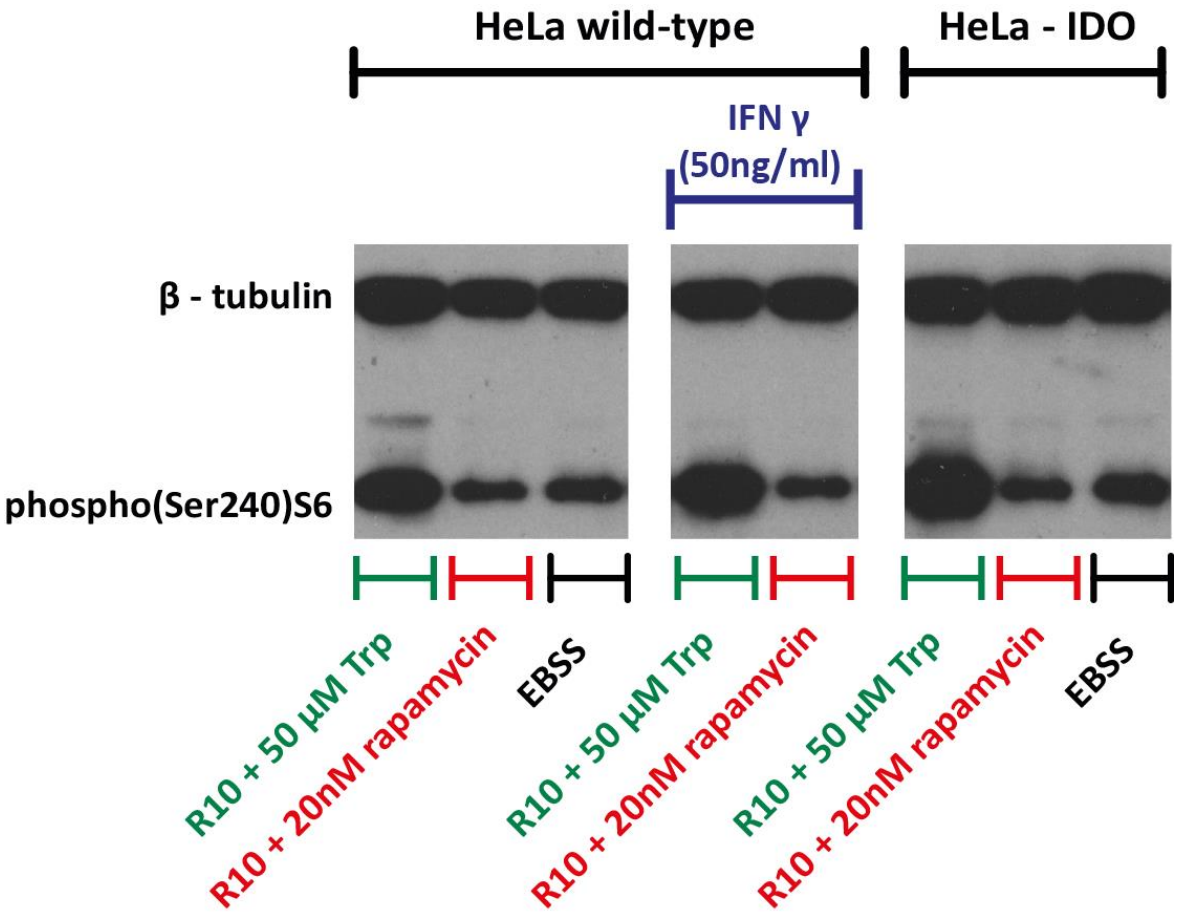

2.5b. Kynurenines per se do not inhibit phosphorylation of S6 at Ser240.

Western blots of cell lysates after 24 hours of culture – 4 hours after media change to EBSS in the relevant groups – revealing that mTORC1 activity as evidenced by phosphorylation of S6 at Ser240 is similar in wild-type cells and in IFN-γ treated or IDO transfected HeLa cells when cultured in tryptophan excess to prevent complete tryptophan depletion in the media.

2.6. At low tryptophan levels there is a direct dose response relationship between mTORC1 pathway activity and extracellular tryptophan concentration in both HeLa and EG7 cell lines.

Following on from these experiments, a way was sought to address whether mTORC1 inhibition by tryptophan deprivation is an all-or-nothing affair or whether a dose response relationship exists. As initial experiments showed, extracellular tryptophan concentrations as low as 3µM were sufficient to keep mTORC1 activity levels near normal.

Unfortunately experiments utilizing FCS containing media cannot properly address the effects of extracellular tryptophan concentrations in the sub 1-2µM range, as this is the amount commonly present in 10% FCS that is bound to albumin and cannot be accurately measured by HPLC.

To address this issue, HeLa and EG7 cell lines were incubated in FCS-free media with predetermined tryptophan concentrations for 2-3 hours to reduce the effects of prolonged growth factor withdrawal. There was a relatively linear relationship between the extent of S6 phosphorylation and amount of extracellular tryptophan at concentrations below 1µM in both EG7 and HeLa wild-type cell lines (Figures 2.6a.&b.)

The effect was more difficult to quantify in the HeLa IDO cell line using a single time point approach with starting tryptophan concentrations below 1µM as tryptophan was rapidly catabolised completely, resulting in maximal inhibition of S6 phosphorylation. A time-based approach was used, harvesting cells and supernatants at frequent time-points arriving at similar results (Figure 2.6b.) , though interestingly the IDO expressing cells appeared to show a steeper dose response curve – that is to say they were able to maintain higher mTORC1 activity levels for the same extracellular tryptophan concentrations.

Figure 2.6. Dose response relationship between mTORC1 activity and extracellular tryptophan levels

EG7 wild-type cells were plated in 6 well plates in tryptophan and FCS-free T0 media at a concentration of $2*10^5$ cells/ml. Individual treatment groups were supplemented with tryptophan at a range of final concentrations. After 2 hours supernatants were collected and analysed by HPLC to determine tryptophan levels, while cells were lysed and probed for phospho(Ser240)S6 by western blotting. The resulting blots were digitised and quantified using ImageJ software. Results were normalised to the amount of β-tubulin detected for each sample on the same blotting membrane.

2.6a. EG7 wild-type cells exhibit a linear dose response relationship between mTORC1 activity and extracellular tryptophan concentration at sub 1µM tryptophan levels

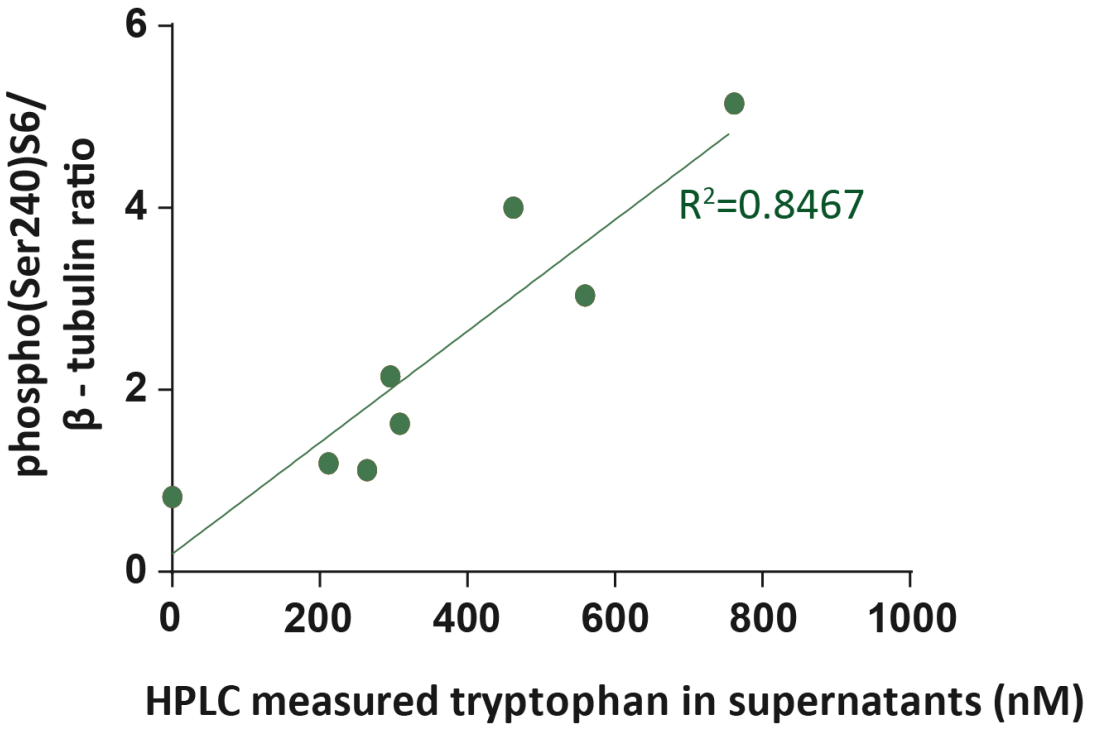

2.6a. Dose-response curve of S6 phosphorylation at Ser240 in response to extracellular tryptophan concentrations in EG7 wild-type cells.

Plot of normalised values of phospho (Ser240)S6 versus measured final tryptophan concentrations in media revealing a near linear dose-effect relationship at tryptophan levels < 1µM.

HeLa wild-type and IDO transfected cells were plated in R10 media, incubated for 12 hours to ensure adherence and then washed twice with PBS briefly prior to the addition of FCS and tryptophan-free T0 media. For HeLa wild-type treatment samples different amounts of added tryptophan (0-2000nM) were added and 4 hours later supernatants were collected and analysed by HPLC while cells were harvested and their lysates probed by western blotting for phosphorylated (Ser240) S6 and β-tubulin. 4μM tryptophan was added to all HeLa-IDO groups; they were then harvested at 30 minute intervals for 3.5 hours, by which point extracellular tryptophan was depleted.

2.6b. HeLa wild-type and IDO transfected cells also exhibit a linear dose response relationship between mTORC1 activity and extracellular tryptophan concentration at sub 1uM tryptophan levels

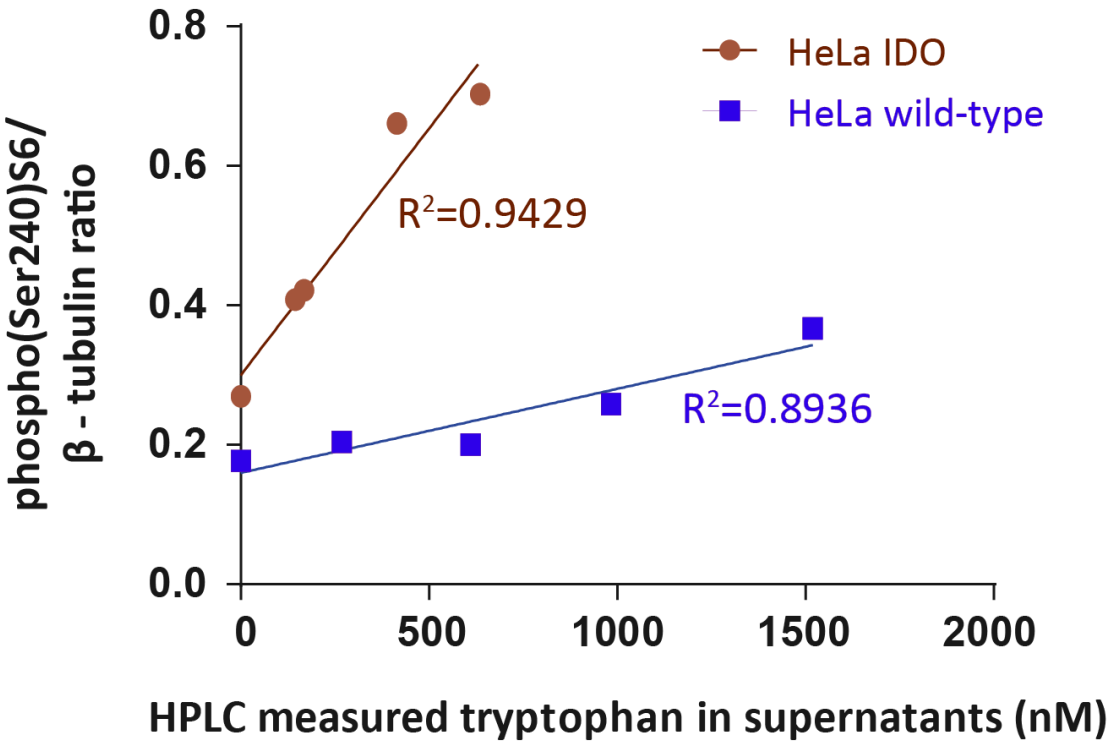

2.6b. Dose-response curve of S6 phosphorylation in response to extracellular tryptophan concentrations in HeLa wild-type cells. Normalised phospho(Ser240)S6 values were obtained for each sample and plotted against measured tryptophan concentrations in the supernatants of the same samples. In both wild-type and IDO transfected cells the dose response curve could be approximated reasonbly well by a linear relationship with a reasonably good fit (R^2=0.9429 and 0.8936 for IDO transfected and wild-type cells respectively. Of note the slope of the curves thus obtained were significantly different (P=0.00057).

2.7. Complex mTORC1- tryptophan dose response curves in EG7 cell lines at low tryptophan concentrations.

As comparison of quantitative results from western blots across different gels is fraught with difficulty, a method was developed to detect phosphorylation of S6 by flow cytometric analysis of intracellular staining (Figure 2.7.) .This technique offers several advantages: quantitation is robust and effects can be seen both at the individual cell and at the population level. Moreover there in no hard limit on the number of samples that could be tested in a single experiment

Using this method the dose response relationship between extracellular tryptophan levels and mTORC1 activity as expressed by phosphorylation levels of S6 at Ser240 was clarified (Figure 2.8.). Moreover the increased sensitivity offered by flow cytometry highlighted two phenomena that were hinted at by previous experiments using western blots as readouts:

Firstly there appeared to be a “dip” in the dose response curve in all EG7 cell lines at tryptophan concentrations around 1μM – the same level where the GCN2 pathway is switched off, and this is apparent both in the proportion of cells expressing high levels of phospho(ser240)S6 cells and the median fluorescent intensity (“FI”) of the population.

Secondly the EG7-IDO transfected cell line showed much higher levels of S6 phosphorylation at Ser240 compared with wild-type and GFP transduced cells at all tryptophan levels, including positive controls. However it was not clear whether was directly due to the presence of actively expressed IDO or due to genetic/epigenetic changes accumulated by IDO-expressing cell clones to allow their continuing survival and proliferation changes: cells that were originally derived from the IDO-transfected clone but had subsequently lost IDO expression as seen by the lack of GFP expression showed identical levels of mTORC1 activity to actively IDO expressing cells when placed together in the same culture and were thus exposed to the same type of effective chronic tryptophan deprivation.

Figure 2.7. Validation of a flow cytometry based phospho(Ser240)S6 staining protocol.

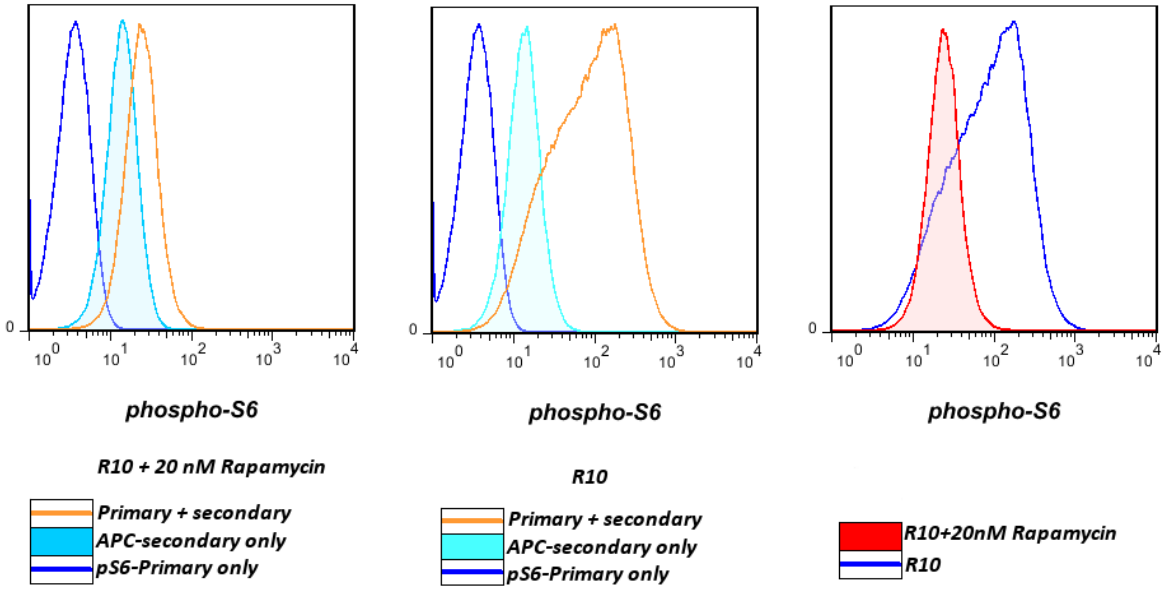

2.7. Validation of Flow Cytometry based phospho(Ser240)S6 staining protocol.

EG7-C7 cells were cultured for 1 hour in R10 +/- 20nM rapamycin and were then harvested , fixed and stained with rabbit anti-phospho(Ser240)S6 primary and APC conjugated $F(ab')_2$ anti-rabbit-IgG at 1:100 dilutions using the e-Biosciences fixation and permeabilisation buffers.

Figure 2.8. Complex pattern of mTORC1 dose response curve to low extracellular tryptophan concentrations.

EG7-GFP and EG7-IDO-GFP transfected cells were cultured in T0 media for 1 hour. Different amounts of tryptophan were added to individual treatment groups as well as in R10 +/- 20nM rapamycin as positive and negative controls respectively. Cells were harvested, fixed, permeabilised and stained for phospho(Ser240)S6 and analysed by flow cytometry.

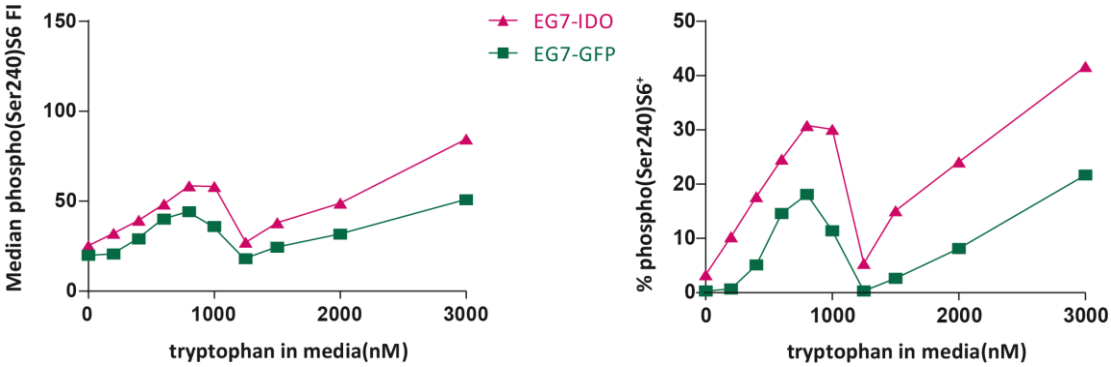

2.8. Dose-response curve of S6 phosphorylation in response to extracellular tryptophan concentrations.

Graphs of mTORC1 activity plotted against tryptophan concentration in plating media as measured by levels of phosphorylation of S6 at Ser240 in 2 different ways:
(Left panel): absolute levels of median FI of anti-phospho(Ser240)S6.
(Right panel): percentage of live cells staining high for phospho(Ser240)S6 .
The results seen were similar in both cases: there was a clear dose response curve with higher levels of tryptophan in the media associated with increased levels of mTORC1 activity. At sub 1µM tryptophan levels the dose response curve was linear as seen in the earlier experiments, however there was a dip at the 1-1.5 µM level. This was true in both the GFP and GFP-IDO groups. HeLa GFP cells exhibited consistently lower levels of mTORC1 activity at all tryptophan levels compared with IDO-GFP transfected cells ($p<0.0001$ by 2 way ANOVA).

2.8. Discussion

2.8.1. Nutrient starvation and cancer

Tumour cells need a continuous supply of nutrients to proliferate. While their propensity to accumulate genetic changes may be able to confer immunity to several –or all even – checkpoints that would normally shut down progression through the cell cycle in response to nutrient starvation, nevertheless the complete lack of essential nutrients will invariably result in a block to cell growth. Multiple essential homeostatic mechanisms will fail and eventually cell death will ensue unless the cell manages to enter a quiescent nutrient conserving state.

In vitro this is easy to observe; rapidly growing cell lines such as EG7 – derived from a murine thymoma - can only survive under conditions of complete nutrient starvation for very limited periods of time. EG7 cells transfected so that they express GFP and IDO constitutively grow significantly slower to controls transfected with GFP alone. What's more there seems to be a strong selection pressure against constitutive IDO expression in vitro so that it is difficult to maintain homogeneous highly active GFP-IDO expressing population in culture over several passages.

This was one of the reasons why a HeLa cell line transfected with IDO was used for many experiments in this chapter; HeLa cells - being slower growing - tolerate nutrient starvation better, and can be used for experiments spanning longer time-scales. In addition IDO-GFP expression in transfected cell lines is much more stable and experiments utilising it are easier to reproduce.

This "autocrine" effect of IDO expressing cells might appear counterintuitive at first sight. It has to be remembered however, that in vivo there is a constant supply of nutrients to the tumour microenvironment via the circulation. While this often is much constrained compared with healthy tissue it still allows for a continuous supply of tryptophan – and other nutrients – so that IDO activity would result in a dramatic reduction of extracellular tryptophan levels but not complete depletion.

Tumour cells therefore have a window of opportunity to get a competitive advantage compared to somatic cells – and in particular cells of the immune system - if they can carry on functioning and proliferating under tryptophan depleted conditions. Bypassing cell cycle controls is a common mechanism employed by multiple types of tumours, however it is the ability to continue growing in the face of tryptophan scarcity that is critical in this setting.

2.8.2. Hypothesis: IDO expression exerts a direct effect on tumour cell growth through the TORC1 and GCN2 pathways.

The mTORC1 pathway is at the centre of a network integrating growth and nutrient availability signals that feeds down to multiple pathways regulating growth, proliferation and survival. It is known to be inhibited under conditions of nutrient starvation, therefore it is a likely target for the effects of tryptophan depletion caused by IDO activity.

In addition, under conditions of extreme amino acid starvation the GCN2 pathway is also known to be activated; there are multiple feedback and feed-forward loops linking the two pathways.

In view of these facts, these two pathways were set as the initial targets of this research project ; the hypothesis that was set out to be explored in the first chapter was that IDO expression can effectively result in tryptophan depletion in the tumour microenvironment with knock-on effects on mTORC1 and GCN2 activity. A secondary hypothesis was that IDO expressing cells would potentially respond in a different way to tryptophan expression than non-IDO expressing cells.

2.8.3. Choice of experimental systems and methods.

To simulate IDO activity in the microenvironment two separate experimental methods can be used. In an indirect approach media containing reduced but defined tryptophan content can be used to stimulate the catabolic effect of IDO. On the other

hand a direct approach involves using tumour cell lines either genetically engineered to express IDO constitutively or induced by the action of IFN-γ.

The indirect approach allows a more physiological approximation of the processes that take place in the tumour microenvironment and takes into account the possible effects of kynurenine metabolites. Its main drawback is that it is practically very difficult to establish reproducible experimental conditions that focus on the effects close to the point of complete tryptophan starvation starting from standard media:

The speed of tryptophan utilisation depends on cell densities and in transgenic lines also on the level of IDO expression- both of which show a certain amount of variability. While this is not large, when added to the inherent uncertainty of the starting tryptophan concentration in FCS containing media, it makes estimating the timepoint where tryptophan is close to be used up (sub 1µM levels) very difficult, particularly across experiments.

In the end a combination approach had to be used depending on the actual cell lines and readouts for each experiment. Tryptophan depleted media based on tryptophan-free RPMI 1640 were heavily utilised as they shortened the timescales needed for complete tryptophan catabolism from the media and thus minimised the risk of additional nutrient depletion confounding the results.

In order to derive useful results in the 0-1µM tryptophan concentration zone experiments were carried out either using fixed timepoints with variable starting tryptophan concentrations or fixed starting concentrations and variable timepoints, both arriving at similar results.

HPLC was an extremely valuable tool that allowed the determination of final tryptophan concentrations in culture supernatants allowing direct links to be drawn between measured levels of mTORC1 activity and cotemporaneous extracellular tryptophan concentrations. In addition it was the only technique that could unequivocally confirm IDO activity via the detection of kynurenine as it is known that IDO expression on its own under certain circumstances does not guarantee its metabolic activity.

In terms of the techniques used to measure mTORC1 and GCN2 activity, initially western blotting was used as it was well established in the literature and at the time considered to be the gold standard. Unfortunately this method placed significant limitations in terms of experimental design: there was a relatively low ceiling on the number of samples that could be assessed per experiment particularly if quantification was important – results can only be reliably quantified within each gel. An additional issue was that during sample preparation there was no way of reliably exclude dead or dying cells potentially confounding the results if they made up a significant proportion of the sample in question.

In view of this, as soon as a flow cytometry based approach to measure mTORC1 activity became available this was tested and adapted for use in further experiments. This was particularly important for the experiments described in the following chapters involving mixed populations of murine splenocytes and human peripheral blood lymphocytes that otherwise could not be usefully assessed by western blotting.

Unfortunately there was no commercially available phospho-GCN2 antibody that was suitable for flow cytometric analysis; even the supply of the original antibody was limited so it could only be used in a small number of experiments.

2.8.4. Significance of experimental findings.

The initial pilot experiments described in the first chapter confirmed both that the mTORC1 pathway was active and suppressible by rapamycin in EG7 and HeLa derived cell lines and that prolonged culture in tryptophan depleted media – made using tryptophan-free RPMI and 10% FCS – caused its inhibition.

Significantly mTORC1 inhibition was seen much earlier in groups containing IDO expressing cells; HPLC analysis of supernatants confirmed that in these groups tryptophan was being used up much more rapidly. Moreover the growth rates of IDO expressing groups in tryptophan depleted media were similar to controls exposed to 20nM rapamycin that was sufficient to fully suppress mTORC1 activity.

In order to establish the levels of tryptophan that were necessary to maintain mTORC1 activity a series of experiments was carried out titrating the amount of tryptophan and FCS available in media. The results confirmed that at least 1µM of tryptophan was necessary to achieve levels of mTORC1 activity that were visibly higher than baseline. In addition the effect of additional tryptophan was not dependent and additive to the effect of FCS.

What was more interesting was the direct comparison of GCN2 and mTORC1 pathway activity in HeLa wild-type cells compared to an IDO transfected line. In both cases the GCN2 pathway was activated and the mTORC1 pathway was inhibited in the absence of tryptophan; however HeLa IDO cells seemed to be able to maintain levels of mTORC1 activity and suppress GCN2 activation at low tryptophan levels (sub 1µM) whereas these levels were insufficient in wild-type cells.

This effect was further examined by quantitation of the dose-response curve of mTORC1 activity at low tryptophan levels initially by image analysis of western blots and eventually by flow cytometry. This revealed essentially a linear relationship between extracellular tryptophan concentration and mTORC1 activity at sub 1µM levels for both IDO expressing and wild-type cells both in HeLa and EG7 cell lines. Importantly however the mTORC1 pathway in IDO expressing cell lines appeared less sensitive so its activity could be maintained at lower tryptophan concentrations.

This result would be consistent with a mechanism being activated in IDO expressing cells that allows them to compensate for the scarcity of extracellular tryptophan. While it is definitely conceivable that this could be by virtue of "resetting" the metabolic rheostat, a more intriguing possibility is offered by recent experimental results by Silk et al[128] : these suggest that a high affinity tryptophan transporter is expressed by IDO expressing allowing them to more efficiently scavenge tryptophan from the environment.

Whatever the actual mechanism involved, the implication is that tryptophan depletion caused by IDO does affect the tumour cells themselves by virtue of its effects on mTORC1 and GCN2. Cancer cells finding themselves in a microenvironment stripped of tryptophan by virtue of IDO action would therefore need to develop mechanisms

to counteract that to continue growing – these mechanisms would be valid targets for pharmacological modification.

2.8.5. Outstanding issues

The aforementioned results were derived experiments on a murine thymoma and a human cervical cancer cell line. While there is no reason to assume the molecular mechanisms involved are not applicable more universally, given more time and resources additional experiments with different cell lines and if possible fresh tumour tissue would strengthen these findings.

Kynurenine was shown to not significantly affect mTORC1 activity and cell growth at levels much higher than those likely to arise in vivo; however it is conceivable that it may contribute to altering the sensitivity of the mTORC1 pathway to extracellular levels and this will have to be addressed in future experiments.

Additional experiments focusing on the GCN2 aspect would have been needed to clarify its complex interplay with the mTORC1 pathway. Unfortunately the lack of usable reagents - the phospho-GCN2 antibody was unavailable for a prolonged period of time by the only company supplying it and in any case was not suitable for flow cytometry – limited the information that could be gleaned.

Specifically it might have been possible to explain the apparent “dip” in the mTORC1 – tryptophan dose response curve that can be seen in both IDO expressing and non-expressing cell lines at extracellular tryptophan concentrations between 1-2µM as this is the level where GCN2 activity is switched off and thus potentially inactivate a positive feedback loop.

Finally it would be interesting to see if blocking the putative tryptophan transporter described in Silk et al[128] restores the mTORC1 dose response curve of IDO cells to that of wild-type cells as that would further substantiate its possibility of being a target for drug development.

Chapter 3. The effects of tryptophan depletion on the m-TOR pathway in murine T cells

3.0. Introduction

An increasing body of evidence is pointing towards the mTORC1 pathway being a central pivot around which critical decisions are made regarding T cell fate following stimulation by cognate peptide[129]. As experimental results from the previous chapter demonstrated, IDO activity – either by tumour cells themselves or alternatively by other cells induced to express IDO – can result in a microenvironment deficient in tryptophan. This has direct implications for all cells present or recruited to that environment and in particular for any T lymphocytes that take part in the immunomonitoring process.

Experiments described in this chapter will attempt to address the effects of tryptophan depletion on T cells stimulated by cognate peptide primarily utilising two transgenic mouse models- OT-I[130] and DO11.10[131] mice. These are genetically engineered to constitutively express a transgenic TCR resulting in a majority of their T cells being able to be stimulated reproducibly by cognate peptide in repeat experiments without the need for prior ex-vivo expansion. Moreover this allows experiments to look at the effects on naïve T cells stimulated for the first time by cognate peptide that otherwise would not be practically feasible.

The initial thrust of the experiments was directed at looking into how the mTORC1 pathway is modulated by tryptophan depletion at early stages (<24 hours) after cognate peptide induced stimulation of $CD4^+$ and $CD8^+$ T cells and whether an immediate phenotypic effect was observable. Subsequent experiments looked at later downstream effects of tryptophan depletion in cell fate pathways that have been shown to be modulated by mTORC1 activity in T cells such as Tbet and FoxP3 expression [129]. Finally the effect of tryptophan depletion on cytokine production by activated $CD8^+$ T cells was explored; had more time been available similar assays would have been done for $CD4^+$ T cells, in particular to identify a shift to a suppressive cytokine profile suggestive of the induction of true regulatory $CD4^+$ T cells.

3.1. Establishment of an efficient staining protocol for the detection of mTORC1 pathway activation in murine T cells using flow cytometry

The 0.5% PFA/90% Methanol Flow cytometry fixing/staining protocols previously described in literature[127] was compared with a modified version of the eBioscience™ one using proprietary buffers (Figure 3.1a.) The latter offered superior cell recovery and fluorochrome persistence albeit with a reduced signal to noise ratio and was chosen as it allowed use of a wider range of surface staining reagents and allowed optimal use of animal tissue .

To mimic the events taking place during T cell activation in vivo, the OT-1 transgenic mouse model system was used. These mice express constitutively a transgenic TCR receptor binding a heptapeptide, SIINFEKL, when presented by the H2k Class I MHC. Initial experiments showed that >95% of all $CD8^+$ T cells in OT-I mice (Figure 3.1b., left panel) express this receptor and therefore can be activated when appropriately exposed to the cognate peptide.

It became apparent that fluorochrome-conjugated SIINFEKL-H2k tetramers could not be used as staining reagents as they caused rapid (<20min) activation of the mTORC1 axis during the staining process (Figure 3.1b., right panel).

Nevertheless, the high expression of the transgenic TCR in OT-I $CD8^+$ T cells allows for practical purposes the use anti-CD8b surface staining to delineate the population of $CD8^+$ OT-I splenocytes potentially sensitive to activation by adequately presented SIINFEKL peptide.

Similarly, in order to investigate the effects of tryptophan depletion on $CD4^+$ T cells, the DO11.10 mouse strain was used that express a transgenic TCR that is specific for the chicken ovalbumin $OVA_{323-339}$ peptide in >97% of its peripheral T cells. (Figure 3.1c.)

For further experiments the general gating strategy outlined in (Figure 3.1d.) was used to identify the splenocyte subpopulations for subsequent flow cytometric analysis.

Figure 3.1: Establishing a flow cytometry protocol for assessing phosphorylation of S6 in murine splenocytes

OT-I Splenocytes were plated in R10 media in 96 well plates alone, with 500ng/ml PMA/Ionomycin or in wells pre-coated with 10µg/ml anti-CD3 and 5µg/ml anti-CD28. ("anti-CD3/CD28")- and harvested 4 hours later. Cells were stained for surface antigens and with a vital dye. The samples were split and stained according to 2 different protocols.

3.1a. Comparison of intracellular staining protocols

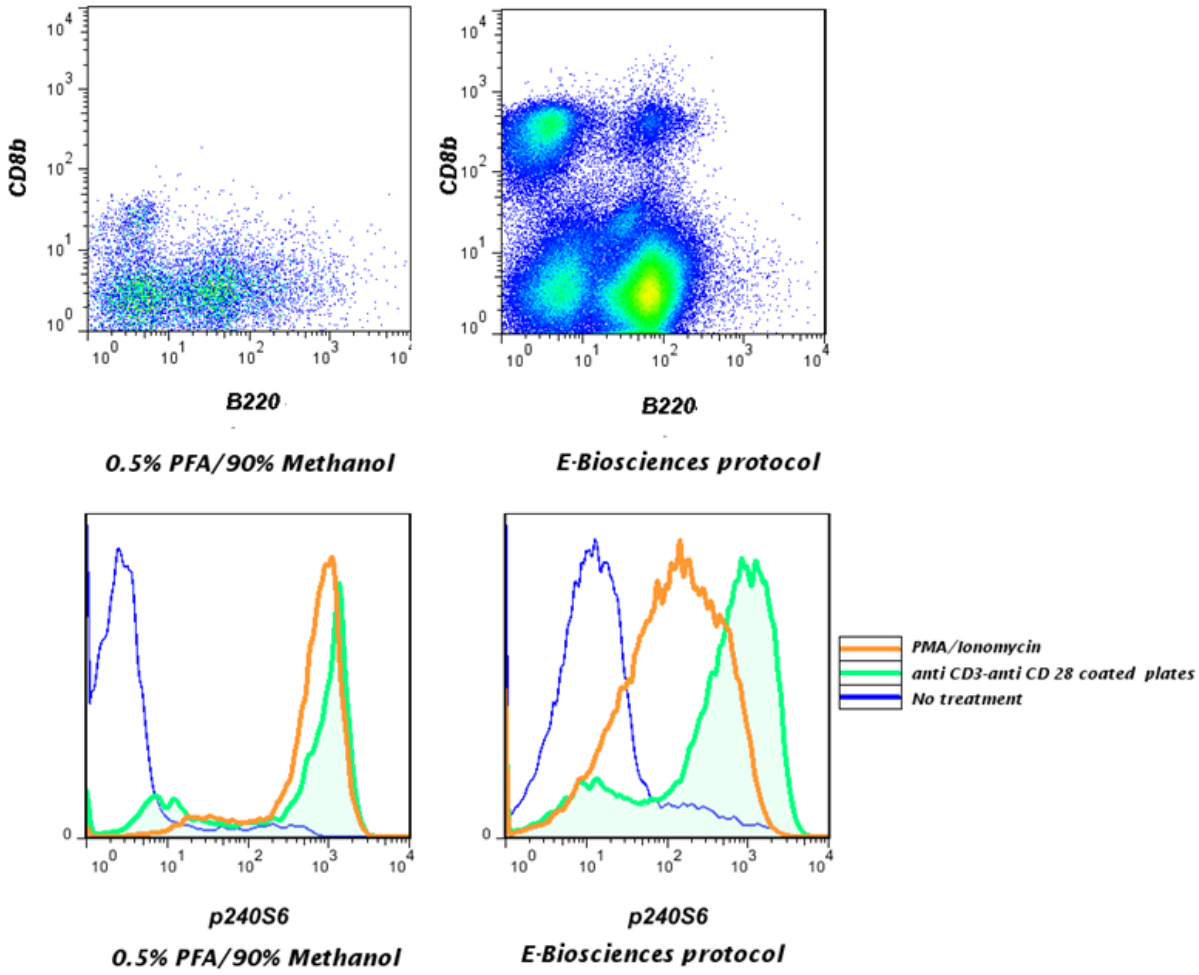

3.1a. The e-Biosciences staining protocol is superior to 0.5% PFA/methanol for multicolour flow cytometric analysis of phosphorylated S6 by intracellular staining.

(Top panel): Pseudocolor dot plots of anti-CD3/CD28 treated groups. There were 12 times more live cells retrieved using the e-Biosciences protocol as compared to the 0.5% PFA/90% Methanol from the same starting sample. Staining for several different surface antigens and fluorochromes was markedly degraded with decreased signal to noise ratios

(Bottom panel): phospho(Ser240)S6 Histograms for the $B220^{-}CD8b^{+}$ populations under different treatment conditions.

Naive OT-1 splenocytes were harvested and stained for phospho(Ser240)S6 directly or after a 20 min incubation in R10 media in 96 well plates with PE-conjugated SIINFEKL-$H2_k$ tetramer at 37°C.

3.1b. Effect of Tetramer Staining on S6 phosphorylation

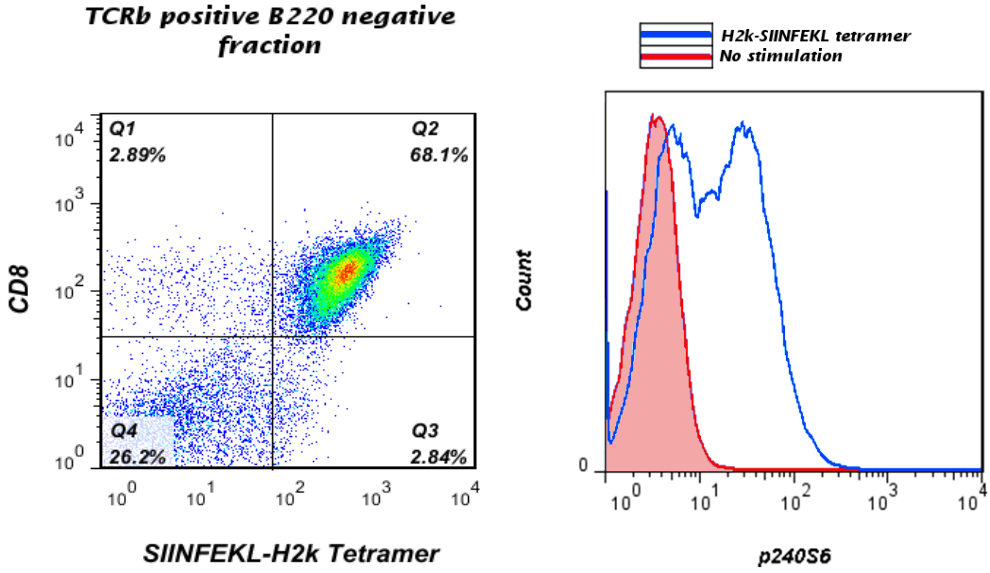

3.1b. SIINFEKL-H2k Tetramer staining results in rapid mTORC1 pathway activation.
(Left panel): Pseudocolor dot plot demonstrating that >95% of $CD8^+$ T cells express the transgenic TCR receptor binding SIINFEKL when presented by $H2_k$.
(Right panel): Overlaid histogram plots of tetramer stained and unstained samples.

3.1c. Use of the DO11.10 transgenic model for investigating $CD4^+$ T cell activation by cognate peptide

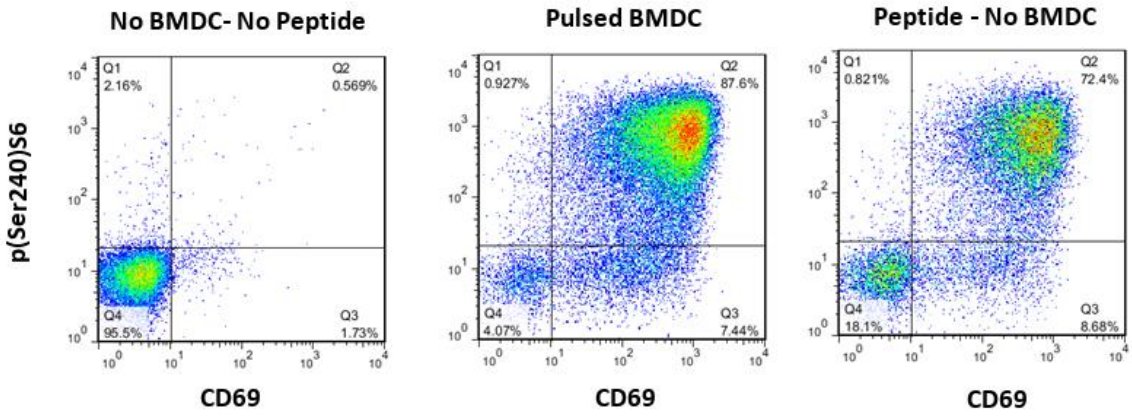

3.1c. DO11.10 $CD4^+$ T cells respond to stimulation by OVA323-339 by activating their mTORC1 pathway. DO11.10 splenocytes were plated in R10 media on their own, with 1µM $OVA_{323-339}$ peptide or with BMDCs pulsed with $OVA_{323-339}$. They were harvested 18 hours later, stained and analysed by flow cytometry. Above: Pseudo-colour dot plots of CD69 versus phospho(Ser240)S6 gated on $B220^-CD4^+$ live cells.

3.1d. Gating strategy

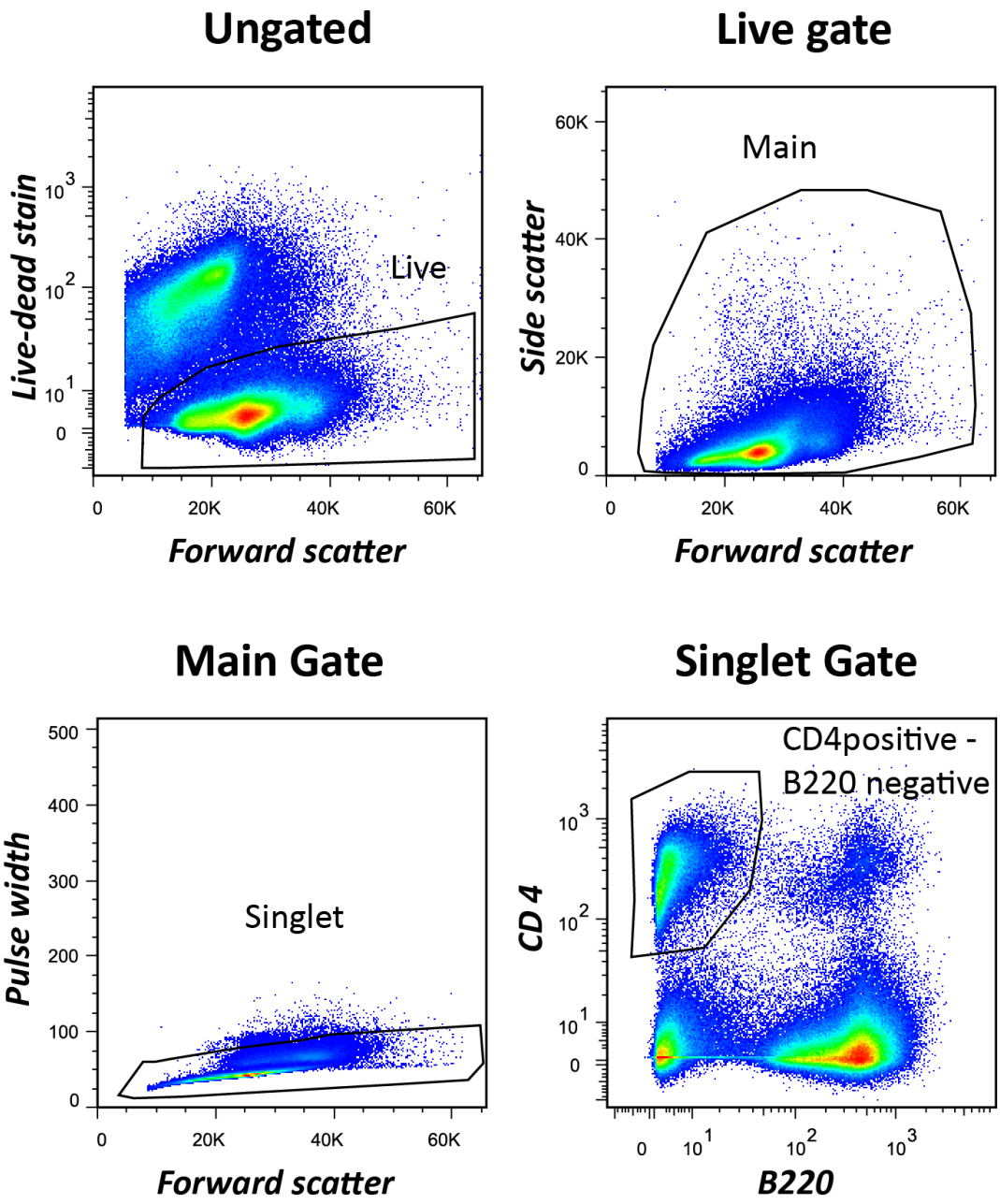

3.1d. General gating strategy for identifying T cells among whole splenocyte population.
To identify T cell subpopulations for further analysis the same general gating strategy was used in all experiments: first a live-dead stain was used to identify dead/non-viable cells that were gated out. Subsequently forward and side scatter gates were used to exclude cell debris and bubbles in the media. A pulse-width base gate then excluded cell doublets/clumps. Finally the B220 positive populations were excluded and the appropriate subgroup – in this case $CD4^+$ splenocytes - were included in the final gate.

3.2. CD69 can be used as a marker for TCR mediated T cell activation in the presence of mTORC1 axis inhibition and is not significantly affected by tryptophan or FCS deprivation.

CD69 is one of the earliest surface markers of T cell activation, appearing within hours of activation and with a half-life of at least 24h post stimulus withdrawal[132] . To investigate whether it could be used as a marker of T cell activation under conditions that may inhibit the mTORC1 axis, OT-I splenocytes were activated for up to 24h in the presence of rapamycin.

Surface expression of CD69 after 7 hours of stimulation was not reduced by rapamycin as measured as the proportion of all $CD8b^+$ splenocytes staining positive for CD69 by flow cytometry (Figure3.2a., top panel). In fact the median CD69 FI of the $CD8b^+$ population was significantly higher in the rapamycin treated groups at both the 7 and 22 hour timepoints (Figure3.2a., bottom panel).

The use of peptide pulsed bone marrow derived dendritic cells (BMDCs) resulted in similar levels of CD69 upregulation for significantly lower peptide concentrations than when peptide was added directly to the splenocytes; the addition of 20nM rapamycin again did not significantly alter the extent of CD69 upregulation irrespective of the mode of peptide presentation (Figure3.3b., left panel).

It should be noted that the rapamycin concentration used - 20 μM - was sufficient to almost completely block phosphorylation of S6 at Ser240 (see Figure3.3a.)

Finally, in order to be able to use CD69 as a reliable marker of T cell exposure to cognate antigen in the presence of nutrient deficient conditions, it was confirmed that its expression was not significantly affected in a temporal or quantitative manner by the absence of tryptophan and/or FCS in the culturing media of stimulated splenocytes (Figure3.2b.)

Figure 3.2. CD69 as a marker of cognate peptide mediated activation

OT-I splenocytes were plated in R10 either alone or with 1µM SIINFEKL peptide in the presence or absence of 20nM rapamycin. Cells were harvested at pre-specified timepoints, fixed, stained and analysed by flow cytometry.

3.2a. Rapamycin does not inhibit CD69 upregulation following CD8+ T cell activation by cognate peptide

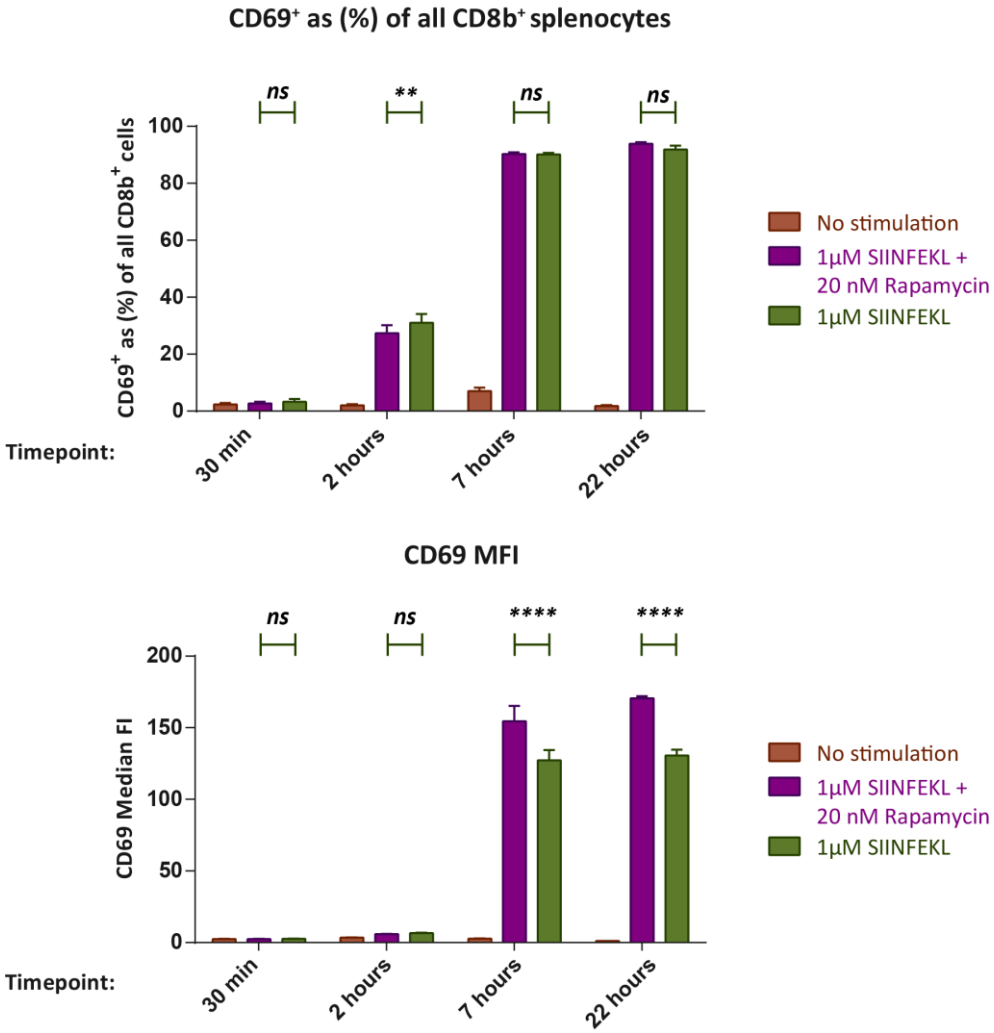

3.2a. Rapamycin does not inhibit CD69 upregulation following CD8+ T cell activation by cognate peptide.

(Top panel) Graph illustrating that rapamycin has a minimal effect in terms of altering the proportion of $B220^{-}$ $CD8b^{+}$ T cells up-regulating CD69 when stimulated by 1µM SIINFEKL. Apart from the 2 hour timepoint, where there was a small detectable statistically significant difference ($p=0.0049$ by Sidak's multiple comparisons test) at all other timepoints there was no detectable effect.

(Bottom panel) In contrast, exposure to rapamycin resulted in significantly higher levels of CD69 expression as early as 7 hours as measured by median fluorescent intensity ($p<0.0001$ by Sidak's multiple comparisons test).

OT-I splenocytes were plated with OT-I BMDCs pulsed with 100nM SIINFEKL peptide in media containing 10%FCS (R10 or tryptophan depleted T10) or no FCS (R0 or tryptophan-free T0), harvested at pre-specified timepoints, stained and analysed by flow cytometry. OT-I splenocytes were also plated in R10 with unpulsed BMDCs as controls ("No peptide" group).

3.2b. CD69 upregulation is not affected by lack of FCS or tryptophan

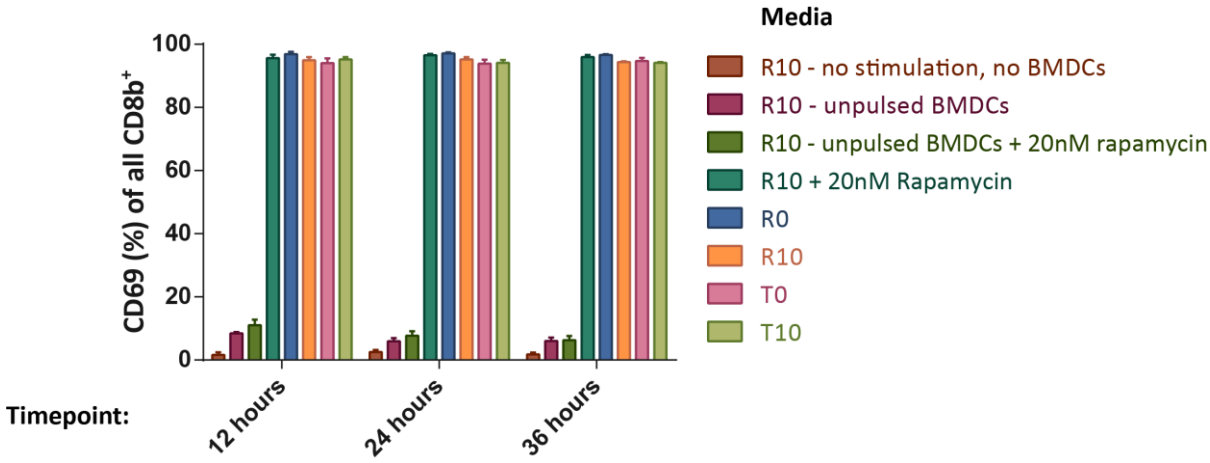

3.2b. Upregulation of CD69 in $CD8b^+$ OT-I splenocytes in response to cognate peptide is not significantly affected by tryptophan or FCS deprivation.

Graph shows fraction (as percentage) of the total $B220^-$ $CD8^+$ population that stained high for CD69. There was no significant difference ($p>0.05$ by Sidak's multiple comparisons test) between any of the treatment groups where peptide-pulsed DCs were used.

3.3. The mTORC1 pathway of murine CD8$^+$ T cells is activated by presentation of cognate peptide

A series of experiments was carried out to establish the baseline levels of mTORC1 pathway activation in naive OT-I CD8$^+$ T cells stimulated by cognate peptide. Two different model systems were explored –splenocytes directly stimulated by free peptide, or by peptide pulsed bone-marrow derived dendritic cells (BMDCs). The results of a typical experiment are summarised in Figure 3.3.

In both systems CD8$^+$ OT-1 T cells are activated fully –in terms of CD69 expression - by 24h in the presence of adequate amounts of SIINFEKL peptide. BMDCs pulsed with 50nM peptide were sufficient to achieve >95% CD69 upregulation rates. Using native splenic APCs with directly added peptide required four times higher peptide concentration to achieve similar levels of activation (Figure 3.3b., left panel).

CD69 staining correlated strongly with phospho(Ser240)S6 staining at this timepoint (Figure 3.3b., middle panel). Moreover the CD69 positive fraction appeared to stain uniformly with similar median fluorescent intensities at all peptide concentrations (Figure 3.3b, right panel as a typical example) This was suggestive that once a particular cell was sufficiently stimulated to upregulate surface CD69 expression the same stimulus was sufficient to trigger mTORC1 pathway activation and thus S6 phosphorylation.

Figure 3.3. The mTORC1 pathway is activated in CD8⁺ OT-I splenocytes stimulated by cognate peptide.

CD11c⁺ BMDCs were pulsed with SIINFEKL peptide at a range of concentrations (0-200nM) for 2 hours at 37°C and were added to splenocytes in R10 media at a 1:10 ratio ("DC" group). Splenocyte only groups ("NoDC") had SIINFEKL peptide directly added to media. Control groups ("+ Rapa") had 20nM rapamycin added at the outset. 24 hours later cells were harvested, fixed and analysed by flow cytometry.

3.3a. The mTORC1 pathway of CD8⁺ OT-I splenocytes is activated after 24 hours of stimulation by cognate peptide.

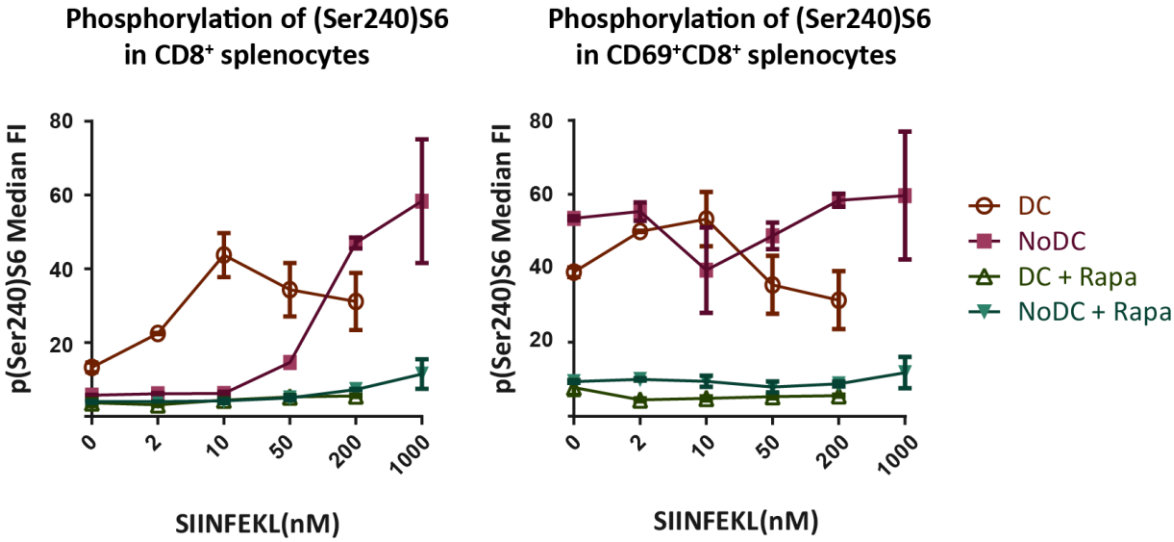

3.3a. Phosphorylation of S6 at Ser240 is upregulated in CD8⁺ OT-I splenocytes after 24 hours of activation by cognate peptide.

(Left panel): Summary graph confirming that stimulation by cognate peptide results in increased phosphorylation of S6 at Ser240 at all concentrations sufficient to elicit CD69 upregulation both in the DC and NoDC groups. S6 phosphorylation is inhibited as expected in the negative control groups treated with rapamycin.

(Right panel): Summary graph demonstrating that within the CD69⁺ subpopulation the extent of S6 phosphorylation at Ser240 is uniform at all peptide concentrations and similar for both the DC and NoDC group.

3.3b. Activation of the mTORC1 pathway correlates strongly with T cell activation in response to cognate peptide.

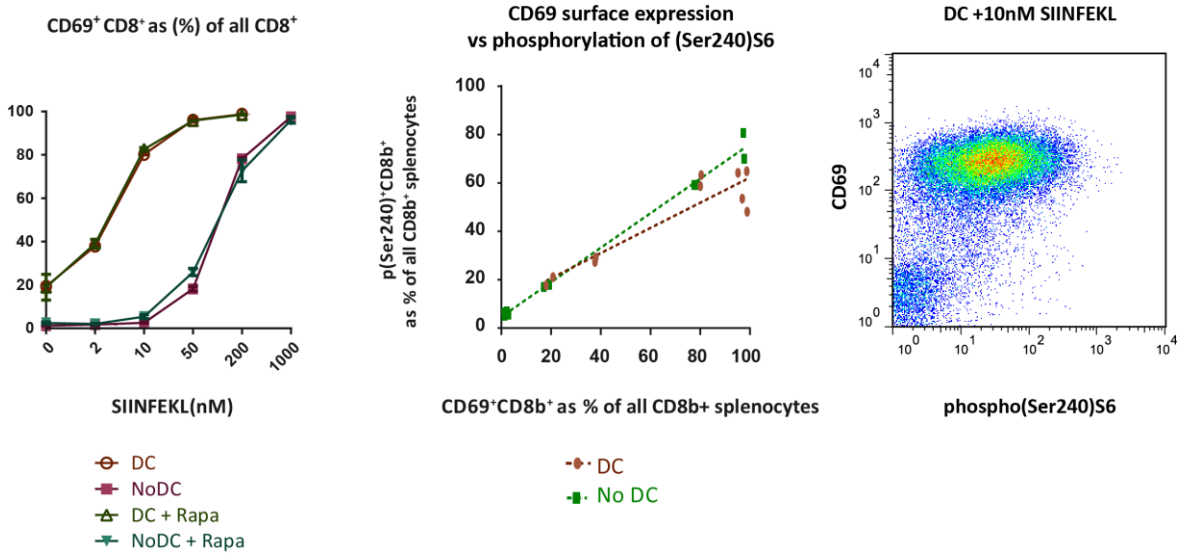

3.3b. Phosphorylation of S6 at Ser240 is closely associated with CD69 upregulation.

(Left panel) Summary graph demonstrating that the percentage of $CD8b^+$ OT-I splenocytes upregulating CD69 after 24 hours of stimulation by cognate peptide is not significantly affected by inhibition of the mTORC1 pathway by 20nM rapamycin at all SIINFEKL concentrations and regardless of whether pulsed DCs were used or not ($p>0.2$ by 2 way ANOVA). DCs were clearly able to more effectively stimulate $CD8^+$ splenocytes at lower peptide concentrations.

(Middle panel): Summary plot of the relative proportion of $CD8^+$ cells upregulating surface CD69 expression versus the proportion exhibiting high levels of S6 phosphorylation at Ser240 for each treatment condition demonstrating a close association between mTORC1 pathway activation and T cell activation following TCR engagement by cognate peptide. A very strong correlation for both the DC and NoDC groups was seen (Pearson r of 0.9281 and 0.9964 respectively corresponding to P values <=0.0001)

(Right panel): Pseudocolor dot plot of a representative sample from this experiment demonstrating that the association between mTORC1 activation and cognate peptide induced T cell activation exists at the single cell level – virtually all cells exhibiting high levels of (Ser240)S6 phosphorylation exhibit high levels of surface CD69 expression.

3.4. Determination of the timecourse of S6 phosphorylation at Ser240 following TCR engagement.

A series of experiments –representative results of which are shown in (Figure 3.4) - were carried out to determine the timecourse of events following TCR engagement with regards to S6 phosphorylation at serine 240 as this is known to be primarily phosphorylated by S6Kinase via the mTORC1 axis as a result of TCR engagement [133].

At early timepoints - up to 7 hours - following activation all $CD8^+$ T cells encountering antigen show similar levels of S6 phosphorylation at Ser240 as measured by median fluorescent intensity (FI) of the phospho(Ser240)S6 binding antibody. Reducing the amount of antigen used results in fewer cells activated, however all activated cells reach similar levels of phospho(Ser240)S6 fluorescent intensity (Figure3.4a.). This increase in FI is only partially inhibited by 20nM rapamycin (Figure3.4b.)

At later timepoints (7-24h) and with continuous stimulation there is a gradual shift to overall higher levels of phospho(Ser240)S6 FI (Figure3.4b.) Addition of 20nM rapamycin prevents this shift and results in significantly reduced phosphorylation of S6 at Ser240, however it does not return it to baseline unstimulated levels.

Using the current model system it was difficult to obtain reproducible data for later time points as tryptophan became limiting as early as 24 hours even with R10 media (Figure3.4c.). Furthermore, late activation of the mTORC1 pathway was observed in several experiments in tryptophan depleted groups e.g. (Figure3.4d.) possibly as part of a negative feedback loop involving autophagy[134].

Figure 3.4. Determination of the timecourse of S6 phosphorylation at Ser240 following TCR engagement.

OT-I splenocytes were plated with BMDCs pulsed with SIINFEKL peptide +/- 20nM rapamycin, harvested at pre-specified timepoints, fixed ,permeabilised, stained and analysed by flow cytometry.

3.4a. mTORC1 activation in CD8^{+} T cells is not complete until 12hours after the onset of stimulation by BMDC presented cognate peptide

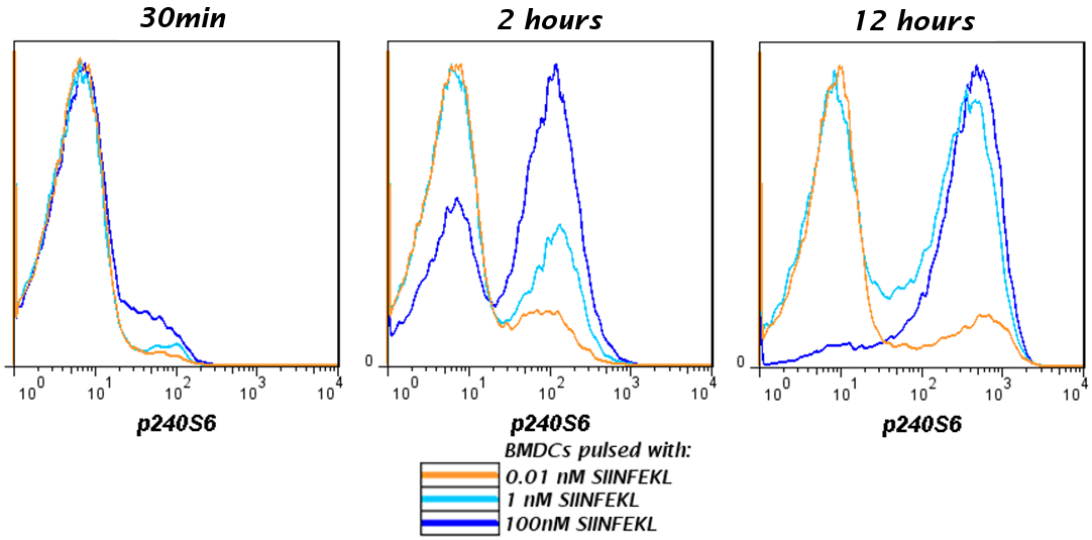

3.4a. Phosphorylation of S6 at Ser240 does not reach maximum levels until 12hours after the onset of stimulation by BMDC presented cognate peptide.

Overlapping fluorescent intensity histograms for phospho(Ser240)S6 gated on live B220^{-} CD8b^{+} cells demonstrating that while phosphorylation of S6 at Ser240 can be detected as early as 30 min after the onset of stimulation regardless of the stimulus strength, nevertheless maximum levels of phosphorylation – both in terms of the proportion of cells exhibiting high levels of phospho(Ser240)S6 and in median FI – are not reached for 12 hours.

3.4b. Rapamycin only partially inhibits the phosphorylation of S6 at Ser240 in response to BMDC presented cognate peptide

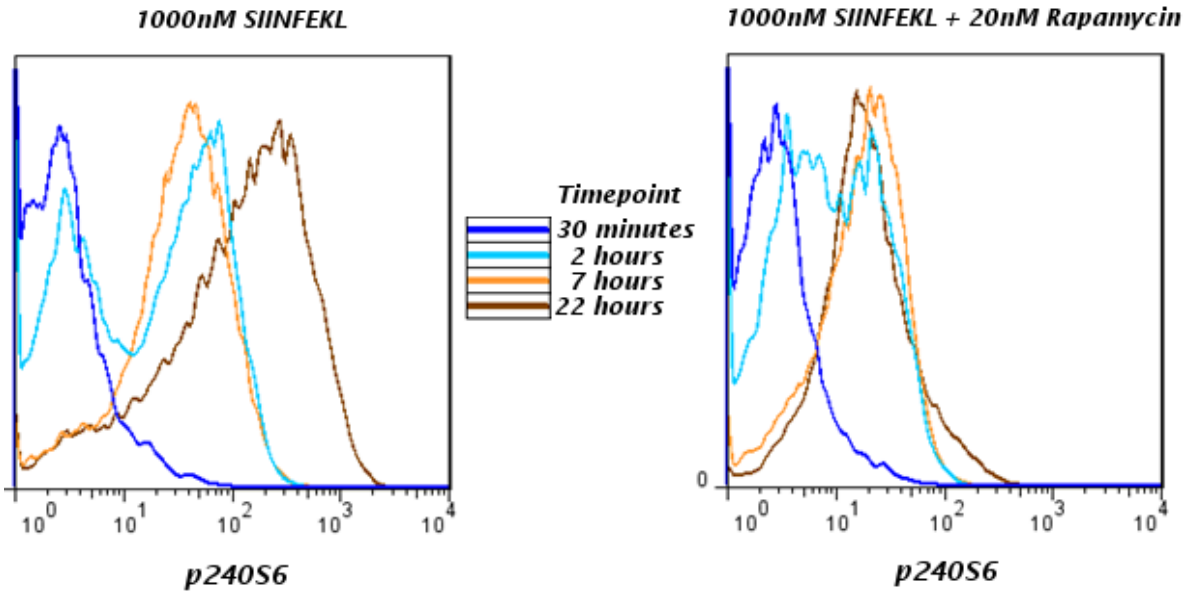

3.4b. Rapamycin only partially inhibits phosphorylation of S6 at Ser240 in OT-I cells stimulated by cognate antigen.

Overlapping fluorescent intensity histograms of phospho(Ser240)S6 gated on live $B220^-$ $CD8b^+$ cells are shown above for individual timepoints. It is clear that while 20nM rapamycin significantly reduces phosphorylation of S6 at Ser240 at all timepoints, inhibition is not complete and this is particularly evident at early timepoints.

OT-I splenocytes were plated with BMDCs pulsed with 100nM SIINFEKL peptide in 96 well plates at a density of $5*10^6$/ ml, harvested at pre-specified timepoints and analysed by flow cytometry.

3.4c. Tryptophan becomes limiting in normal media at late timepoints

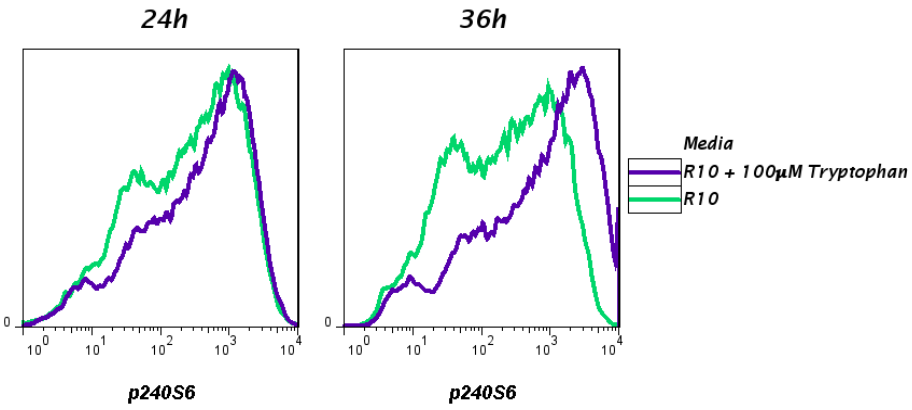

3.4c. Tryptophan becomes limiting even in cells cultured in R10 media beyond 24 hours. Above: FI histograms of $CD8^+$ OT-I splenocytes cultured in R10 media; the addition of 100µM tryptophan maintains high levels of S6 phosphorylation at Ser240 beyond 24 hours.

3.4d. mTORC1 pathway reactivation at late timepoints under tryptophan starvation

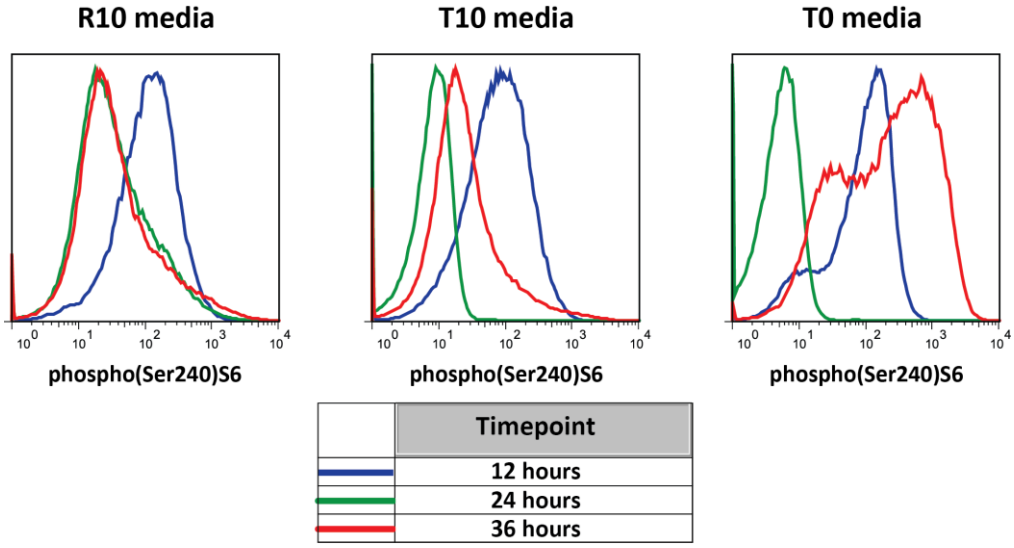

3.4d. Late activation of the mTORC1 pathway by tryptophan starvation in cognate peptide stimulated OT-I CD8+ T cells. FI histograms of phospho(Ser240)S6 gated on live $B220^-CD8b^+$ cells cultured in R10 ***(left panel)***, tryptophan depleted T10 ***(middle panel)*** or tryptophan and FCS-free T0 ***(right panel)*** media revealing that while there is an early inhibition of mTORC1 activity at 24hours *(green lines)* under conditions of tryptophan deprivation , by 36 hours the pathway is reactivated as evidenced by increasing levels of phospho(Ser240)S6 *(red lines)*.

3.5. Determination of the timecourse of mTOR phosphorylation at Ser2481 following TCR engagement.

Auto-phosphorylation of mTOR at Ser2481 is known to be required for mTORC1 dependant phosphorylation of S6Kinase; initial studies had suggested that it was not sensitive to rapamycin treatment or amino acid withdrawal[135] . Recent studies however have shown that it correlates positively with the degree of kinase activity of both mTORC1 and mTORC2 complexes, and conditions that lead to diminished mTORC1 activity such as amino-acid withdrawal or rapamycin inhibit its autophosphorylation by mTORC1 but not necessarily mTORC2[136]

At very early timepoints – as early as 20min post stimulation, and before CD69 is expressed on the surface - mTOR is phosphorylated at Ser2481, however the process is reversed by 1h (Figure 3.5a.). Under conditions of continuous stimulation, phosphorylation levels gradually increase over the course of 24 hours (Figure 3.5b.).

It should be noted that the presence of unpulsed BMDCs is able on its own to drive a low level of persistent phosphorylation of mTOR at Ser2481, however this does not seem to change over time and is not associated with other markers of T cell activation such as surface CD69 upregulation.

Figure 3.5. Determination of the timecourse of mTOR phosphorylation at Ser2481 following TCR engagement in CD8+ OT-I splenocytes.

OT-I splenocytes were plated in R10 either alone or in the presence of mature BMDCs that had been pulsed for 2 hours with 100nM SIINFEKL peptide; as control groups OT-I splenocytes exposed to unpulsed mature DCs were included. At pre specified timepoints cells were harvested and analysed by flow cytometry.

3.5a. Early Phosphorylation of mTOR at Ser2481 following stimulation by cognate peptide in CD8⁺ T cells

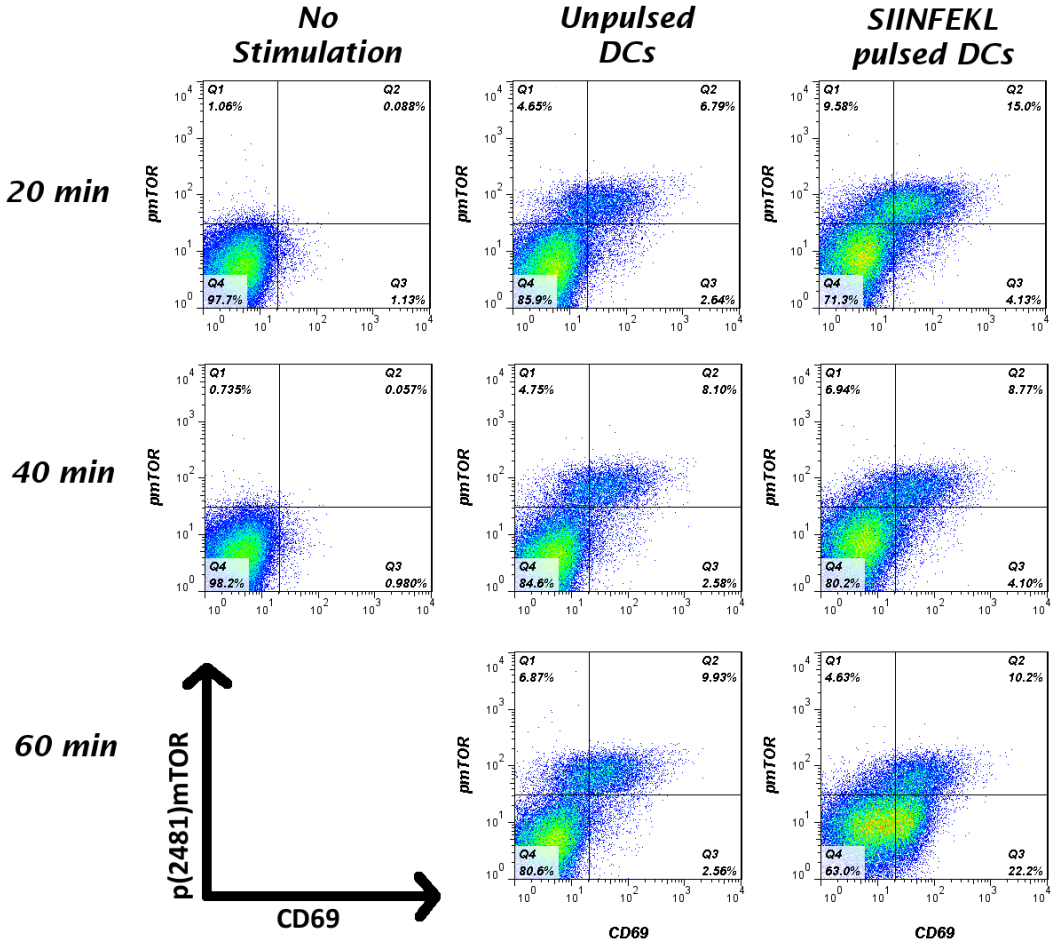

3.5a. Early phosphorylation of mTOR at Ser2481 following activation by cognate peptide. Pseudocolor dot plots of CD69 versus phospho(Ser2481)mTOR gated on live $B220^{-}CD8b^{+}$ cells, demonstrating that $CD8^{+}$ OT-I splenocytes show evidence of very early phosphorylation of mTOR at Ser2481 after exposure to peptide pulsed BMDCs preceding upregulation of surface CD69. Unpulsed BMDCs on their own cause a small baseline increase in the levels of phospho(Ser2481)mTOR that does not change over time.

OT-I splenocytes were plated in R10 media in the presence or absence of 1µM SIINFEKL peptide, harvested at pre-specified timepoints and analysed by flow cytometry.

3.5b. Late Phosphorylation of mTOR at Ser2481 following stimulation by cognate peptide in CD8⁺ T cells

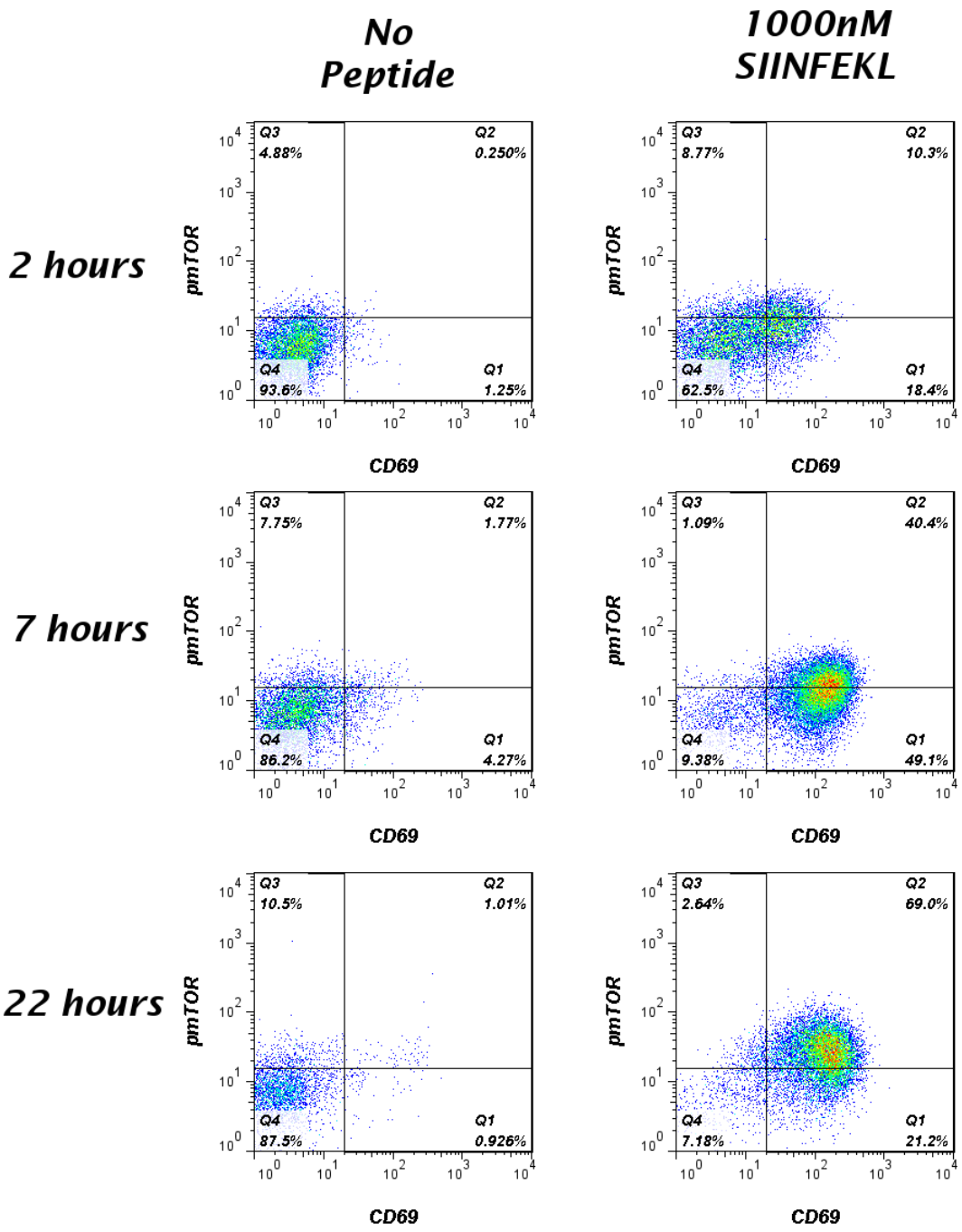

3.5b. Late phosphorylation of mTOR at Ser2481 following activation by cognate peptide. Pseudocolor dot plots of CD69 versus phospho(Ser2481)mTOR gated on B220⁻ CD8b⁺ cells demonstrating progressively increasing levels of phosphorylation of mTOR at Ser2481 over the course of the first 24 hours after the onset of stimulation by cognate peptide in OT-I CD8⁺ splenocytes

3.6. Rapamycin inhibits phosphorylation of S6 at Ser240 and Ser236 but not of mTOR at Ser2481 at 24 hours after activation

To confirm that in $CD8^+$ splenocytes the mTORC1 pathway is the major pathway leading to S6 phosphorylation after the initial stages of T cell activation, Rapamycin was used as in inhibitor in a series of experiments (Figure 3.6.) at a concentration (20nM) that was known not to inhibit early events in $CD8^+$ T cell activation (e.g. see Figure 3.2.).

The results verified that culturing in 20nM rapamycin nearly completely inhibited S6 phosphorylation both at residue 240 that are known to be phosphorylated primarily by S6Kinase, but also at residue 236 which is also downstream of the MAPK/ERK pathway.

Interestingly, phosphorylation of mTOR itself at residue 2481 was not affected. Phosphorylation of mTOR as part of mTORC1 but not mTORC2 at this residue has been reported to be sensitive to inhibition by rapamycin, and mTORC2 pathway activity downstream of TCR signalling may explain this finding.

Figure 3.6. Rapamycin inhibits phosphorylation of S6 at Ser240 and Ser236 but not of mTOR at Ser2481

OT-I splenocytes were plated with BMDCs pre-pulsed with 100nM SIINFEKL peptide in R10 media with or without 20nM rapamycin, harvested 24 hours later, fixed, permeabilised, stained and analysed by flow cytometry. Controls were also plated with unpulsed DCs in R10 media.

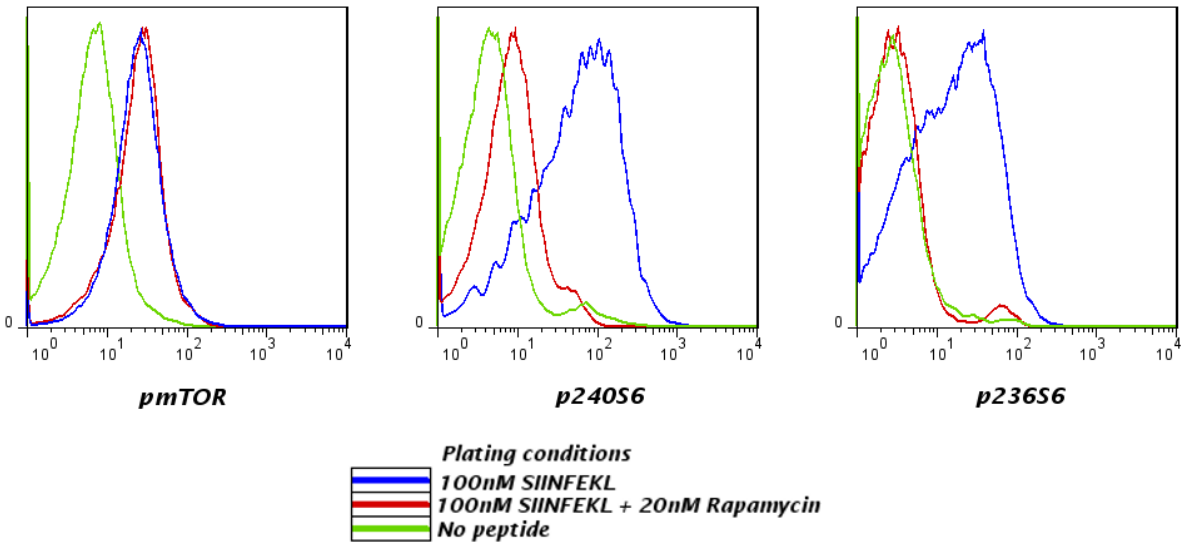

3.6. Rapamycin inhibits phosphorylation of S6 at Ser240 and Ser236 but not of mTOR at Ser2481. FI histograms of phospho(Ser2481)mTOR, phospho(Ser240)S6 and phospho(Ser236)S6 gated on live $B220^{-}$ $CD8b^{+}$cells demonstrating that while 20nM rapamycin is sufficient to inhibit phosphorylation of S6 at both Ser240 ***(middle panel)*** and Ser236 ***(right panel)***, it has no effect on phosphorylation of mTOR at Ser2481 ***(left panel)***.

3.7. Lack of tryptophan and/or FCS modifies the pattern of S6 phosphorylation at early and late timepoints in CD8$^+$ OT-I T cells stimulated by cognate high affinity peptide.

To investigate the effects of tryptophan depletion on the mTORC1 pathway in activated CD8$^+$ T cells, a series of experiments was carried out utilising media made using custom made tryptophan-free RPMI1640.

As FCS invariably contained a certain amount of tryptophan that was highly variable between batches (resulting in final concentrations in 10% FCS containing media ranging from just under 1µM to over 5µM) the effect of media containing no FCS was also investigated.

At all timepoints before 24 hours it was apparent that stimulating CD8$^+$ T cells in a low tryptophan environment resulted in slower phosphorylation of S6 at Ser240/244 with significantly reduced MFI at 12 and up to 24 hours (Figure 3.7a.).

Phosphorylation of S6 at Ser236 followed a similar pattern in CD8$^+$ T cells placed in media containing 10% FCS; however there was a significant late (>24h) increase in phospho(Ser236)S6 at 24h and later timepoints in 0% FCS media (Figure 3.7b.).

In view of the significant potential of low FCS concentrations in media for confounding the effect of tryptophan deprivation further experiments all used 10%FCS based media. Where possible media using dialysed FCS was used together with tryptophan-free RPMI with additional tryptophan added separately as needed. This guaranteed a much more reliable baseline as dialysed FCS consistently contained < 1µM tryptophan.

It should be noted that media made using dialysed FCS may be missing additional micronutrients and growth factors with a molecular weight <10000 that do not bind to larger serum proteins as compared to standard media. Comparison positive controls in all experiments utilising these media included normal media to exclude a significant effect caused by their absence.

Figure 3.7. Lack of tryptophan or FCS inhibits S6 phosphorylation at early and late timepoints in CD8⁺ OT-I T cells.

OT-I splenocytes were plated with BMDCs pulsed with 100nM SIINFEKL peptide in RPMI 1640 media with ("R") or without ("T") 25µM tryptophan and with ("10") or without ("0") 10% FCS, harvested at specific timepoints and analysed by flow cytometry.

3.7a. Lack of tryptophan inhibits S6 phosphorylation at Ser240

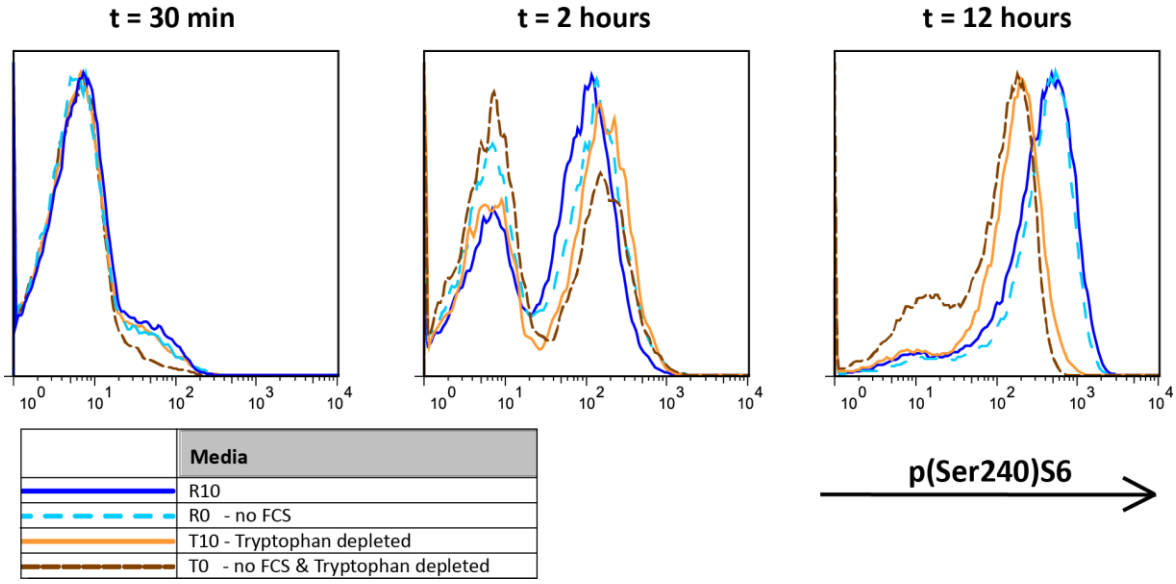

3.7a. Lack of tryptophan inhibits S6 phosphorylation at Ser240 in OT-I CD8+ splenocytes stimulated by cognate peptide.

FI plots of phospho(Ser240)S6 demonstrating that already after 2 hours of stimulation tryptophan depletion reduces the proportion of cells exhibiting high levels of phospho(Ser240)S6. By 12 hours there is an additional effect on the extent of phosphorylation at Ser240 with tryptophan depleted groups exhibiting lower levels.

3.7b. Lack of tryptophan inhibits S6 phosphorylation at Ser236, but lack of FCS has an overriding effect at later timepoints

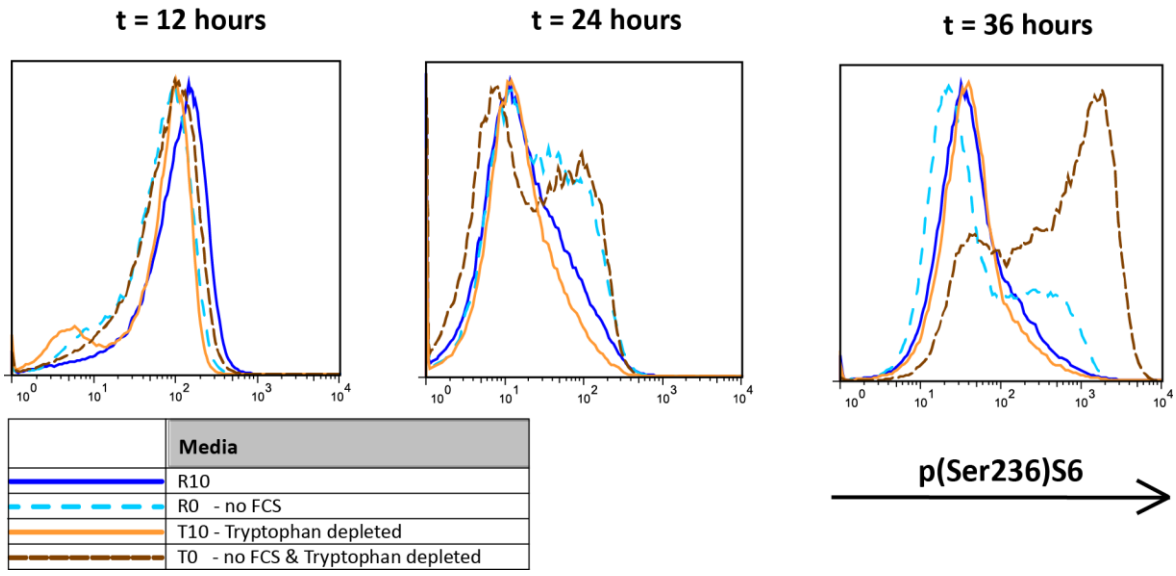

3.7b. Lack of tryptophan inhibits S6 phosphorylation at Ser236 in OT-I CD8$^+$ splenocytes stimulated by cognate peptide, but lack of FCS has an overriding effect at later timepoints

Overlapping FI histograms of phospho(Ser236)S6 demonstrating that tryptophan depletion also reduces the phosphorylation of S6 at Ser236 as measured by median FI; the effect is visible in the groups with 10% FCS containing media all the way to 36 hours. However in the 0% FCS containing media there was a significant increase of phospho(Ser236)S6 at 24h and later timepoints that was particularly pronounced in the T0 (no FCS, no tryptophan) group.

3.8. Tryptophan deprivation impedes CD69 upregulation and mTORC1 pathway activation in CD8$^+$ cells stimulated by low affinity peptides.

The OT-I tumour model was used again to further look into the effect of tryptophan deprivation on CD8$^+$ cells when stimulated by low affinity cognate peptide - as may often be the case when first encountering neo-antigens presented by tumour cells. In addition to SIINFEKL additional peptides were used that have previously been shown[137] to have lower affinity for the transgenic TCR.

As expected, the dose response curves for these peptides were shifted (Figure 3.8a., top panels). Higher concentrations of the lower affinity peptides were necessary to elicit the same activation response as measured by the proportion of CD8$^+$ splenocytes upregulating CD69. These results were in keeping with peptide affinities already reported in literature [136].

The shapes of the curves and relative peptide strength was similar in both normal and tryptophan depleted media. However, for the lower affinity peptides, T cell activation at low peptide concentrations was significantly reduced when the splenocytes were stimulated in low tryptophan conditions (Figure 3.8a., lower panel)

Using phosphorylation of S6 at Ser240 as a marker of mTORC1 activity it was obvious that tryptophan depletion resulted in marked and highly significant reduction in mTORC1 activity post stimulation by cognate peptide regardless of peptide affinity or concentration, though the extent of inhibition was less for weaker stimuli (Figure 3.8b/c.).

To control for the possibility that these results were explained by a direct effect on T cell activation alone, the CD69$^+$ subset was analysed separately (Figure 3.8d.). It is clear that the inhibitory effect is just as pronounced in this subgroup which only includes activated splenocytes and the effect is similar in magnitude to that seen in the whole CD8$^+$ population.

The effect of tryptophan deprivation was not all-or-none; instead at increasing tryptophan concentrations there was a corresponding increase in the extent of upregulation of the mTORC1 pathway as evidenced by increasing levels of phosphorylation of S6 at Ser 240 (Figure 3.8e.).

Figure 3.8. Effects of tryptophan deprivation on CD8⁺ OT-I splenocytes after 18 hours of stimulation with low affinity cognate peptide.

10^6 freshly harvested OT-I splenocytes were plated in dT10 in 96 well plates. At t=0 hours a pre-defined amount of cognate peptide and tryptophan to each well was added so that the final culture volume was 200µl. 6 different peptides were used that were known to have different binding affinities to the OT-I TCR. The cells were harvested after 18 hours, fixed permeabilised and stained for flow cytometric analysis.

3.8a. CD8⁺ splenocyte activation by low affinity peptide is inhibited by tryptophan deprivation

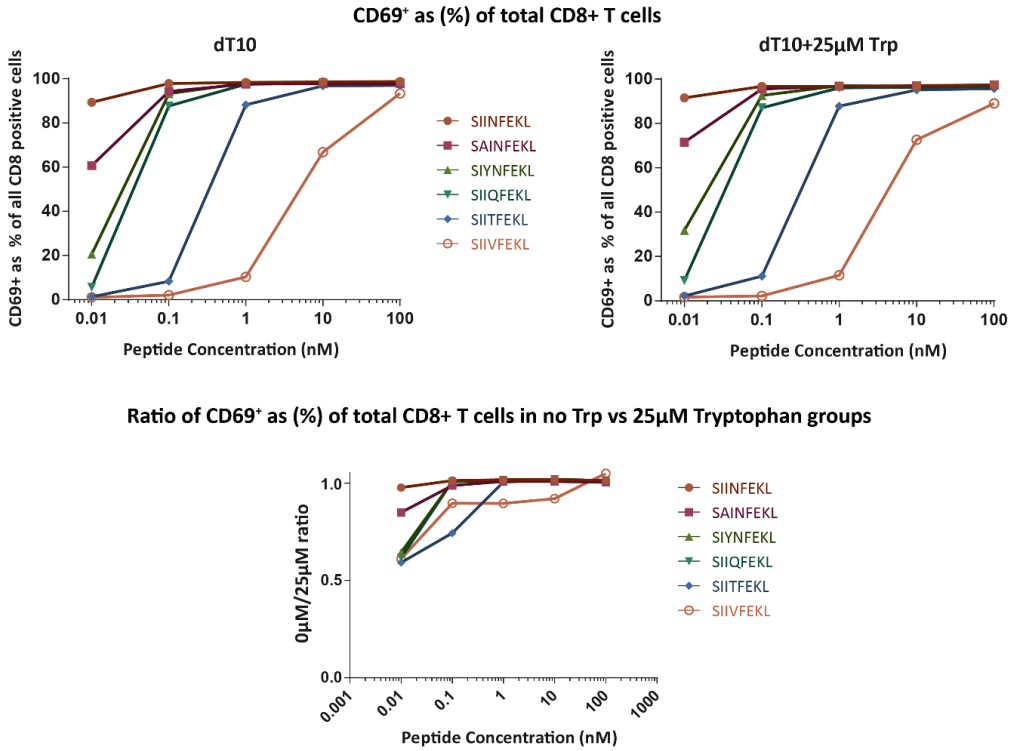

3.8a. CD8⁺ T cell activation as measured by CD69 upregulation is impeded by tryptophan deprivation in OT-I T cells stimulated by low concentrations of low affinity cognate peptide.

(Top panels) : Graphs clearly demonstrating that reducing affinity of the peptides to the TCR results in shifted dose response curves in terms of CD8⁺ T cells activation as measured by CD69 upregulation; low affinity peptides require significantly ($p<0.005$ by 2 way ANOVA) higher peptide concentrations to have the same effect in both tryptophan depleted and tryptophan replete media.

(Bottom panel): The effect of tryptophan starvation in terms of CD69 upregulation only becomes visible when lower affinity peptides are used at concentrations not sufficient to fully activate the CD8⁺ cells. In this experiment the effect was statistically significant ($p<0.05$ by Sidak's multiple comparisons test) for the SIYNFEKL, SIIQFEKL, SIITFEKL and SIIVFEKL groups at the 10pM range.

3.8b. mTORC1 pathway activation in response to cognate peptide is inhibited in tryptophan deprived CD8⁺ splenocytes

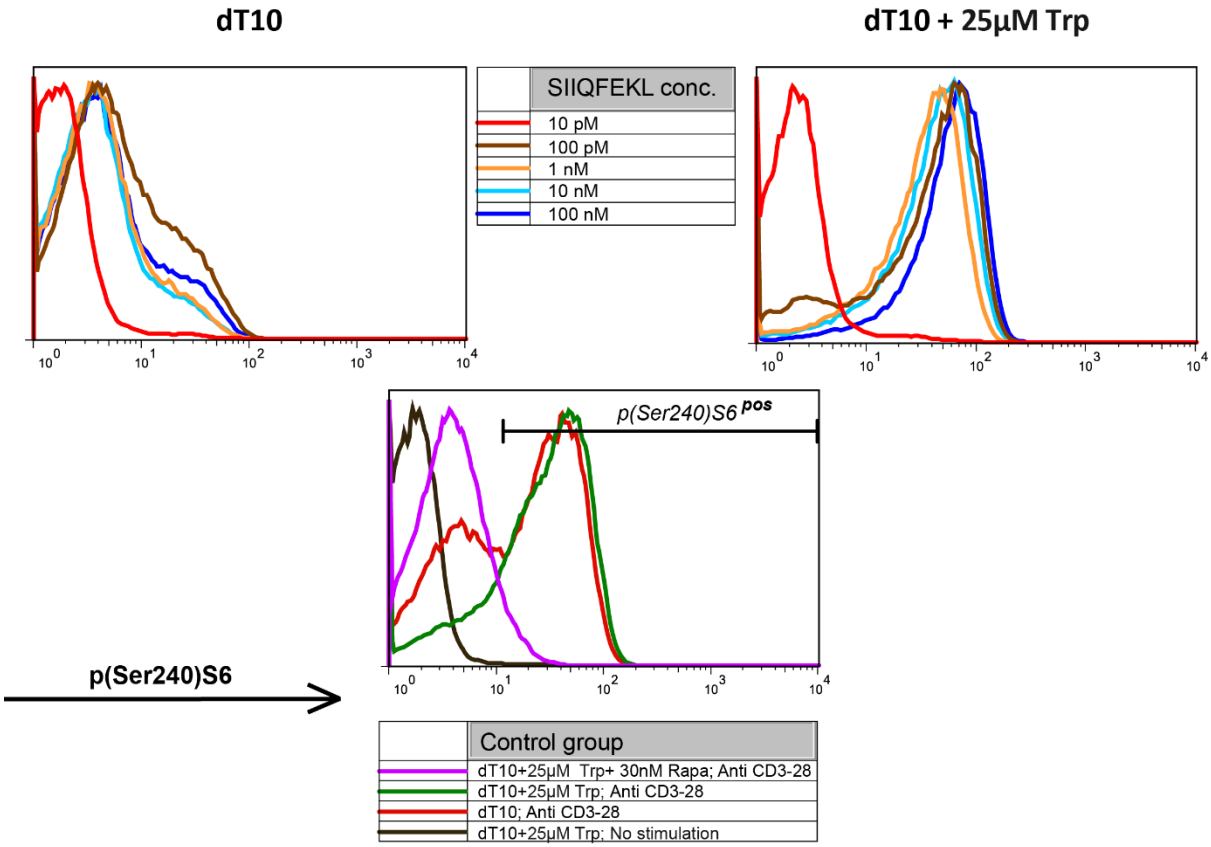

3.8b. Tryptophan starvation results in inhibition of phosphorylation of S6 at Ser240 in CD8⁺ OT- I T cells stimulated by cognate petides regardless of peptide concentration.

Typical histograms demonstrating markedly reduced phosphorylation of S6 at Ser240 in tryptophan starved OT-I CD8b⁺T cells in response to stimulation by cognate peptide (top left: tryptophan starved group; top right: tryptophan replete; bottom: control groups as comparison.)

3.8c. mTORC1 inhibition in response to tryptophan deprivation occurs regardless of the strength of the TCR stimulus

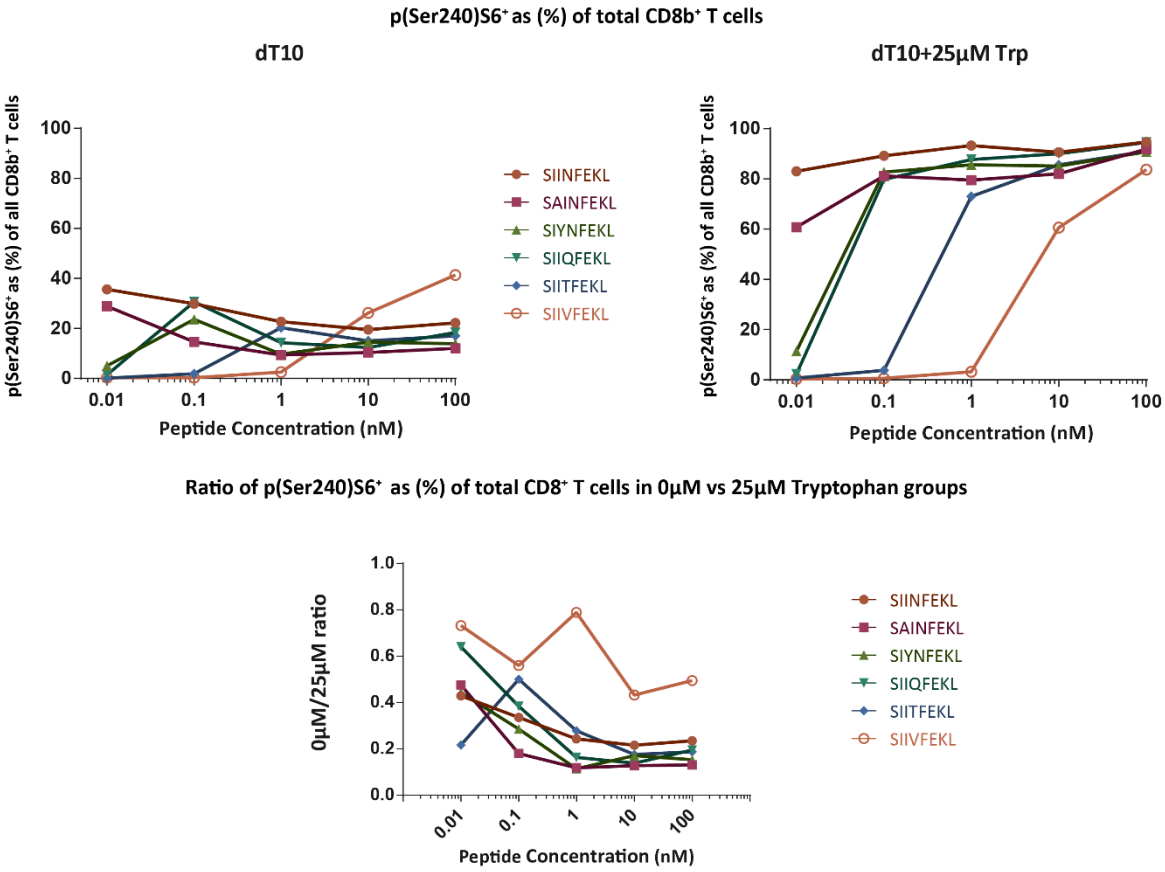

3.8c. Tryptophan starvation results in inhibition of phosphorylation of S6 at Ser240 in CD8$^+$ OT- I T cells stimulated by cognate petides regardless of peptide concentration or affinity.

Summary graphs demonstrating the dramatic effect of tryptophan deprivation in terms of S6 phosphorylation at Ser240 in all treatment groups regardless of stimulating peptide affinity or concentration.

(Top panels): Plots of the proportion of all CD8b$^+$ T cells exhibiting increased levels of S6 phosphorylation at Ser240 for different stimulating peptides and at different concentrations in tryptophan poor (dT10, left panel) and tryptophan enriched (dT10+25µM Tryptophan, right panel) media. The difference between the 2 media groups was highly statistically significant ($p<0.0001$ by 2 way-ANOVA).

(Bottom panel): Plot of the ratio of the phospho(Ser240)S6$^+$ populations for the same peptide concentration in tryptophan poor vs. tryptophan rich media. In all cases and regardless of the peptide concentration or affinity the ratio was <1. The effect was smaller for lower affinity peptides (e.g. SIIVFEKL) but still observable even at concentrations where the level of CD8$^+$ T cell activation as defined by CD69 upregulation was low.

3.8d. Activated CD8⁺ splenocytes' mTORC1 pathway is not protected from inhibition in response to tryptophan deprivation

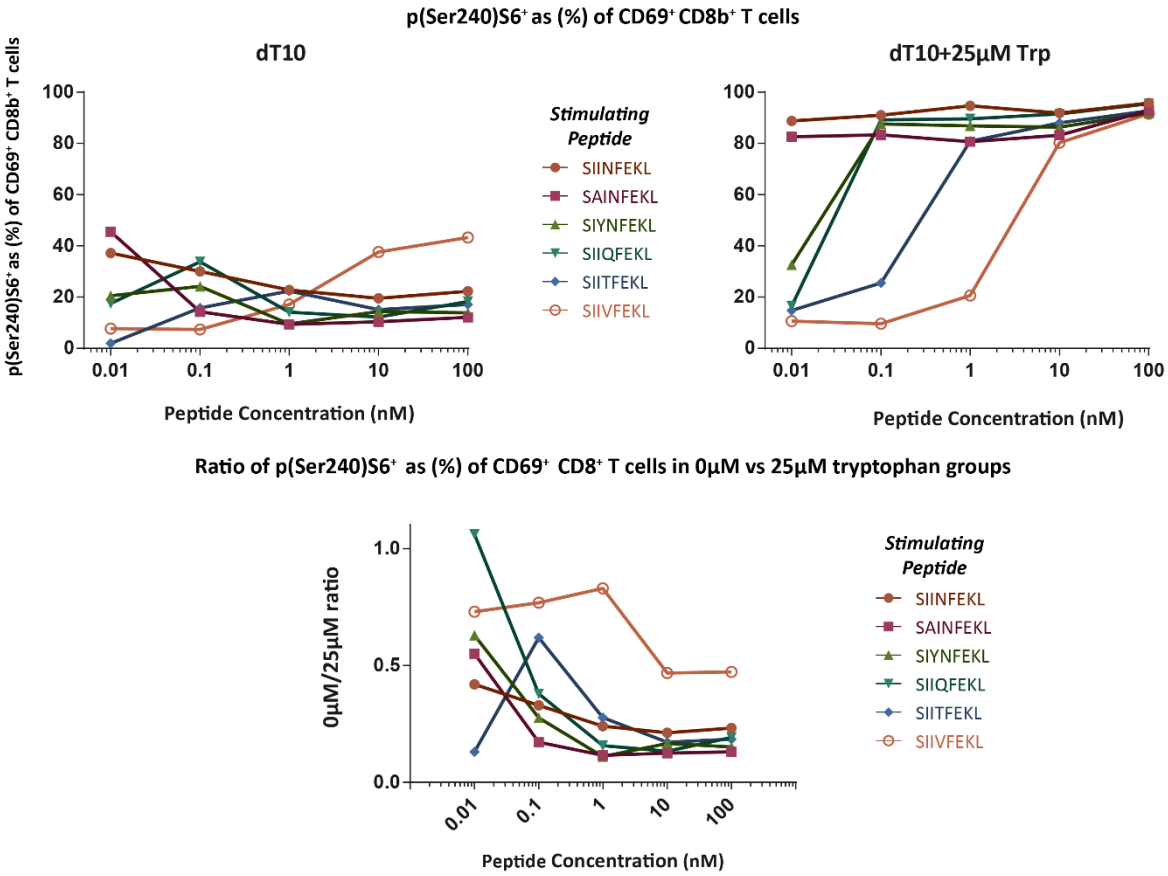

3.8d. The CD69⁺ subpopulation of activated CD8⁺ OT-I splenocytes also exhibits significant inhibition of phosphorylation of S6 at Ser240 in response to tryptophan deprivation regardless of cognate peptide concentration or affinity.

The effect of tryptophan deprivation was visible and highly significant ($p<0.0001$ by 2 way-ANOVA) even on the CD69 positive fraction of CD8b⁺ cells regardless of peptide affinity and for almost all peptide concentrations where reliable results could be measured. Results for low peptide concentrations of low affinity peptides should be viewed with caution due to the small numbers of cells involved (see Figure 3.8a).

3.8e. mTORC1 pathway activation is proportional to signal intensity and to tryptophan availability

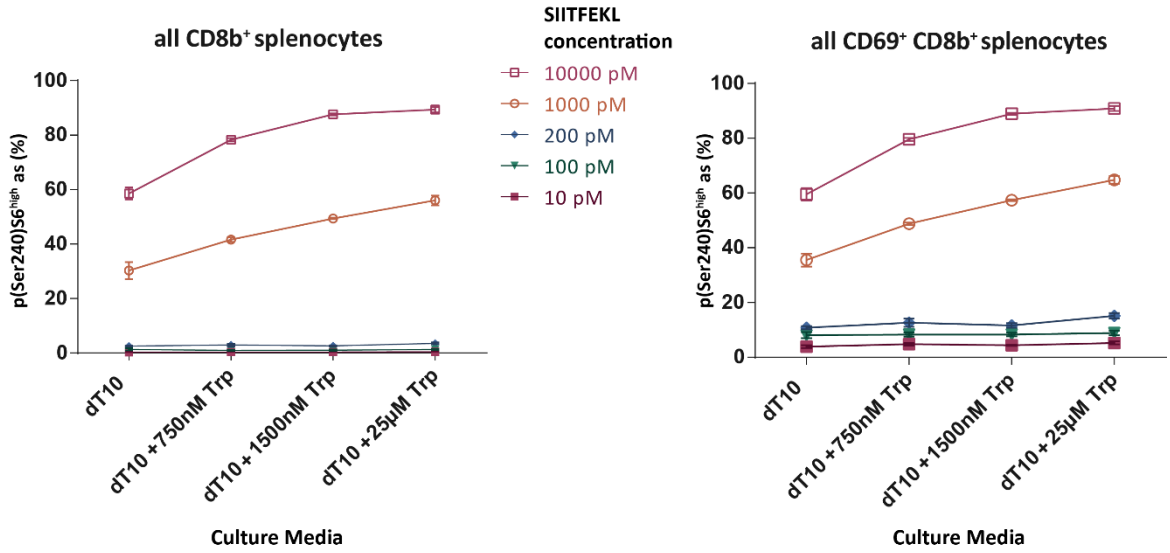

3.8e. The extent of phosphorylation of S6 at Ser240 is proportional both to stimulus strength and to the amount of available tryptophan in the media.

Summary graphs plotting the proportion of either the entire CD8b$^+$ splenocyte population ***(left panel)*** or the CD69$^+$ activated CD8$^+$ subpopulation ***(right panel)*** against the tryptophan concentration in the culture media for different concentrations of stimulating SIITFEKL peptide.

3.9. Tryptophan depletion results in impaired mTORC1 pathway activity in $CD4^+$ DO11.10 splenocytes stimulated by cognate peptide

To see whether the effects of tryptophan depletion in $CD8^+$ splenocytes were also observable in murine $CD4^+$ T cells a series of experiments was carried out utilising the DO11.10 transgenic model. DO11.10 splenocytes were stimulated with $OVA_{323-339}$ - the cognate peptide for the transgenic TCR expressed in >90% of DO11.10 $CD4^+$ splenocytes. Tryptophan depleted "dT10" media - containing custom tryptophan-free RPMI1640 and dialysed FCS - was used as the baseline media.

Initial experiments (Figure 3.9a.) showed that, similarly to results in $CD8^+$ OT-I cells, stimulation with high affinity peptide produced similar levels of activation as measured by CD69 upregulation regardless of the media tryptophan concentration.

More importantly, subsequent experiments confirmed a highly significant effect in media containing low tryptophan concentrations on the phosphorylation of S6 at Ser240 (Figure 3.9b.) that was markedly reduced both when the entire $CD4^+$ population (Figure 3.9b., bottom left panel) and the activated $CD69^+CD4^+$ subpopulation population (Figure 3.9b., bottom right panel) were looked at.

Figure 3.9. Effects of tryptophan deprivation on CD4⁺ splenocytes after 18 hours of stimulation with cognate peptide in the DO11.10 model

10^6 freshly harvested DO 11.10 splenocytes were plated in dT10 in 96 well plates. At t=0 hours a pre-defined amount of cognate peptide ("ISQ"= $OVA_{323-339}$) and tryptophan was added to each well so that the final culture volume was 200µl. As positive controls, wells pre-coated with anti-CD3/CD28 were used. The cells were harvested after 18 hours, fixed permeabilised and stained for flow cytometric analysis.

3.9a. CD69 upregulation after 18 hours in DO11.10 CD4⁺ Splenocytes

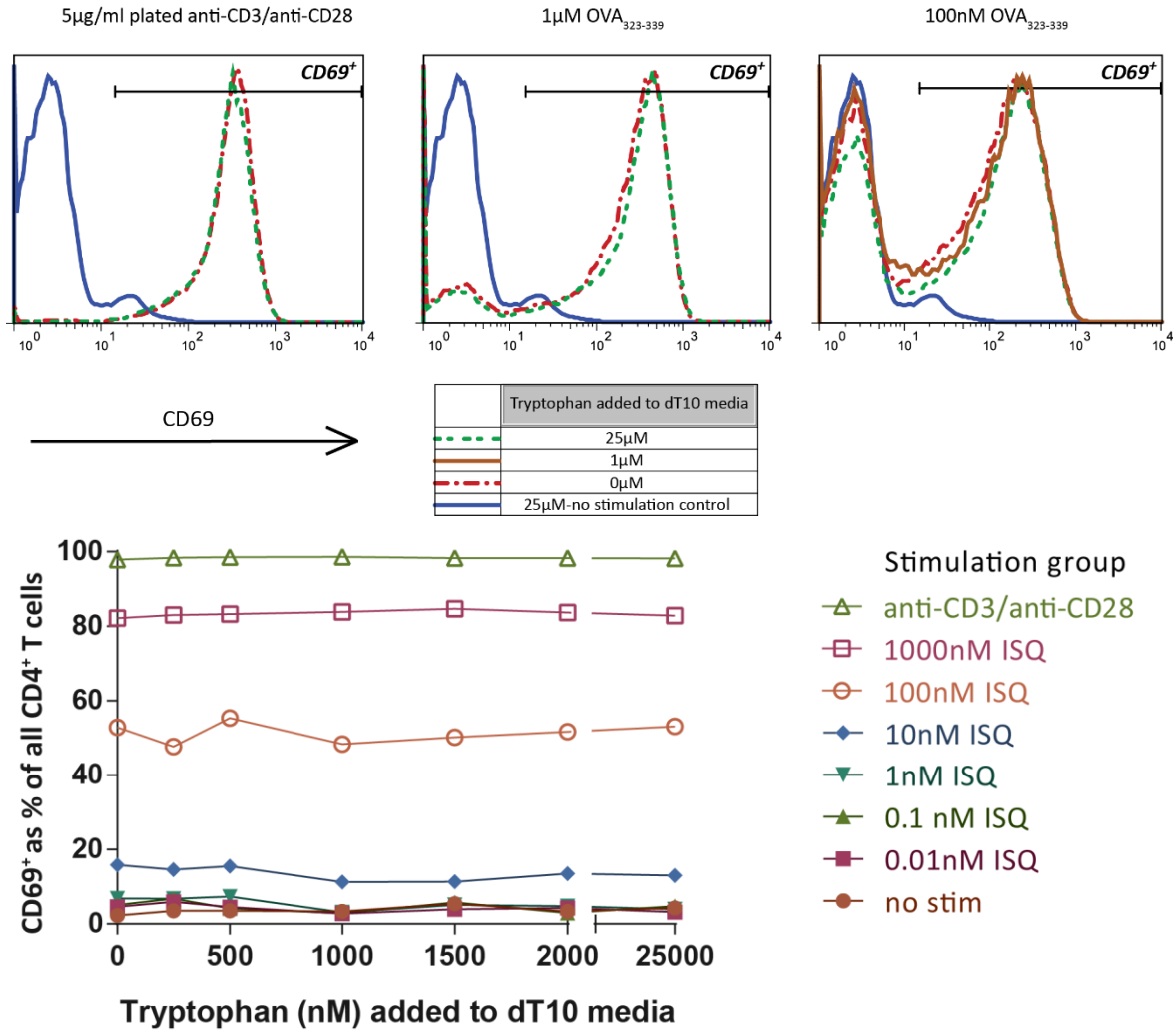

3.9a. CD69 upregulation after 18 hours is not affected by lack of tryptophan in culture. $CD4^+$ T cell activation as measured by the extent of CD69 upregulation is not affected by tryptophan concentration in cultured media in response to both plated anti-CD3/CD28 and cognate peptide.

(Top panels): Typical histograms demonstrating essentially identical CD69 upregulation responses for the same stimulus in all tryptophan groups.

(Bottom panel)*:* Summary graph showing flat dose response curves for CD69 expression at all cognate peptide concentrations.

3.9b. Phosphorylation of S6 at Ser240 in DO11.10 CD4⁺ splenocytes

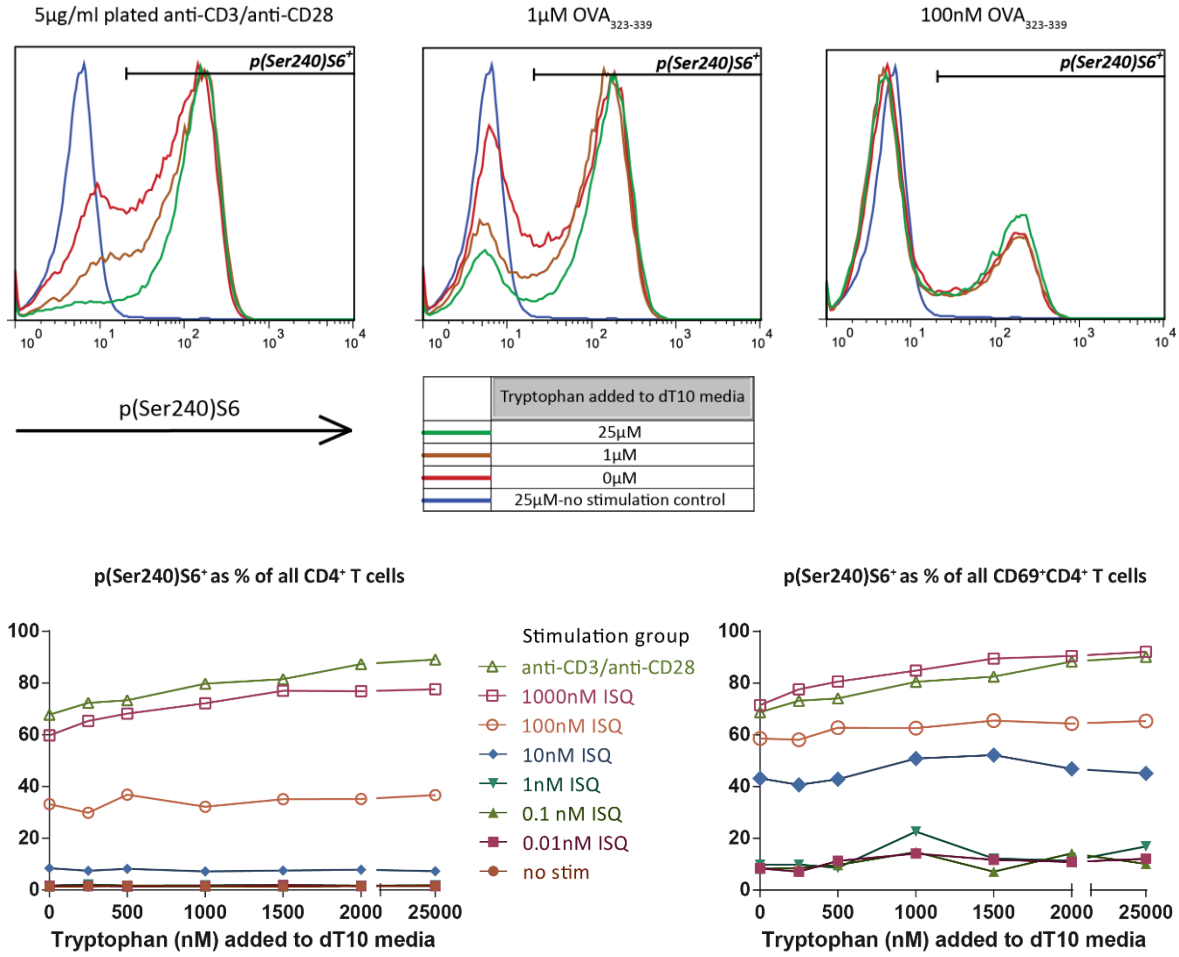

3.9b. Lack of tryptophan in media results in reduced mTORC1 activity as measured by phosphorylation of S6 at Ser240 in CD4⁺ DO11.10 splenocytes after 18 hours of stimulation. Graphs demonstrating the effect of tryptophan deprivation in culture media of CD4⁺ DO11.10 splenocytes stimulated with either plate bound anti-CD3/CD28 or high (>100nM) cognate peptide concentrations for 18 hours.

(Top panels): Typical histograms demonstrating significantly reduced phospho(Ser240)S6 in CD4⁺ DO11.10 splenocytes when stimulated by plated anti-CD3/CD28 and cognate peptide at high concentrations.

(Bottom left graph): A significant ($p<0.05$ by 2-way ANOVA) reduction in the relative size of the phospho(Ser240)S6⁺ populations was seen in groups stimulated by 5µg/ml anti-CD3/CD28 and 1µM $OVA_{323-339}$ cognate peptide.

(Bottom right graph): The effect was even more evident and statistically significant when the CD69⁺ CD4⁺ subpopulation was analysed ($p<0.005$ by 2 way ANOVA).

3.10. Proliferation of murine splenocytes in response to stimulation by cognate peptide is inhibited by tryptophan deprivation

Deprivation of tryptophan, an essential amino-acid, is expected to have a significant effect on the proliferative capability of highly metabolically active cells - such as T cells activated by cognate peptide. A series of experiments was therefore devised to investigate this further and in particular establish whether there was a significant interaction with the strength of the stimulus.

Initial experiments using non-specific stimulation with plate bound anti-CD3/CD28 (Figure 3.10a., right panels) using tryptophan depleted "T10" media revealed the dramatic effect of tryptophan deprivation. Cells cultured in media without additional tryptophan failed to proliferate; the addition of tryptophan rescued the proliferative capability of these cells.

Follow-up experiments using cognate peptide in the OT-I and DO11.10 transgenic murine models (Figure 3.10a., left panels) confirmed that this was also true when the stimulation was mediated by direct TCR activation by cognate peptide.

A series of experiments (Figure 3.10b.) then demonstrated that the inhibitory effect was not all or nothing – instead the amount of proliferation was directly related to the tryptophan concentration in the culture media. Tryptophan concentrations of >2μM were needed to obtain maximal proliferation levels

Stimulation signals of lower strength (i.e. use of lower concentrations of cognate peptide) resulted as expected in lower levels of maximal proliferation. Accordingly lower levels of tryptophan were sufficient under these circumstances to support these.

Figure 3.10. Murine T cell proliferation is severely impaired by tryptophan deprivation.

Freshly harvested murine splenocytes were stained with CFSE and immediately plated in 48well plates pre-coated with anti-CD3/ CD28 at a concentration of 10^6 / well in 1ml of tryptophan depleted dT10 media. At the same time cognate peptide (SIINFEKL for OTI splenocytes and $OVA_{323-339}$ for DO11.10 splenocytes) was added in separate non pre-coated wells. At t=0 tryptophan was added to the wells. The cells were subsequently - at 60 hours for OT-I and 84 hours for DO11.10 groups - harvested, fixed, permeabilised and stained for flow cytometric analysis.

3.10a. Lack of tryptophan inhibits the proliferation of $CD8^+$ and $CD4^+$ splenocytes in response to activating stimuli.

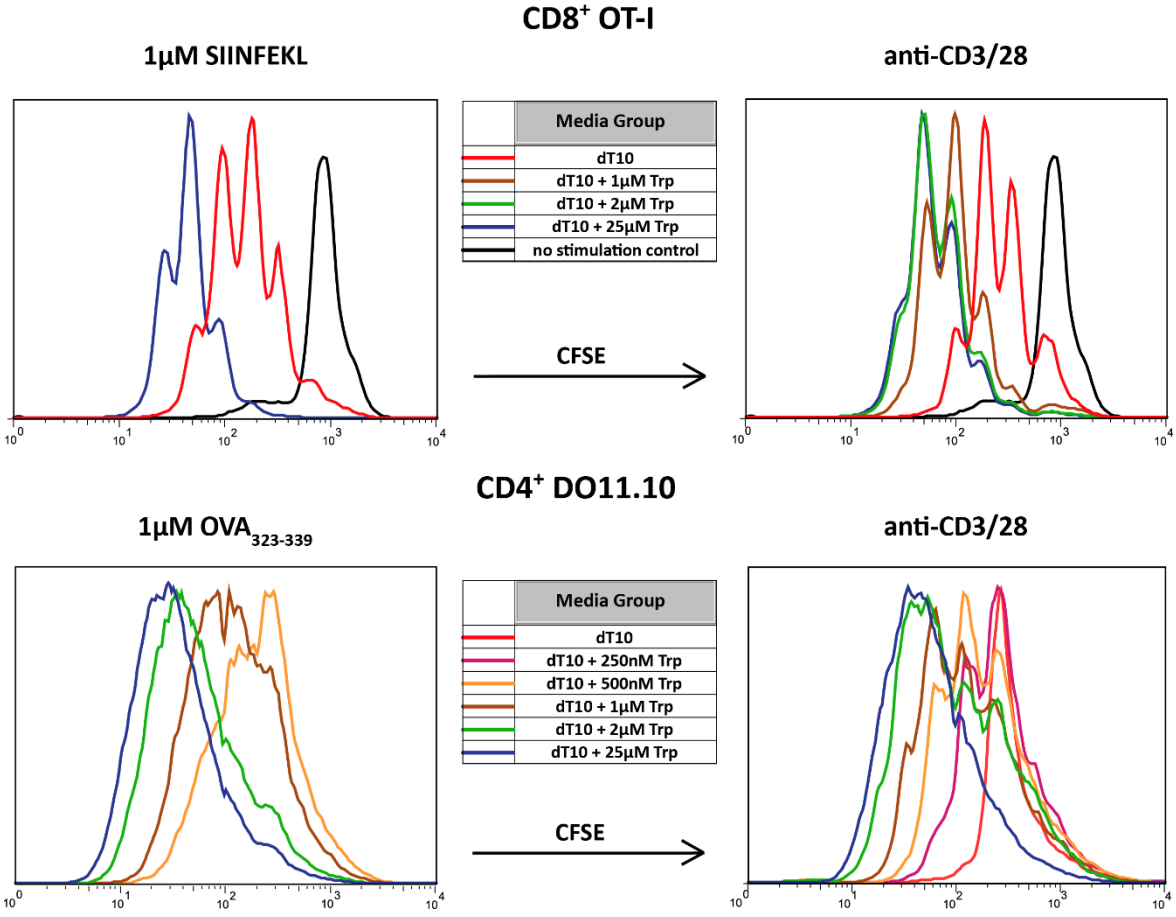

3.10a. Tryptophan deprivation inhibits proliferation in OT-I $CD8^+$ and DO11.10 $CD4^+$ splenocytes in response to activating stimuli. Typical histograms demonstrating the dramatic effect of tryptophan deprivation in inhibiting both $CD4^+$ ***(top panels)*** and $CD8^+$ ***(bottom panels)*** splenocyte proliferation in response to cognate peptide ***(left panels)*** or pre-coated plates with anti-CD3/CD28 ***(right panels)***.

3.10b. Murine CD8⁺ and CD4⁺ T cell proliferation in response to cognate peptide is directly related to available tryptophan.

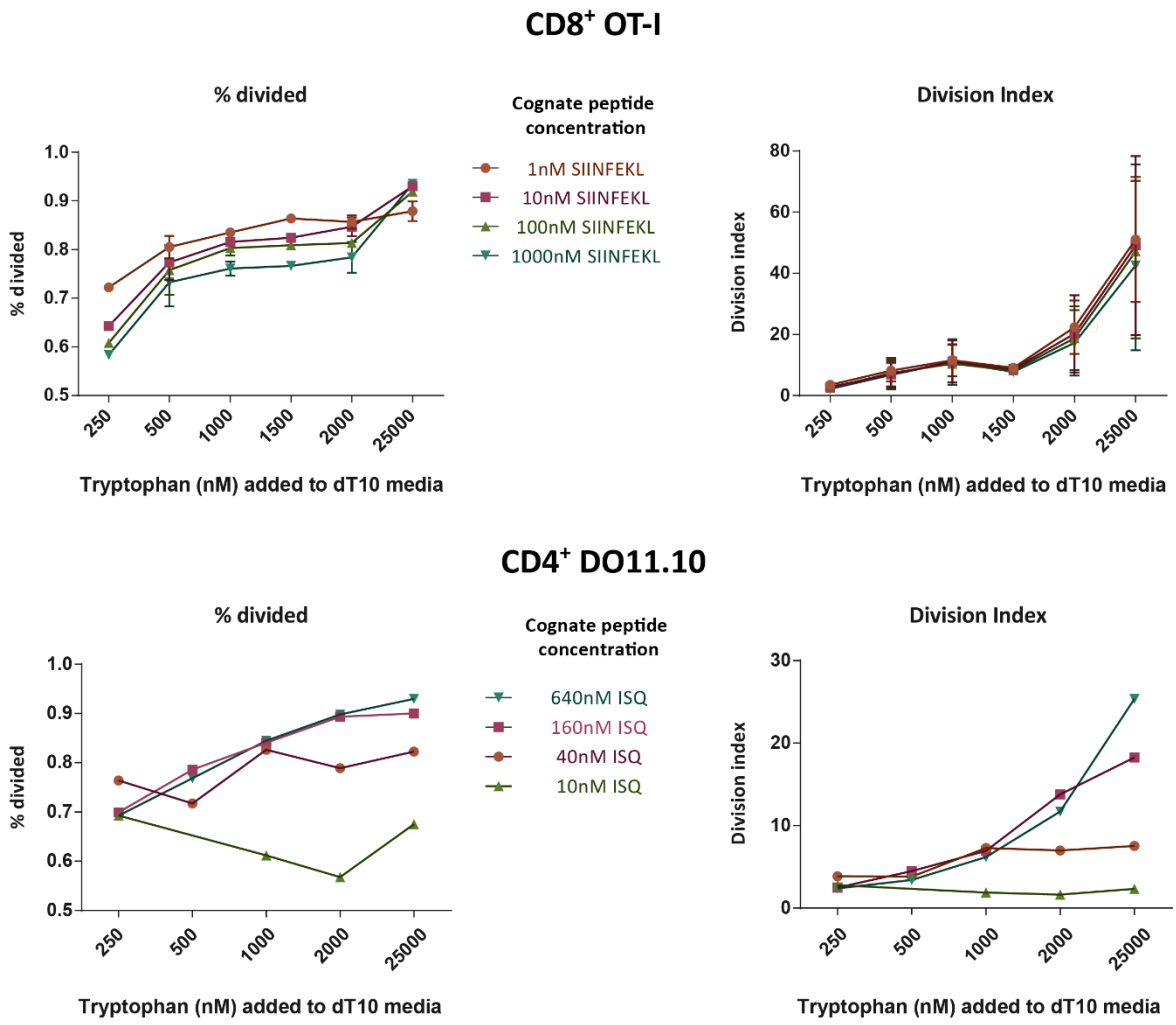

3.10b. The ability of CD8⁺ OT-I and CD4⁺ DO11.10 splenocytes to proliferate in response to cognate peptide is directly related to the available tryptophan in culture media.

Summary graphs demonstrating the inhibitory effect of tryptophan deprivation on splenocyte proliferation in response to stimulation by cognate peptide in the OT-I ***(top panels)*** and DO11.10 ***(bottom panels***) models. The left panels illustrate the (%) of the starting T cell population that divided whereas the right panels plot the division index (= total number of division in the given subpopulation / number cells in the starting culture)

The effect – as measured by the division index - was evident and highly statistically significant in all cases where the strength of stimulation was sufficient to trigger proliferation in >80% of the splenocytes.($p<0.001$ as measured by 2 way ANOVA).

At higher signal strengths in the DO11.10 model, higher tryptophan levels (>2µM) were necessary to achieve maximal proliferation.

3.11. CD25 expression in murine T cells is modified by tryptophan deprivation at early and late timepoints after stimulation by cognate peptide.

In order to further investigate the phenotypic effects of tryptophan deprivation on cognate peptide stimulated T cells a set of experiments was carried out looking at the surface expression of CD25. This is a surface receptor for IL-2; its surface expression is normally upregulated early after T cell activation; however in the presence of IL2 it is then internalised as it binds to its ligand so that after a few days only select subpopulations express it[138].

During early timepoints (<24h) after T cell stimulation with cognate peptide, tryptophan deprivation resulted in markedly decreased levels of CD25 surface expression both in the OT-I $CD8^+$ model and in the DO11.10 $CD4^+$ models. (Figure 3.11a.)

On the other hand 84 hours after stimulation continuous tryptophan deprivation had the exact inverse effect: high levels of CD25 expression were maintained in the tryptophan deprived groups, while surface CD25 was markedly downregulated in the tryptophan replete groups (Figure 3.11b.)

In both cases the size of the effect was proportional to amount of tryptophan available in culture media with at least 2μM tryptophan concentrations being necessary at baseline.

Figure 3.11. CD25 expression pattern following T cell stimulation by cognate peptide is altered by tryptophan deprivation

10^6 freshly harvested OT-I and DO11.10 splenocytes were plated in tryptophan depleted dT10 media in 96 well plates. At t=0 hours a pre-defined amount of cognate peptide and tryptophan was added to each well so that the final culture volume was 200µl. The cells were harvested after 18 hours, fixed permeabilised and stained for flow cytometric analysis.

3.11a.Tryptophan deprivation impedes early CD25 upregulation in response to cognate peptide in CD4⁺ and CD8⁺ murine splenocytes

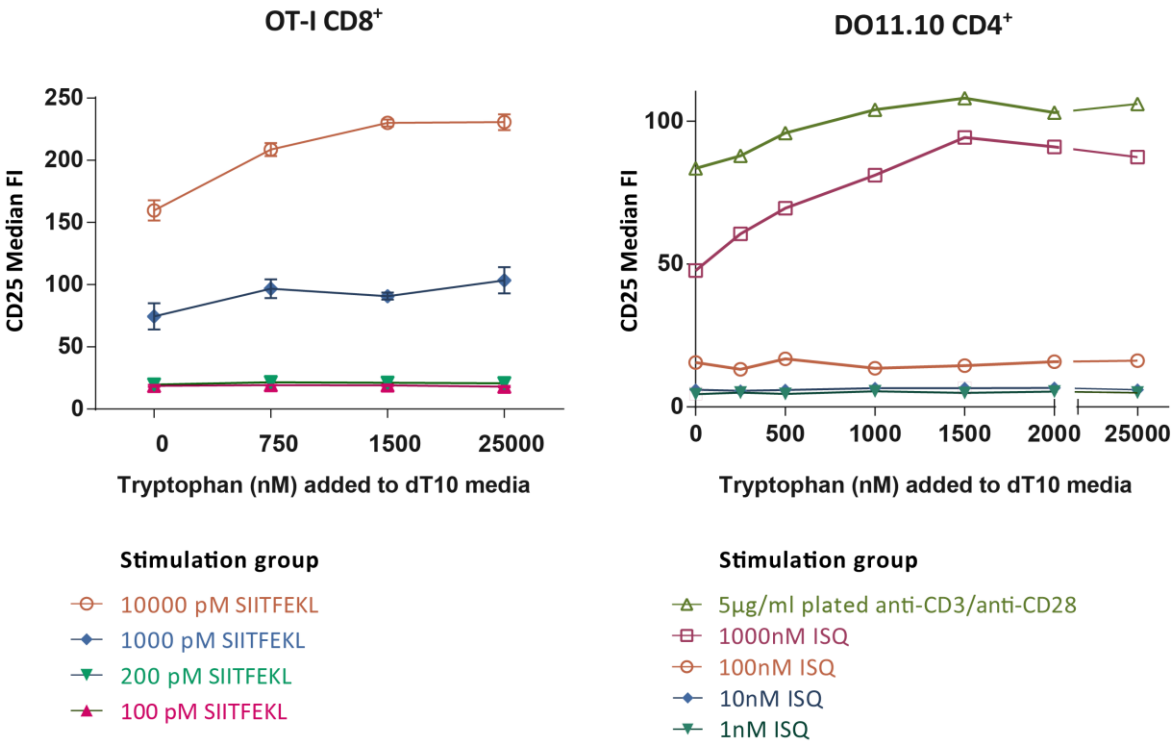

3.11a.Tryptophan deprivation results in reduced upregulation of surface expression of CD25 in CD8⁺ OT-I splenocytes and CD4⁺ DO11.10 splenocytes after 18 hours of stimulation by cognate peptide.

Summary graphs demonstrating the effect of different tryptophan concentrations in culture media on CD25 upregulation in CD8⁺ OT-I ***(left panel)*** and CD4⁺ DO11.10 ***(right panel)*** splenocytes after 18hours of stimulation with either 5µg/ml of anti-CD3/CD28 or a range of concentrations of cognate peptide (SIITFEKL for OT-I and $OVA_{323-339}$ ="ISQ" for DO11.10).

There was no significant effect detected for low cognate peptide concentrations that were in any case insufficient to elicit a significant CD25 upregulation. The effect was highly significant however at both the anti-CD3/CD28 stimulated groups and the 1µM $OVA_{323-339}$ group as well as the 1nM and 10nM SIITFEKL groups ($p < 0.0005$ in the 1µM $OVA_{323-339}$ group and <0.0001 in the SIITFEKL groups by Sidak's multiple comparisons test)

3.11b. Tryptophan deprivation delays CD25 downregulation 84 hours after stimulation by cognate peptide in murine T cells

Freshly harvested murine splenocytes were plated in 48well plates at a concentration of 10^6 / well in 1ml of tryptophan depleted dT10 media. At t=0 tryptophan and cognate peptide (SIINFEKL for OTI splenocytes and $OVA_{323-339}$ for DO11.10 splenocytes) was added in different concentrations in appropriate wells. At t=84 hours the cells were harvested, surface stained and fixed for flow cytometric analysis.

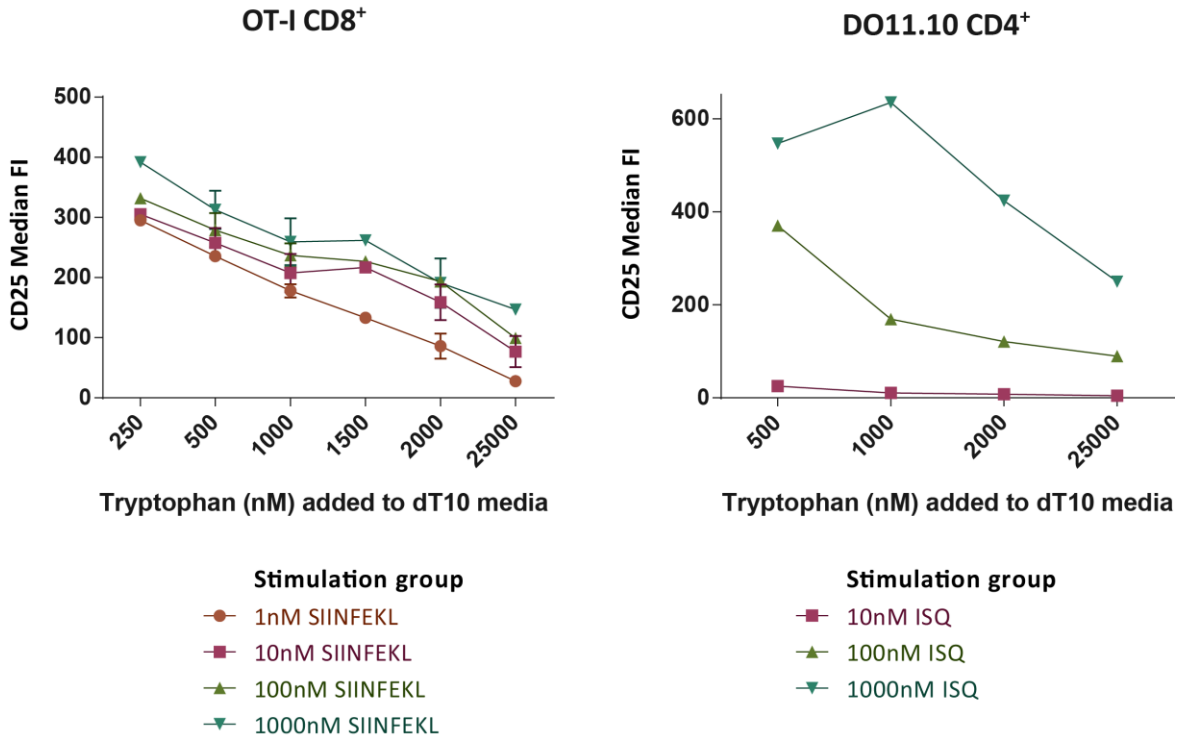

3.11b. Tryptophan deprivation prevents surface CD25 downregulation after 84 hours of stimulation with cognate peptide CD25 in $CD8^+$ OT-I and $CD4^+$ DO11.10 splenocytes.

Summary graphs demonstrating the effect of different tryptophan concentrations in culture media on surface CD25 expression in $CD8^+$ OT-I ***(left panel)*** and $CD4^+$ DO11.10 ***(right panel)*** splenocytes after 84 hours of stimulation with a range of concentrations of cognate peptide (SIINFEKL for OT-I and $OVA_{323-339}$ ="ISQ" for DO11.10).

In both the OT-I $CD8^+$ and DO11.10 $CD4^+$ T cell models there was a highly significant ($p<0.0001$ and $p<0.0002$ by 2 way ANOVA respectively) effect; tryptophan depleted groups exhibited much higher levels of CD25 surface expression than tryptophan replete groups.

3.12. Tbet expression in activated murine CD8$^+$ T cells is impeded by tryptophan deprivation.

Tbet upregulation is a critical event in T cell fate determination following stimulation [139] ; to investigate this further a series of experiments were carried out to investigate the effect tryptophan deprivation had on this process.

Stimulation of CD8$^+$ OT-I splenocytes by both plate bound anti-CD3/CD28 and cognate peptide resulted in significant Tbet upregulation after 84 hours that was significantly inhibited by culture in tryptophan depleted ("dT10") media (Figures 3.12a/b.). Again this was not an all or nothing event, the reduction was proportional to the amount of tryptophan in the media and at least 2µM tryptophan was needed to achieve the maximal Tbet response.

Furthermore, Tbet expression could be rescued by the late addition of tryptophan even if no additional tryptophan was present in the initial culture media for the first 48 hours after stimulation (Figure 3.12b.). In this type of experimental conditions the effect on Tbet expression closely followed the effect on mTORC1 pathway activation as expressed by phosphorylation of S6 at Ser240.

Subsequent experiments using the plated anti-CD3/CD28 stimulation model (Figure 3.12c.), demonstrated that continuous stimulation was not necessary for the rescue effect – splenocytes that were removed from the pre-coated plates and placed into fresh wells would also upregulate Tbet to the same extent as splenocytes that were left in the original wells.

In addition it was shown that mTORC1 pathway inhibition by rapamycin could partly but not completely prevent the rescue of Tbet expression by the late addition of tryptophan.

Figure 3.12. Tbet expression in stimulated OT-I CD8⁺ T cells is inhibited by tryptophan depletion

3.12a.Upregulation of Tbet expression in stimulated CD8⁺ splenocytes is inhibited by prolonged tryptophan deprivation

10^6 freshly harvested OT-I splenocytes were plated in 1 ml of tryptophan depleted dT10 media in 48 well plates pre coated with anti-CD3/ CD28. At t=0 tryptophan was added to each well. The cells were harvested after 84 hours, fixed, permeabilised and stained for flow cytometric analysis.

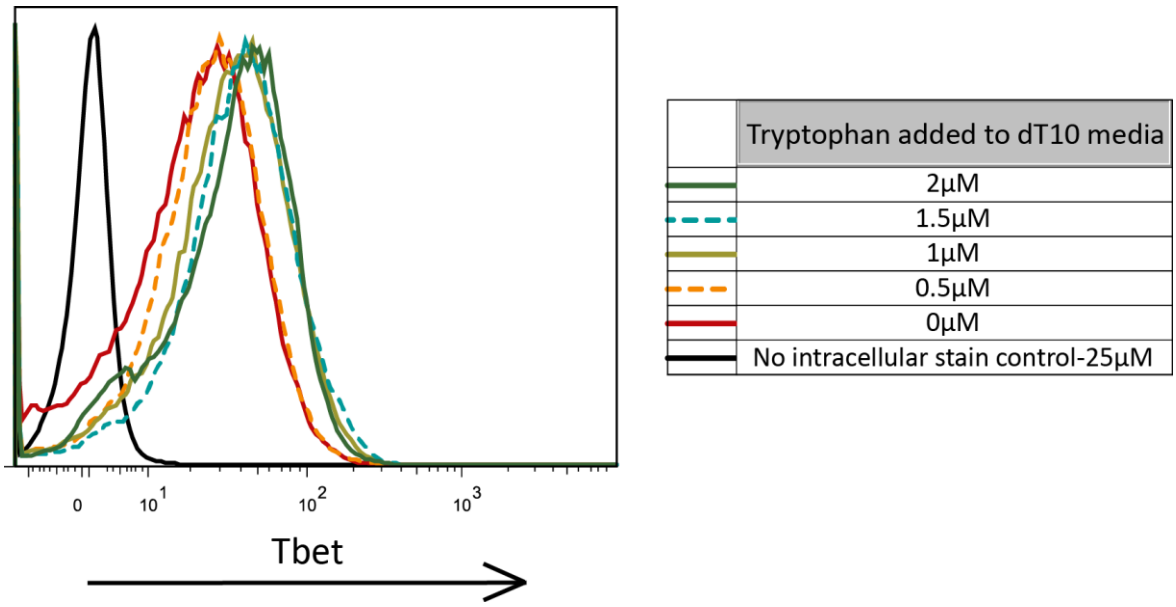

3.12a. Tbet expression in CD8b+ OT-I splenocytes after 84 hour of stimulation by plated anti-CD3/ CD28 is inhibited by tryptophan deprivation.

Typical histograms demonstrating Tbet expression of CD8b⁺ OT-I splenocytes cultured in media with different tryptophan concentrations.

3.12b. Late addition of tryptophan leads to mTORC1 pathway activation and rescues Tbet expression in OT-I CD8⁺ splenocytes stimulated by cognate peptide under low tryptophan conditions.

10^6 freshly harvested OT-I splenocytes were plated in 48 well plates in 1 ml of tryptophan poor T10 media. 1µM cognate peptide (SIINFEKL) was added to each well at t=0. After 48 hours a variable amount of tryptophan (+/- 20nM rapamycin for control groups) was added. The cells were harvested 15 hours later, fixed, permeabilised and stained for flow cytometric analysis.

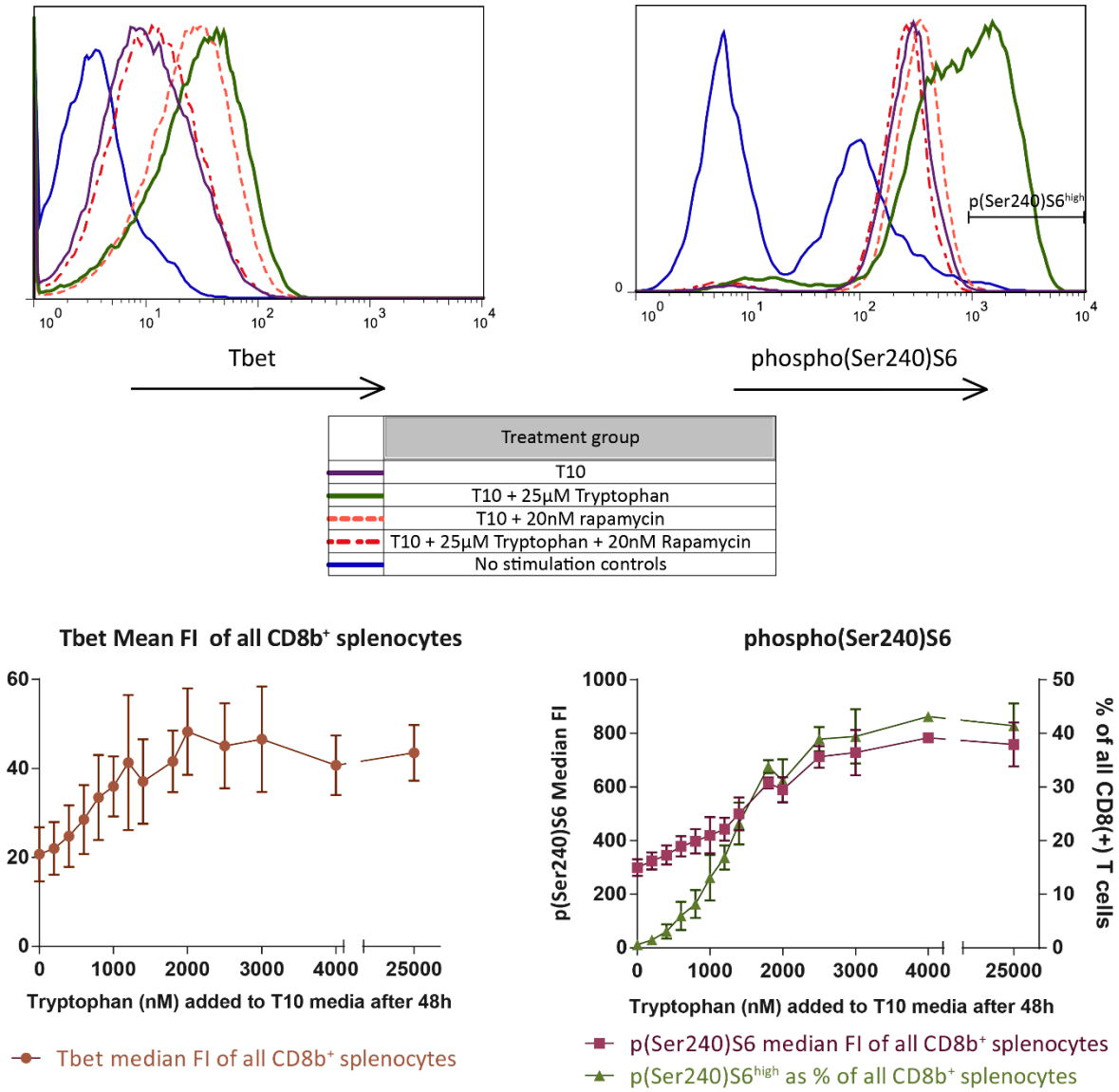

3.12b. Addition of tryptophan after 48 hours leads to late mTORC1 pathway activation and rescues Tbet expression in OT-I CD8b⁺ splenocytes stimulated by cognate peptide in tryptophan depleted media. Typical histograms ***(top panels)*** and summary plots **(bottom panels)** demonstrating how the addition of tryptophan even after 48hours of culture in tryptophan poor media results in increased Tbet expression in CD8b⁺ splenocytes ***(left panels)*** . This is mirrored by the effect on S6 phosphorylation at Ser240 ***(right panels)*** and both effects measured were highly statistically significant ($p<0.0001$ by 2 way ANOVA).

3.12c. Tbet rescue in response to tryptophan is not dependent on continuous stimulation and is partially inhibited by rapamycin.

10^6 freshly harvested OT-I splenocytes were plated in 1 ml of T10 in 48 well plates pre coated with anti-CD3/CD28. After 48 hours cells were either left in the original wells or moved to fresh wells not pre-coated with stimulating antibodies. In both groups a variable amount of tryptophan (+/- 20nM rapamycin for control groups) was added immediately afterwards. The cells were harvested 24 hours later, fixed, permeabilised and stained for flow cytometric analysis.

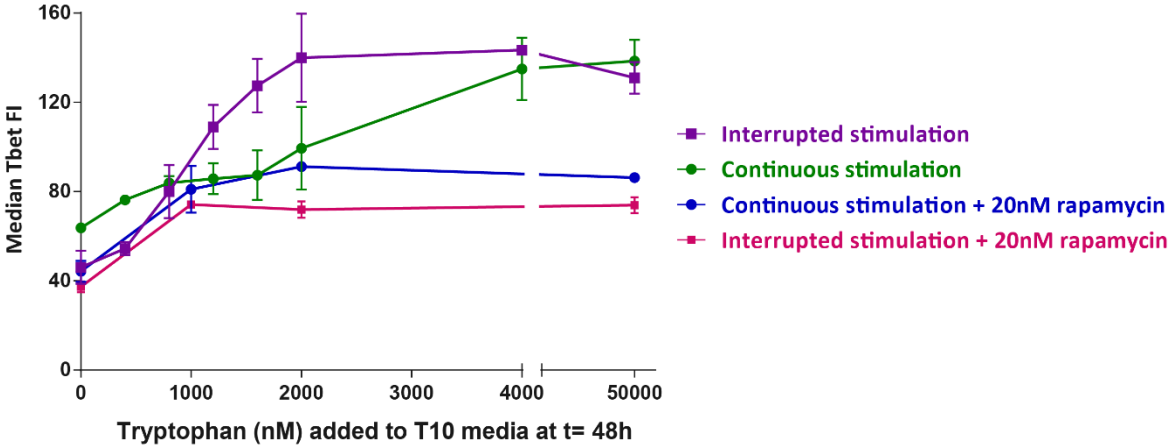

3.12c. The rescue of Tbet expression by the late addition of tryptophan to OT-I splenocytes stimulated under tryptophan deprived conditions is not dependent on the presence of continuous stimulation but is partially inhibited by rapamycin.

Summary results for $CD8b^+$ splenocytes confirming the highly statistically significant ($p<0.0001$ by 2 way ANOVA) effect of tryptophan rescue on Tbet expression regardless of whether there was continuing stimulation after tryptophan was added. There was no statistically significant difference in the extent of rescue between continuously stimulated groups and groups where the cells were removed from the pre-coated plates ($p=0.6736$ by 2 way ANOVA). Of note, while the addition of tryptophan did not completely prevent Tbet rescue in response to added tryptophan this was incomplete.

3.13. Tryptophan availability affects the size of the FoxP3^{+}CD25^{high} CD4^{+} subpopulation in murine CD4^{+} cells following stimulation by plated anti-CD3/CD28

To investigate the possibility that tryptophan depletion may contribute to the known effect of IDO expression in promoting Treg accumulation, experiments were carried out to investigate the effect of tryptophan deprivation on the size of the FoxP3^{+}CD25^{high} CD4^{+} subpopulation.

Initial experiments using BALBc splenocytes stimulated by plated anti-CD3/CD28 revealed that the relative size of the FoxP3^{+}CD25^{high} CD4^{+} subpopulation after 84 hours of continuous stimulation was significantly higher in splenocytes stimulated in tryptophan depleted media (Figure 3.13a/b.) – the relative size of the population almost doubled. Interestingly this effect was abrogated by adding as little as 2µM tryptophan as late as 48 hours after the onset of stimualtion. The addition of 20nM rapamycin at t=0 had a similar effect.

CFSE-staining based proliferation analysis of these subpopulations (Figure 3.13c.) revealed that cells within the FoxP3^{+}CD25^{high} CD4^{+} subpopulation proliferated in all treatment groups less well than the CD4^{+} population as a whole. Importantly however, tryptophan depletion did not affect their proliferation rate, while that of the CD4^{+} population as a whole was significantly affected.

This suggested that the expansion of this population was primarily as a result of the reduced proliferation of the FoxP3^{-} population.

The need for continuous stimulation for this effect to take place was assessed in experiments again utilising the plated anti-CD3/CD28 stimulation model (Figure 3.13d.). The addition of tryptophan as late as 48 hours after the onset of stimulation was sufficient to prevent the expansion of the FoxP3^{+}CD25^{high} CD4^{+} subpopulation, regardless of whether there was continuous stimulation or not from that timepoint forward. On the other hand , tryptophan added later than 72 hours did not prevent the relative expansion of this subpopulation regardless of the nature of stimulation.

Figure 3.13. Tryptophan depletion affects the size of the FoxP3^{+} CD25^{high} CD4^{+} subpopulation in stimulated murine T cells.

BALBc splenocytes were harvested, stained with CFSE and then immediately plated in 48 well plates pre-coated with anti-CD3/CD28 in 1 ml of T10 media. At t=0 and t=48 hours tryptophan and/or 20nM rapamycin were added to appropriate wells. The cells were harvested at t=84 hours, fixed, permeabilised and stained for flow cytometric analysis.

3.13a. Tryptophan depletion increases the relative size of the FoxP3^{+} CD25^{high} CD4^{+} population after 84hours of anti-CD3/CD28 stimulation

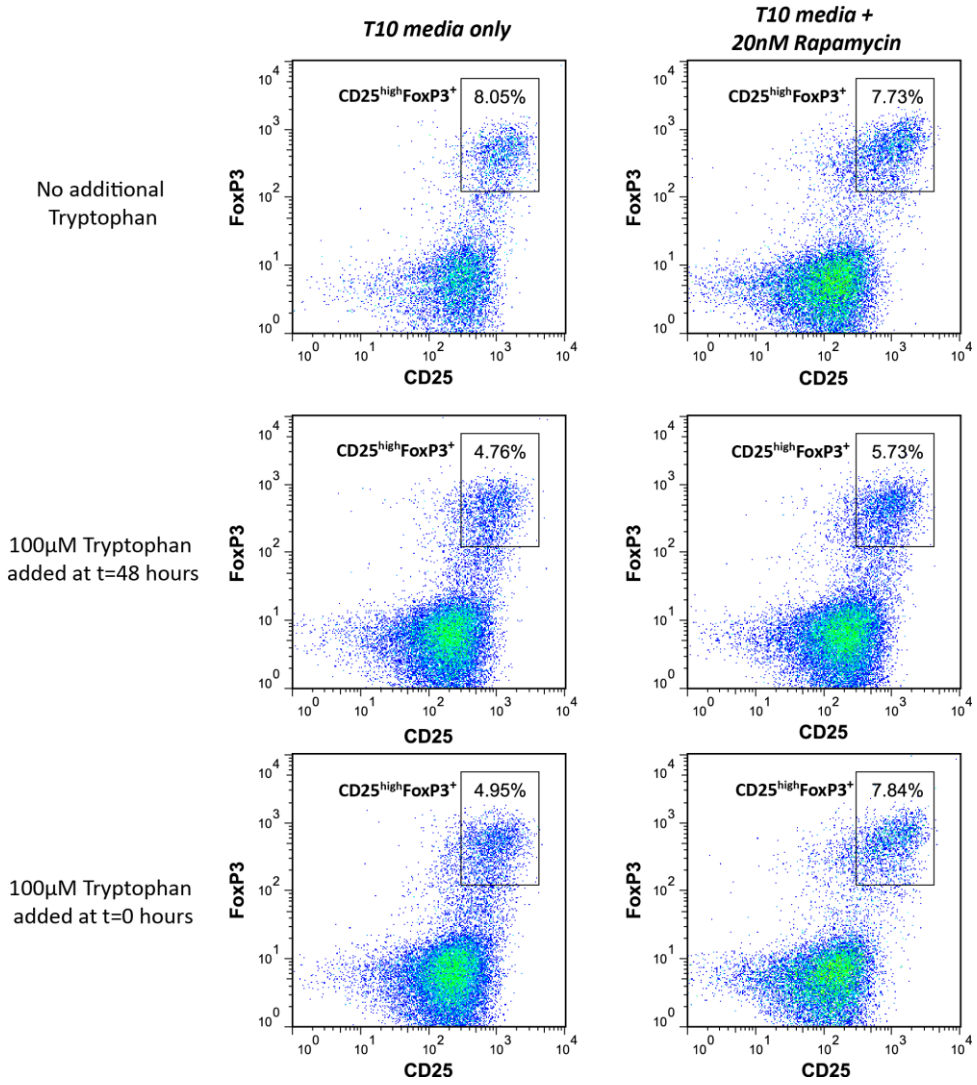

3.13a. Tryptophan depletion increases the relative size of the FoxP3+ CD25high CD4+ population after 84hours of anti-CD3/CD28 stimulation. Typical pseudocolor dot plots demonstrating that in tryptophan deprived groups the proportion of CD4^{+} splenocytes belonging in the CD25^{high}FoxP3^{+} subgroup was higher that in groups where tryptophan was added either straight away or even after 48 hours. The presence of rapamycin seemed to dull this effect, particularly when added at early timepoints.

3.13b. Tryptophan depletion increases the relative size of the FoxP3^{+} CD25^{high} CD4^{+} population after 84hours of anti-CD3/CD28 stimulation

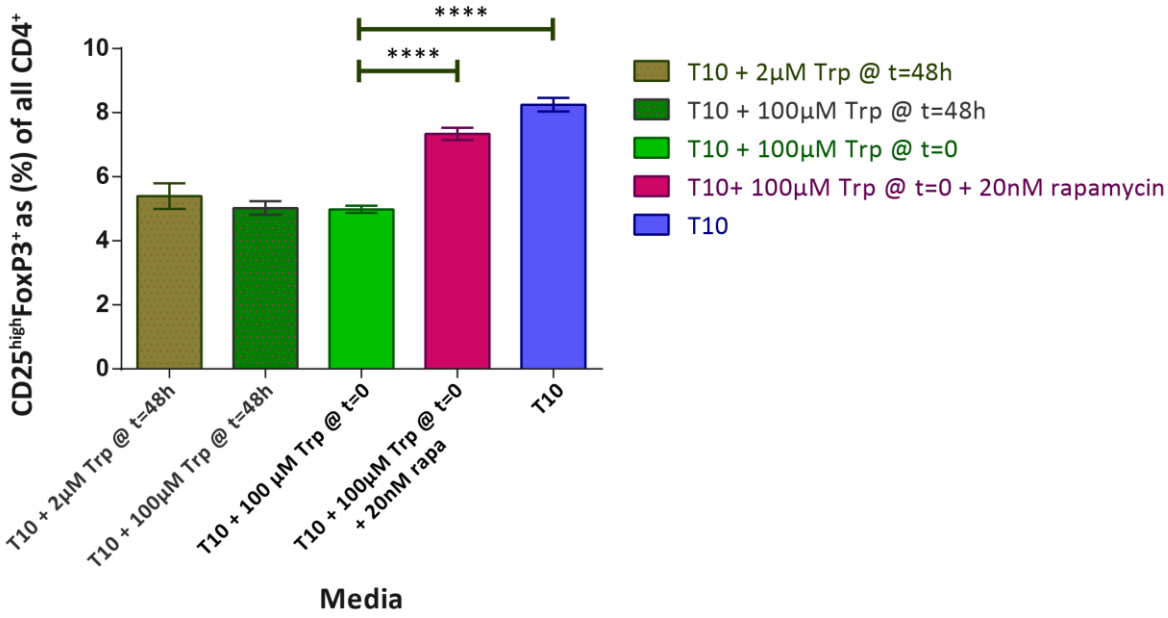

3.13b. Tryptophan depletion increases the relative size of the FoxP3+ CD25high CD4+ population after 84hours of anti-CD3/CD28 stimulation.

Summary graph demonstrating that the size of the CD4^{+}CD25^{high}FoxP3^{+} subgroup at 84 hours after the onset of stimulation is significantly ($p<0.0001$ by ANOVA) higher in the absence of tryptophan in culture media. The effect is reversed by the addition of at least 2µM tryptophan as late as 48 hours after the onset of stimulation and partially mimicked by the addition of rapamycin at t=0.

3.13c. Tryptophan deprivation does not affect the proliferative capability of the FoxP3⁺ CD25^{high} CD4⁺ subpopulation as much as the total CD4⁺ population.

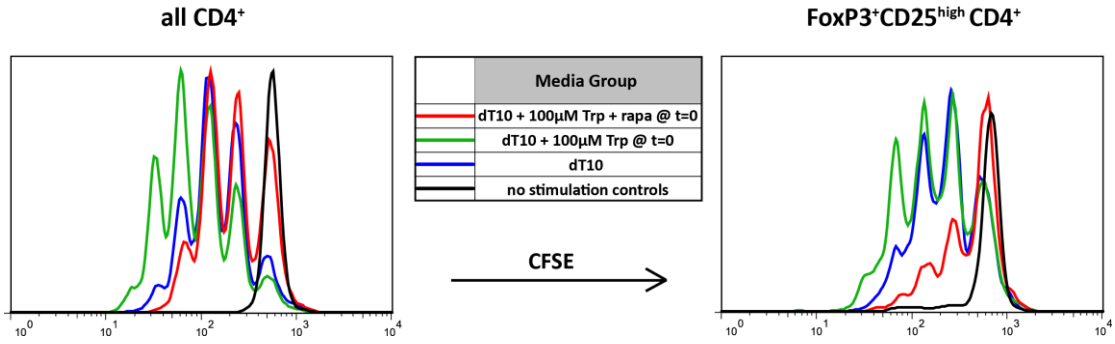

3.13c. The ability of FoxP3+CD25highCD4+ cells to proliferate is not significantly altered by tryptophan depletion in contrast to the ability of CD4⁺ cells as a whole.

(Top panels): typical histograms demonstrating the effect of tryptophan depletion on CD4⁺ T cells as a whole as compared with the CD25^{high}FoxP3⁺ subgroup.

(Bottom panels): Summary graphs of CFSE proliferation analysis revealing that even in the tryptophan replete groups, cells belonging to the CD25^{high}FoxP3⁺CD4⁺ subpopulation proliferated significantly less in response to stimulation by anti-CD3/CD28 as compared with the total CD4⁺ group. Interestingly however, the proliferation parameters of the CD25^{high}FoxP3⁺CD4⁺ subpopulation were much less affected by the presence or absence of tryptophan in media; this was in stark contrast to the effect on the whole CD4⁺ group where as previously shown tryptophan depletion resulted in significant inhibition of proliferation.

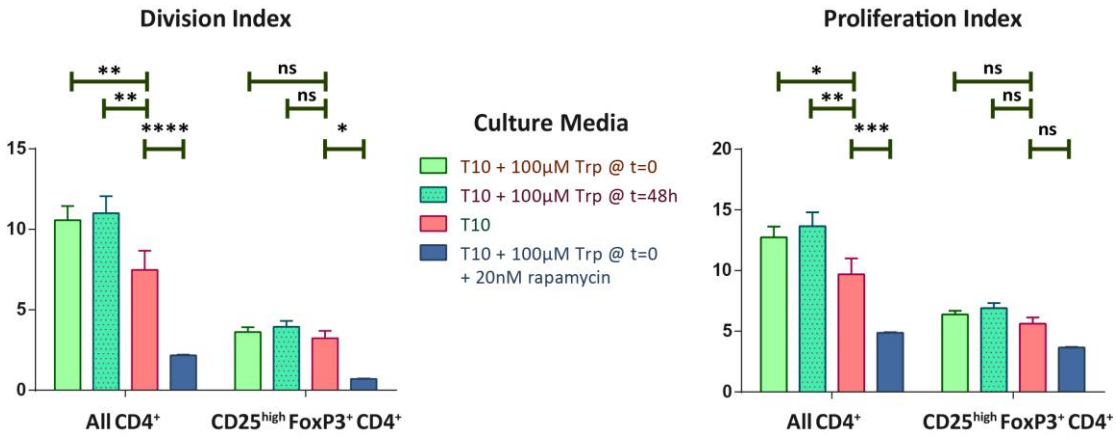

3.13d. The effect of tryptophan depletion on the CD25^{high}FoxP3^{+}CD4^{+} splenocyte population is not dependent on continuous stimulation

DO11.10 splenocytes were harvested and then immediately plated in 48 well plates pre-coated with anti-CD3/CD28 in 1 ml of T10 media. At t=72hours the wells were split 1:1 with fresh T10 media so that half the cells were left in the original wells and half were replated in new uncoated wells. Tryptophan was added to some wells at t=0, 48 or 72 hours. The cells were harvested 2 days later at t=108 hours, fixed, permeabilised and stained for flow cytometric analysis.

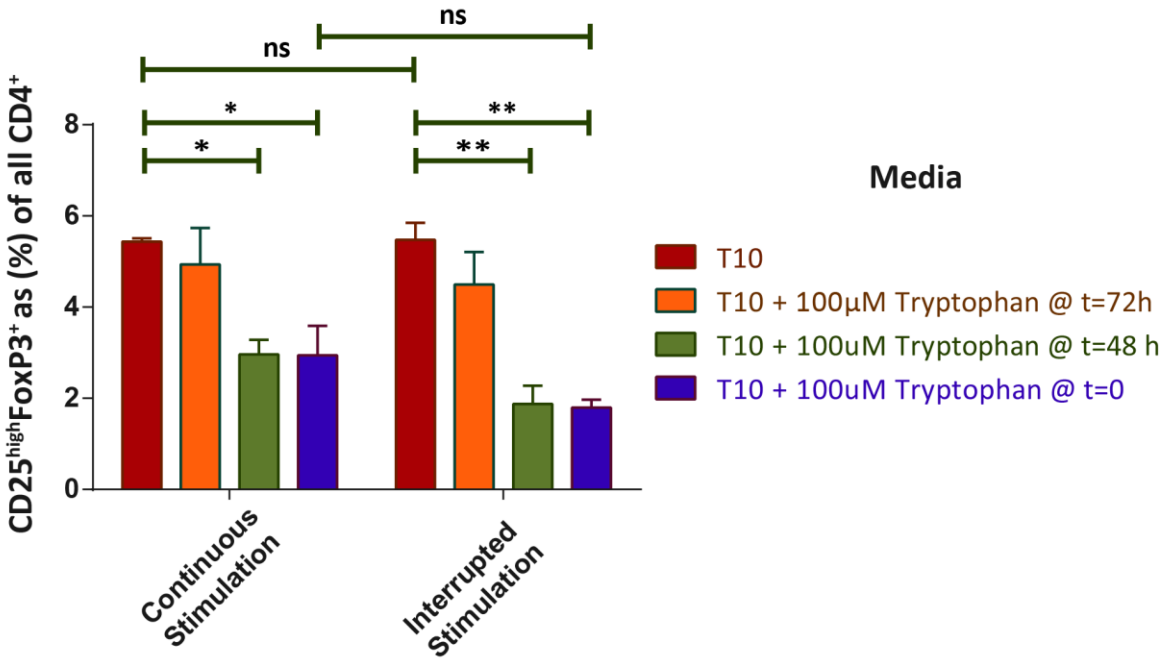

3.13d. Continuous stimulation by anti-CD3/CD28 is not necessary for the effects of tryptophan depletion on the relative size of the CD25^{high}FoxP3^{+} CD4^{+} splenocyte population.

Summary graphs reconfirming the effect of tryptophan deprivation on the realtive size of the CD25^{high}FoxP3^{+} CD4^{+} subpopulation that remained significant in the treatment groups exposed to both continuous and interrupted anti-CD3/CD28 stimulation ($p<0.05$ and $p<0.005$ respectively by 2-way ANOVA with Sidak's multiple comparisons test). Interruption of stimulation by anti-CD3/CD28 did not cause a significant difference in the relative size of CD25^{high}FoxP3^{+} CD4^{+} subpopulations when groups with similar exposure to tryptophan in the media were looked at.

3.14. Lack of tryptophan modifies the secreted cytokine profile of $CD8^+$ T cells stimulated by cognate peptide.

To further investigate the physiological effects of tryptophan depletion on activated T cell function ELISA assays were done on supernatants of OT-I splenocytes stimulated with SIINFEKL peptide. In supernatants from cultures of splenocytes stimulated by cognate peptide in tryptophan depleted media levels of IFN-γ and IL-2 were reduced and this was detectable as early as 11hours after the onset of stimulation and could be seen as late as 36 hours.

The effect was more obvious and highly statistically significant for IFN-γ; it could be reproduced by the addition of 20nM rapamycin or 100nM pp242 in tryptophan replete media – a typical experiment is shown in (Figure 3.14.).

Figure 3.14. Tryptophan depletion reduces cytokine production by OT-I CD8⁺ splenocytes in response to stimulation by cognate peptide.

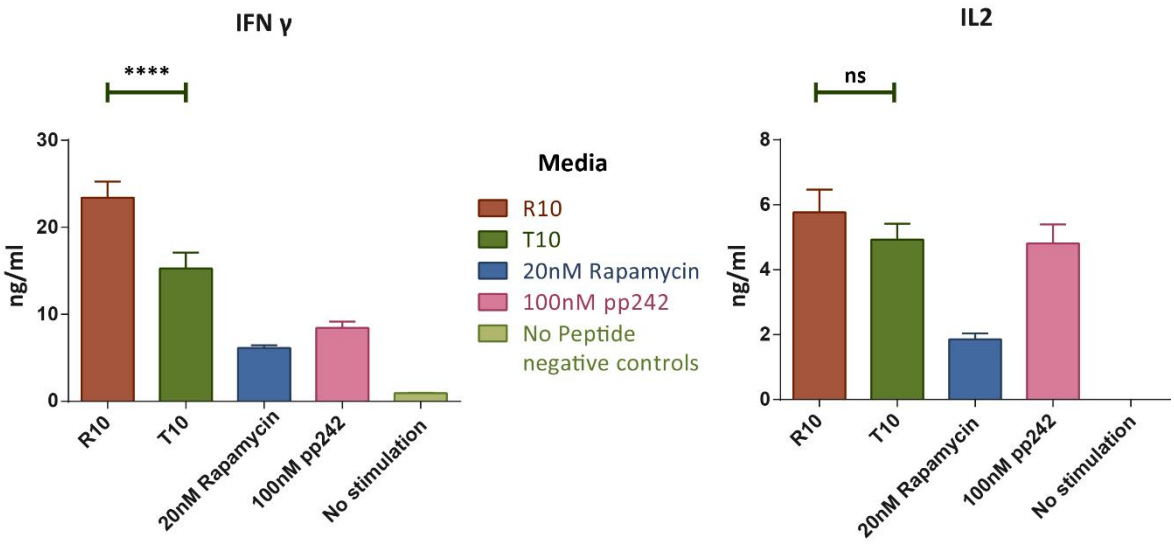

3.14. Culture in tryptophan depleted media reduces IFN-γ and IL2 production of OT-I splenocytes stimulated by cognate peptide.

OT-I splenocytes were harvested and freshly plated at 10^6/well in 96 well plates in media with ("R") or without ("T") 25μM tryptophan. 20nM rapamycin and 100nM pp242 were added to specific wells. Supernatants were harvested at 17 hours and analysed by ELISA for the presence of IFN-γ **(left panel)** and IL2 **(right panel).** The reduction in IFN-γ production as compared to the R10 control group was highly significant in all groups ($p<0.0001$ by Sidak's multiple comparisons test). IL2 production was also reduced but this experiment was underpowered to reach statistical significance.

3.15. Discussion

3.15.1. Cell fate and the mTORC1 pathway in murine T cells

Activation of the mTORC1 pathway in T cells occurs early in response to engagement of cognate peptide to the T cell receptor (TCR), however the extent of activation depends to a large extent on the immunological context – parameters such as the presence of co-stimulatory surface molecules or cytokines and whether the T cell in question is naïve or not can significantly alter the temporal and intensity pattern of mTORC1 activity.

This is to be expected with mTORC1 being at the crossroads of several pathways integrating nutrient availability and growth signalling information to guide the cellular metabolic response to its environment. Importantly, it appears that at least in T cells this pathway has an additional role: an increasing body of evidence is now painting a picture where mTORC1 activity acts as a rheostat that determines the fate of the activated T cell and guides its decision to follow a specific specialisation route (e.g. cytotoxic vs. memory) or become anergic and refractory to further stimulation.

3.15.2. Hypothesis: Tryptophan depletion alters the response of the mTORC1 pathway in murine T cells to stimulation by cognate peptide and alters their developmental fate

IDO expression has been shown to have a number of effects on T cells such as an increase in the population of regulatory T cells and reduction in cytotoxic T cell activity and numbers. As this closely corresponds to the effects seen under conditions of mTORC1 inhibition, the question arose as to whether IDO's immunomodulatory effects on T cells can be mediated in a large part via its tryptophan depleting action on the local microenvironment.

This forms the underlying hypothesis around which the experiments described in the second and third chapter of this thesis were designed; in the second chapter the focus is on using murine models that allow a more physiological approach to look at events following T cell stimulation by cognate peptide

3.15.3. Choice of experimental systems and methods

While activation of freshly harvested T cells from murine spleens with plated stimulating anti-CD3 and anti-CD28 antibodies ("anti-CD3/CD28") provides a quick and relatively reliable way to access large homogenously activated T cell populations, there was the risk that this type of activation is not physiological and might not accurately reflect the signalling processes occurring during cognate peptide mediated TCR activation; in particular the effect of antigen presenting cells could not be modelled and signalling strength was fixed.

Fortunately at this point in time there are several transgenic mice strains available that have been genetically engineered to express high levels of TCRs for which cognate antigens are well defined. The OT-I and DO11.10 strains have been designed to recognise specific fragments of ovalbumin presented by MHC class I molecules in the former and MHC class II molecules ion the latter case. They therefore present ideal models for $CD8^+$ and $CD4^+$ T cell activation by cognate peptide respectively.

The ability to use cognate peptide allowed experimental designs were signalling strength could be varied in terms of peptide concentration, but more importantly in the OT-I model by using peptides with different affinities for the transgenic TCR as these are well described in the literature[137] .

While initial experiments used bone-marrow derived dendritic cells ("BMDCs") pre-pulsed with antigenic peptides, subsequent experiments confirmed that these were not essential due to the presence of DCs in the spleens and resulted in similar levels of T cell activation. In later experiments peptides were therefore added directly to media as this removed an additional element of variability – the quality of the BMDCs – and reduced the number of animals needed for the experiments.

Tryptophan-free RPMI was again utilised as the basis for culture media, as it allowed controlling the amount of tryptophan available in culture. For experiments where fine tuning tryptophan levels was important and in particular where the target starting tryptophan concentration in media was sub 2µM, dialysed FCS was used to make up

experimental media as stimulation and proliferation of splenocytes in <10% FCS containing media was suboptimal.

In terms of techniques the use of flow cytometry was essential as it allowed co-culture of multiple cell types together in a more physiological setting without the need for complicated sorting procedures pre-stimulation or pre-harvesting that would run the risk of modifying the readout variables – phosphorylation of S6 in particular can change relatively rapidly in response to cell stress and the staining protocol had to be optimised to minimise the time harvested cells were exposed to washing/staining steps prior to fixation.

An additional benefit of multicolour flow cytometry is that it allowed simultaneous analysis of different T cell populations at the cellular level with multiple quantifiable readouts; up to 9 stains could be used concurrently and depending on the specific setup 4-5 of them could be used as experimental readouts. This was of particular value in the case of proliferation analysis where CFSE labelling allowed a direct comparison of the effects on different subpopulations within the same treatment groups.

3.15.4. Significance of results

The initial pilot experiments determined the optimal protocol to be used for detecting mTORC1 activity in murine splenocytes by flow cytometry and confirmed that in both the OT-I and DO11.10 model systems the mTORC1 pathway was activated upon stimulation by cognate peptide in $CD8^+$ and $CD4^+$ T cells respectively.

In addition CD69 was confirmed to be an early marker of T cell activation that was not affected by mTORC1 inhibition; it could therefore be used in subsequent experiments to identify the subset of T cells activated by a given stimulus.

An early observation that could be made based on this fact was that on a cellular level all activated cells – as defined by cells exhibiting increased levels of surface CD69 - expressed similar levels of mTORC1 at a given timepoint and in the presence of normal culture media; on a population level mTORC1 activity levels - as expressed by

phosphorylation of S6 at Ser240 – were directly proportional to the extent of CD69 activation.

To further define the events taking place after TCR engagement by cognate peptide, timecourse experiments were carried out; these confirmed that early downstream events leading to phosphorylation of mTOR itself at Ser2481 – thought to be important for further downstream mTORC1 activity – took place as early as 20 minutes after activation; early evidence of mTORC1 activity itself in the form of S6 phosphorylation at Ser240 could be seen as soon as 30 minutes after stimulation.

However, not all T cells were activated at the same time – even under optimal stimulating conditions it took more than 7 hours for the majority of T cells to exhibit elevated levels of S6 phosphorylation; moreover mTORC1 activity as measured by the median fluorescent intensity (MFI) of phospho(Ser240)S6 continued to increase all the way up to 24 hours after stimulation and this was mirrored by increased levels of phosphorylation of mTOR at Ser(2481).

Using standard media it was difficult to follow patterns of mTORC1 activity for longer than 24 hours unless low cell plating concentrations were used as nutrients – and in particular tryptophan – became limiting. What's more, if tryptophan or FCS depleted media were used, after an initial period of inhibition a paradoxical spike of mTORC1 activity could be detected; this is likely related to a feedback effect triggered by initiation of autophagy under these conditions and has been previously described in the literature.

In any case initial experiments clearly indicated that culture in tryptophan depleted media did result in reduced mTORC1 activity within 12 hours after the onset of stimulation by high levels of high affinity peptide in both $CD4^+$ and $CD8^+$ T cells

A series of experiments subsequently tried to clarify the effects of tryptophan depletion under conditions where stimulation was of lower intensity – either in terms of cognate peptide concentration, affinity or both. From these experiments a number of important observations could be made:

Firstly at low tryptophan concentrations (<2μM) there was a similar linear dose response curve between tryptophan concentration and mTORC1 activity to that seen in the tumour cell lines. On one hand the baseline and maximum levels of mTORC1 activity depended critically on the strength of the stimulus; below a level sufficient to trigger CD69 upregulation, no significant mTORC1 activity could be detected. On the other hand, even in cells showing evidence of activation in terms of raised CD69 levels, mTORC1 activity was significantly reduced in the absence of tryptophan and the effect was if anything more prominent under strong stimuli. Finally, when low affinity stimuli were used, tryptophan deprivation actually resulted in a lower proportion of $CD8^+$ T cells becoming activated in terms of CD69 upregulation – this effect was not seen in $CD4^+$ T cells as no well-defined lower affinity peptides were available to be used when these experiments were carried out.

These findings suggest that tryptophan has a permissive effect on mTORC1 activation in both $CD4^+$ and $CD8^+$ T cells; the triggering stimulus has to come from the TCR, however in the absence of sufficient tryptophan availability mTORC1 activity is dramatically inhibited.

The fact that low tryptophan concentrations also impede $CD8^+$ T cell activation in the presence of low concentrations of low affinity peptides is particularly relevant with regards to tumour immunomonitoring , as this is exactly the situation that is likely to arise in the tumour microenvironment: tumour cells expressing high affinity neoantigens at high densities are likely to become rapidly eliminated in any case; it is cancer cells expressing low levels of weekly immunogenic antigens that are more likely to escape and cytotoxic lymphocytes would effectively become anergic against them under conditions of tryptophan depletion.

In any case, further experiments showed that even T cells that become activated under low tryptophan conditions are significantly affected; their proliferative capability is dramatically impaired as is their ability to secrete proinflammatory cytokines.

In addition, in $CD8^+$ T cells Tbet expression is significantly reduced by 72 hours after the onset of stimulation under tryptophan depleted conditions. This effect is

reversible by the addition of tryptophan as late as 48 hours after the onset of stimulation and this rescue is not dependant on ongoing stimulation.

Interestingly, adding tryptophan at this time point also stimulated the mTORC1 axis with a virtually identical dose response curve. Similar to the results in tumour cell lines was this was almost linear in the 0-1µM range and there was even a hint of a brief "dip" in the 1-2µM range, possibly suggestive of similar feedback mechanisms relating to the GCN2 pathway kicking in.

In $CD4^+$ cells the most dramatic effect was seen in the $FoxP3^+CD25^{high}$ subpopulation that is traditionally thought to comprise mainly of T_{reg} cells. There was a significant relative expansion of this population under low tryptophan conditions. While the question of the provenance of these cells was not directly addressed, proliferation analysis suggested that the proliferation rate of the $FoxP3^+CD25^{high}$ population was not significantly altered by tryptophan deprivation - in stark contrast to the effect on the overall $CD4^+$ population that were significantly impeded. This effect was also not dependent on continuous stimulation and adding tryptophan as late as 48 hours after the onset of stimulation would prevent this expansion regardless.

3.15.5. Outstanding issues

Overall, the effects of tryptophan deprivation on stimulated $CD4^+$ and $CD8^+$ murine T cells fit in well with what the expected effects of IDO expressing cells in lymphocytic populations in the whole animal and it is highly likely that tryptophan depletion is responsible to a large part for these effects.

Unfortunately, it was not possible to repeat the experiments using media pre-conditioned by IDO expressing cells similar to those described in for human lymphocytes in the third results chapter as this would have clarified the role of kynurenine and its metabolites. A few pilot experiments were carried out but were hampered by a number of practical issues, the most important of which was the relative low levels of IDO expression in the EG7-IDO transfected cell line; this combined with this cell line's rapid growth rate resulted in media that were depleted

of multiple nutrients as well as tryptophan and not suitable for use. A newly cloned EG7 line expressing high levels of constitutive IDO activity was derived but couldn't be used due to a lack of time.

A more important issue is the nature of the detected expanded $FoxP3^{+}CD25^{high}$ subpopulation; a number of open questions remain, the most important of which are whether this population is expressing FoxP3 stably, and whether it behaves functionally like a regulatory T cell population.

The role of Tbet in the $CD4^{+}$ T cell population unfortunately couldn't be assessed in the current set of experiments due to difficulties in establishing a staining panel that would allow simultaneous measurement of the $FoxP3^{+}CD25^{high}$ population, CFSE staining and Tbet, however it should be trivial to assess on its own in future experiments or with the use of more advanced flow cytometers.

An additional point worth commenting on is that throughout these experiments it was assumed that phosphorylation of S6 at Ser240 directly reflects mTORC1 activity. While this is certainly the case to a large extent – and rapamycin negative controls were used in all experiments where this was measured to confirm this is true – there was evidence of the role of additional pathways leading to S6 phosphorylation at Ser240 as in some cases rapamycin could not reduce phosphorylation levels to those seen in unstimulated T cells.

It is important to note that the used of dialysed media was mandated by the need to investigate extracellular tryptophan concentrations in the 0-2µM range that would be impossible to achieve using normal media. While it is conceivable that some of the effects described in these experiments could be attributable partially to the lack of other micronutrients or low molecular weight growth factors, experiments using normal FCS based media yielded similar results, particularly where complete tryptophan depletion was achieved through prolonged culture of active IDO expressing cell lines. This issue was partially addressed in the human setting via the use of normal FCS media pre-conditioned by tryptophan-consuming cell lines as seen in Chapter 4, and a similar approach could be used in the murine setting to strengthen these findings.

Chapter 4. The effects of tryptophan depletion on the m-TOR pathway in human T cells and subsequent T cell fate.

4.0. Introduction

The experiments described in the previous chapter illustrated the effects murine splenocytes would experience when exposed to tumour microenvironments where there is sufficient IDO activity to deplete tryptophan. In order to find out if these findings held true in the human immune system a series of experiments were devised to identify and optimise a model of T cell stimulation that would allow the same parameters to be measured as in the mouse models.

Once this was achieved, a series of experiments could be carried out initially utilising T cells derived from healthy human volunteers and then from melanoma patients to assess the validity and reproducibility of the findings.

In a final set of experiments, the direct effect of IDO activity was assessed by utilising a model where media were preconditioned by culture with IDO expressing cells and then used for culture of stimulated human lymphocytes.

4.1. Optimising experimental methods for investigating the effect of tryptophan deprivation and IDO activity on human T cells.

In the murine setting transgenic models (such as OT-I and DO11.10 mice) allow the use of cognate peptide to stimulate T cells under different conditions to investigate the effect changes in the microenvironment such as IDO activity have on the processes triggered by this activation.

In the human setting this is clearly not feasible; while immortalised human T cell lines expressing uniform T cell receptors exist, the changes needed to allow these cells to survive in long term cultures make it difficult to be able to extrapolate any findings regarding signal transduction pathways to cells freshly collected let alone to in the vivo situation.

Therefore an effort was made to develop an experimental model where freshly isolated human T cells could be used without the need for any additional manipulation other than stimulation.

Several different techniques exist in the literature for the non-antigen specific stimulation of human T-cells, the most common ones being the use of stimulating anti-CD3 antibodies together with stimulating anti-CD28 antibodies ("anti-CD3/CD28"), the use of PHA and the use of PMA-Ionomycin.

As tryptophan depleted dT10 media (made using tryptophan-free RPMI1640 and dialysed FCS) was planned to be utilised for experiments where the role of starting media tryptophan concentration was going to be a variable, this rather than standard R10 media was used for this set of experiments to establish the optimal conditions for stimulating human T cells

In the first instance the optimal protocol for using pre-plated anti-CD3/CD28 was sought via a series of experiments (Figure 4.1a.) A plating concentration of 10µg/ml anti-CD3 and 5 µg/ml anti-CD28 was found to offer the best combination of stimulation as measured by the percentage of $CD4^+$ and $CD8^+$ cells upregulating CD69 after 18 hours and proliferation as measured by CFSE staining after 60hours.

Phosphorylation of S6 at Ser240 could also be detected optimally at this concentration which was therefore used for further experiments.

Use of anti-CD3/CD28 at these plating concentrations was then compared with both PMA/Ionomycin and PHA as methods for non-specifically stimulating human PBL derived splenocytes (Figure 4.1b.-c.).

PMA/Ionomycin resulted in consistently high levels of T cell activation; however it also resulted in very high levels of mTORC1 pathway activation that were only marginally suppressible by rapamycin (Figure 4.1b.). Furthermore when used for proliferation assays there was significant downregulation of CD4 surface expression (Figure 4.1c.) greatly limiting its usefulness in flow cytometry experiments with $CD4^+$ populations as readouts.

The use of PHA on the other hand resulted in consistently lower levels of CD69 upregulation as compared with anti-CD3/CD28 (data not shown). Unfortunately, it could not be used in CFSE assays due to excessive toxicity (figure 4.1c.).

As the planned experiments would involve both manipulation of the mTORC1 pathway, CFSE labelling and flow cytometry based analysis of unseparated PBL, it was therefore decided to use plated anti-CD3/CD28 for all future studies using human T cells.

Figure 4.1. Stimulating anti-CD3/CD28 is the optimal method for non-specifically activating human T cells

96 well plates were pre-coated with human stimulating anti-CD3 and anti-CD28 antibodies ("anti-CD3/CD28") diluted in PBS in concentrations ranging from 1 to 10µg/ml. 10^6 freshly collected human blood cone derived PBL were plated in each well in 200µl of dT10 tryptophan depleted media with the addition of tryptophan to a final concentration of 25 µM and fixed, stained and analysed by flow cytometry.

4.1a. Human PBL stimulated by plated anti-CD3/CD28 activate their mTORC1 pathway

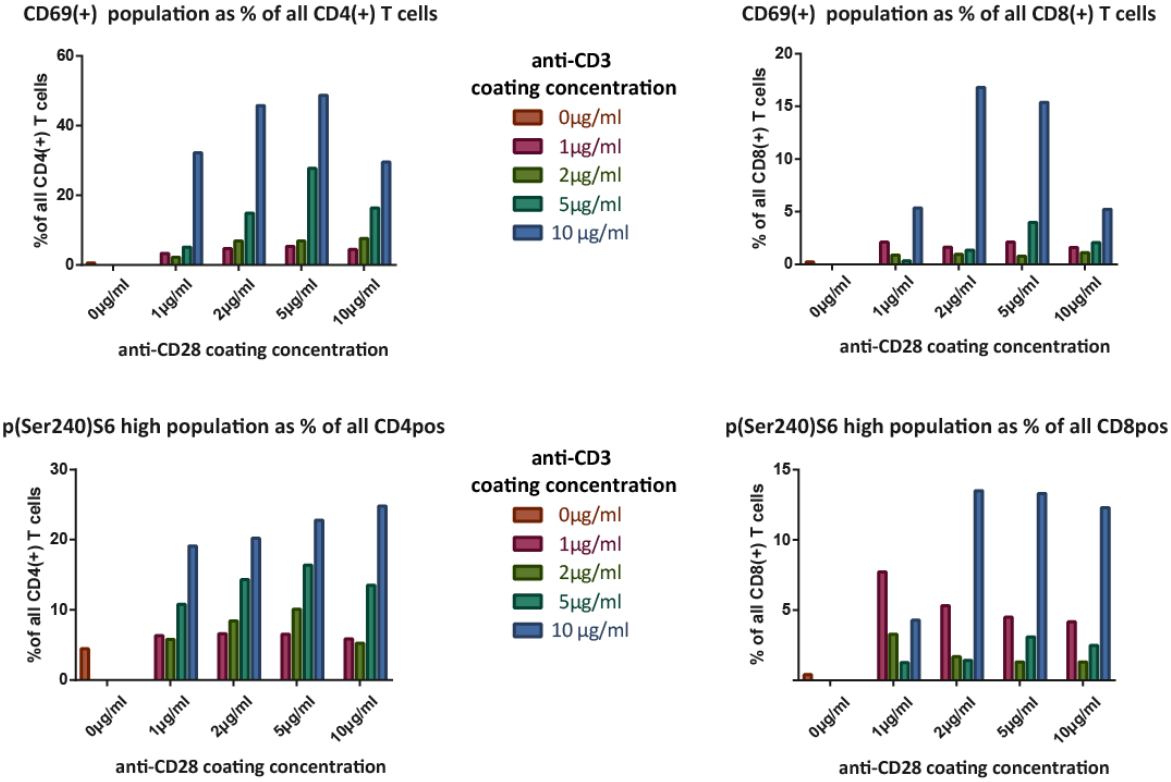

4.1a. Human PBL are stimulated by plated anti-CD3/CD28 as seen by surface CD69 expression with a concomitant increase in S6 Ser240 phosphorylation levels. Summary graphs demonstrating $CD4^+$ ***(left panels)*** and $CD8^+$ ***(right panels)*** T cell activation in terms of surface CD69 expression ***(top panels)*** and phosphorylation of S6 at Ser240 ***(bottom panels)*** in response to different concentrations of coating stimulating anti-CD3 and anti-CD28 antibodies.

Human blood cone derived PBL were plated in dT10+25µM tryptophan in 96 well plates at a concentration of 10^6 cells/ well and cultured for 18h. Stimulating conditions included wells pre- coated with 10µg/ml anti-CD3 and 5µg/ml anti-CD28, PMA/Ionomycin at 50ng/ml and 500ng/ml final concentrations and PHA at 5µg/ml final concentration. Control groups included non-stimulated cells and wells where rapamycin was added to a final concentration of 30nM.

4.1b.PMA/Ionomycin stimulation activates the mTORC1 axis in human T cells but is not suppressible by rapamycin

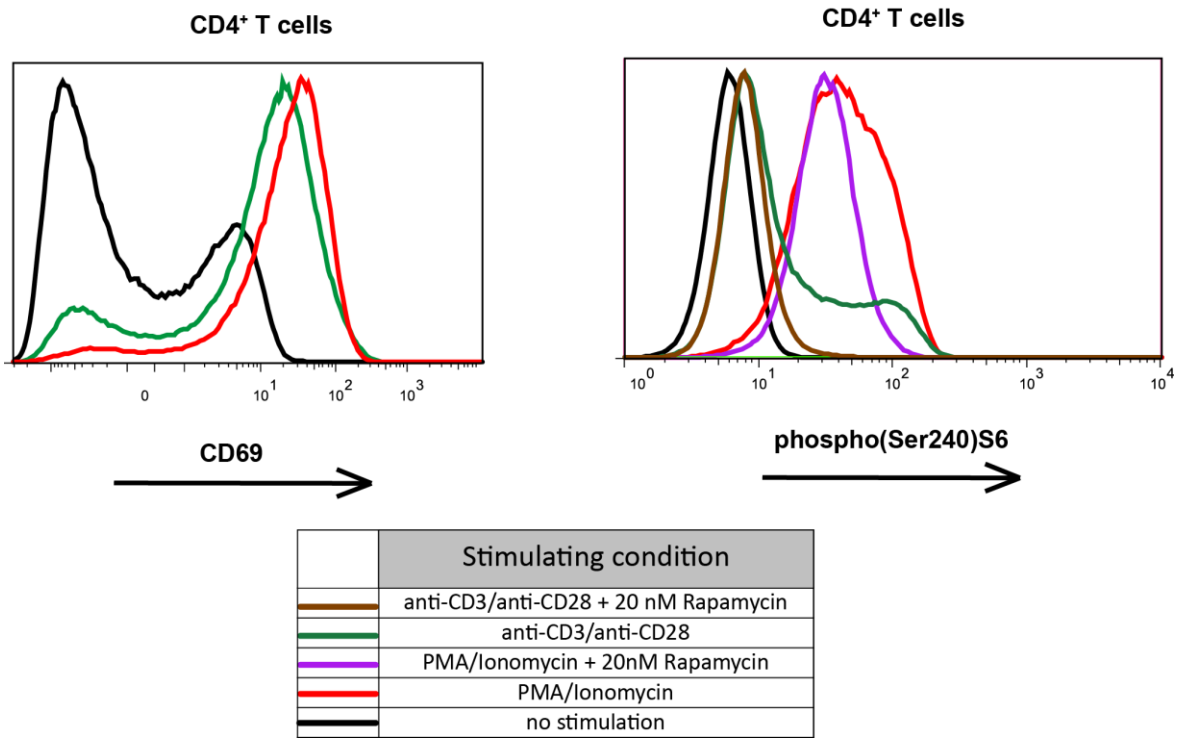

4.1b. Stimulation of human T cells by PMA/Ionomycin results in high levels of S6 phosphorylation at Ser240 that is not suppressible by 20nM rapamycin unlike anti-CD3/CD28 stimulation.

Typical histogram plots of surface CD69 expression ***(left panel)*** and phospho(Ser240)S6 ***(right panel)***. The PMA/Ionomycin treated cell groups exhibited similar levels of CD69 upregulation and much higher levels of mTORC1 pathway activation as evidenced by increased phosphorylation of S6 at Ser240 as compared with groups stimulated by anti-CD3/CD28. However the effect on S6 phosphorylation was incompletely inhibited by 30nM rapamycin – a concentration sufficient to almost completely abolish the effect on anti-CD3/CD28 stimulated groups.

4.1c. Stimulation by anti-CD3/CD28 is superior to PMA/Ionomycin and PHA for CFSE based analysis of proliferating human T cells.

10^6 human blood cone-derived PBL were plated in dT10 + 25uM tryptophan in 48 well plates for 60 hours. Stimulating conditions included wells pre- coated with 10µg/ml anti-CD3 and 5µg/ml anti-CD28, PMA/Ionomycin at 50ng/ml and 500ng/ml final concentrations and PHA at 5µg/ml final concentration.

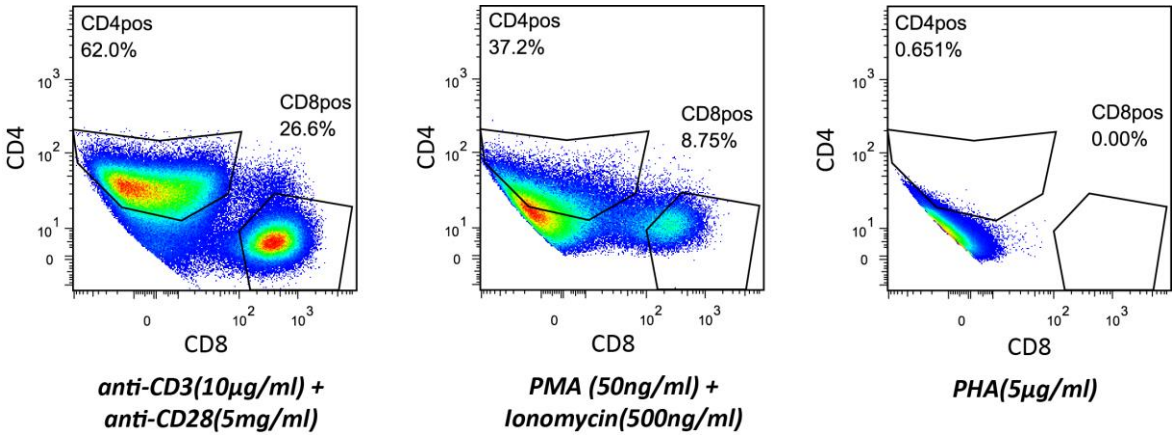

4.1c. Stimulation by anti-CD3/CD28 is superior to PMA/Ionomycin and PHA for CFSE based flow cytometric analysis of proliferating human blood cone derived T cells.

Typical pseudocolour dot plot diagrams of cells harvested after 60h of stimulation. Use of pre-coated anti-CD3/CD28 ***(left panel)*** did not result in significant change in the pattern of CD4 and CD8 expression when compared with unstimulated cells; both populations were easy to identify. Stimulation with 5µg/ml PHA resulted in severe toxicity and eradication of the CD4+ and CD8+ populations ***(right panel)***. The use of PMA resulted in significant downregulation of both CD8 and especially CD4 surface expression ***(middle panel***).

4.2. Upregulation of CD69 in human T cells stimulated by anti-CD3/CD28 is not affected by tryptophan deprivation.

One important limitation of using fresh unmodified human lymphocytes with anti-CD3/CD28 is that there is high variability in the degree of response of samples from different donors to stimulation – different T cell subsets respond differentially to stimulation by anti-CD3/CD28[140] and the marked genetic and immunologic heterogeneity in human populations ensure that it is very unlikely that samples from healthy unselected volunteers will have identical T cell compositions ; this was another reason why it was essential to carry out the optimisation experiments outlined in section 4.1.

In order to be able to carry out statistical analysis, positive control groups from each donor can be utilized to normalize results from that specific donor. Nevertheless as sometimes the fraction of T cells responding to anti-CD3/CD28 can be low the use of an activation marker is important to allow analysis of the T cell subpopulations responding to stimulation.

CD69 is an early surface marker of T cell activation that can be used in flow cytometry based analysis to detect effects that are limited to the activated subpopulations, as well as identify differences in the size of the activated population.

A number of experiments was carried out using tryptophan concentration in the media as the main variable (Figure 4.2.) For samples from the same donor, the T cell response to anti-CD3/CD28 stimulation - as measured by CD69 upregulation – was not affected by the amount of tryptophan in culture media for both $CD4^+$ and $CD8^+$ T cells.(Figure 4.2a.)

The effect held true across many donors when the normalised results were analysed (Figure 4.2b.); there was overall no detectable effect of tryptophan concentration by 2 way ANOVA in either $CD8^+$ or $CD4^+$ T cells ($p=0.28$). Therefore, similar to the murine models, CD69 expression can be used as a proxy marker for T cell activation in experiments using media tryptophan concentrations as a variable.

Figure 4.2. The CD69 response in human T cells stimulated by anti-CD3/CD28 is not affected by tryptophan deprivation.

10^6 human blood cone derived PBL were plated in tryptophan depleted dT10 media in each well of 96 well plates pre- coated with 10µg/ml anti-CD3 and 5µg/ml anti-CD28. Tryptophan at appropriate concentrations for each group was added at 0 hours; the cells were harvested after 18 hours, fixed, permeabilised and stained for flow cytometric analysis.

4.2a. Upregulation of CD69 in response to anti-CD3/CD28 is not affected by early tryptophan deprivation.

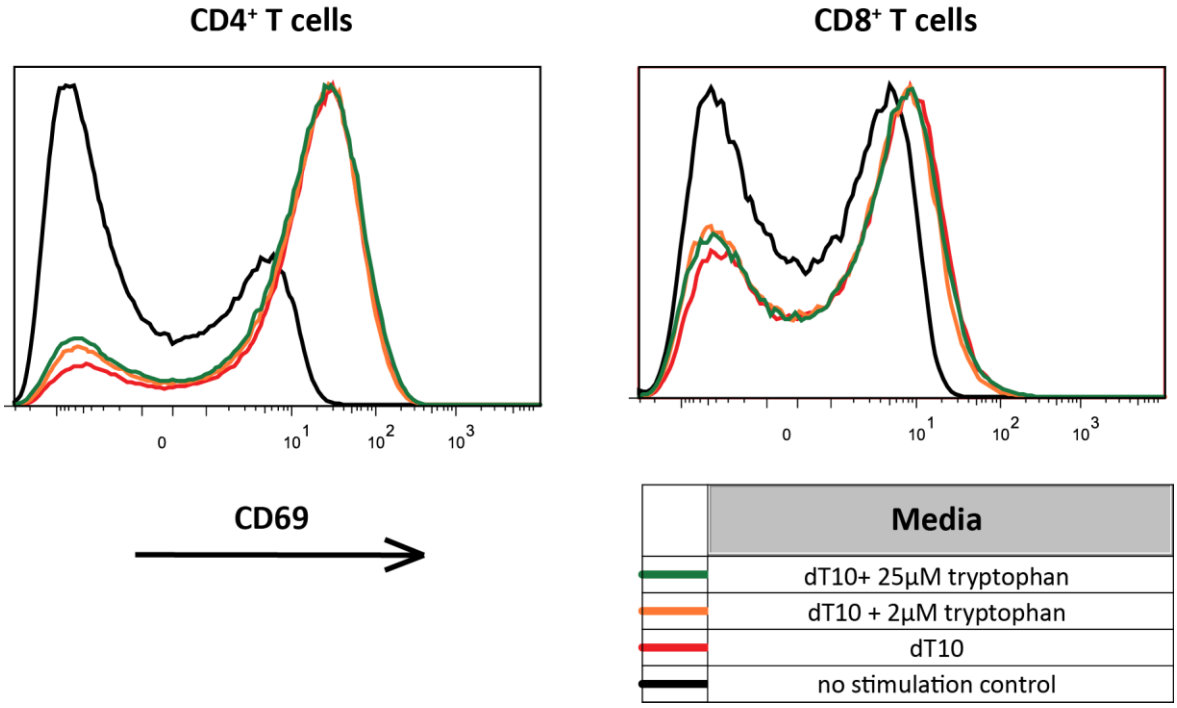

4.2a. The early upregulation of surface CD69 expression in human $CD4^+$ and $CD8^+$ T cells responding to stimulating anti-CD3 and anti-CD28 is not affected by tryptophan deprivation in samples derived from the same donor.

Typical FI histograms of surface CD69 expression in $CD4^+$ ***(left panel)*** and $CD8^+$***(right panel)*** populations from samples derived from the same donor demonstrating no significant effect of tryptophan on the extent of CD69 upregulation.

4.2b. Tryptophan deprivation does not affect the ability of human T cells to become activated in response to anti-CD3/CD28

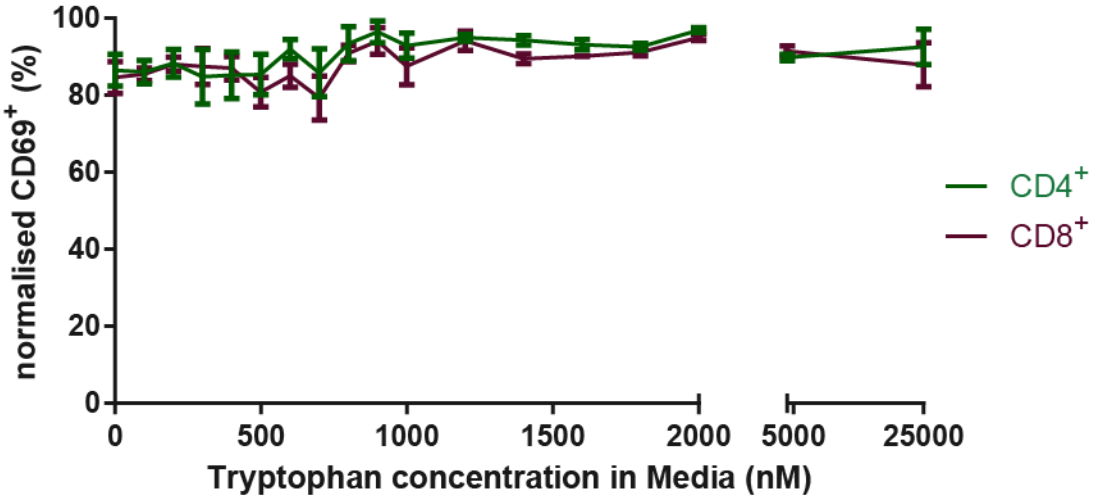

4.2b. Tryptophan deprivation does not affect the activation of human PBL-derived $CD4^+$ and $CD8^+$ T cells by stimulating anti-CD3/CD28 as measured by surface CD69 upregulation. Summary graph of results from 3 separate experiments. In each sample a measurement was made of the CD69 high population as a proportion of the $CD4^+$ or $CD8^+$ T cell subset .Values from each sample were normalised to the highest measurement in samples derived from the same donor to correct for variation between different blood donors. The results are plotted as arithmetic mean +/- SE. There was no significant difference between the different tryptophan concentrations by 2 way ANOVA (overall p=0.28); all adjusted p values between different tryptophan concentrations by Dunnett's multiple comparisons test were >0.8.

4.3. Early mTORC1 pathway activation in human $CD4^+$ and $CD8^+$ T cells stimulated by plated anti-CD3/CD28 is impeded by tryptophan depletion in culture media.

Once a protocol for reliably stimulating human PBL derived lymphocytes was established further experiments were carried out to confirm that the mTORC1 pathway sensitivity to tryptophan depletion that was seen in the murine model also existed in human lymphocytes.

Initial experiments showed that this was indeed the case (Figure 4.3a.): 18 hours after the onset of stimulation the percentage of both $CD4^+$ and $CD8^+$ T cells exhibiting an activated mTORC1 pathway – as evidenced by high levels of S6 phosphorylation at Ser240 - was 60% lower in treatment groups cultured in tryptophan depleted media as compared with those cultured in full media.

As samples from individual donors exhibited significant inter-donor variation in the extent of maximum mTORC1 pathway activation as measured by the proportion of T cells exhibiting high levels of phosphorylated S6 at Ser240, to allow statistical analysis the results from samples of each donor were normalised to the samples of that donor exhibiting the maximal response (Figure 4.3b.)

This confirmed that the effect was highly statistically significant in both $CD4^+$ and $CD8^+$ T cells ($p<0.0001$ by ANOVA). In addition it was apparent that there was a clear dose response curve with increasing amounts of tryptophan in media leading to increased mTORC1 pathway activation; at least 1µM tryptophan needed to be added to tryptophan depleted media to achieve near maximal phosphorylation levels of S6 at Ser240.

Figure 4.3. Early mTORC1 pathway activation in stimulated human CD4⁺ and CD8⁺ T cells is severely inhibited by tryptophan deprivation.

Human blood cone derived PBL were plated in 200 µl of tryptophan depleted dT10 media in 96 well plates pre- coated with 10µg/ml CD3 and 5µg/ml anti-CD28 at a concentration of 10^6 cells /well. Tryptophan was added at 0 hours in the relevant groups; the cells were harvested after 18 hours, fixed, permeabilised and stained for flow cytometric analysis.

4.3a. Culture in tryptophan depleted media inhibits mTORC1 activity in human CD4⁺ and CD8⁺ T cells stimulated by plate bound anti-CD3/CD28.

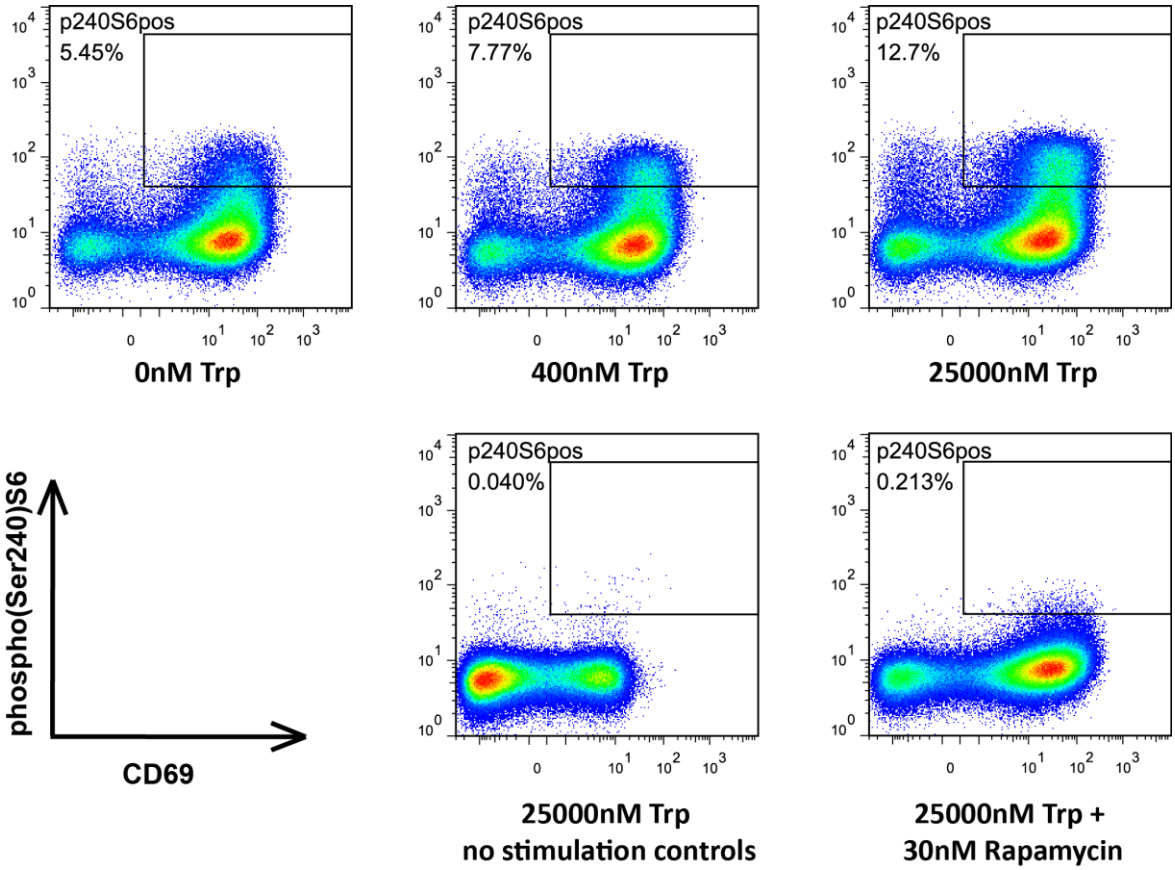

4.3a. Culture in tryptophan depleted media inhibits phosphorylation of S6 at Ser(240) in human CD4⁺ and CD8⁺ T cells after 18 hours of stimulation by plate bound anti-CD3/CD28 . Typical pseudocolor dot plots of $CD4^+$ $CD3^+$ populations after 18 hours of stimulation with plated anti-CD3/CD28.

Top panels: Representative plots for PBL stimulated in dT10 with different amounts of tryptophan.

Bottom panels: control groups .

4.3b. mTORC1 activity in activated human CD4⁺ and CD8⁺ T cells is directly related to the amount of tryptophan available in the media

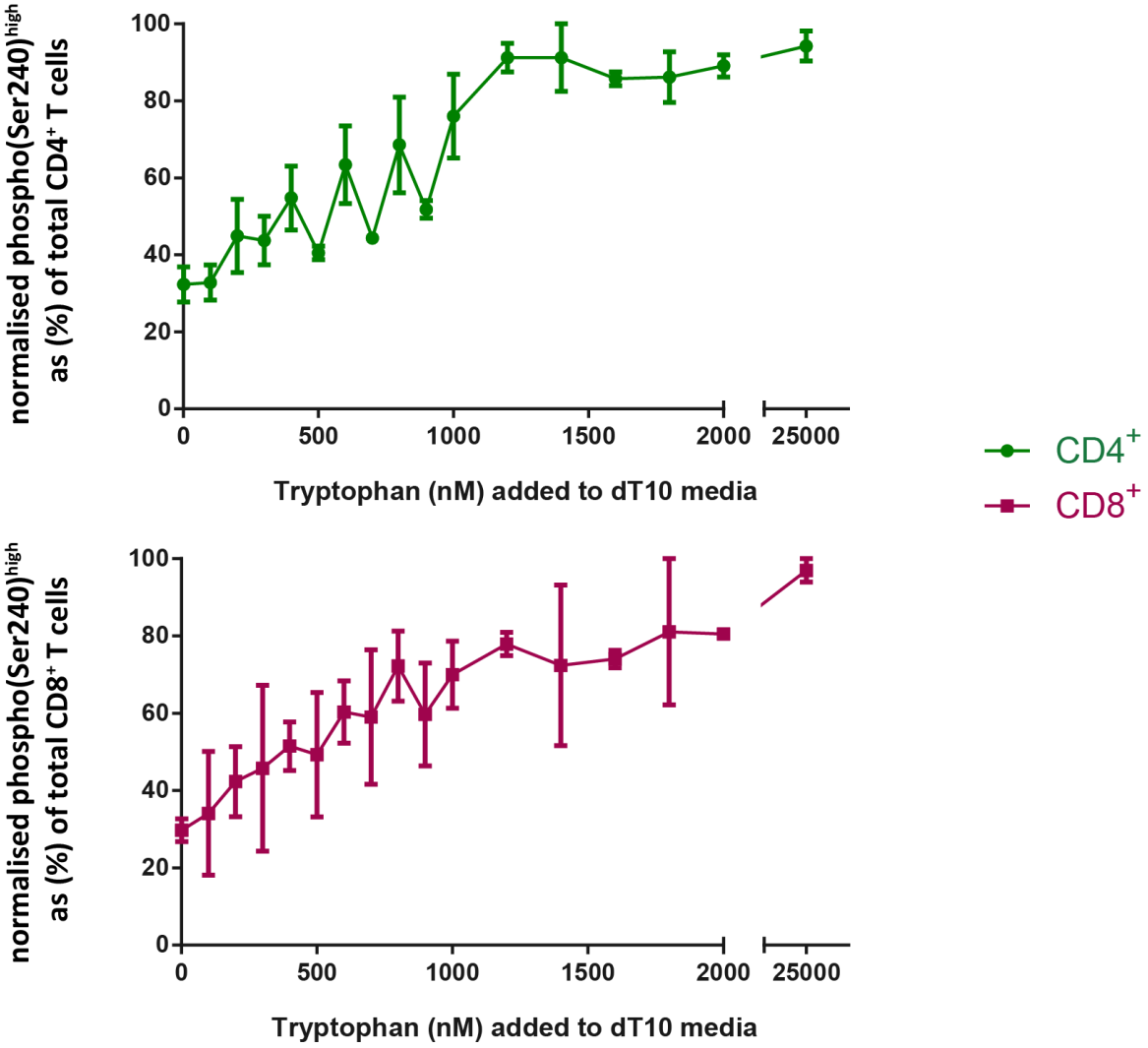

4.3b. The amount of available tryptophan in media is directly proportional to the extent of S6 phosphorylation at Ser(240) in human CD4⁺ and CD8⁺ T cells after 18 hours of stimulation by plate bound anti-CD3/CD28.

Plots demonstrating the effect of increasing media tryptophan concentrations on the extent of S6 phosphorylation at Serine 240 after 18h stimulation with plate bound anti-CD3/CD28. The results from specimens from each donor were normalised to the positive control group from that donor. The effect of tryptophan was statistically significant at the $p < 0.0001$ level by ANOVA for both CD4⁺ and CD8⁺ T cells.

4.4. Proliferation of human $CD4^+$ and $CD8^+$ T cells is severely inhibited in tryptophan depleted media.

The next set of experiments set out to clarify the sensitivity of the human T cell proliferative response to conditions of tryptophan deprivation. Again, plates pre-coated with stimulating anti-CD3/CD28 was used as a non-specific driver of T cell proliferation in combination with dT10 as the baseline tryptophan depleted media.

Similar to the murine systems culture in tryptophan depleted media resulted in profound inhibition of proliferation both in the $CD4^+$ and $CD8^+$ T cell populations (Figure 4.4.). In particular while the addition of 25µM tryptophan up to 24 hours after the onset of stimulation could fully rescue the proliferative response, later additions were less effective; by 72 hours the effect was negligible (Figure 4.4a.).

Furthermore, and again similar to the murine system, the extent of proliferation was directly related to the tryptophan concentration in the culture media, notably however much higher concentrations of tryptophan (>4µM) were needed for the T cells to reach their maximum proliferative potential (Figure 4.4b.).

Figure 4.4. Human T cell proliferation is severely impaired by tryptophan deprivation.

Human blood cone derived PBL were stained with CFSE; 10^6 cells were immediately plated in 1ml of dT10 in each well of 48 well plates pre- coated with 10µg/ml CD3 and 5µg/ml anti-CD28. Tryptophan was added at 0/24/48/72 hours in the relevant groups; the cells were harvested after 90 hours, fixed, permeabilised and stained for flow cytometric analysis.

4.4a. Lack of tryptophan for more than 24 hours inhibits the proliferation of CD8⁺ and CD4⁺ splenocytes in response to activating stimuli.

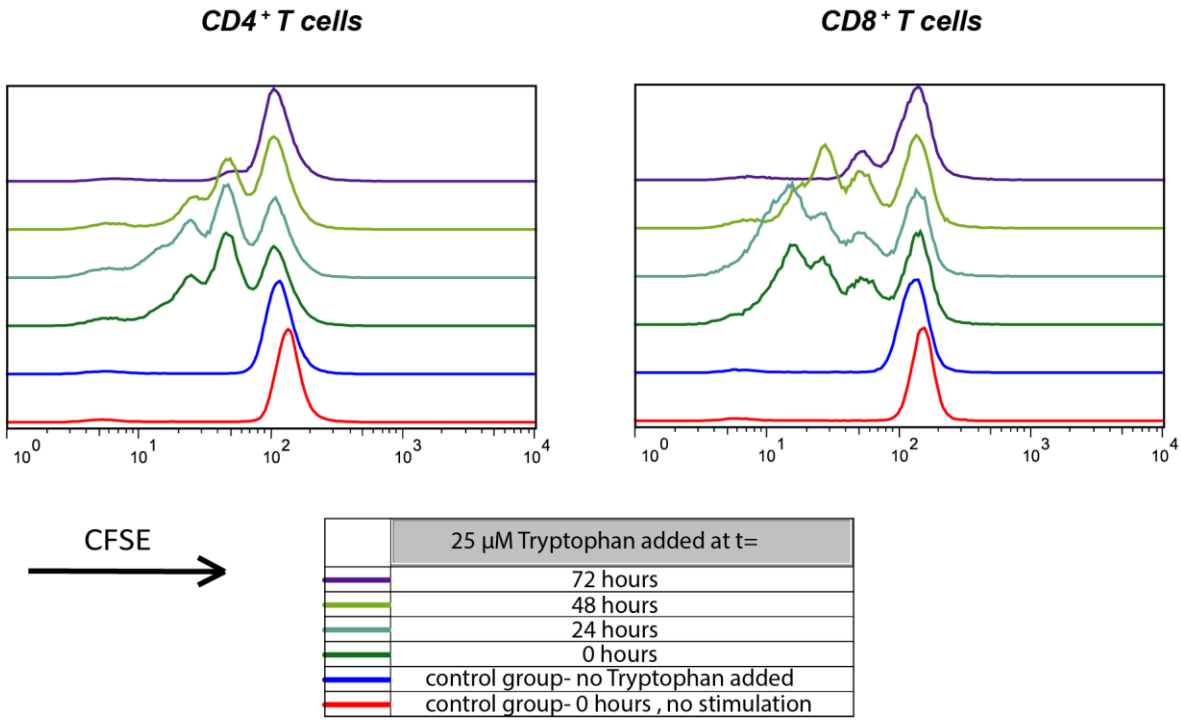

4.4a. Tryptophan deprivation for more than 24 hours inhibits the proliferation of human CD8⁺ and CD4⁺ T cells in response to plated anti-CD3/CD28.

Representative CFSE histogram plots of CD4⁺ ***(left panel)*** and CD8+ ***(right panel)*** T cells after 90 hours in wells pre-coated with anti-CD3/CD28. Lack of tryptophan results in complete inhibition of proliferation of both CD4+ and CD8+ T cells as measured by CFSE dilution. The late addition of tryptophan rescues proliferation with diminishing effects after 24 hours.

4.4b. Human CD8⁺ and CD4⁺ T cell proliferation in response to anti-CD3/CD28 is directly related to available tryptophan

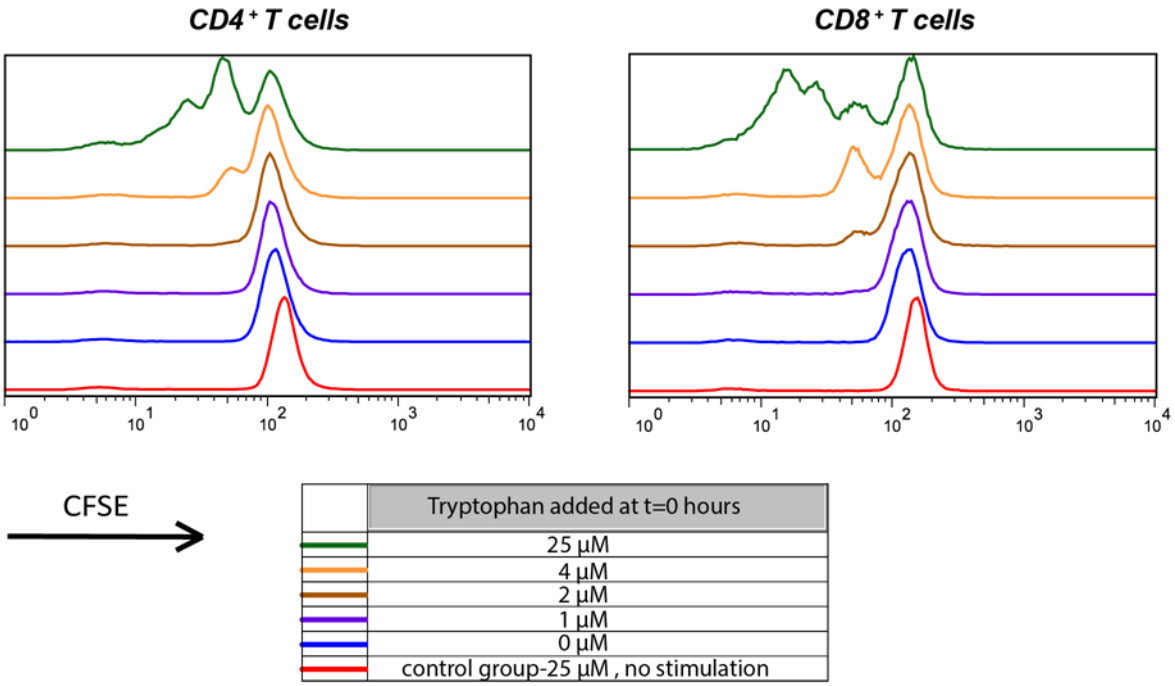

4.4b. The ability of human CD8+ and CD4⁺ T cells to proliferate in response to plated anti-CD3/CD28 is directly related to available tryptophan in culture media.

Representative CFSE histogram plots of CD4⁺ ***(left panel)*** and CD8⁺ ***(right panel)*** T cells after 90 hours in wells pre-coated with anti-CD3/CD28. The extent of inhibition is dependent on the magnitude of tryptophan depletion; concentrations of 4µM tryptophan are not sufficient to reach levels of proliferation achievable under saturating tryptophan conditions.

4.5. Tbet expression in human T cells responding to stimulation is impeded by tryptophan deprivation.

Tbet expression in human lymphocytes is an important early event after stimulation that has a significant effect on determining the future cell fate. A series of experiments was therefore carried out to investigate if tryptophan deprivation has a similar effect on human T cells to that seen in experiments in murine models.

Early experiments revealed that significant Tbet upregulation could be seen as early as 90 hours after stimulation. The lack of tryptophan resulted in significantly reduced Tbet expression both in $CD4^+$ and $CD8^+$ T cells. Furthermore, more than 2μM of tryptophan was needed to be present in baseline culture media to reach levels of Tbet expression that were achievable in saturating tryptophan conditions - e.g. (Figure 4.5a.).

Interestingly, Tbet expression could be rescued by adding tryptophan as late as 72 hours after the onset of stimulation – 18 hours prior to harvesting the cells - in both $CD4^+$ and $CD8^+$ T cells, though it should be noted that the effect of adding tryptophan to media at 72 hours did lead to marginally reduced Tbet levels compared with positive controls that did not reach statistical significance.

Figure 4.5. Tbet upregulation in human blood cone derived T cells in response to plated anti-CD3/CD28 is dependent on the presence of sufficient amounts of tryptophan in culture media.

Fresh human blood cone derived PBL from healthy volunteers were immediately plated in 1ml of tryptophan depleted dT10 media in each well of a 48 well plate pre- coated with 10µg/ml CD3 and 5µg/ml anti-CD28 at a concentration of 10^6 cells/well. Tryptophan was added at 0/24/48/72 hours in the relevant groups; the cells were harvested after 90 hours, fixed, permeabilised and stained for flow cytometric analysis.

4.5a. Tbet expression in human T cells responding to stimulation is impeded by tryptophan deprivation.

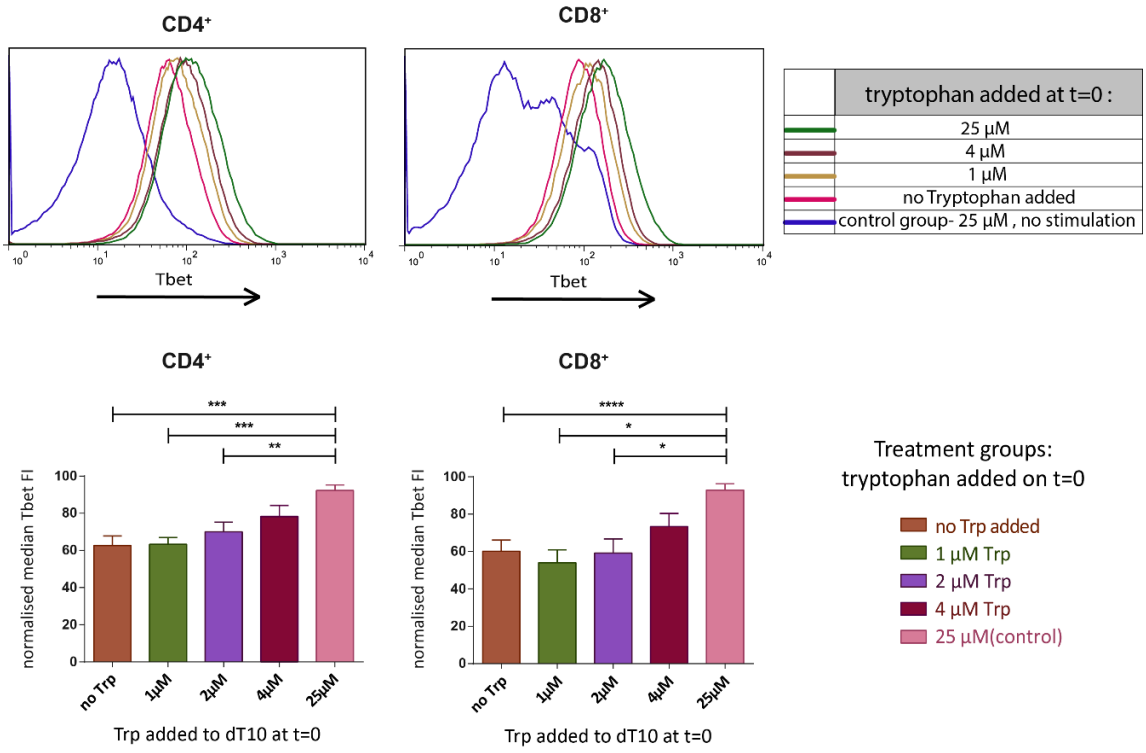

4.5a. Tbet expression in human T cells responding to stimulation by plated anti-CD3/CD28 is impeded by tryptophan deprivation.

(Top panels)*:* Tbet expression histograms from representative samples showing patterns of Tbet upregulation in response to stimulation in tryptophan deprived environments in both $CD4^+$ ***(left panels***) and $CD8^+$ ***(right panels)*** T cell populations.

(Bottom panels): Statistical analysis of results from 3 separate experiments involving 6 individual healthy blood donors. To account for staining variability between experiments and for donor variability measured Tbet median FIs were normalised for each donor to the highest measured Tbet FI for that donor in the particular experiment. The upregulation of Tbet expression is markedly reduced in the absence of tryptophan in the media. Addition of tryptophan at t=0 improves the response, but the addition of more than 2µM is needed before the response approaches that of the positive controls.

4.5b. Late addition of tryptophan rescues Tbet expression in human T cells responding to stimulation in tryptophan deprived conditions.

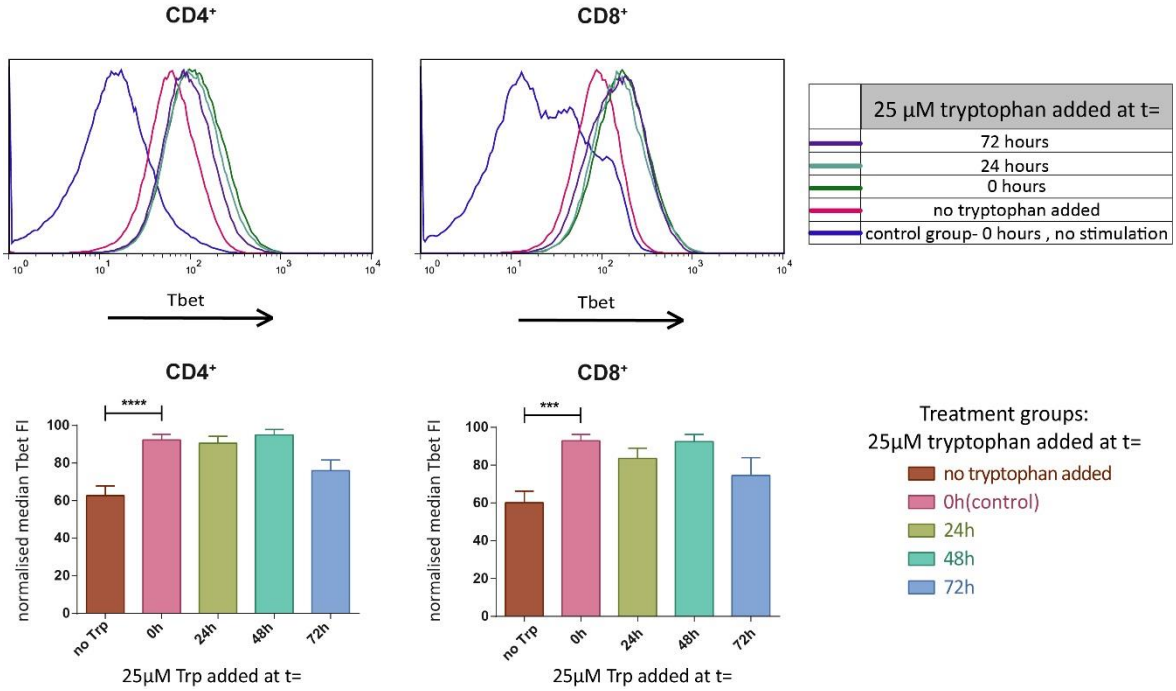

4.5b. Tbet expression in human T cells responding to anti-CD3/CD28 mediated stimulation in tryptophan deprived conditions is rescued by the addition of tryptophan as late as 3 days after the onset of stimulation.

(Top panels): Tbet expression histograms from representative samples showing patterns of Tbet upregulation in $CD4^+$ **(*left panels*)** and $CD8^+$ **(*right panels*)** T cell populations of samples where tryptophan was added at different timepoints after the onset of stimulation.

(Bottom panels): Statistical analysis of results from 3 separate experiments involving 6 individual healthy blood donors. To account for staining variability between experiments and for donor variability measured Tbet median FIs were normalised for each donor to the highest measured Tbet FI for that donor in the particular experiment. The plots demonstrate clearly that the addition of 25µM tryptophan at later timepoints as late as 48 hours after the onset of stimulation can rescue the full response seen in the positive control groups ($p<0.0001$ and $p=0.0002$ by Dunnatt's multiple comparisons test for the $CD4^+$ and $CD8^+$ subgroups respectively). Adding tryptophan 72 hours after the onset of stimulation results in an intermediate picture where there is a trend for increased Tbet compared to the no tryptophan controls that fails to reach statistical significance.

4.6. Tryptophan deprivation increases the relative size of the FoxP3^{+} CD25^{high} CD4^{+} T cell subgroup following stimulation with plate bound anti-CD3/CD28 without altering overall levels of CD25 expression.

To further investigate whether in human T cells tryptophan deprivation also results in a relative expansion of the FoxP3^{+}CD25^{high} CD4^{+} T cell subgroup, a series of experiments was carried out again utilising tryptophan depleted dT10 media and plates pre-coated with stimulating anti-CD3/CD28 as the stimulus.

Similar to the experiments in the murine systems, stimulation in tryptophan depleted media resulted in a marked relative expansion (almost 2x in most samples) of the FoxP3^{+} CD25^{high} CD4^{+} T cell subgroup as compared to positive controls cultured in tryptophan replete media (Figure 4.6a.)

While there was significant inter-donor variability on the absolute size of this subpopulation as a percentage of the whole CD4^{+} subpopulation, nevertheless when the results were normalised to account for this the effect of culture in tryptophan depleted media was clearly visible and highly significant (Figure 4.6b.)

The addition of tryptophan in the media within the first 24 hours after the onset of stimulation did prevent this expansion, however additional tryptophan at later timepoints was insufficient to completely abolish this effect.

It is worth noting that in the human model tryptophan depletion did not affect the level of overall CD4^{+} CD25 expression unlike what was seen in the murine model (Figure 4.6c.).

Figure 4.6. Tryptophan deprivation increases the relative size of the FoxP3⁺ CD25^{high} CD4⁺ T cell subgroup following stimulation without altering overall levels of CD25 expression.

Fresh human blood cone derived PBL from healthy volunteers were immediately plated in 1ml of tryptophan depleted dT10 media in each well of a 48 well plate pre- coated with 10µg/ml CD3 and 5µg/ml anti-CD28 at a concentration of 10^6 cells/well. Tryptophan was added at 0/24/48/72 hours in the relevant groups; the cells were harvested after 90 hours, fixed, permeabilised and stained for flow cytometric analysis.

For statistical analysis results from 3 separate experiments involving 6 individual healthy blood donors were used. To account for staining variability between experiments and for donor variability, results were normalised for each donor to the highest value across samples of that donor in the particular experiment.

4.6a. The relative size of the FoxP3⁺ CD25^{high} CD4⁺ subpopulation in human T cells is increased following stimulation under tryptophan deprived conditions.

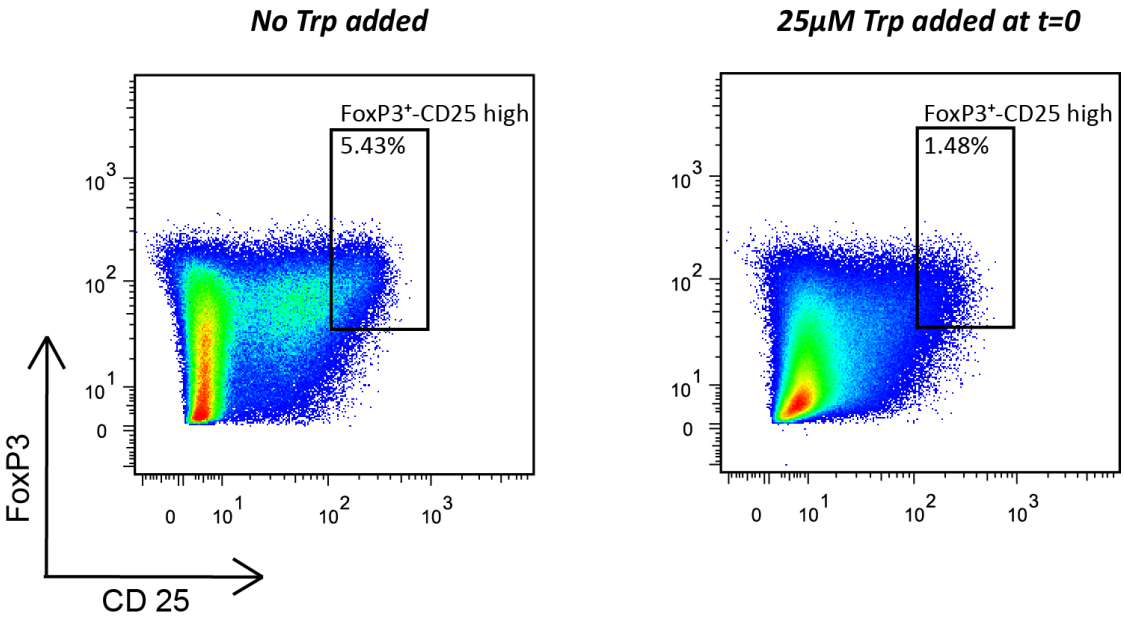

4.6a. The relative size of the FoxP3+CD25high CD4+ subpopulation in human T cells is increased following stimulation by plated anti-CD3/CD28 in tryptophan deprived conditions.

Pseudo-color dot plots from representative samples demonstrating that stimulation of human blood cone derived PBL with plate bound anti-CD3/CD28 under tryptophan depleted conditions results in proportionally larger FoxP3⁺CD25^{high} CD4⁺ T cell subpopulations.

4.6b. The late addition of tryptophan only partially prevents an increase in the relative size of the FoxP3⁺ CD25^{high} CD4⁺ subpopulation in human T cells following stimulation under tryptophan deprived conditions.

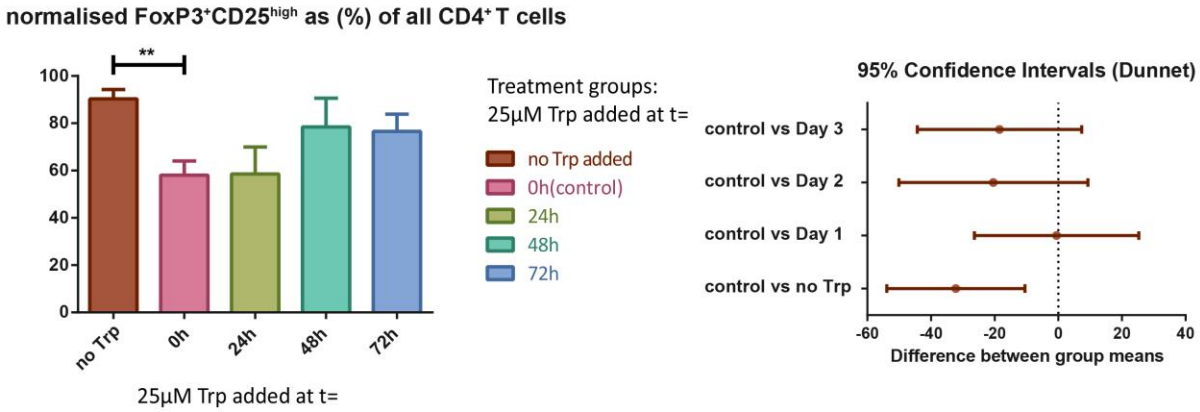

4.6b. The late addition of tryptophan only partially prevents an increase in the relative size of the FoxP3⁺CD25^{high} CD4⁺ subpopulation in human T cells following stimulation by anti-CD3/CD28 under tryptophan deprived conditions. ***(Left panel)*** Summary plot demonstrating that tryptophan depleted groups exhibited a highly statistically significant (p=0.001) relative enlargement of the FoxP3+CD25^{high} CD4⁺ T cell subpopulation as compared with the groups where 25µM tryptophan was added at 0 and 24h; while there was a trend for an increase at the 48h and 72h groups it did not reach statistical significance (p>0.05, ***right panel***).

4.6c. CD25 upregulation in human T cells in response to anti-CD3/CD28 is not significantly altered by tryptophan depletion.

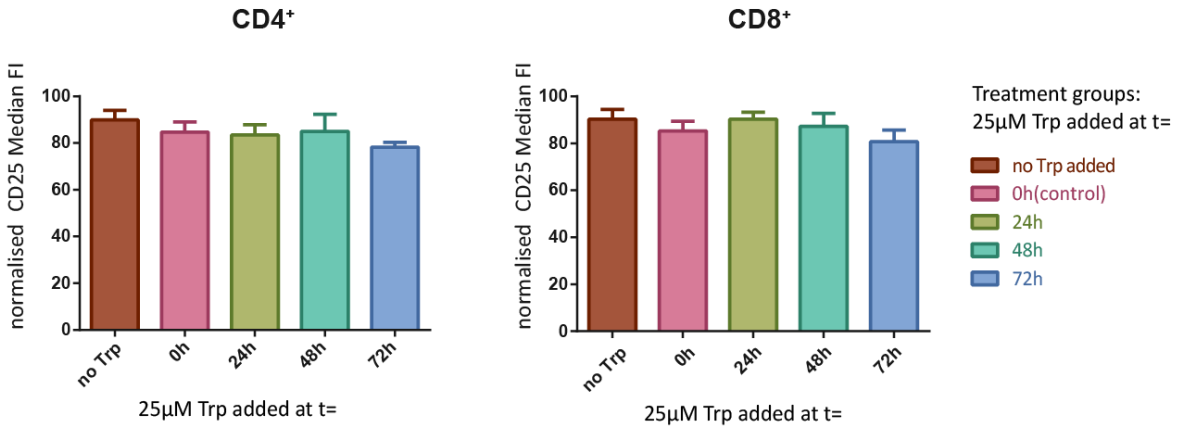

4.6c. Tryptophan depletion does not significantly affect continuing CD25 surface expression after 90h of stimulation of human CD4⁺ and CD8⁺ T cells by anti-CD3/CD28. Summary plots demonstrating that there was no significant difference either in surface expression of CD25 as measured in terms of normalised CD25 median FI among both the CD4⁺ ***(left panels)*** or CD8⁺ ***(right panels)*** T cell populations between tryptophan starved groups and groups were tryptophan was added at timepoints as late as 72 hours after the onset of stimulation.

4.7. The phenotype of $CD4^+$ and $CD8^+$ T cells of human melanoma patients following stimulation is influenced by tryptophan availability.

In order to investigate whether the tryptophan depletion effects seen on human T cells derived from fresh blood cones of healthy volunteers was reproducible and applicable in a clinical setting, fresh PBL were isolated from blood donated by human stage III-IV melanoma patients and used for a set of similar experiments. Plated anti-CD3/CD28 was again used for stimulation purposes, and tryptophan depleted dT10 media was used as the baseline media to which additional tryptophan was added at particular timepoints.

Results from this sets of experiments (summarised in Figure 4.7.) confirmed the observations seen in previous experiments using healthy donors although again there was marked inter-patient variability: Tbet expression was markedly reduced when tryptophan depleted media was used, however it could be rescued by the addition of tryptophan as late as 72 hours after the onset of stimulation in both $CD4^+$ and $CD8^+$ cells (Figure 4.7a.)

Similar to the results seen in healthy volunteer samples, surface CD25 expression after 90 hours of stimulation in the $CD4^+$ subpopulation was not affected by tryptophan depletion; however there was a small but highly statistically significant effect seen in the $CD8^+$ population where there was decreased upregulation under tryptophan depleted conditions (Figure 4.7b.)

Importantly a relative expansion of the $FoxP3^+$ $CD25^{high}$ $CD4^+$ T cell subgroup was again seen in the absence of tryptophan after 90 hours (figure 4.7c.); addition of tryptophan later than 72 hours was again unable to prevent this expansion.

Figure 4.7. Tryptophan depletion affects the activation patterns of T cells from human melanoma patients.

Fresh human peripheral blood derived PBL from stage III-IV melanoma patients were immediately plated in 1ml of tryptophan depleted dT10 media in each well of a 48 well plate pre- coated with 10µg/ml CD3 and 5µg/ml anti-CD28 at a concentration of 10^6 cells/well. Tryptophan was added at 0/24/48/72 hours in the relevant groups; the cells were harvested after 90 hours, fixed, permeabilised and stained for flow cytometric analysis.

For statistical analysis results from 4 separate experiments involving 11 individual donors were used. To account for staining variability between experiments and for donor variability, results were normalised to the mean of positive control samples (stimulated in dT10 media with 25µM tryptophan added immediately) for that patient. Each point represents the average of results for a given patient at that specific treatment group.

4.7a. Tryptophan depletion inhibits Tbet upregulation in T cells from human melanoma patients

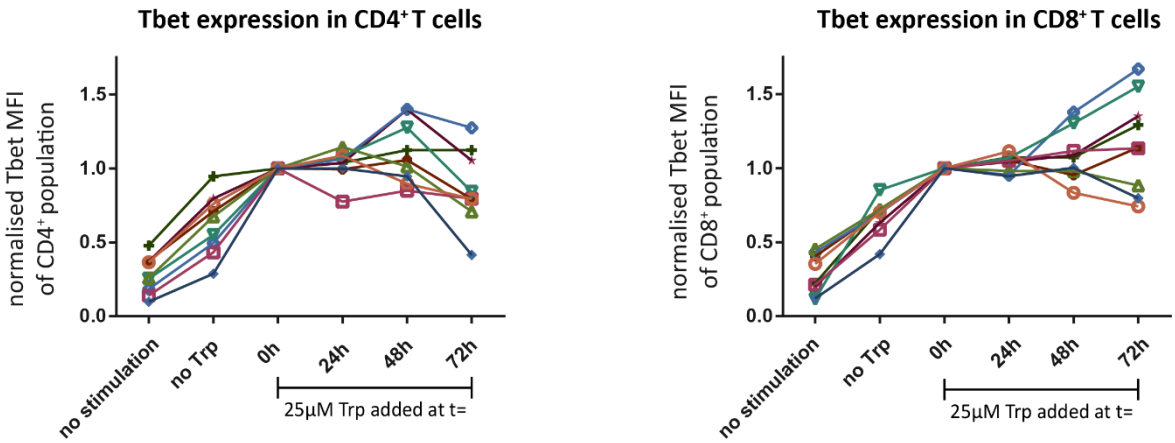

4.7a. Tryptophan depletion inhibits Tbet upregulation in CD4+ and CD8+ T cells from human melanoma patients in response to stimulation by anti-CD3/CD28.
In both $CD4^+$ ***(left panel)*** and $CD8^+$ ***(right panel***) T cell populations there was statistically significant reduction ($p<0.0001$ and $p<0.05$ respectively by Dunnett's multiple comparisons test) in the extent of Tbet upregulation in the groups where no additional tryptophan was added.

4.7b. Tryptophan depletion has a limited effect on CD25 upregulation of T cells from human melanoma patients

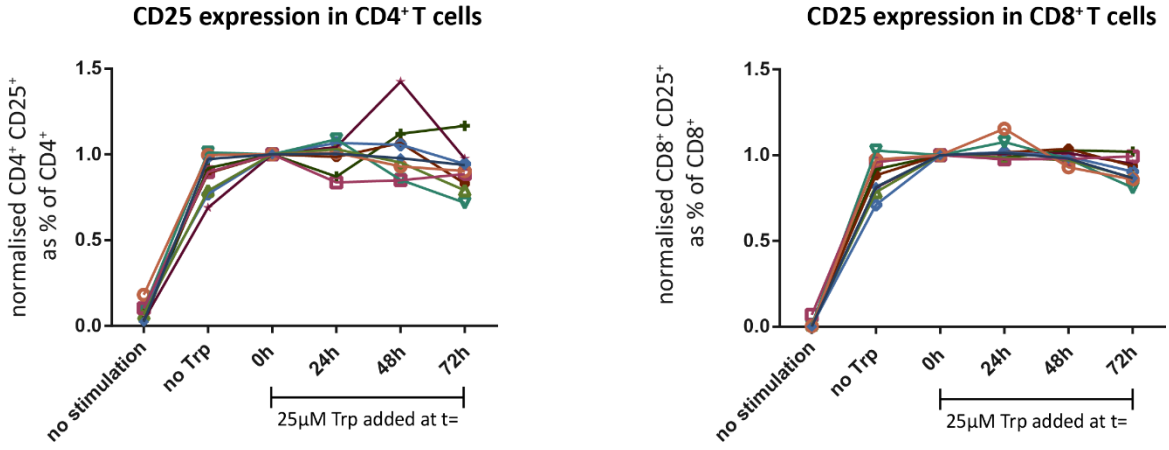

4.7b. The effect of tryptophan depletion on upregulation of surface CD25 expression in $CD4^+$ and $CD8^+$ T cells from human melanoma patients stimulated by plated anti-CD3/CD28 is limited. There was no significant difference ($p>0.05$ by 2-way ANOVA) seen between treatment groups in the $CD4^+$ T cell population ***(left panel)*** in terms of CD25 upregulation . In the $CD8^+$ T cell population ***(right panel)*** there was a small but statistically significant ($p<0.0001$) between treatment groups- in the no tryptophan group surface CD25 upregulation was marginally reduced.

4.7c. The relative size of the FoxP3$^+$ CD25^{high} CD4$^+$ subpopulation in T cells from human melanoma patients is increased following stimulation under tryptophan deprived conditions.

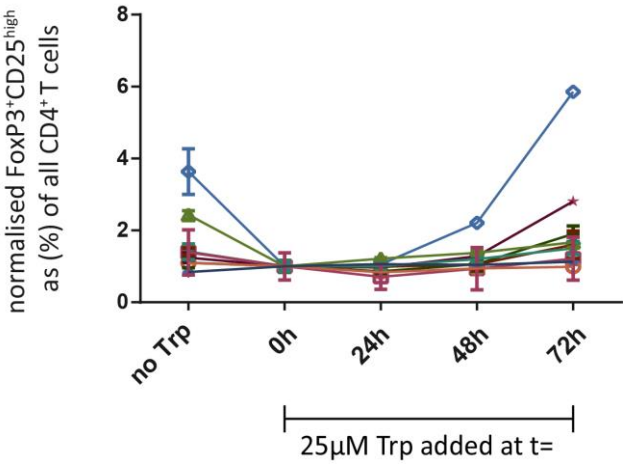

4.7c. The relative size of the FoxP3$^+$ CD25^{high} CD4$^+$ subpopulation in T cells from human melanoma patients is increased following stimulation by plated anti-CD3/CD28 in tryptophan deprived conditions. The FoxP3$^+$CD25^{high} subpopulation of $CD4^+$ T cells was significantly expanded both in the no tryptophan groups and in the 72 hour group ($p<0.0001$ by Dunnett's multiple comparisons test).

4.8. Stimulation of naïve human $CD4^+$ cells under tryptophan deprived conditions results in reduced CD25 and Tbet expression but an expanded $FoxP3^+$ $CD25^{high}$ population

As the T cell populations in PBL obtained from human volunteers invariably contain a mix of naïve and memory T cells and stimulation by anti-CD3/CD28 indiscriminately activates all of these a series of experiments was carried investigating the effect of tryptophan depletion on a relatively pure naïve $CD4^+$ T cell population obtained by using a commercially available negative selection kit on donor healthy volunteer derived PBL. Again to account for inter-donor variability the results from each donor were normalised to positive control groups from that donor.

The first observation that came out of these experiments was that the timecourse of events was significantly slower in naïve $CD4^+$ T cells; both surface CD25 and intracellular Tbet expression at 90 hours after the onset of stimulation was not significantly higher than that seen in unstimulated controls (Figure 4.8a.).

After 186 hours however upregulation of surface CD25 and intracellular Tbet was clearly visible in the positive control groups (Figures 4.8b.-c.). Moreover, at this timepoint tryptophan depletion had a clear effect in inhibiting CD25 expression (Figure 4.8c.). The effect on Tbet was less clear-cut in the total naïve population, but was clearly evident in the $CD25^+$ fraction that was likely representative of the activated subpopulation (Figure 4.8b).

An expansion of the $FoxP3^+$ $CD25^{high}$ subgroup was also seen at this timepoint (Figure 4.8c.), however the experiment was underpowered to reach statistical significance.

Figure 4.8. Tryptophan depletion affects the activation patterns of naïve human CD4⁺ T cells.

Naïve CD4⁺ T cells were isolated from fresh human blood cone derived PBL using the Miltenyi Biotech naïve CD4⁺ T Cell isolation kit II; from the same blood cones unseparated PBL as well as the naïve CD4⁺ T cell depleted fraction were used as controls. $2*10^5$ cells were immediately plated in 1ml of tryptophan depleted dT10 media in each well of a 48 well plate pre-coated with 10µg/ml CD3 and 5µg/ml anti-CD28. Tryptophan was added at 0/24/48/72 hours in the relevant groups; the cells were harvested after 90 or 186 hours, fixed, permeabilised and stained for flow cytometric analysis.

To account for donor variability, results were normalised to the mean of positive control samples (stimulated in dT10 media with 25µM tryptophan added immediately) of the naïve CD4⁺ cell depleted fraction for that donor.

4.8a. Human naïve CD4⁺ cells stimulated by anti-CD3/CD28 for 90 hours do not show signs of activation

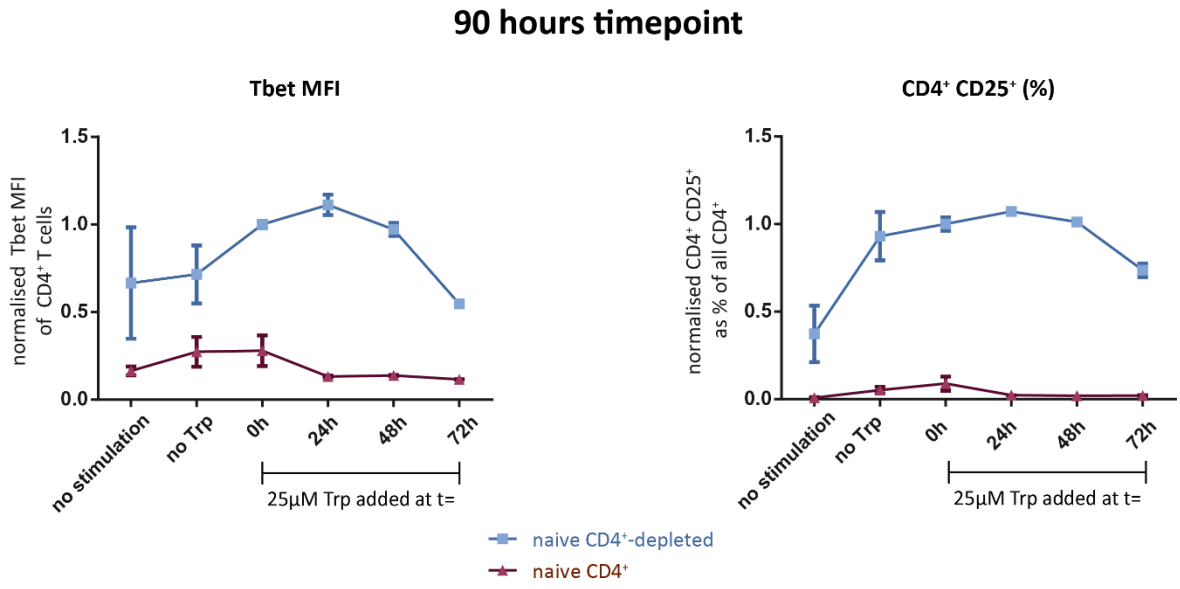

4.8a. Stimulation of human naïve CD4⁺ T cells by plated anti-CD3/CD28 does not trigger upregulation of surface CD25 expression or intracellular Tbet expression at 90 hours after the onset of stimulation.

Graphs summarising findings with regards to CD25 and Tbet upregulation after 90 hours; results plotted as mean +/- SE from duplicate samples from 2 donors and normalised to account for inter-donor variability. Tbet levels ***(left panel)*** and surface CD25 expression ***(right panel)*** in the naïve CD4⁺ group were very low across all treatment conditions and not significantly different from no stimulation control groups.

4.8b. Tryptophan depletion results in markedly reduced levels of Tbet in human naïve CD4⁺ cells activated after 7 days of stimulation.

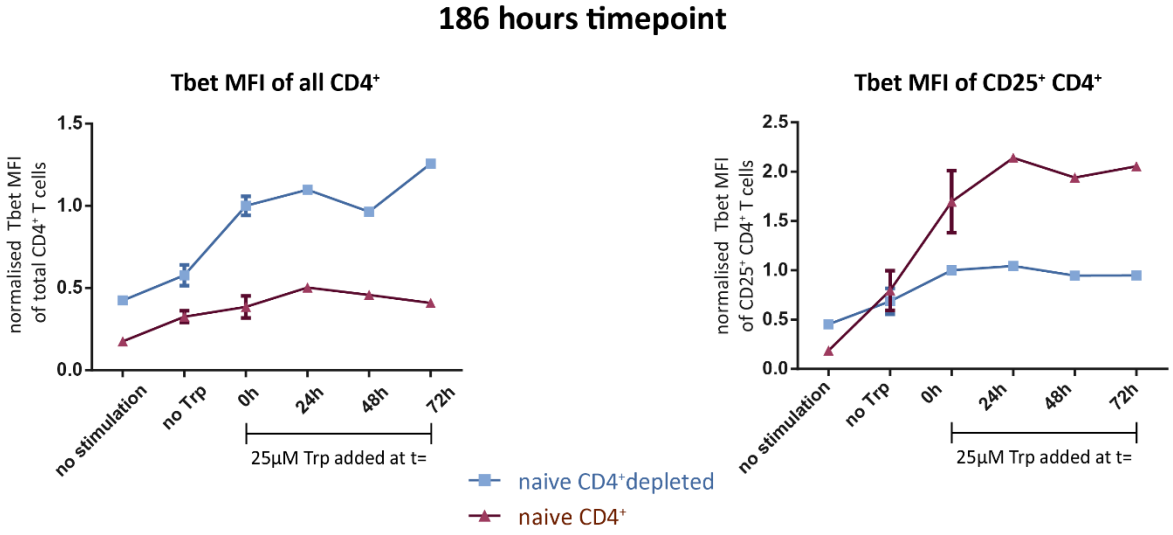

4.8b. Tryptophan depletion results in markedly reduced levels of Tbet expression in human naïve CD4⁺ cells after 7 days of stimulation by anti-CD3/CD28.

Graphs summarising findings with regards to Tbet upregulation after 186 hours; results plotted as mean +/- SE from duplicate samples from 2 donors and normalised to account for inter-donor variability. By the 186 hours timepoint Tbet levels in the naïve CD4⁺- group ***(left panel)*** approached those seen in the unstimulated control group. While a trend was seen for a reduction in Tbet levels in the tryptophan starved groups, the experiment was underpowered for this to be statistically significant.

The effect of tryptophan deprivation in naïve CD4⁺ T cells became more apparent when the CD25⁺ CD4⁺ subpopulation was analysed ***(right panel)***. The magnitude of the effect on this subpopulation was large at 186 hours and statistically significant ($p<0.05$ by Sidak's multiple comparisons test). Delay in adding tryptophan for up to 72 hours post activation did not result in a measurable difference in Tbet levels at this timepoint for any of the groups.

4.8c. Tryptophan depletion results in reduced levels of surface CD25 expression but an increase in the relative size of the FoxP3⁺ CD25^{high} CD4⁺ subpopulation in human naïve CD4⁺ cells after 7 days of stimulation.

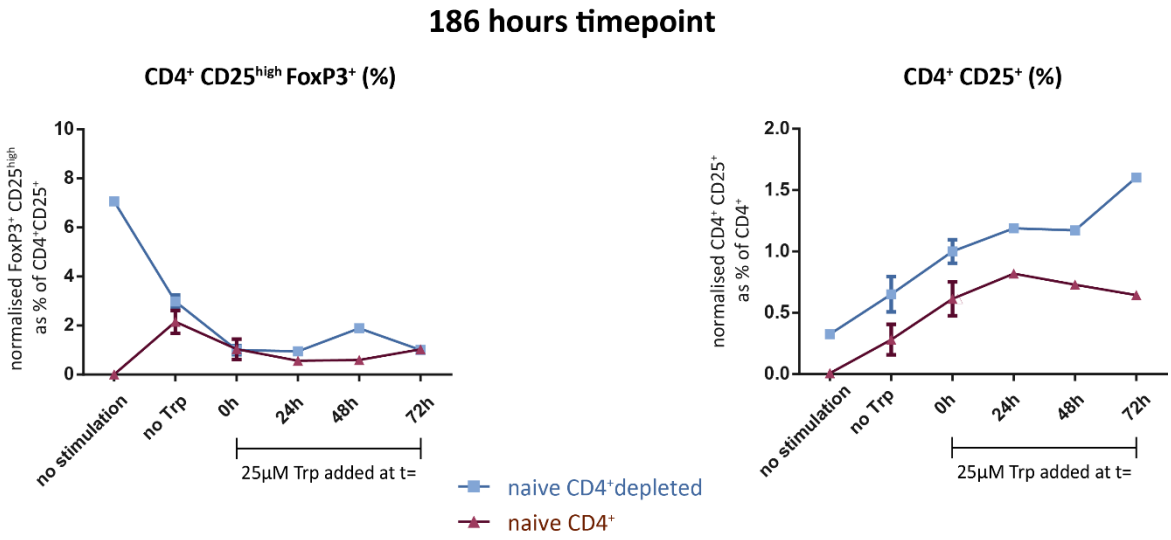

4.8c. Tryptophan depletion results in reduced levels of surface CD25 expression but an increase in the relative size of the FoxP3⁺ CD25^{high} CD4⁺ subpopulation in human naïve CD4⁺ cells after 7 days of stimulation with anti-CD3/CD28.

Graphs summarising findings with regards to CD25 upregulation and FoxP3 expression after 186 hours; results plotted as mean +/- SE from duplicate samples from 2 donors and normalised to account for inter-donor variability.

(Right panel): After 186 hours of stimulation significant upregulation of CD25 could be seen in the naïve groups; there was a trend for reduced surface CD25 expression in the tryptophan starved groups but the experiment was underpowered to confirm its statistical significance (p=0.19 by Sidak's multiple comparisons test).

(Left panel): There was a clear trend for an increased proportion of FoxP3⁺CD25^{high} expressing cells amongst both the naïve and naïve depleted CD4⁺ T cell groups, however the experiment was insufficiently powered to demonstrate this at the p<0.05 level in the naïve CD4⁺-depleted group.

4.9. The inhibitory effect of media preconditioned by active IDO expressing tumour cells on activated human T cells is reversed by the addition of tryptophan.

IDO expression by tumour cells is known to produce inhibitory effects on T cells not dissimilar to those seen in the experiments carried out earlier in this chapter when T cells were cultured under tryptophan deprived conditions. To ascertain whether tryptophan consumption by IDO expressing cells is one of the main ways this effect is mediated, a series of experiments was carried out on PBL derived from healthy volunteers stimulated by plated anti-CD3/CD28 in media preconditioned by IDO expressing cells.

For this purpose a genetically modified HeLa cell line was utilised that had been transduced to express active human IDO together with GFP("HeLa-IDO" cells)[128]. Initial experiments confirmed the ability of transfected HeLa-IDO cells to rapidly convert tryptophan to Kynurenine in media and established the optimal parameters for future experiments (Figure 4.9a.) – it was important to find culture conditions for the HeLa-IDO cells that would result in adequate levels of tryptophan depletion in the media without the confounding effect of additional reduction in the levels of other essential nutrients

To allow a valid comparison to be made, control media were preconditioned in a similar way utilising wild-type HeLa cells as well as HeLa cells transfected with GFP but not IDO ; additional controls included preconditioned media mixed 1:1 with tryptophan depleted dT10 media as well as non-preconditioned R10 media, dT10 media.

Initial experiments confirmed that the use of pre-conditioned media did not affect the ability of either $CD4^+$ or $CD8^+$ T cells to become activated by plated anti-CD3/CD28 as seen by surface CD69 expression after 14 hours ($p=0.4621$ by ANOVA, results not shown).

On the other hand, IDO preconditioned media had a dramatic effect on mTORC1 activity in both $CD4^+$ and $CD8^+$ T cells, as seen by significantly reduced levels of phosphorylation of S6 at Ser240 (Figure 4.9b.) after 14 hours of stimulation. It is

important to note that the addition of 25uM tryptophan prevented this effect, while the use of a 1:1 mix of pre-conditioned media with tryptophan depleted dT10 media failed to do so.

Likewise, after 72 hours of stimulation a highly significant effect could be seen in terms of inhibition of Tbet expression in both $CD4^+$ and $CD8^+$ T cells that could be completely prevented by the addition of 25µM tryptophan to the HeLa-IDO pre-treated media at t=0.

In addition - and similar to the results seen when tryptophan depleted dT10 media was used - the relative size of the $FoxP3^+$ $CD25^{high}$ population was twice as large in the groups cultured in HeLa-IDO pre-treated media; again this effect was completely reversed by the addition of 25µM tryptophan in the starting media.(Figure 4.9c.)

Finally, proliferation of both $CD4^+$ and $CD8^+$ T cells was dramatically inhibited by culture in HeLa IDO preconditioned media both in terms of the proportion of the starting cells dividing and in terms of the amounts of divisions the proliferating cells underwent (Figure 4.9d.). The addition of 25µM tryptophan at the outset led to proliferation levels identical or even better than those seen in media preconditioned by non IDO expressing HeLa cells.

Figure 4.9. Tumour cells expressing active IDO modify the phenotype of T cells in their vicinity by tryptophan depletion.

At t=0 HeLa wild-type ("HeLa-wt"), HeLa GFP("HeLa-GFP") and HeLa GFP-IDO("HeLa-IDO") transduced cell lines were cultured in 100ml of R10 media at a range of concentrations; at 24 and 72 hours supernatant was collected, freshly filtered and stored. 80 µl aliquots were analysed in duplicate by HPLC for tryptophan and kynurenine content. Culture for 72 hours with initial cell concentrations of 10^5 cells/ml was used to obtain preconditioned media used in subsequent T cell experiments that were immediately filtered and stored at 4˚C.

4.9a. HeLa IDO cells express functional IDO and are able to quickly convert tryptophan to kynurenine in vitro.

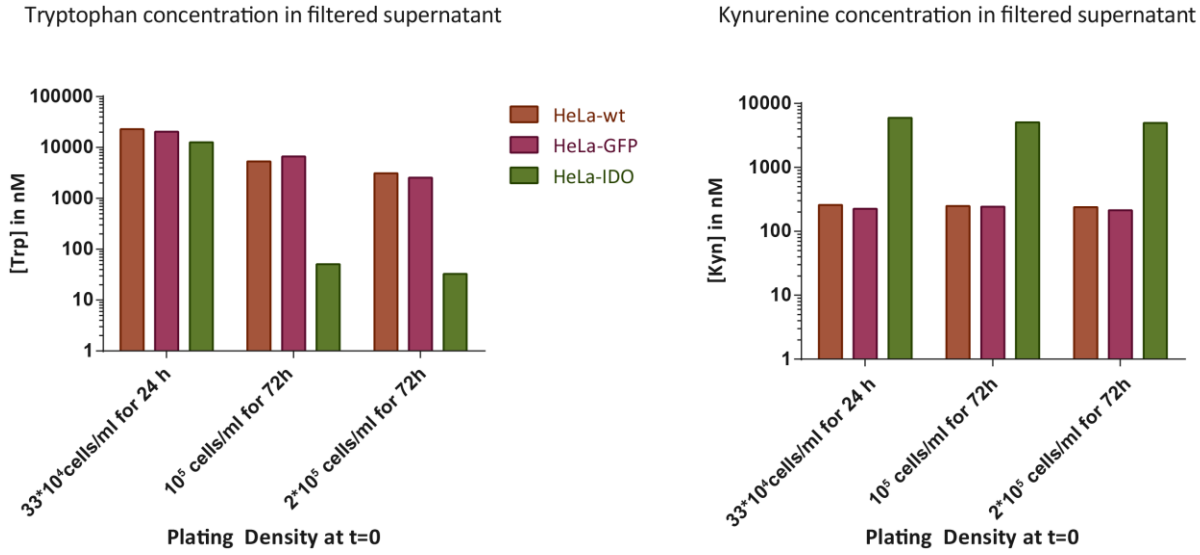

4.9a. Tryptophan levels are significantly reduced with a concomitant increase in kynurenine levels in supernatants from HeLa-IDO cultures after 72 hours.

(Left panel): While there was evidence of significant tryptophan consumption in all groups by 72 hours, it was only in the HeLa-IDO groups that it was virtually used up (<50nM tryptophan remaining); a plating concentration of 10^5 cells/ml was sufficient for this effect. Utilising higher HeLa-IDO plating densities for shorter time periods (e.g. 24 hours in this case) resulted in levels of IDO activity insufficient to effectively deplete tryptophan from media.

(Right panel): In all HeLa wild-type and HeLa-GFP groups kynurenine production was minimal and barely registered above background noise (range 212-257nM); in all HeLa-IDO group supernatants kynurenine could be detected at significant amounts (>4µM) consistent with active IDO expression.

$8*10^5$ fresh human blood cone derived PBL were plated in 200µl of media in a 96 well plate pre- coated with 10µg/ml CD3 and 5µg/ml anti-CD28. Media used included fresh R10 and dT10 as well as HeLa culture supernatants prepared as above. Control groups included multiple negative controls in non pre-coated wells; additional 25 µM tryptophan or 30nM rapamycin were also added in specific groups. The cells were harvested after 14 or 72 hours, fixed, permeabilised and stained for flow cytometric analysis. Results were normalised for each leucocyte donor to the positive control group (R10 media) to account for inter-donor variation.

4.9b. Culture in media pre-conditioned by IDO expressing cells results in impeded mTORC1 activity in human CD4⁺ and CD8⁺ T cells.

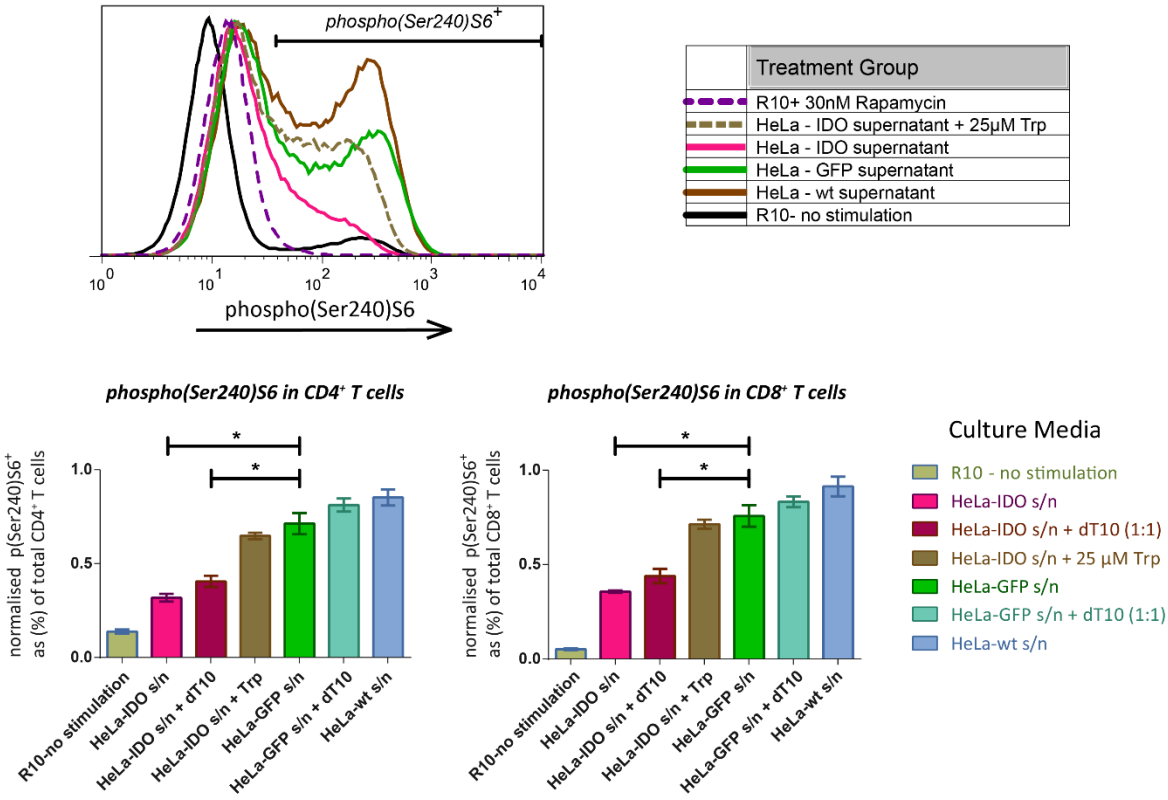

4.9b. Culture in media pre-treated by IDO expressing cells results in impeded phosphorylation of S6 at Ser240 in human T cell lymphocytes responding to stimulation by anti-CD3/CD28 by 14 hours.

(Top panel): Typical histograms of phospho(Ser240)S6 FI of CD4⁺ T cells from selected typical samples demonstrating the profound inhibitory effect HeLa-IDO preconditioned media types on mTORC1 activity as expressed by phosphorylation of S6 at Ser240.

(Bottom panels): Summary diagrams outlining the effect of HeLa-IDO preconditioned media on the mTORC1 pathway of CD4⁺ ***(left panel)*** and CD8⁺ ***(right panel)*** T cells as expressed by the percentage of cells staining positive for phosphorylated S6 at Ser240 (see top panel). Culture in HeLa-IDO preconditioned media significantly ($p<0.05$ by Dunnett's multiple comparisons test) inhibited S6 phosphorylation, and the addition of fresh tryptophan depleted dT10 media did not reverse this; in contrast, the addition of 25µM tryptophan at t=0 does.

4.9c. Culture in media pre-conditioned by IDO expressing cells results in inhibition of Tbet expression following stimulation in human CD4⁺ and CD8⁺ T cells.

10^6 fresh human blood cone derived PBL from healthy volunteers were plated in 1ml of media in each well of 48 well plates pre- coated with 10µg/ml CD3 and 5µg/ml anti-CD28. Media used included fresh R10 and dT10 as well as HeLa culture supernatants prepared as above. Control groups included preconditioned media with additional tryptophan and/or mixed 1:1 with tryptophan depleted dT10 media. The cells were harvested after 72 hours, fixed, permeabilised and stained for flow cytometric analysis. Results were normalised for each leucocyte donor to the positive control group (R10 media) to account for interdonor variation.

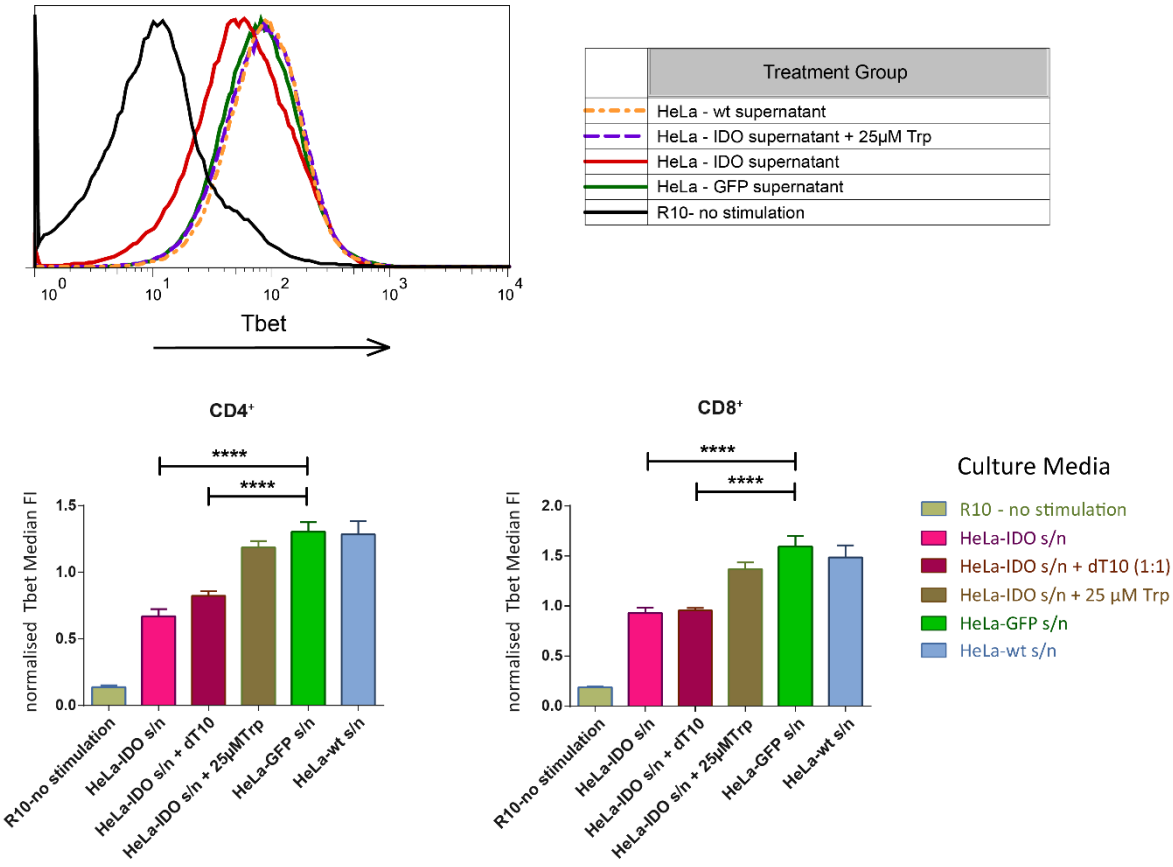

4.9c. Culture in media pre-conditioned by IDO expressing cells results in inhibition of Tbet expression following stimulation by anti-CD3/CD28 for 72 hours in human CD4⁺ and CD8⁺ T cells.

(Top panel): Typical histogram plots of Tbet expression in CD4⁺ T cells demonstrating reduced Tbet expression in cells cultured in HeLa-IDO pre-treated media.

(Bottom panels): Summary graphs demonstrating that Tbet upregulation in CD4⁺ ***(left panel***) and CD8⁺ ***(right panel)*** T cells is significantly decreased after 72h of stimulation by anti-CD3/CD28 by culturing in media preconditioned by active IDO expressing cells ($p<0.001$ by Dunnett's multiple comparisons test); the addition of tryptophan at t=0 abrogated this effect, while using a 1:1 mix of HeLa-IDO pre-conditioned and dT10 tryptophan depleted media did not rescue Tbet expression.

4.9d. Culture in media pre-conditioned by IDO expressing cells results in a relative expansion of the FoxP3⁺CD25^{high}CD4⁺ subpopulation in human T cell lymphocytes responding to stimulation by anti-CD3/CD28.

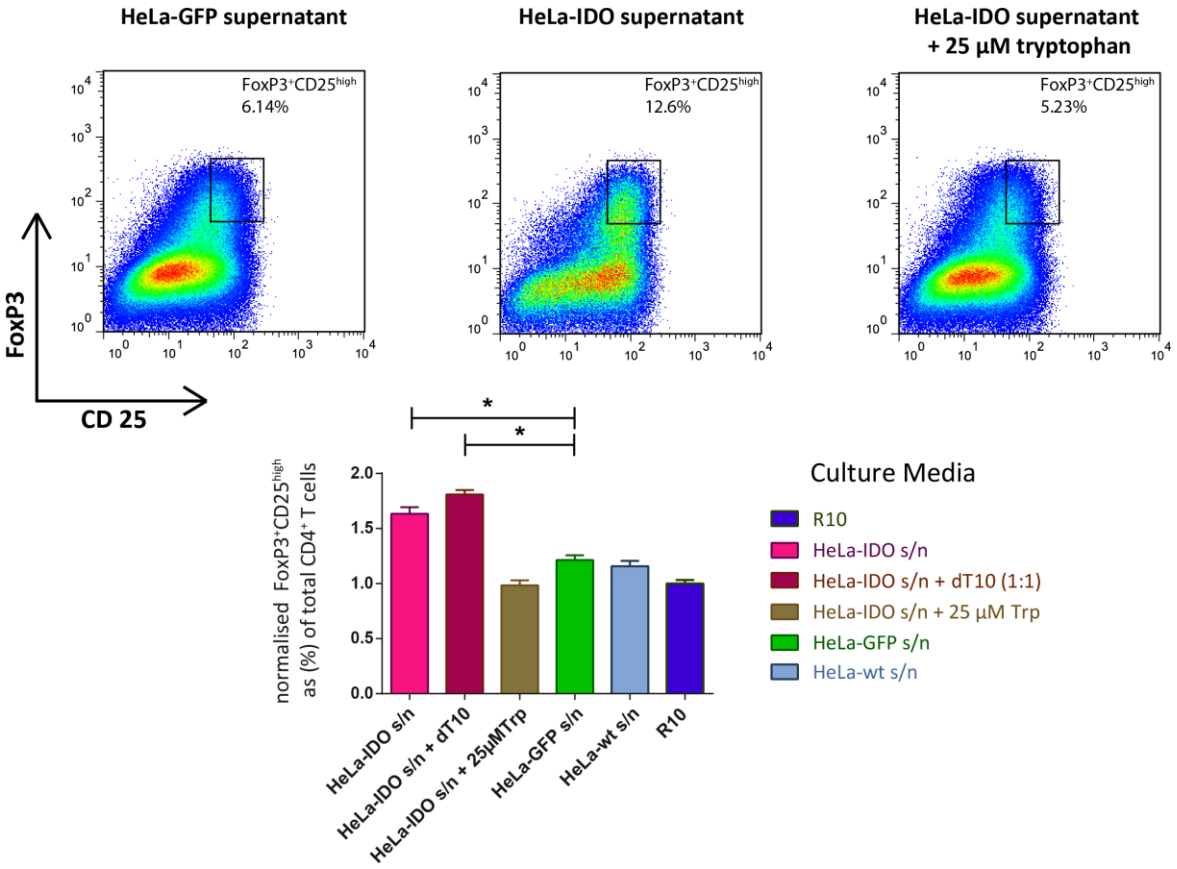

4.9d. Culture in media pre-conditioned by IDO expressing cells results in a relative expansion of the FoxP3⁺CD25^{high}CD4⁺ subpopulation in human T cell lymphocytes following stimulation by anti-CD3/CD28 for 72 hours.

(Top panels): Typical dot plots of CD4⁺ T cells of healthy volunteers after 72 hours of stimulation by anti-CD3/CD28 demonstrating an expansion of the FoxP3⁺CD25^{high}CD4⁺ subpopulation in cells cultured in HeLa-IDO pre-conditioned media as opposed to media preconditioned by HeLa-GFP cells; the effect was abrogated by the addition of 25µM tryptophan at t=0

(Bottom graph): Summary graph demonstrating a significant ($p<0.0001$ by Dunnett's multiple comparisons test) relative increase in the size of the FoxP3⁺CD25^{high}CD4⁺ subpopulation in cells cultured in HeLa-IDO pre-treated media as opposed to HeLa-GFP/wild-type or fresh R10 media. The effect was similar in size to that seen in cells cultured in fresh dT10 tryptophan poor media and could be abrogated by the addition of 25µM tryptophan at t=0 but not by culture in a 1:1 mix of HeLa-IDO pre-conditioned and dT10 tryptophan depleted media.

4.10. Discussion

4.10.1. The regulation of T cell fate and the mTORC1 pathway in human T cells via modulation of tryptophan availability.

The results outlined in chapter 2 paint a clear picture of the role of tryptophan availability in regulating the mTORC1 pathway in murine T cells following TCR activation by cognate peptide. The underlying molecular pathways are very similar in the human and murine immune system – both the role of mTORC1 axis in guiding cell fate and of IDO activity in modulating immune responses has been shown to exist in human systems.

It is therefore appropriate to ask the question of whether these results are applicable to the human immune system and specifically as this would expand our understanding of the way the tumour microenvironment impacts on tumour immunosurveillance and expand our options for combating immune escape mechanisms.

4.10.2. Hypothesis: IDO activity directly affects the response of the mTORC1 pathway in activated human T cells via reducing tryptophan availability in the local microenvironment and thereby alters their developmental fate.

The primary hypothesis behind the experiments described in the third chapter is that IDO exerts its immunomodulatory activity on human T cells to a large extent via its ability to deplete the microenvironment from tryptophan. The premise is that this has knock-on effects on the mTORC1 pathway of activated T cells that as a result alter their developmental fate to adopt a phenotype that is more permissive towards tumour growth and immune-escape.

4.10.3. Choice of experimental systems and methods

Experimenting with cells of human origin places significant limitations on experimental design. The biggest difference compared with the models used to investigate the murine system is the difficulty in establishing a system that properly replicates TCR activation by cognate peptide in vivo. The frequency of human T cells with specificity for specific peptides in the average sample from a human volunteer is vanishingly small unless the volunteer has previously been exposed to that particular peptide; even then ex vivo enrichment would be necessary to have access to a sufficient number of cells to experiment with. These cells however would no longer be naive and would already have undergone a fair amount of "programming" as a result of the processes necessary to obtain them; interpretation of results based on their use would be difficult and unlikely to be generalizable.

For the same reasons using immortalised cell lines expressing a particular TCR are fraught with difficulty; the techniques used to immortalise a cell line are likely to result in changes in the activity patterns of the mTORC1 pathway and in any case the developmental fate of these cells after activation is likely to differ in multiple aspects from those of freshly isolated lymphocytes.

In view of this a number of techniques commonly used to non-specifically activate human lymphocytes were evaluated; in the end stimulation with anti-CD3/anti-CD28 plated stimulating antibodies was chosen, as it functions without bypassing the normal TCR complex altogether and activates mTORC1 using the same pathways. What's more, it does not result in significant CD4 or CD8 downregulation and does not interact with CFSE staining thus perfectly complementing a flow cytometric approach.

In addition to lymphocytes obtained from healthy human volunteers, lymphocytes derived freshly collected blood samples of stage III and IV melanoma patients were used to both confirm that the findings were not affected by the process of lymphocyte extraction and generalizable to a clinically relevant population.

It should be noted that both in the case of samples from healthy volunteers and in samples from melanoma patients there was a significant amount of inter-donor variation in almost all parameters – most significantly in the proportion of cells responding to antiCD3/28 stimulation and to the intensity of stimulation as measured e.g. by maximum MFI of phospho(Ser240)S6. This was not surprising as humans exhibit a great deal of genetic heterogeneity – unlike inbred mouse strains – and moreover their immune systems are exposed to a variety of stimuli throughout their lifetime that cannot be controlled in any practical way.

In order to be able to interpret results from experiments with multiple donors, a normalisation procedure had to be used – typically using a positive control sample from each donor as the baseline for normalising all samples for that donor. This has the additional benefit of being able to aggregate results from experiments analysed on different days carried out following the same protocol as any variation in experimental procedures could be controlled. In this fashion the samples from melanoma patients were all processed fresh, avoiding any potential interference caused by the freeze-thawing process that would otherwise be necessary.

In an attempt to more finely delineate the effect of tryptophan depletion on naïve $CD4^+$ T cells a commercially available kit was used to isolate naïve $CD4^+$ cells via negative selection. Although the technique was not optimised and the experiment was primarily a pilot, nevertheless useful conclusions could be drawn to guide future experiments.

Finally, aiming to more closely mimic the effect of IDO action, media preconditioned by constitutionally IDO expressing tumour cell lines were used. Pilot experiments had demonstrated that this was preferable to using co-cultures of live cells as it was impossible to achieve tryptophan depletion in standard media within a timeframe where the exhaustion of additional nutrients would not confound the results. While feeding the cells with tryptophan-free media might have mitigated this to some extent, this would also result in removal of cytokines from the cell culture, significantly altering the parameters of the observed system.

4.10.4. Significance of results

Initial pilot experiments confirmed that mTORC1 activity – as measured by increased levels of phosphorylated S6 at Ser240 – could be seen shortly after T cell activation both in human $CD4^+$ and $CD8^+$ T cells. Furthermore the ability of these cells to be stimulated by plated anti-CD3/CD28 – as measured by the upregulation of surface CD69 – was not significantly altered in the absence of tryptophan; this was not surprising as anti-CD3/CD28 is a strong stimulus and analogous to high levels of high affinity peptide in the murine model where again there was no effect seen on CD69 expression.

Importantly, subsequent experiments confirmed the presence of a nearly linear dose response curve between mTORC1 activity and extracellular tryptophan concentration at tryptophan levels ≤ 1μM in both $CD4^+$ and $CD8^+$ T cells.

Furthermore the hypothesis that Tbet upregulation following stimulation by anti-CD3/CD28 is inhibited by tryptophan deprivation was confirmed both for $CD4^+$ and $CD8^+$ human lymphocytes whether they were derived from healthy volunteers or melanoma patients. Likewise a relative expansion of the $CD4^+FoxP3^+CD25^{high}$ population was observed under conditions of tryptophan scarcity that also resulted in a dramatic inhibition of proliferation in both $CD4^+$ and $CD8^+$ T cells.

In addition a pilot experiment utilising a purified naïve $CD4^+$ population also revealed a similar effect on Tbet and a relative increase of the $FoxP3^+CD25^{high}$ population though repeat experiments would be needed to confirm this result.

Finally, a concluding set of experiments demonstrated that all these effects of tryptophan deprivation (proliferation, mTORC1 inhibition, Tbet repression and $CD4^+$ $FoxP3^+CD25^{high}$ expansion) could be mimicked by media that had been pre-conditioned by culturing HeLa cells genetically modified to express active IDO. Significantly, these effects were not seen when media similarly preconditioned by IDO non expressing cells were used; the addition of 25μM tryptophan on the other hand did abolish these effects while that of fresh tryptophan-free media didn't.

It can therefore be surmised that tryptophan depletion is one of the main mechanisms through which IDO expression in the tumour microenvironment can directly affect T lymphocytes and impair their ability to partake in effective tumour immunosurveillance.

4.10.5. Outstanding issues

An important limitation in the experiments described in this chapter is the use of anti-CD3/CD28 to activate T cells instead of cognate antigen; this limitation is not easy to overcome without compromising other aspects of the model system although the similarity in the results observed suggests that similar mechanisms are operating in the human and murine system.

Similar to the case in experiments in the mice described earlier, an important issue that needs to be addressed is the nature of the detected $FoxP3^{+}CD25^{high}$ subpopulation and whether it truly corresponds to an expanded T_{reg} population.

Additional experiments would need to be carried out on the naïve $CD4^{+}$ T cell system to optimise culture conditions and confirm that the results are reproducible; similar experiments could be carried using naïve $CD8^{+}$ cells though obtaining suitable culture conditions will be more challenging in the absence of $CD4^{+}$ cells in the co-culture.

Chapter 5: Concluding Remarks and future directions

The experiments conducted as part of this research project have illuminated several aspects of the underlying molecular mechanisms through which IDO exerts its immunomodulatory effects.

Tryptophan deprivation from the local microenvironment has clearly been shown to have a central role in dampening the immune response and undoubtedly can be co-opted by tumour cells to contribute to immune escape.

The mTORC1 axis is evidently involved in this process; while it is likely that additional pathways such as the GCN2 axis are co-ordinately manipulated, the mTORC1 pathway and its downstream effectors have unequivocally been shown to be inhibited in tryptophan deprived conditions with dramatic results for cell growth, proliferation and phenotype.

It is important to point out that these effects also apply to the cancer cells themselves who have to develop mechanisms to counteract them so they can continue to grow and proliferate.

The clinical implications of these results point out to two different potential avenues for oncological treatments:

Firstly the tumour cell compensatory mechanisms could be targeted directly e.g. if a high affinity tryptophan transporter was identified on tumour cells but not expressed in immune cells then an inhibitor would considerably impede their ability to grow or even drive them to necrosis if the relevant cellular checkpoints had been inactivated.

Secondly the effect of IDO could be targeted either directly – by enzyme inhibitors, or indirectly e.g. by providing excess tryptophan. The latter approach might need to be complemented by techniques that improve nutrient delivery to the tumour bed such as certain VEGF inhibitors that drive the formation of mature rather than leaky vessels.

In the context of immunotherapy it might not even be necessary to have continuous IDO inhibition – as most of the effects of IDO affect T cells that are in the process of

becoming activated and prior to adopting their final cell fate it is conceivable that short bursts of IDO inhibition with or without manipulation of the downstream pathways might be sufficient to drive a strong immune response in the presence of additional stimuli (e.g. a tumour vaccine/ anti CTLA-4 or anti PD-1 antibody etc.)

Ultimately these are hypotheses that would need to be tested initially in animal models and then in humans; there are already trials of IDO inhibitors on the way in humans and their results are eagerly awaited.

In the meanwhile there are numerous basic immunological questions that remain to be addressed. Due to lack of time and resources several lines of investigation were not pursued in this project that could quickly provide additional information; in particular cytokine release profiles of the stimulated human T cells could easily be obtained and analysed by ELISA.

Additional cell fate indicators could be looked for; pilot experiments (not included in this report) were suggestive for a reciprocal increase in Eomesodermin levels when Tbet expression was reduced as a result of tryptophan depletion.

Immortalised clonal human lymphocytes could be used to confirm the findings on human lymphocytes stimulated by cognate peptide; inhibitors upstream of mTORC1 (e.g. of PI3K or Akt) or affecting parallel pathways (e.g. MEK/ERK) could further elucidate the importance of individual parts of the signalling cascade on the effects of IDO and provide additional targets for pharmacological manipulation.

Autophagy is another process that is closely associated with the mTORC1 pathway; it is known to be activated by cellular starvation but an active mTORC1 pathway inhibits it[141] ; it is highly likely that in a microenvironment where IDO is active and results in mTORC1 inhibition , autophagy would be triggered and may well act as a compensatory mechanism.

Finally, IDO is not the only immunomodulatory mechanism described that results in depletion of an essential amino-acid[142] – e.g. arginase expression by myeloid derived suppressor cells has been well described[143]. It is highly likely that in those cases as well the mTORC1 pathway would be involved with similar downstream effects altering the

immune response; experiments set up to confirm this would be relatively straightforward to set up and validate the concept.

Hopefully the results and investigational avenues opened up by this project will lead to an improved understanding of the role of IDO and similar nutrient depleting mechanisms in modulating the immune response and provide new options for immunotherapy against cancer.

Appendices

Appendix I: Materials and Methods

Unless otherwise specified results reported represent typical findings from experiments carried out in triplicate; where shown error bars represent standard errors unless specifically mentioned otherwise in the figure legend.

Included in brackets "[]" are the product identification / catalogue numbers for the particular product provided by the named supplier.

I.1. Antibodies

I.1.1. Conjugated Cell surface antibodies

Conjugated cell surface antibodies were obtained from e-Bioscience:

Anti-mouse antibodies against the following surface proteins were used: CD4-PE-Cy7 [25-0041-82], CD8b-FITC [11-0083-82] and CD8b–PerCP-eFluor® 710 [46-0083-80], CD69-PE [12-0691-83], TCRβ-PE [12-5961-82], CD25-APC-eFluor® 780 [47-0251-82], CD25-PE [12-0251-82].

Anti-human antibodies against the following surface proteins were used: CD25-Alexa Fluor® 488 [53-0259-42], Anti-Human-Vα24Jα18TCR eFluor® 660 [50-5806-42], CD8a PE-Cy7 [25-0088-42], CD3-APC-eFluor® 780 [47-0036-42] , CD4 PerCP-eFluor® 710 [46-0047-42] , CD69-APC [17-0699-42] , CD45RO-eFluor® 450[48-0457-42] – the latter being dual anti-human/mouse specific.

These were all used at a 1:200 dilution.

I.1.2. Intracellular antibodies

Antibodies to the following intracellular proteins were procured from Cell Signalling Technology®:

phospho(Ser240/244)S6 *[#2215],* Alexa Fluor647-phospho(Ser235/236)S6 *[#4851],* S6 [#2217], phospho(Ser2481)mTOR [#2974], phospho(Ser371)p70S6Kinase [#9208],

GCN2[#3302], phospho(Thr898)GCN2 [#3301], phospho(Thr308)-Akt [#2965] and phospho(Ser473)Akt [#4060] .

Anti-human Foxp3-PE [12-4777-42], anti-mouse Foxp3-APC [17-5773-82] and anti-Human/Mouse Tbet eFluor® 660 [50-5825-82] were obtained from e-Bioscience.

APC conjugated $F(ab')_2$ Fragment Goat anti-rabbit IgG(H+L) was from Jackson ImmunoResearch Laboratories, Inc.

For the purposes of flow cytometry all these were used at a 1:100 dilution unless otherwise specified.

I.1.3. Western blotting antibodies

For western blotting phospho-antibodies were used at 1:1000 , non-phospho at 1:2000 and anti-rabbit-HRP at 1:10000 unless otherwise specified.

Monoclonal mouse anti β-tubulin Antibody (#T4026) was from Sigma® and was used at a 1:5000 dilution for western blotting.

Polyclonal Goat anti mouse-HRP Ig was from DakoCytomation(#P0447)and was used at 1:20000 dilution.

Affinity purified goat anti-rabbit IgG (H&L)-HRP [#7074] was from Cell Signalling Technology® and was used at 1:10000 dilution

I.1.4. Functional antibodies

Functional grade purified Anti-mouse CD3 [16-0032-85] and CD28 [16-0281-85] and anti-human CD3 [16-0038-85] and CD28 [16-0289-85] was procured from e-Bioscience. In experiments involving both murine splenocytes and human PBL plating concentrations of 10µg/ml anti-CD3 and 5µg/ml anti-CD28 were used unless otherwise specified.

I.2. Mice, cell lines and cell culture

OT-1 and DO11.10 transgenic mice were bred in the Biomedical Services Unit, John Radcliffe Hospital, and used for ex-vivo experiments under the authority of a UK Home Office Project License.

All media used for cell culture work contained 50u/ml penicillin and 50µg/ml streptomycin; for murine cells 50µM 2-Mercaptoethanol was also present.

Unless otherwise specified:

- Cell lines were bulked up in Corning Flasks but plated in 6 well plates with fresh media prior to experiments
- Cell suspensions were spun for 5 minutes in room temperature at 1500 rpm.
- Media were warmed to 37˚C prior to use.
- 96-well plates were flat-bottomed for cell culture and round-bottomed for flow cytometry.

The murine EG7 cell line - derived from the C57BL/6 mouse lymphoblastic T cell lymphoma line EL4 by transduction with an ovalbumin encoding vector conferring aminoglycoside resistance[144] - was maintained in "*R10*" media- RPMI1640 with 10% Fetal Calf Serum ("FCS"); 0.4mg/ml Geneticin® (#11811-031, Invitrogen) was added to maintain ovalbumin expression.

The human cervical cancer HeLa cell line and its derivative transfected lines[128] were also maintained in R10 media.

GFP and IDO-GFP stably transfected clones of the aforementioned cell lines were kindly provided by Dr J.Silk; they were derived from the original lines by using the lentiviral pHR-SIN-BX-IRES-EM vector, which was designed to allow concurrent translation of both GFP and IDO from the polygenic transcript.

Stable transfection was confirmed prior to experiments using flow cytometry for GFP expression and kynurenine production for functional IDO expression.

To investigate the effects of tryptophan deprivation tryptophan-free RPMI 1640 (UK Hyclone Reserves,#RR11774.01) was used as the base media to which varying amounts of tryptophan and/or FCS were added, the most common combinations being “T10” with 10% FCS, “R0” with 25mM tryptophan and “T0” with no tryptophan or FCS. FCS normally contains variable amounts of tryptophan, typically in the 1-2μM range for a 10% solution as measured by HPLC (results not shown) as well as non measurable amounts bound directly to albumin[142].

For all experiments using EG7 or HeLa cell Lines the cells were plated in 6-well plates at $2*10^5$ cells/ml unless otherwise specified.

Human Interferon γ (Peprotech, [#300-02]) was used at a final concentration of 50ng/ml as an IDO-inducing agent for HeLa wild-type cell lines.

To simplify setting up 96 well plate experiments “2x” stocks of Media were prepared with double the amount of additives that when diluted 1:1 with tryptophan-free RPMI1640 would produce the same final concentrations as stock media.

Rapamycin (Sigma-Aldrich, [#R0395]) was kept as 1mg/ml stock in DMSO at -20°C and apart from initial titration experiments was used at 20nM final concentration.

For experiments using non antigen specific T cell stimulation, flat bottom 96 well plates were coated with anti-CD3 and anti-CD28 for 2 hours at 37°C and were washed 3 times in PBS prior to plating.

I.3. Bone Marrow Derived Dendritic Cell Related Procedures

I.3.1. BMDC preparation

Femora and tibia from freshly sacrificed mice were carefully dissected using aseptic technique and their ends cut using sharp sterile scissors. Bone marrow was flushed using warmed RPMI1640 and the resulting solution was passed through a cell strainer and spun down. The pellet was resuspended in 2ml of RBC Lysis buffer (5 Prime Gmbh,#2900040) and left at room temperature for 1.5min prior to the addition of 20ml R10 and a further spin-down. The resulting pellet was then resuspended in 20ml of R10 prior to counting.

Cells were then plated in 6 well plates with 5ml R10 with GM-CSF (obtained as hybridoma supernatant) and IL-4 (Peprotech,[#214-14]) at final concentrations of 10ng and 20ng/ml respectively at a density of 10^6 cells/ well. BMDCs were fed again after 72 and 144 hours gently aspirating 3ml from each well and replacing with fresh media supplemented with IL-4 and GM-CSF to reach the same final concentrations. Where appropriate LPS from E.Coli O26: B6 (Sigma, [#L8274]) was added 12h prior to harvest at a 1:100000 dilution (10mg/ml stock).

I.3.2. BMDC harvesting

Floating and semi-adherent cells were harvested by gently aspirating with a Pasteur pipette 4-5 times. Cells were then spun, counted and a small aliquot was stained with CD40 and CD11c to ascertain maturation status and CD11c purity; if <50% then the $CD11c^+$ fraction was further enriched by MACS using CD11c-beads (Miltenyi Biotech, clone N418, [#130-052-001]) and LS columns (Miltenyi Biotech,[#130-042-401]) using the manufacturer's protocol. Post MACS repeat flow cytometric analysis using CD11c stain took place to establish actual CD11c numbers.

I.3.3. BMDC peptide pulsing

$CD11c^+$ BMDCs were resuspended in mR10 media containing SIINFEKL peptide at appropriate dilutions and were incubated for 2-4h at 37°C in 5% CO_2 atmosphere. They were then washed at least twice prior to their further use in experiments.

I.4. Splenocyte Related Procedures

I.4.1. Splenocyte harvesting

Fresh spleens were individually mashed up in warmed up R10, passed through a cell strainer and spun .The pellet was resuspended in 2ml of RBC lysis buffer and left at room temperature for 1.5min prior to the addition of 20ml R10 and a further spin-down. The resulting pellet was then resuspended in 20ml of R10 prior to counting.

I.4.2. Splenocyte plating for tryptophan depletion experiments

100µl of "2x" media were added to 96 well plates as per experimental design with additives such as rapamycin where appropriate. Pulsed and unpulsed DCs were spun three times and resuspended each time in Trp-free RPMI1640. Following the last spin the resuspension volume was calculated aiming at a final concentration of $2*10^6$ cells/ml. 50µl were then added to the appropriate wells. The same procedure was carried out for the splenocytes but with the final resuspension at $2*10^7$ cells/ml aiming at a final well volume of 200µl with 10^7 splenocytes and 10^6 DCs.

I.4.3. Supernatant harvesting.

100µl of media were removed carefully from each well, spun down and supernatant was stored at-80°C for future analysis by HPLC/ELISA.

I.5. Human lymphocyte procedures

I.5.1. Sources of human leucocytes

2 sources were used to obtain human peripheral blood mononuclear cells ("PBMC") for experimental purposes:

Leukocyte Reduction System ("LRS") cones were procured through NHS Blood and Transplant (NHSBT) – these were obtained as a matter of course in the process of eliminating contaminating leucocytes from blood products at the point of collection from healthy volunteers who had provided written informed consent for the use of any blood products for research in an anonymous fashion. The cones were stored in room temperature and transferred to the lab for processing within 24 hours

Fresh blood was collected from patients who had provided informed consent as part of the ORB Biobank Project. 50 ml of blood was collected from each patient via simple venepuncture in 10 ml BD Vacutainer tubes [# 368480] , containing 171 IU sodium heparin and transferred in room temperature fresh to the lab within 4 hours of collection for further processing.

I.5.2. Peripheral blood leucocyte isolation

Peripheral Blood leucocytes ("PBL") were isolated from both LRS cones and fresh heparinised blood as follows:

Using strict aseptic procedure the LRS cone ends were severed using a scalpel blade and blood was eluted with neat RPMI 1640 warmed up to room temperature to bring the final volume to 150ml. In a similar fashion fresh patient blood collected in vacutainers was transferred to collecting tubes and also brought to a final volume of 150 ml with RPMI 1640.

15 ml of Lymphoprep (Stemcell technologies, [# 07851]) was then aliquoted in 50ml Falcon tubes to each of which 30ml of blood/RPMI 1640 mix was slowly layered. Each tube was then spun at 2000rpm for 30 minutes with the final break off and the PBL

layers were then immediately removed with a sterile pastette to a fresh collecting tube, where fresh RPMI was added to a final volume of 50ml. These tubes were then spun at 1500 rpm for 15 minutes with the final break on to fully wash the Lympoprep; after discarding the supernatant the volume was brought up to 50 ml again and the tubes when then spun at 1000rpm for 10 min with break on. After discarding the supernatant – which at this point should contain the platelets – the pellet would be resuspended in media appropriate for subsequent experiments. Where exact control of media tryptophan concentrations was essential, the last resuspension would be in tryptophan free media and an additional washing step with a further spin at 1500rpm for 5 min followed by resuspension in tryptophan free media would take place.

I.5.3. Naïve T cell isolation.

Naïve $CD4^+$ T cells were isolated from LRS cone derived PBMCs using the ” Naive CD4+ T Cell Isolation Kit II, human” [order no 130-094-131] by Miltenyi Biotech using the included protocol.

I.6. Flow Cytometry procedures

All procedures were carried out on ice, protected from direct light, and using ice cold reagents; incubations were carried out on ice in the dark; centrifuges were refrigerated to 4°C.

For quick analysis of unfixed cells using ≤4 fluorochromes the BD FACSCalibur™ platform was used; for analysis of fixed cells with more than 4 fluorochromes the CyAN™ ADP 9 Colour Analyzer by Beckman Coulter was employed.

I.6.1. Tetramer staining

Where appropriate prior to surface antibody staining the cells were spun down, supernatants discarded and pellets resuspended in 10µl of PE- $H2^K$-SIINFEKL tetramer conjugate for 30 min at 37°C.

I.6.2. Staining for FACSCalibur flow cytometer

Plates are washed with PBS/0.5%FCS twice; cells were resuspended in 50µl of surface Antibody mix in PBS/0.5%FCS and left for 20 min on ice in the dark. They were then washed twice, prior to resuspension in 200-400µl of PBS/0.5%FCS. Immediately prior to analysis propidium iodide(Sigma,# P4170) was added at a final concentration of 10µg/ml.

I.6.3. Staining for CyAN flow cytometer

Plates were initially washed with PBS twice prior to a 20 minute incubation with 50µl/well with the mastermix of vital (LIVE⁄DEAD® Fixable Aqua Dead Cell Stain, Invitrogen #L34957, used at a 1:300 dilution) and surface stains for the particular experiment. Plates were then washed twice and 100µl/well of fixation buffer was added.

Cells were left at 4°C in the dark for a minimum of one hour until all timepoints were collected for a particular experiment so that further processing and analysis could take place in tandem.

Permeabilisation and staining with primary and secondary intracellular antibodies was carried out as per e-Biosciences protocol. Fixed cells were left in the dark at 4°C prior to analysis that took place at most 12h after the last staining step.

Early experiments were carried out using an alternative protocol described by Sinclair et al[145] using 0.5%PFA for 15 minutes at room temperature as a fixative and 90% Methanol for 15 min at -20°C as a permeabilising agent, but comparison of the two methods showed similar qualitative results with much better yields for the e-Biosciences Method that was used for subsequent experiments.

I.6.4. Data analysis

A minimum of 10^4 relevant events were collected, stored ungated and the data analysed with FlowJo software v 7.6.5 (©TreeStar Inc.) on a workstation running Windows 7 as the operating system.

The gating strategy involved gating out dead cells followed by removing pulse width, FS and SS outliers – see Figure 3.1d. for a typical gating approach. Statistical analysis and graph plotting was done using Graphpad PRISM v6.

I.7. Western Blotting Procedures

I.7.1. Stock solutions

Tris-Glycine 10x : 250mMol Trizma® Base*(Sigma,#T1503)* with 192mM Glycine*(Sigma,#G8898)* in distilled water

Tris-Cl*(Sigma,#T3253)* : 0.5M, pH adjusted to 6.8 and 1.5M pH adjusted to 8.8

SDS*(Sigma,#3771)* : 10% Solution in water

APS*(Sigma,#A3678)* : 10% Solution in water ,kept in 100µl aliquots at -20°C

Acryl:Bis 30%*("Protogel",National Diagnostics,# ELR-210-010P)*

*:*30%w/v Acrylamide: methylene Bis Acrylamide 37.5:1 Solution

Sample Reducing Agent **:**DTT(*Sigma,#D9163*) kept as 30x 1.25M stock in 50µl aliquots at -20°C.

Molecular weight Marker: Novex® Sharp Pre-stained Protein Standard *(Invitrogen, #LC5800)*

I.7.2. Gradient Gels

NuPAGE® Novex® Bis Tris 1.5mm Mini Gels 4-12% (Invitrogen,# NP0336) were used in a Invitrogen Xcell SureLock™ MiniCell system.

I.7.3. In-house made gels

For single concentration gels the BioRad Mini-PROTEAN Tetra© Electrophoresis system was used. Gels were prepared fresh using the BioRad Mini-PROTEAN Tetra© Casting Module using the following recipes:

	Separating gel			Stacking Gel	
	8%	10%	12%	4%	6%
Distilled water	6.48ml	5.43ml	4.33ml	6ml	5.34ml
Tris-Cl	5ml-***1.5M, pH 8.8***			2.5ml-***0.5M, pH 6.8***	
Acryl:Bis 30%	4.25ml	5.3ml	6.4ml	1.34ml	2ml
10%SDS	0.16ml			0.1ml	
10%APS	0.1ml			0.05ml	
TEMED	0.01ml			0.01ml	
Total Volume	16ml			10ml	

I.7.4. Buffers

Lysis Buffer:	This was stored as stock at -20°C and was made of deionised water with 50nM HEPES *(Sigma Aldritch,# 3537),* 100 mM NaCl, 10 mM EDTA, 1% Triton® X-100 *(Sigma-Aldritch, T8532),* $Na_4P_2O_7$ 4mM, Na_3VO_4 *(Sigma Aldritch,# 450243),* NaF *(Sigma Aldritch,# S7920),* Pefabloc®SC *(Sigma Aldritch,# 76307)* and 1 tablet/20ml of Protease inhibitor cocktail "Complete, Mini" (Roche, #11836153001).
Sample Buffer:	3x SDS Sample Buffer*(New England Biolabs, #B7703S)*
Running buffer for in-house gels:	25mM Tris Base, 19.2mM Glycine and 0.1% SDS in deionised water.
Running buffer for gradient gels:	NuPAGE® MES-SDS Running Buffer*(#NP0002)* or NuPAGE® MOPS-SDS Running Buffer*(#NP0001)* both from Invitrogen.
Transfer Buffers :	25mM Tris Base,19.2mM Glycine and 0.1% SDS in deionised water; methanol was included according to the nature of the proteins to be blotted (40% if <20kDa, 20% if <150kDa and 0% otherwise)
Blocking/Dilution buffer:	PBS/0.1% TWEEN®20 (Sigma,#P5927) /5% w/v Bovine Serum Albumin- Fraction V purified lyophilized powder, Essentially γ-globulin free (Sigma-Aldritch, #A3059)
Washing Buffer**:**	PBS/0.1% TWEEN®20

I.7.5. Sample Preparation for Western Blotting

For adherent cell lines media were washed away from plates with ice cold PBS. Ice cold lysis buffer (100µl/10^6 cells) was added to the wells; the cells were then lysed in situ using a combination of cell scraping and gentle repeated pipetting.

For non-adherent cell lines cell suspensions were spun down in 15ml Falcon tubes; supernatants were discarded and pellets were resuspended in ice cold PBS and transferred to 2ml Eppendorf tubes that were spun again at 3000rpm for 5min.Supernatants were discarded and the pellets were lysed by the addition of 100µl Lysis Buffer/10^6cells and gently pipetting up and down.

Resulting Lysates were tumbled end over for 90 minutes and then spun down for 15 minutes at 13000rpm at 4°C. Supernatants were then collected, aliquoted, and snap frozen in dry ice and stored at -80°C if not used immediately.

The protein concentration in each sample was determined using the Pierce BCA assay kit[#23225] following manufacturer's instructions. Samples were diluted with lysis buffer as appropriate to ensure equal loading volumes and protein contents and were mixed with DTT and sample buffer prior to heating for 5 min at 95°C. They were then immediately cooled in ice, spun down and loaded on the electrophoresis gels.

I.7.6. Gel Running and Blotting

Gels were run at 200V constant Voltage until the blue marker dye reached the end of the gel. They were then blotted onto nitrocellulose paper *(Amersham Hybond™-C Extra,[#RPN303E])* using a Hoefer semi-dry transfer unit using 35mA/gel over 90 min.

I.7.7. Membrane staining

The resulting membranes were placed in blocking solution for 1 hour at room temperature and were washed in PBS/0.1%TWEEN®20 three times. At this point

membranes were cut if appropriate and were left overnight in primary antibody solution.

The next day they were washed again 3 times in PBS/0.1% TWEEN and secondary antibody solution was applied for 1 hour at room temperature. A single wash in PBS/0.5% TWEEN was then followed by 2 more in PBS/0.1%TWEEN, at which point the membrane was developed using ECL Plus Western Blotting Detection Reagents *(GE Healthcare ,[#GZRPN2132]).* Kodak® BioMax™ XAR Film was then immediately exposed to it in a dark room and following its development scanned using a Canoscan LIDE200 scanner; alternatively images were recorded with the use of a GE chemiluminescence detector.

I.7.8. Image analysis & quantification

Western Blot images were quantitated using ImageJ software v1.42q (public domain software, http://rsb.info.nih.gov/ij[146] as described in the accompanied instruction manual. Briefly the steps undertaken were as follows:

- Western blots images were either scanned from photographic film or directly recorded through a chemiluminescence scanner in 8 bit greyscale.

- The built in "Analyse>Gels>Plot Lanes" function was used to identify individual gel lanes.

- Profile plots were then obtained for each lane representing the relative pixel density (proportional to the amount of detected antigen) plotted against lane length; each detected band was therefore represented as a peak on this plot.

- For each lane the start and stop points of each peak were demarcated to account for background noise using the built-in "straight line" tool

- Each peak was then individually selected using the built-in "wand" tool and then the "Analyse>Gels>Label Peaks" function was used to allow correct peak identification.

- The programme automatically calculated the “area under the curve” (AUC) for each peak - this is proportional to the amount of antigen detected by the western blotting procedure.

- Within each lane the AUC of each band detected was compared to the AUC of the standard band (typically β-tubulin) and a ratio obtained.

- This value represents the relative density of the band of interest and can be compared with that of the same band on different lanes of the same gel.

- For comparison of bands across multiple gels, identical blotting and staining reagents and procedures were used and a standard sample had to be run in both gels to allow normalisation of results prior to comparison.

I.8. HPLC Analysis

Tryptophan and kynurenine concentrations in supernatants was measured by HPLC. Briefly, supernatants were treated with 30%(w/v) trichloroacetic acid for 15 minutes at 4°C and then centrifuged at 10000g for 30min . Resulting supernatants were injected into a *Zorbax SB-C18 column (Agilent Technologies, USA)* on a Knauer Smartline HPLC system with a variable wavelength Knauer smalrtline 26000 UV detector and a Biotek HPLC565 autosampler.

Kynurenine was detected as a single peak at a wavelength of 365nm and tryptophan at 280nm. Quantification and verification of peak location was carried out by running a series of standards with known tryptophan and kynurenine concentrations at the same run and subsequently establishing a normal curve for AUC values versus standard concentrations and extrapolating using GraphPad Prism version 6 on a workstation running Windows 7 operating system.

Appendix II: List of abbreviations

4E-BP1	: eukaryotic translation initiation factor 4E binding protein 1
a.a.	: Amino Acids
AAR	: amino acid response
AMPK	: 5' adenosine monophosphate-activated protein kinase
AHR	: aryl hydrocarbon receptor
anti-CD3/CD28	: plated anti-CD3 and anti-CD28 T lymphocyte stimulating antibodies
β2m	: β2 microglobulin
BMDC	: bone marrow derived dendritic cells
CIA	: Collagen-induced arthritis
CFSE	: Carboxyfluorescein succinimidyl ester
DC	: dendritic cells
EAE	: experimental autoimmune encephalomyelitis
EBSS	: Earle's balanced salt solution
EG7	: thymoma cell line
FI	: fluorescent intensity
FCS	: Fetal Calf Serum
GCN2	: general control nonderepressible 2
IDO	: indoleamine 2,3-dioxygenase (EC 1.13.11.52)
IDO2	: indoleamine 2,3-dioxygenase 2
IFN-γ	: Interferon gamma
mTOR	: mechanistic (or mammalian – old nomenclature) target of rapamycin
mTORC1	: mTOR complex 1
mTORC2	: mTOR complex 2
MHC	: Major histocompatibility complex
MFI	: median fluorescent intensity
NAD	: nicotinamide dinucleotide
NK cell	: natural killer cell
NKT cell	: natural killer T cell
PBMC	: Peripheral blood mononuclear cells
RAG 1/2	: Recombination Activating Gene 1/2
rpm	: rotations per minute
Ser	: Serine residue
TDO	: tryptophan 2,3-dioxygenase
TIL	: tumour infiltrating lymphocyte
Treg	: regulatory T cell
tRNA	: transfer RNA

Appendix III: Index of figures

Appendix IV: References

1. Ehrlich, P. Über den jetzigen stand der karzinomforschung. *Ned Tijdschr Geneeskd* **5,** 273–290 (1909).
2. Burnet, F. M. The concept of immunological surveillance. *Prog. Exp. Tumor Res.* **13,** 1–27 (1970).
3. Pantelouris, E. M. Absence of thymus in a mouse mutant. *Nature* **217,** 370–371 (1968).
4. Stutman, O. Tumor development after 3-methylcholanthrene in immunologically deficient athymic-nude mice. *Science* **183,** 534–536 (1974).
5. Stutman, O. Chemical carcinogenesis in nude mice: comparison between nude mice from homozygous matings and heterozygous matings and effect of age and carcinogen dose. *J. Natl. Cancer Inst.* **62,** 353–358 (1979).
6. Dunn, G. P., Old, L. J. & Schreiber, R. D. The three Es of cancer immunoediting. *Annu. Rev. Immunol.* **22,** 329–360 (2004).
7. Ikehara, S., Pahwa, R. N., Fernandes, G., Hansen, C. T. & Good, R. A. Functional T cells in athymic nude mice. *Proc. Natl. Acad. Sci. U. S. A.* **81,** 886–888 (1984).
8. Dighe, A. S., Richards, E., Old, L. J. & Schreiber, R. D. Enhanced in vivo growth and resistance to rejection of tumor cells expressing dominant negative IFN gamma receptors. *Immunity* **1,** 447–456 (1994).
9. Kaplan, D. H. *et al.* Demonstration of an interferon γ-dependent tumor surveillance system in immunocompetent mice. *Proc. Natl. Acad. Sci.* **95,** 7556–7561 (1998).
10. Russell, J. H. & Ley, T. J. Lymphocyte-mediated cytotoxicity. *Annu. Rev. Immunol.* **20,** 323–370 (2002).
11. Street, S. E., Cretney, E. & Smyth, M. J. Perforin and interferon-gamma activities independently control tumor initiation, growth, and metastasis. *Blood* **97,** 192–197 (2001).
12. Street, S. E. A., Trapani, J. A., MacGregor, D. & Smyth, M. J. Suppression of lymphoma and epithelial malignancies effected by interferon gamma. *J. Exp. Med.* **196,** 129–134 (2002).

13. Shinkai, Y. *et al.* RAG-2-deficient mice lack mature lymphocytes owing to inability to initiate V(D)J rearrangement. *Cell* **68,** 855–867 (1992).
14. Shankaran, V. *et al.* IFNgamma and lymphocytes prevent primary tumour development and shape tumour immunogenicity. *Nature* **410,** 1107–1111 (2001).
15. Dunn, G. P., Bruce, A. T., Ikeda, H., Old, L. J. & Schreiber, R. D. Cancer immunoediting: from immunosurveillance to tumor escape. *Nat Immunol* **3,** 991–998 (2002).
16. Girardi, M. *et al.* The distinct contributions of murine T cell receptor (TCR)gammadelta+ and TCRalphabeta+ T cells to different stages of chemically induced skin cancer. *J. Exp. Med.* **198,** 747–755 (2003).
17. Swann, J. B. *et al.* Type I natural killer T cells suppress tumors caused by p53 loss in mice. *Blood* **113,** 6382–6385 (2009).
18. Dunn, G. P. *et al.* A critical function for type I interferons in cancer immunoediting. *Nat. Immunol.* **6,** 722–729 (2005).
19. Langowski, J. L. *et al.* IL-23 promotes tumour incidence and growth. *Nature* **442,** 461–465 (2006).
20. Simson, L. *et al.* Regulation of carcinogenesis by IL-5 and CCL11: a potential role for eosinophils in tumor immune surveillance. *J. Immunol. Baltim. Md 1950* **178,** 4222–4229 (2007).
21. Smyth, M. J., Crowe, N. Y. & Godfrey, D. I. NK cells and NKT cells collaborate in host protection from methylcholanthrene-induced fibrosarcoma. *Int. Immunol.* **13,** 459–463 (2001).
22. Vesely, M. D., Kershaw, M. H., Schreiber, R. D. & Smyth, M. J. Natural Innate and Adaptive Immunity to Cancer. *Annu. Rev. Immunol.* **29,** 235–271 (2011).
23. Smyth, M. J. *et al.* Perforin-mediated cytotoxicity is critical for surveillance of spontaneous lymphoma. *J. Exp. Med.* **192,** 755–760 (2000).
24. Donehower, L. A. *et al.* Mice deficient for p53 are developmentally normal but susceptible to spontaneous tumours. *Nature* **356,** 215–221 (1992).
25. Boshoff, C. & Weiss, R. AIDS-related malignancies. *Nat. Rev. Cancer* **2,** 373–382 (2002).

26. Chaturvedi, A. K. *et al.* Elevated risk of lung cancer among people with AIDS. *AIDS Lond. Engl.* **21,** 207–213 (2007).

27. Kirk, G. D. *et al.* HIV infection is associated with an increased risk for lung cancer, independent of smoking. *Clin. Infect. Dis. Off. Publ. Infect. Dis. Soc. Am.* **45,** 103–110 (2007).

28. Krynitz, B. *et al.* Risk of skin cancer and other malignancies in kidney, liver, heart and lung transplant recipients 1970 to 2008--a Swedish population-based study. *Int. J. Cancer J. Int. Cancer* **132,** 1429–1438 (2013).

29. Vajdic, C. M. *et al.* Cancer incidence before and after kidney transplantation. *JAMA J. Am. Med. Assoc.* **296,** 2823–2831 (2006).

30. Penn, I. Malignant melanoma in organ allograft recipients. *Transplantation* **61,** 274–278 (1996).

31. Moloney, F. J. *et al.* A population-based study of skin cancer incidence and prevalence in renal transplant recipients. *Br. J. Dermatol.* **154,** 498–504 (2006).

32. Reuschenbach, M., von Knebel Doeberitz, M. & Wentzensen, N. A systematic review of humoral immune responses against tumor antigens. *Cancer Immunol. Immunother. CII* **58,** 1535–1544 (2009).

33. Albert, M. L. & Darnell, R. B. Paraneoplastic neurological degenerations: keys to tumour immunity. *Nat. Rev. Cancer* **4,** 36–44 (2004).

34. Albert, M. L. *et al.* Tumor-specific killer cells in paraneoplastic cerebellar degeneration. *Nat. Med.* **4,** 1321–1324 (1998).

35. Ferradini, L. *et al.* Analysis of T cell receptor variability in tumor-infiltrating lymphocytes from a human regressive melanoma. Evidence for in situ T cell clonal expansion. *J. Clin. Invest.* **91,** 1183–1190 (1993).

36. Zorn, E. & Hercend, T. A natural cytotoxic T cell response in a spontaneously regressing human melanoma targets a neoantigen resulting from a somatic point mutation. *Eur. J. Immunol.* **29,** 592–601 (1999).

37. Koebel, C. M. *et al.* Adaptive immunity maintains occult cancer in an equilibrium state. *Nature* **450,** 903–907 (2007).

38. Clark, W. H., Jr *et al.* Model predicting survival in stage I melanoma based on tumor progression. *J. Natl. Cancer Inst.* **81,** 1893–1904 (1989).

39. Schumacher, K., Haensch, W., Röefzaad, C. & Schlag, P. M. Prognostic significance of activated CD8(+) T cell infiltrations within esophageal carcinomas. *Cancer Res.* **61,** 3932–3936 (2001).

40. Zhang, L. *et al.* Intratumoral T cells, recurrence, and survival in epithelial ovarian cancer. *N. Engl. J. Med.* **348,** 203–213 (2003).

41. Galon, J. *et al.* Type, density, and location of immune cells within human colorectal tumors predict clinical outcome. *Science* **313,** 1960–1964 (2006).

42. Restifo, N. P. *et al.* Loss of functional beta 2-microglobulin in metastatic melanomas from five patients receiving immunotherapy. *J. Natl. Cancer Inst.* **88,** 100–108 (1996).

43. Von Boehmer, L. *et al.* NY-ESO-1-specific immunological pressure and escape in a patient with metastatic melanoma. *Cancer Immun.* **13,** 12 (2013).

44. Khong, H. T., Wang, Q. J. & Rosenberg, S. A. Identification of multiple antigens recognized by tumor-infiltrating lymphocytes from a single patient: tumor escape by antigen loss and loss of MHC expression. *J. Immunother. Hagerstown Md 1997* **27,** 184–190 (2004).

45. Takahashi, H. *et al.* FAS Death Domain Deletions and Cellular FADD-like Interleukin 1β Converting Enzyme Inhibitory Protein (Long) Overexpression: Alternative Mechanisms for Deregulating the Extrinsic Apoptotic Pathway in Diffuse Large B-Cell Lymphoma Subtypes. *Clin. Cancer Res.* **12,** 3265–3271 (2006).

46. Shin, M. S. *et al.* Mutations of Tumor Necrosis Factor-related Apoptosis-inducing Ligand Receptor 1 (TRAIL-R1) and Receptor 2 (TRAIL-R2) Genes in Metastatic Breast Cancers. *Cancer Res.* **61,** 4942–4946 (2001).

47. Hinz, S. *et al.* Bcl-XL protects pancreatic adenocarcinoma cells against CD95- and TRAIL-receptor-mediated apoptosis. *Oncogene* **19,** 5477–5486 (2000).

48. Dong, H. *et al.* Tumor-associated B7-H1 promotes T-cell apoptosis: A potential mechanism of immune evasion. *Nat. Med.* (2002). doi:10.1038/nm730

49. Villablanca, E. J. *et al.* Tumor-mediated liver X receptor-alpha activation inhibits CC chemokine receptor-7 expression on dendritic cells and dampens antitumor responses. *Nat. Med.* **16,** 98–105 (2010).

50. Wrzesinski, S. H., Wan, Y. Y. & Flavell, R. A. Transforming growth factor-beta and the immune response: implications for anticancer therapy. *Clin. Cancer Res. Off. J. Am. Assoc. Cancer Res.* **13,** 5262–5270 (2007).

51. Herber, D. L. *et al.* Lipid accumulation and dendritic cell dysfunction in cancer. *Nat. Med.* **16,** 880–886 (2010).

52. Terabe, M. & Berzofsky, J. A. Immunoregulatory T cells in tumor immunity. *Curr. Opin. Immunol.* **16,** 157–162 (2004).

53. Gabrilovich, D. I. & Nagaraj, S. Myeloid-derived suppressor cells as regulators of the immune system. *Nat Rev Immunol* **9,** 162–174 (2009).

54. Wei, S. *et al.* Plasmacytoid dendritic cells induce CD8+ regulatory T cells in human ovarian carcinoma. *Cancer Res.* **65,** 5020–5026 (2005).

55. Srivastava, M. K., Sinha, P., Clements, V. K., Rodriguez, P. & Ostrand-Rosenberg, S. Myeloid-Derived Suppressor Cells Inhibit T-Cell Activation by Depleting Cystine and Cysteine. *Cancer Res* **70,** 68–77 (2010).

56. Harden, J. L. & Egilmez, N. K. Indoleamine 2,3-Dioxygenase and Dendritic Cell Tolerogenicity. *Immunol. Invest.* **41,** 738–764 (2012).

57. Leklem, J. E. Quantitative aspects of tryptophan metabolism in humans and other species: a review. *Am. J. Clin. Nutr.* **24,** 659–672 (1971).

58. Platten, M., Wick, W. & Eynde, B. J. V. den. Tryptophan Catabolism in Cancer: Beyond IDO and Tryptophan Depletion. *Cancer Res.* **72,** 5435–5440 (2012).

59. Kanai, M. *et al.* Tryptophan 2,3-dioxygenase is a key modulator of physiological neurogenesis and anxiety-related behavior in mice. *Mol. Brain* **2,** 8 (2009).

60. Yamamoto, S. & Hayaishi, O. Tryptophan pyrrolase of rabbit intestine. D- and L-tryptophan-cleaving enzyme or enzymes. *J. Biol. Chem.* **242,** 5260–5266 (1967).

61. Godin-Ethier, J., Hanafi, L.-A., Piccirillo, C. A. & Lapointe, R. Indoleamine 2,3-Dioxygenase Expression in Human Cancers: Clinical and Immunologic Perspectives. *Clin. Cancer Res.* **17,** 6985–6991 (2011).

62. Taylor, M. W. & Feng, G. S. Relationship between interferon-gamma, indoleamine 2,3-dioxygenase, and tryptophan catabolism. *FASEB J.* **5,** 2516–2522 (1991).

63. Pfefferkorn, E. R. & Guyre, P. M. Inhibition of growth of Toxoplasma gondii in cultured fibroblasts by human recombinant gamma interferon. *Infect. Immun.* **44,** 211–216 (1984).

64. Ozaki, Y., Edelstein, M. P. & Duch, D. S. The actions of interferon and antiinflammatory agents of induction of indoleamine 2,3-dioxygenase in human peripheral blood monocytes. *Biochem. Biophys. Res. Commun.* **144,** 1147–1153 (1987).

65. Fukunaga, M. *et al.* Studies on tissue and cellular distribution of indoleamine 2,3-dioxygenase 2: the absence of IDO1 upregulates IDO2 expression in the epididymis. *J. Histochem. Cytochem. Off. J. Histochem. Soc.* **60,** 854–860 (2012).

66. Meininger, D. *et al.* Purification and kinetic characterization of human indoleamine 2,3-dioxygenases 1 and 2 (IDO1 and IDO2) and discovery of selective IDO1 inhibitors. *Biochim. Biophys. Acta* **1814,** 1947–1954 (2011).

67. Metz, R. *et al.* Novel tryptophan catabolic enzyme IDO2 is the preferred biochemical target of the antitumor indoleamine 2,3-dioxygenase inhibitory compound D-1-methyl-tryptophan. *Cancer Res.* **67,** 7082–7087 (2007).

68. Fatokun, A. A., Hunt, N. H. & Ball, H. J. Indoleamine 2,3-dioxygenase 2 (IDO2) and the kynurenine pathway: characteristics and potential roles in health and disease. *Amino Acids* (2013). doi:10.1007/s00726-013-1602-1

69. Witkiewicz, A. K. *et al.* Genotyping and expression analysis of IDO2 in human pancreatic cancer: a novel, active target. *J. Am. Coll. Surg.* **208,** 781–787; discussion 787–789 (2009).

70. Löb, S. *et al.* IDO1 and IDO2 are expressed in human tumors: levo- but not dextro-1-methyl tryptophan inhibits tryptophan catabolism. *Cancer Immunol. Immunother. CII* **58,** 153–157 (2009).

71. Byrne, G. I., Lehmann, L. K. & Landry, G. J. Induction of tryptophan catabolism is the mechanism for gamma-interferon-mediated inhibition of intracellular Chlamydia psittaci replication in T24 cells. *Infect. Immun.* **53,** 347–351 (1986).

72. Däubener, W. *et al.* Restriction of Toxoplasma gondiiGrowth in Human Brain Microvascular Endothelial Cells by Activation of Indoleamine 2,3-Dioxygenase. *Infect. Immun.* **69,** 6527–6531 (2001).

73. Bozza, S. *et al.* A Crucial Role for Tryptophan Catabolism at the Host/Candida albicans Interface. *J. Immunol.* **174,** 2910–2918 (2005).

74. Munn, D. H. *et al.* Prevention of allogeneic fetal rejection by tryptophan catabolism. *Science* **281,** 1191–1193 (1998).

75. Yan, Y. *et al.* IDO Upregulates Regulatory T Cells via Tryptophan Catabolite and Suppresses Encephalitogenic T Cell Responses in Experimental Autoimmune Encephalomyelitis. *J. Immunol.* **185,** 5953–5961 (2010).

76. Criado, G., Šimelyte, E., Inglis, J. J., Essex, D. & Williams, R. O. Indoleamine 2,3 dioxygenase–mediated tryptophan catabolism regulates accumulation of Th1/Th17 cells in the joint in collagen-induced arthritis. *Arthritis Rheum.* **60,** 1342–1351 (2009).

77. Chen, S.-Y. *et al.* Suppression of collagen-induced arthritis by intra-articular lentiviral vector-mediated delivery of Toll-like receptor 7 short hairpin RNA gene. *Gene Ther.* **19,** 752–760 (2012).

78. Munn, D. H. *et al.* GCN2 Kinase in T Cells Mediates Proliferative Arrest and Anergy Induction in Response to Indoleamine 2,3-Dioxygenase. *Immunity* **22,** 633–642 (2005).

79. Opitz, C. A., Wick, W., Steinman, L. & Platten, M. Tryptophan degradation in autoimmune diseases. *Cell. Mol. Life Sci. CMLS* **64,** 2542–2563 (2007).

80. Opitz, C. A. *et al.* An endogenous tumour-promoting ligand of the human aryl hydrocarbon receptor. *Nature* **478,** 197–203 (2011).

81. Fallarino, F. *et al.* The Combined Effects of Tryptophan Starvation and Tryptophan Catabolites Down-Regulate T Cell Receptor ζ-Chain and Induce a Regulatory Phenotype in Naive T Cells. *J. Immunol.* **176,** 6752–6761 (2006).

82. Huang, A. *et al.* Serum tryptophan decrease correlates with immune activation and impaired quality of life in colorectal cancer. *Br. J. Cancer* **86,** 1691–1696 (2002).

83. Weinlich, G., Murr, C., Richardsen, L., Winkler, C. & Fuchs, D. Decreased serum tryptophan concentration predicts poor prognosis in malignant melanoma patients. *Dermatol. Basel Switz.* **214,** 8–14 (2007).

84. Okamoto, T. *et al.* Transcriptional regulation of indoleamine 2,3-dioxygenase (IDO) by tryptophan and its analogue : Down-regulation of the indoleamine

2,3-dioxygenase (IDO) transcription by tryptophan and its analogue. *Cytotechnology* **54,** 107–13 (2007).

85. Brandacher, G. *et al.* Prognostic value of indoleamine 2,3-dioxygenase expression in colorectal cancer: effect on tumor-infiltrating T cells. *Clin. Cancer Res. Off. J. Am. Assoc. Cancer Res.* **12,** 1144–1151 (2006).

86. Ino, K. *et al.* Indoleamine 2,3-dioxygenase is a novel prognostic indicator for endometrial cancer. *Br. J. Cancer* **95,** 1555–1561 (2006).

87. Nakamura, T. *et al.* Expression of indoleamine 2, 3-dioxygenase and the recruitment of Foxp3-expressing regulatory T cells in the development and progression of uterine cervical cancer. *Cancer Sci.* **98,** 874–881 (2007).

88. Witkiewicz, A. *et al.* Expression of indoleamine 2,3-dioxygenase in metastatic pancreatic ductal adenocarcinoma recruits regulatory T cells to avoid immune detection. *J. Am. Coll. Surg.* **206,** 849–854; discussion 854–856 (2008).

89. Astigiano, S. *et al.* Eosinophil granulocytes account for indoleamine 2,3-dioxygenase-mediated immune escape in human non-small cell lung cancer. *Neoplasia N. Y. N* **7,** 390–396 (2005).

90. Inaba, T. *et al.* Role of the immunosuppressive enzyme indoleamine 2,3-dioxygenase in the progression of ovarian carcinoma. *Gynecol. Oncol.* **115,** 185–192 (2009).

91. Ino, K. *et al.* Inverse correlation between tumoral indoleamine 2,3-dioxygenase expression and tumor-infiltrating lymphocytes in endometrial cancer: its association with disease progression and survival. *Clin. Cancer Res. Off. J. Am. Assoc. Cancer Res.* **14,** 2310–2317 (2008).

92. Uyttenhove, C. *et al.* Evidence for a tumoral immune resistance mechanism based on tryptophan degradation by indoleamine 2,3-dioxygenase. *Nat. Med.* **9,** 1269–1274 (2003).

93. Munn, D. H. & Mellor, A. L. Indoleamine 2,3-dioxygenase and tumor-induced tolerance. *J. Clin. Invest.* **117,** 1147–1154 (2007).

94. Holmgaard, R. B., Zamarin, D., Munn, D. H., Wolchok, J. D. & Allison, J. P. Indoleamine 2,3-dioxygenase is a critical resistance mechanism in antitumor T cell immunotherapy targeting CTLA-4. *J. Exp. Med.* **210,** 1389–1402 (2013).

95. Pilotte, L. *et al.* Reversal of tumoral immune resistance by inhibition of tryptophan 2,3-dioxygenase. *Proc. Natl. Acad. Sci. U. S. A.* **109,** 2497–2502 (2012).

96. Gwinn, D. M. *et al.* AMPK phosphorylation of raptor mediates a metabolic checkpoint. *Mol. Cell* **30,** 214–226 (2008).

97. Hardie, D. G. AMP-activated/SNF1 protein kinases: conserved guardians of cellular energy. *Nat. Rev. Mol. Cell Biol.* **8,** 774–785 (2007).

98. Sancak, Y. *et al.* The Rag GTPases Bind Raptor and Mediate Amino Acid Signaling to mTORC1. *Science* **320,** 1496–1501 (2008).

99. Sancak, Y. *et al.* Ragulator-Rag Complex Targets mTORC1 to the Lysosomal Surface and Is Necessary for Its Activation by Amino Acids. *Cell* **141,** 290–303 (2010).

100. Kim, E., Goraksha-Hicks, P., Li, L., Neufeld, T. P. & Guan, K.-L. Regulation of TORC1 by Rag GTPases in nutrient response. *Nat Cell Biol* **10,** 935–945 (2008).

101. Inoki, K., Li, Y., Zhu, T., Wu, J. & Guan, K.-L. TSC2 is phosphorylated and inhibited by Akt and suppresses mTOR signalling. *Nat. Cell Biol.* **4,** 648–657 (2002).

102. Ma, L., Chen, Z., Erdjument-Bromage, H., Tempst, P. & Pandolfi, P. P. Phosphorylation and functional inactivation of TSC2 by Erk implications for tuberous sclerosis and cancer pathogenesis. *Cell* **121,** 179–193 (2005).

103. Roux, P. P. *et al.* RAS/ERK signaling promotes site-specific ribosomal protein S6 phosphorylation via RSK and stimulates cap-dependent translation. *J. Biol. Chem.* **282,** 14056–14064 (2007).

104. Feng, Z., Zhang, H., Levine, A. J. & Jin, S. The coordinate regulation of the p53 and mTOR pathways in cells. *Proc. Natl. Acad. Sci. U. S. A.* **102,** 8204 –8209 (2005).

105. Yip, C. K., Murata, K., Walz, T., Sabatini, D. M. & Kang, S. A. Structure of the Human mTOR Complex I and Its Implications for Rapamycin Inhibition. *Mol. Cell* **38,** 768–774 (2010).

106. Laplante, M. & Sabatini, D. M. mTOR signaling at a glance. *J Cell Sci* **122,** 3589–3594 (2009).

107. Yonezawa, K., Tokunaga, C., Oshiro, N. & Yoshino, K. Raptor, a binding partner of target of rapamycin. *Biochem. Biophys. Res. Commun.* **313,** 437–441 (2004).

108. Kantidakis, T., Ramsbottom, B. A., Birch, J. L., Dowding, S. N. & White, R. J. mTOR associates with TFIIIC, is found at tRNA and 5S rRNA genes, and targets their repressor Maf1. *Proc. Natl. Acad. Sci. U. S. A.* (2010). doi:10.1073/pnas.1005188107

109. Ikenoue, T., Inoki, K., Yang, Q., Zhou, X. & Guan, K.-L. Essential function of TORC2 in PKC and Akt turn motif phosphorylation, maturation and signalling. *EMBO J* **27,** 1919–1931 (2008).

110. Sarbassov, D. D. *et al.* Prolonged rapamycin treatment inhibits mTORC2 assembly and Akt/PKB. *Mol. Cell* **22,** 159–168 (2006).

111. Zhang, P. *et al.* The GCN2 eIF2{alpha} Kinase Is Required for Adaptation to Amino Acid Deprivation in Mice. *Mol Cell Biol* **22,** 6681–6688 (2002).

112. Kilberg, M. S., Shan, J. & Su, N. ATF4-dependent transcription mediates signaling of amino acid limitation. *Trends Endocrinol. Metab.* **20,** 436–443 (2009).

113. Kilberg, M. S., Pan, Y.-X., Chen, H. & Leung-Pineda, V. Nutritional control of gene expression: how mammalian cells respond to amino acid limitation. *Annu. Rev. Nutr.* **25,** 59–85 (2005).

114. Pan, Y.-X., Chen, H., Thiaville, M. M. & Kilberg, M. S. Activation of the ATF3 gene through a co-ordinated amino acid-sensing response programme that controls transcriptional regulation of responsive genes following amino acid limitation. *Biochem. J.* **401,** 299–307 (2007).

115. Yu, L. *et al.* Termination of autophagy and reformation of lysosomes regulated by mTOR. *Nature* **advance online publication,** (2010).

116. Chen, Y.-J., Tan, B. C.-M., Cheng, Y.-Y., Chen, J.-S. & Lee, S.-C. Differential regulation of CHOP translation by phosphorylated eIF4E under stress conditions. *Nucleic Acids Res* **38,** 764–777 (2010).

117. Jin, H.-O. *et al.* Activating transcription factor 4 and CCAAT/enhancer-binding protein-[beta] negatively regulate the mammalian target of rapamycin via

Redd1 expression in response to oxidative and endoplasmic reticulum stress. *Free Radic. Biol. Med.* **46,** 1158–1167 (2009).

118. Kazemi, S. *et al.* A Novel Function of eIF2{alpha} Kinases as Inducers of the Phosphoinositide-3 Kinase Signaling Pathway. *Mol Biol Cell* **18,** 3635–3644 (2007).

119. Kantidakis, T. & White, R. J. A feedback loop between mTOR and tRNA expression? *Cell Cycle* **9,** 2936–2935 (2010).

120. Nii, T. *et al.* Molecular events involved in up-regulating human Na+-independent neutral amino acid transporter LAT1 during T-cell activation. *Biochem. J.* **358,** 693–704 (2001).

121. Edinger, A. L. & Thompson, C. B. Akt Maintains Cell Size and Survival by Increasing mTOR-dependent Nutrient Uptake. *Mol Biol Cell* **13,** 2276–2288 (2002).

122. Rodriguez, P. C. *et al.* Arginase I production in the tumor microenvironment by mature myeloid cells inhibits T-cell receptor expression and antigen-specific T-cell responses. *Cancer Res.* **64,** 5839–5849 (2004).

123. Delgoffe, G. M. *et al.* The mTOR Kinase Differentially Regulates Effector and Regulatory T Cell Lineage Commitment. *Immunity* **30,** 832–844 (2009).

124. Lee, K. *et al.* Mammalian Target of Rapamycin Protein Complex 2 Regulates Differentiation of Th1 and Th2 Cell Subsets via Distinct Signaling Pathways. *Immunity* **32,** 743–753 (2010).

125. Haxhinasto, S., Mathis, D. & Benoist, C. The AKT-mTOR axis regulates de novo differentiation of CD4+Foxp3+ cells. *J. Exp. Med.* **205,** 565–574 (2008).

126. Araki, K. *et al.* mTOR regulates memory CD8 T-cell differentiation. *Nature* **460,** 108–112 (2009).

127. Rao, R. R., Li, Q., Odunsi, K. & Shrikant, P. A. The mTOR Kinase Determines Effector versus Memory CD8+ T Cell Fate by Regulating the Expression of Transcription Factors T-bet and Eomesodermin. *Immunity* doi:10.1016/j.immuni.2009.10.010

128. Silk, J. D. *et al.* IDO induces expression of a novel tryptophan transporter in mouse and human tumor cells. *J. Immunol. Baltim. Md 1950* **187,** 1617–1625 (2011).

129. Heikamp, E. B. & Powell, J. D. Sensing the immune microenvironment to coordinate T cell metabolism, differentiation & function. *Semin. Immunol.* **24,** 414–420 (2012).

130. Clarke, S. R. *et al.* Characterization of the ovalbumin-specific TCR transgenic line OT-I: MHC elements for positive and negative selection. *Immunol. Cell Biol.* **78,** 110–117 (2000).

131. Roy, B. M., Zhukov, D. V. & Maynard, J. A. Flanking Residues Are Central to DO11.10 T Cell Hybridoma Stimulation by Ovalbumin 323-339. *PLoS ONE* **7,** (2012).

132. Testi, R., D'Ambrosio, D., De Maria, R. & Santoni, A. The CD69 receptor: A multipurpose cell-surface trigger for hematopoietic cells. *Immunol. Today* **15,** 479–483 (1994).

133. Salmond, R. J., Emery, J., Okkenhaug, K. & Zamoyska, R. MAPK, Phosphatidylinositol 3-Kinase, and Mammalian Target of Rapamycin Pathways Converge at the Level of Ribosomal Protein S6 Phosphorylation to Control Metabolic Signaling in CD8 T Cells. *J Immunol* **183,** 7388–7397 (2009).

134. Yu, L. *et al.* Termination of autophagy and reformation of lysosomes regulated by mTOR. *Nature* **465,** 942–946 (2010).

135. Peterson, R. T., Beal, P. A., Comb, M. J. & Schreiber, S. L. FKBP12-Rapamycin-associated Protein (FRAP) Autophosphorylates at Serine 2481 under Translationally Repressive Conditions. *J. Biol. Chem.* **275,** 7416 –7423 (2000).

136. Soliman, G. A. *et al.* mTOR Ser-2481 Autophosphorylation Monitors mTORC-specific Catalytic Activity and Clarifies Rapamycin Mechanism of Action. *J. Biol. Chem.* **285,** 7866 –7879 (2010).

137. Zehn, D., Lee, S. Y. & Bevan, M. J. Complete but curtailed T-cell response to very low-affinity antigen. *Nature* **458,** 211–214 (2009).

138. Létourneau, S., Krieg, C., Pantaleo, G. & Boyman, O. IL-2- and CD25-dependent immunoregulatory mechanisms in the homeostasis of T-cell subsets. *J. Allergy Clin. Immunol.* **123,** 758–762 (2009).

139. Oestreich, K. J. & Weinmann, A. S. Transcriptional mechanisms that regulate T helper 1 cell differentiation. *Curr. Opin. Immunol.* doi:10.1016/j.coi.2011.12.004

140. Frauwirth, K. A. & Thompson, C. B. Activation and inhibition of lymphocytes by costimulation. *J. Clin. Invest.* **109,** 295–299 (2002).

141. Kim, J., Kundu, M., Viollet, B. & Guan, K.-L. AMPK and mTOR regulate autophagy through direct phosphorylation of Ulk1. *Nat. Cell Biol.* **13,** 132–141 (2011).

142. Cobbold, S. P. *et al.* Infectious tolerance via the consumption of essential amino acids and mTOR signaling. *Proc. Natl. Acad. Sci. U. S. A.* (2009). doi:10.1073/pnas.0903919106

143. Rodríguez, P. C. & Ochoa, A. C. Arginine regulation by myeloid derived suppressor cells and tolerance in cancer: mechanisms and therapeutic perspectives. *Immunol. Rev.* **222,** 180–191 (2008).

144. Moore, M. W., Carbone, F. R. & Bevan, M. J. Introduction of soluble protein into the class I pathway of antigen processing and presentation. *Cell* **Vol 54,** 777–785 (1988).

145. Sinclair, L. V. *et al.* Phosphatidylinositol-3-OH kinase and nutrient-sensing mTOR pathways control T lymphocyte trafficking. *Nat Immunol* **9,** 513–521 (2008).

146. Schneider, C. A., Rasband, W. S. & Eliceiri, K. W. NIH Image to ImageJ: 25 years of image analysis. *Nat. Methods* **9,** 671–675 (2012).